CRANFIELD UNIVERSITY

TOSIN ONABANJO

TECHNO-ECONOMIC AND ENVIRONMENTAL ASSESSMENT OF GAS TURBINES UTILIZING BIOFUELS

SCHOOL OF ENERGY, ENVIRONMENT AND AGRIFOOD
ENERGY THEME

PhD THESIS

CRANFIELD UNIVERSITY

SCHOOL OF ENERGY, ENVIRONMENT AND AGRIFOOD
ENERGY THEME

Ph.D. THESIS

Academic Year 2011 - 2014

TOSIN ONABANJO

TECHNO-ECONOMIC AND ENVIRONMENTAL ASSESSMENT OF GAS TURBINES UTILIZING BIOFUELS

Supervisor: GIUSEPPINA DI LORENZO

MARCH 2015

ABSTRACT

The continued global reliance on fossil fuels with impact on resource depletion, human health, atmospheric pollution and environmental degradation has necessitated a global drive to integrate renewable fuels such as biodiesels. Biodiesels are described as “fuels composed of fatty acid methyl or ethyl esters and obtained from vegetable oils or animal fats”. Their use in energy generation could diversify the world’s energy mix, reduce fossil fuel dependence, reduce emissions and energy cost to bring about other economic benefits, especially for developing economies and rural communities with lack of adequate access to modern energy. A techno-economic and environmental life cycle assessment is however required to ensure that these fuels are fit for use in engines and meet any regulatory standard and sustainability criteria. This thesis has evaluated the use of Jatropha- and microalgae-biodiesel for power generation in two industrial gas turbines with open and combined cycle configuration. This was achieved using a techno-economic and environmental life cycle impact assessment framework. Comparative fuel assessments have been carried out between biodiesels and fossil fuels. Furthermore, the concept of microbial fuel degradation was examined in gas turbines. The thesis have identified Jatropha biodiesel as a worthwhile substitute for conventional diesel fuel, because it has close performance and emission characteristics to conventional diesel fuel with added advantage of being renewable. The consequent displacement of conventional diesel fuel with Jatropha biodiesel has significant environmental benefits. For economic viability and sustainability of gas turbine operated power plants, energy producers require a minimum monetary amount to recover the added cost of operating 100% Jatropha biodiesel. Other integration mechanisms are also available for utilizing the fuel in engines without compromising on plant’s economic performance. In worst case scenarios, where there are no government incentives, local conditions such as high life cycle cost of electricity, open opportunities for distributed and independent power generation from renewable fuels like Jatropha-biodiesel. Furthermore, this thesis has identified salient energy conversion processes that occur in gas turbine fuels, especially with biodiesels and developed a bio-mathematical model, Bio-fAEG to simulate these processes in gas turbines. This platform is a first step in quantifiable assessment and could enable a better understanding of microbial initiated processes.

Keywords: Biodiesels, Performance, Emissions, Power Generation, Developing Countries

ACKNOWLEDGEMENTS

I would like to acknowledge my project supervisor, Dr Giuseppina Di Lorenzo for her research guidance and support during the course of my PhD. Special thanks to my prior supervisors: Dr Eric Goodger has consistently reviewed and improved the quality of my research. Prof. Pericles Pilidis gave me the opportunity as a researcher in the Department of Power and Propulsion and has provided valuable support at my request. Dr Stephen Ogaji, who was not able to supervise me have given me worthwhile angles for my research. More heartfelt thanks to the Department of Power & Propulsion for subsistence funds and to the following people: Mrs Gill Hargreaves, Nicola Datt and Claire Bellis, for making my journey a smoother ride at one point or the other. I would also like to appreciate colleagues (Chima Ajonu, Iroizan Adasi, Dapo Ajayi, Isaac Bassey, Osasu Osaze and Shuaibu Hyai) who helped me develop confidence in gas turbine theory and performance at the early stages of my PhD. My deepest thanks to Dr Matthew Castrow, Ebi Ogiriki, Karhik Yadiyal, Dr Nkoi Barinyima, Isaiah ThankGod, and Dr Theoklis Nikolaidis for taking out time to help me during my simulations.

Heartfelt appreciation to my husband, Yinka for unending love and research support towards my research career, especially on grey days and during discouraging times. Thank you to Toluwani, my gorgeous easy-going daughter for being so adorable. Special thank you goes to my parents for the motivation, financial and moral support and to my siblings, Gbenga, Niyi and Toyosi for lending a hand and heart. Unforgettable are my parents-in love for constantly praying for me.

Finally, I will use this opportunity to thank the following people: Pastor Biyi Ajala, Pastor Tayo and Moyo Olotu, The Ogiriki family, Mr and Mrs Ajimokatan, Teni Ogundipe, Mr & Mrs Boboye, Dr Sola Adesola, Dr Adegbite and family, Mr and Mrs Okonkwo, Mr and Mrs Hameed for support at one time or the other.

To all my friends and well-wishers, I say a big thank you.

May God bless you all!

DEDICATION

I dedicate this thesis to the person of the HOLY SPIRIT for inspiration and timely intervention. May the LORD's name be praised!

TABLE OF CONTENTS

LIST OF FIGURES

LIST OF TABLES

LIST OF ABBREVIATIONS

AG	Microalgae
Ar	Argon
ASTM	American Society for Testing and Materials
B/C	Benefit-to-Cost
BA	Biofilm Age
BD	Biofilm Depth
BLPD	Billion Litres Per Day
BTOE	Billion Tonnes of Oil Equivalent
C	Carbon
C/H	Carbon-to-Hydrogen
CCGT	Combined Cycle Gas Turbine
CEA	Chemical Equilibrum with Applications
CH_4	Methane
CO	Carbon monoxide
CO_2	Carbon dioxide
DI	Diesel
Di-EGME	Diethylene Glycol Monomethyl Ether
DLN	Dry Low NOx
DZ	Dilution Zone
ED	Electron Donor
EGT	Exhaust Gas Temperature
EIA	U.S. Energy Information Administration
ELCD	European Reference Life Cycle Database
EMF	Exhaust Mass Flow
EPS	Extracellular Polysaccharide
FAME	Fattty Acid Methyl Ester
FAR_{STOIC}	Stoichiometric Fuel-to-Air-Ratio
FBN	Fuel-bound Nitrogen
FF	Flame Front
FMP	Federal Ministry of Power
FPP	Fired Power Plants
GE	General Electric
GHG	Greenhouse Gas
GUI	Graphical User Interphase

GWP	Global Warming Potential
H	Hydrogen
H/C	Hydrogen-to-Carbon
H_2O	Water
H_2S	Hydrogen Sulphide
HHV	Higher Heating Value
HPT	High Pressure Turbine
HRSG	Heat Recovery Steam Generator
HRSG	Heat Recovery Steam Generators
IAWPS	International Association for the Properties of Water and Steam
IEA	International Energy Agency
IPCC	Intergovernmental Panel on Climate Change
IPP	Independent Power Producer
IRR	Internal Rate of Return
ISO	International Standard Organization
IZ	Intermediate zone
JT	Jatropha
KV	Kinematic Viscosity
LCA	Life Cycle Assessment
LCOE	Levelized Cost of Energy/Electricity
LHV	Lower Heating Value
LHV	Lower Heating Value
LMP	Larson Miller Parameter
MIC	Microbial Induced Corrosion
MLPD	Million Litres Per Day
MTBE	Methyl Tertiary-Butyl Ether
N_2	Nitrogen
N_2O	Dinitrogen Oxide
NASA	National Aeronautics and Space Administration
NER	Net Energy Ratio
NERC	Nigerian Electricity Regulatory Commission
NEV	Net Energy Value
NG	Natural Gas
NH_3	Ammonia
NNPC	Nigerian National Petroleum Corporation
NO_3	Nitrate

NO_X	Nitrogen Oxide
NPV	Net Present Value
NREV	Net Renewable Energy Value
O&M	Operation and Maintenance
O_2	Oxygen
O_3	Ozone
OCGT	Open Cycle Gas Turbine
OECD	Organization for Economic Cooperation and Development
OEM	Original Equipment Manufacturer
OPA	Offshore Processing Agreement
PAH	Polycyclic Aromatic Hydrocarbon
PL	Plant Life
PM_{10}	Particulate Matter
PME	Palm Methyl Ester
PO_4	Phosphate
PRé	Product Ecology Consultants
PZ	Primary Zone
RH	Relative Humidity
ROI	Return on Investment
RR	Revenue Requirements
S	Sulphur
SCR	Selective Catalytic Reduction
SIR	Société Ivoirienne de Raffinage
SMD	Sauter Mean Diameter
SO_2	Sulphide
SO_4	Sulphate
SPB	Simple Payback Period
STP	Standard Temperature and Pressure
TAME	Tertiary Amyl Methy Ether
TEA	Terminal Electron Acceptor
TET	Turbine Entry Temperature
TLCC	Total Life Cycle Cost
UHC	Unburnt Hydrocarbon
UNDP	United Nation Development Programme
US LCI	United States Life Cycle Inventory
USAF	United State Air Force

VLCC	Very Large Crude Carrier
VOC	Volatile Organic Carbon
WACC	Weighted Average Cost of Capital
WHO	World Health Organization
X_{acc}	Accessibility Factor
X_{bio}	Overall Biodegradability
X_{in}	Intrinsic Biodegradability

CHAPTER 1

1. INTRODUCTION

1.1 Research Motivation

The motivation for this research in biofuels and gas turbines is based on: i) the demand for renewable fuels, ii) energy demand and crisis in developing and least developed countries, iii) gas turbine potentials and opportunities for renewable energy.

1.1.1 Renewable Fuels

The world depends on fossil fuels —mainly petroleum derived oils, coal and natural gas, for most of its activities including transportation and electricity generation. These fuels are widely accepted as the main contributors to the annual global emissions of carbon dioxide (CO_2), one of the major greenhouse gases (GHGs) resulting from human activities. In 2013, the annual global emissions of CO_2 was said to increase to 36 billion metric tons; a 61% increase in CO_2 emissions from that of 1990, the baseline year of the Kyoto protocol [Le Quéré et al. 2014]. According to International Energy Agency (IEA), 2013 report, 83% of the GHG emissions in 2011 were generated from burning fuels for energy generation with the rest covered by agriculture, industrial processes and waste generation. Also, 42% of the world's CO_2 emissions in 2011 were accounted to two combined sectors in electricity and heat [see figure 1.1].

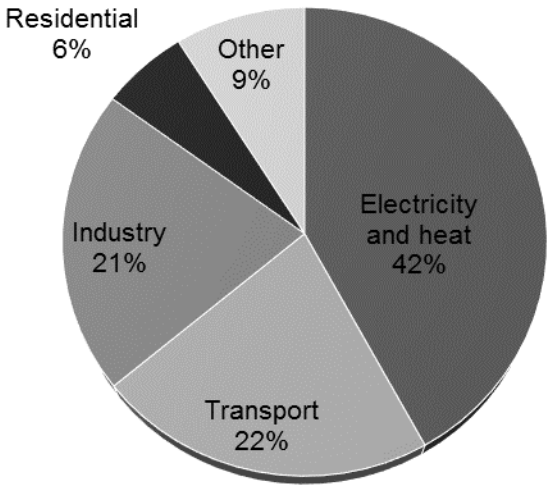

Figure 1.1: World CO_2 emissions by sector in 2011 [IEA, 2013]

Based on current policies and regulations surrounding the use of fossil fuels, the global CO_2 emissions are expected to rise to 45 billion metric tons in 2040 [EIA, 2014a].

Apart from the increase in global emissions of CO_2, the world also faces more damaging effects on the ecosystem with glacial ice melt in the Polar Regions and flooding in many parts of the world, a direct consequence of increasing ambient temperatures and emissions of damaging gases, by a phenomenon referred to as global warming. The emissions of poisonous (toxic) gases during fuel combustion also have great effects on human health. For instance, 1.94 million premature deaths in 2008 across several developing and least developed countries were associated to the use of exposed fossil fuels. 44% of these premature deaths occurred in children under 5 while 2% resulted from lung cancer and overall, it affected more women than men [UNDP/WHO, 2009]. Furthermore, the global petroleum reserves are expected to be depleted in less than 50 years at the present rate of energy consumption.

In order words, continued global reliance on fossil fuels has negative effects on resource depletion, human health, atmospheric pollution and environmental degradation. These effects have necessitated a global drive to integrate renewable fuels such as biofuels.

1.1.2 Energy Demand

Energy is a crucial element in the development and growth of any economy. It is the driving force behind the strong industrial and technological advanced economies and a missing element in poorly advancing economies. Energy is important for powering homes (cooking, heating, lighting and use of appliances), industrial and manufacturing processes, communication, transportation, education, water and waste treatment, health care, research and technology, agriculture, commerce, and security. The lack of adequate energy to power development has strong links with poverty, pollution, greenhouse gas (GHG) emissions and other environmental concerns.

About 12.7 billion tonnes of oil equivalent (BTOE) was said to be the world's energy consumption in 2013, a value that was 79% higher than that of 2002 and primarily supplied by three fossil fuel sources (natural gas-24%, oil-33% and coal-30%) —see Figure 1.2. The highest energy consuming continents were Asia [41%], Europe and Eurasia [23%] and North America [22%], while the least energy consuming ones include the Middle East, Africa, South and Central America —see Figure 1.3.

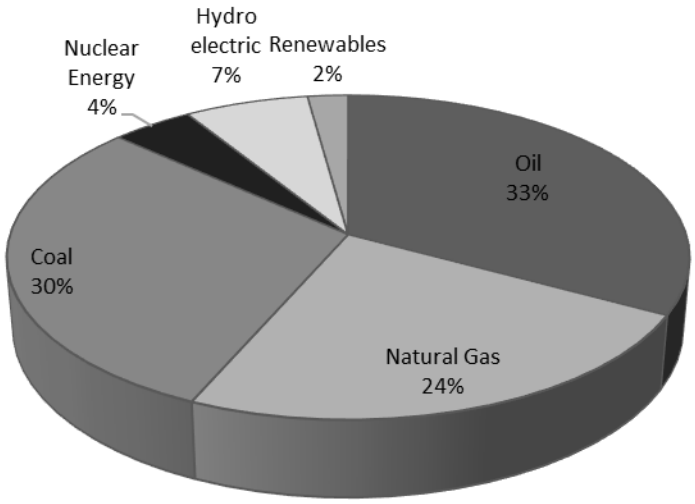

Figure 1.2: World's energy consumption by fuels in 2013[1]

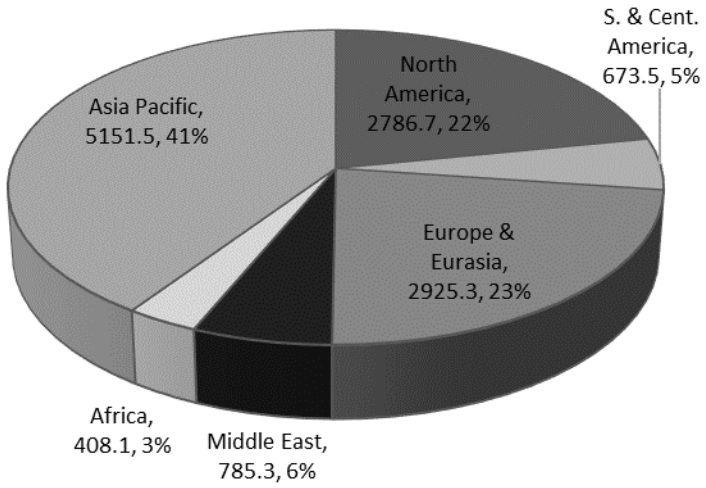

Figure 1.3: World's energy consumption by continent in 2013[1]

According to EIA's International Energy Outlook 2013, the world's energy consumption will increase by 56% through 2010 to 2040, especially for non-Organization for Economic Cooperation and Development (non-OECD) countries [EIA, 2013a]. An updated report in 2014 estimates increase in global oil consumption by more than 33% from 2010 to 2040 with the transportation and industrial sectors accounting for 92% of the fuel demand in 2040. These projections are expected to be driven by fast-emerging economies like China, India and other developing countries, where energy has been in short supply [EIA, 2014a; IEA, 2014].

[1] Extracted from BP, 2014

The current state of energy consumption and future growth therefore calls for urgent advances in renewable energy production, integration and application, especially for economies with relatively high potentials for renewables but lacking sufficient energy.

1.1.2.1 Energy Situation in Developing and Least Developed Countries

According to UNDP/WHO, [2009], about 1.5 billion people, a quarter of the world population are without access to modern electricity. This fraction of the world's population largely belongs to developing and least developed countries —concentrated in Africa and South Asia. Energy supply is of critical concern in these countries, because of the increasing population, energy demand, and power shortages. Most communities are experiencing rapid breakdowns in the energy sector and facing persistent black-outs because of poor infrastructural development, poor maintenance of the limited gas networks and power plants, sub-optimal transmission systems, ageing infrastructures and other local issues. But more importantly, as a result of sole dependence of the energy sector on a single choice of technology and fuel type, often fossil derived fuel.

The energy situation in Africa is peculiar. Africa is about the size of the United States, China, India and Europe combined, having a population of about 1.14 billion —16% of the world's population. In 2013 [see Figure 1.3], it however only utilised 3% of the world's energy consumption [BP, 2014]. This is neither as a result of high energy efficiency nor due to lack of resources but for the lack of sufficient energy supply. As a matter of fact, the continent has huge natural resource bank with vast natural gas and oil proven reserves, nearly account for 15% and 9% respectively of the world's proven reserve [KPMG, 2014]. A large percentage of the natural gas is found in Nigeria and Algeria, while the crude oil reserves are concentrated in Nigeria and Libya [UNECA, 2006]. Similar to the world's energy consumption in 2013, fossil fuels account for over 70%, while hydro-electric capacity and renewables generate only 21% and 4% respectively — see Figure 1.4. Typically, electricity is generated mainly by hydroelectric power in Central and West Africa, oil and gas in West and North Africa, hydroelectric power and coal in South Africa and geothermal in East Africa [UNECA, 2006; ICA, 2008].

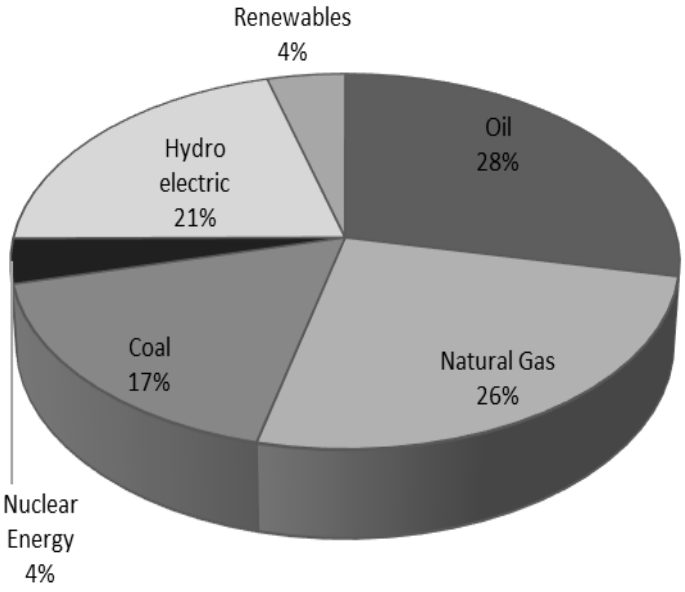

Figure 1.4: Africa's energy consumption by fuels in 2013[a]

The above described energy situation in developing and least developing countries, especially in Africa leaves over two-third of the population in darkness with no access to modern energy. But the current demand for energy, which is expected to increase due to population growth and drive for economic development, provides a unique opportunity for integration of renewable fuels like biofuels.

Since, energy is a critical factor and energy consumption in these countries is expected to increase over the next 50 years [IEA, 2014]; there is the need for an alternative, renewable and sustainable energy source to substitute fossil fuel power generation.

1.1.3 Gas Turbine Potentials and Opportunities for Renewable Energy

Gas turbines are widely advanced with commercial application in industries, especially for power generation, marine, and aviation [Soares, 2008]. One of the key advantages is the large amount of useful work that can be derived from an engine of relatively small size and weight. In principle, it uses compressed working fluid (air) subsequently expanded as hot gas to generate useful power or thrust. This is brought about by progressive series of compression, combustion with fuel where chemical energy is extracted, and expansion of gas in the turbine [Walsh and Fletcher, 2008]. In comparison, with other prime movers such as diesel engines, gas turbines emit relatively lower levels of combustion pollutants [Langston and Opdyke, 1997]. However, when compared to other renewable options such as solar energy, wind energy, the use of

fossil fuels and the emissions of large quantities of CO_2, as well as GHGs such as NOx and CO, make it non-competitive. The way to attain such [2]"renewable" status when compared to present and near future renewable energy forms would require zero or similar emission levels from a life cycle perspective. This can be achieved by capturing the emissions from the engine exhaust or from the fuel or through the use of renewable fuels such as biofuels.

1.2 Research Aim and Objectives

Following the research motivation described above, this research is directed towards achieving the following aim and objectives.

To assess the use of biodiesels in industrial gas turbines from a techno-economic and environmental perspective, and for application in power generation for developing and least developed countries. To achieve this aim, the following objectives were outlined.

- Evaluate the techno-economic performance of gas turbines operating on biofuels, and in comparison to those operating on natural gas and conventional diesel fuel.
- Evaluate the environmental performance of gas turbines operating on the best choice of biodiesel fuel using techno-economic considerations and life cycle perspective.
- Assess the impact of microbial-induced fuel degradation on engine performance.

1.3 Thesis Structure

The thesis has been written in a series of paper-style format due to the multi-disciplinary approach of the study. It consists of eight chapters: first two chapters are introductory, and the following chapters 3-6 cover broad topics on engine performance, emission analysis, economic evaluation and environmental assessment. Chapter 7 deals with microbial-induced fuel degradation. Each of the chapters (3-7) consists of introduction, methodology, results and discussion, conclusion, future work and references. The last chapters (8) provide an abridged version of thesis conclusion and recommendation.

[2] Renewable -net zero carbon emissions

A more detailed overview of each chapter is provided below.

- **Chapter 1** sets the scene for biofuels and gas turbines with an overview on the research motivation, project aim and objectives. Following this thesis structure, the lists of publications and oral or poster presentations that were prepared, published or presented during the course of this research are provided.
- **Chapter 2** presents a general literature review and the boundaries in which the research was conducted. It also highlights the research gap and how the thesis has contributed to knowledge.
- **Chapter 3** assesses the performance of gas turbines operating on different fuels with the view of understanding how these fuels affect engine performance. A consideration is made for the best choice of renewable fuel that could substitute fossil-fuels based on engine performance.
- **Chapter 4** considers the emission performance of engines in relation to the fuels burnt. The best choice of biodiesel fuel that could substitute the use of fossil fuels in gas turbine engines from the view of emissions is highlighted.
- **Chapter 5** presents a techno-economic and environmental framework to assess the economic performance of gas turbine power plants operating on different fuels. The power plants were examined under different scenarios for base load operation and for power generation in Nigeria or similar developing countries.
- **Chapter 6** considers the energy requirement and the environmental burden associated with the use of the “best choice of fuel” using life cycle assessment methodologies via a well-to-wake and a well-to-wheel system boundary.
- **Chapter 7** introduces the concept of bio-fouling in gas turbine fuels and fuel systems and examines the impact of microbial fuel degradation on engine performance. The development of a bio-mathematical model and subsequent integration of the degraded fuels in engine performance model is described.
- **Chapter 8** provides an abridge version of the individual chapter summaries and recommendations.

1.4 Publications and Posters during PhD

1.4.1 Publications

1. Onabanjo, T. O.; Di Lorenzo, G.; Goodger, E. M.; Pilidis, P. 2014. The development of a model for the assessment of bio-fouling in gas turbine system. Journal of Engineering for Gas Turbine and Power, 136(6), 061401 Paper No: GTP-13-1399; doi: 10.1115/1.4026367.

2. Onabanjo, T. O.; Di Lorenzo, G.; Goodger, E. M.; Pilidis, P. 2013. Application of microbial metabolism stoichiometry in modelling bio-fouling assessment in gas turbine liquid fuels. In 13th International Conference on Stability, Handling and Use of Liquid Fuels, Rhodes, Greece, October 6-10 2013.

3. Onabanjo, T. O.; Di Lorenzo, G.; Goodger, E. M.; Pilidis, P. 2013. The development of a model for the assessment of bio-fouling in gas turbine system. In ASME Turbo Expo 2013: Turbine Technical Conference and Exposition. Vol. 2: Aircraft Engine; Coal, Biomass and Alternative Fuels; Cycle Innovations. San Antonio, Texas, USA, June 3–7, 2013.

4. Onabanjo, T. O.; Di Lorenzo, G.; Goodger, E. M.; Pilidis, P. A model for simulating microbial fuel degradation in gas turbines. Submitted to International Biodeterioration & Biodegradation. Manuscript Number: IBB-S-14-00425 (under review)

5. Onabanjo, T. O.; Di Lorenzo. Somorin, Y. Application of Bio-fAEG, a biofouling assessment model in gas turbines and the effect of degraded fuels on engine performance simulations. Prepared for Proceedings of the ASME Power & Energy 2015, June 28-July 2, 2015, San Diego, USA. Technical Publication Number: PowerEnergy2015-49657 (Accepted for Publication)

6. Onabanjo, T. O.; Di Lorenzo. Energy efficiency and environmental life cycle assessment of Jatropha for energy in Nigeria: a “well-to-wheel” perspective. Prepared for Proceedings of the ASME Power & Energy 2015, June 28-July 2, 2015, San Diego, USA. Technical Publication Number: PowerEnergy2015-49654 (Accepted for Publication)

7. Onabanjo, T. O.; Di Lorenzo. Economic Analysis of a Jatropha Biodiesel-fired Power Plant in Nigeria. Prepared for The 3rd Sustainable Thermal Energy Management International Conference (SUSTEM 2015), 7th – 8th July 2015, Newcastle upon Tyne, UK. (Abstract Accepted/Manuscript under review)

8. Onabanjo, T. O.; Di Lorenzo, G. Nikolaidis, T. Pilidis, P. 2014. The effects of fuel degradation on a simulated gas turbine for marine propulsion (Prepared manuscript).

9. Onabanjo, T. O. and Di Lorenzo, G. 2014. Jatropha biodiesel-fuel production in Nigeria: energy balance and environmental life-cycle assessment. Submitted to Applied Energy (Manuscript under review).

1.4.2 Oral/Poster Presentations:

1. Onabanjo, T. O.; Di Lorenzo. 2015. Salient Energy Bio-Conversion Processes Limiting Gas Turbine Engine Performance & Efficiency. Technical presentation for the ASME Power & Energy 2015, June 28-July 2, 2015, San Diego, USA.

2. Onabanjo, T. O.; Di Lorenzo. 2015. Evaluation of Gas Turbine Emission Criterion for Regulatory Review and Methodology of Pricing in Nigeria. Poster to be presented at the ASME Power & Energy 2015, June 28-July 2, 2015, San Diego, USA.

3. Onabanjo, T. O.; Di Lorenzo, G.; Goodger, E. M.; Pilidis, P. 2013. Application of microbial metabolism stoichiometry in modelling bio-fouling assessment in gas turbine liquid fuels. Oral & Poster Presentation at the IASH 2013, the 13th International Conference on Stability, Handling and Use of Liquid Fuels, on October 6-10 2013, Rhodes, Greece

4. Onabanjo, T. O.; Di Lorenzo, G.; Goodger, E. M.; Pilidis, P. 2013. The development of a model for the assessment of bio-fouling in gas turbine system. Presented at the ASME Turbo Expo 2013/ASME International Gas Turbine Institute, on June 3-7, 2013, San Antonio Convention, Texas, USA

5. Onabanjo, T. O. 2012. Bio-Mathematical Techniques. Application in Combustion and Gas Turbine Technologies. Poster presented at the SfAM Postgraduate and Early Career Scientists (PECS), on October 25, 2012, London, UK

6. Onabanjo, T.O 2012. 'Assessing Fuel Degradation in Gas Turbines: Biofilm Model'. Poster presented at the 6th American Society of Microbiologists-Conference on Biofilms, September 29-October 4, 2012, Hyatt Regency, Miami, USA

7. Onabanjo, T.O. 2012. 'A mathematical based model for assessing microbial fuel degradation.' Poster presented at Opportunities for Algal Commercialization, June 20, 2012, Cranfield, UK

1.5 References

[1] British Petroleum (BP). 2014. Historical data workbook in Statistical Review of World Energy. London

[2] Federal Ministry of Power (FMP), 2015. Power Statistics Generated on December 23, 2012. Available on http://www.power.gov.ng/index.php/component/content/article/78-featured/140-power-statistics Last accessed on 07/02/2015

[3] House of Representative Ad-Hoc Committee (HRADC). 2012. Report of the ad-hoc Committee to verify and determine the actual subsidy requirements and monitor the implementation of the subsidy regime in Nigeria", Resolution No. (HR.1/2012). Available on http://premiumtimesng.com/docs_download/KGB%202015%20subsidy.pdf Last accessed on 06/9/2014.

[4] International Energy Agency (IEA). 2013. CO_2 emissions from fuel combustion 2012. Second Edition. IEA Publications, Paris.

[5] International Energy Agency (IEA). 2014. World Energy Outlook 2014. IEA Publications, Paris.

[6] KPMG. 2014. Oil and Gas in Africa: Africa's Reserves, Potential and Prospects of Africa. Available on https://www.kpmg.com/Africa/en/IssuesAndInsights/Articles-Publications/General-Industries-Publications/Documents/Oil%20and%20Gas%20in%20Africa%202014.pdf. Last accessed on 06/9/2014

[7] Langston, S and Opydyke, G. 1997. Introduction to Gas Turbine for non-engineers. Global Gas Turbine News 37(2): 1-9.

[8] Le Quéré, C., Moriarty, R., Andrew, R.M., Peters, G.P., Ciais, P., Friedlingstein, P. et al. 2014. Global Carbon Budget 2014. *Earth System Science Data Discussions* 7, 521-610. doi: http://dx.doi.org/10.5194/essdd-7-521-2014

[9] Nigerian National Petroleum Corporation (NNPC). 2012. Annual Statistical Bulletin. First Edition, NNPC: Abuja.

[10] Soares, C. 2008. Gas turbines: A Handbook of Air, Land, and Sea applications. Amsterdam: Butterworth-Heinemann. London: Elsevier Inc.

[11] The Infrastructural Consortium for Africa (ICA). 2008. Power Supply situation in Africa. Background paper prepared for ICA Annual Meeting 2008. Available on http://www.icafrica.org/fileadmin/documents/Tokyo/Background_paper_Power_Supply_situation_in_Africa_FINAL.pdf Last accessed on 06/9/2014

[12] U.S. Energy Information Administration (EIA). 2013a. International Energy Outlook 2013. Report Number DOE/EIA-0484(2013). Washington. Available on: www.eia.gov/forecasts/ieo/pdf/0484(2013).pdf Last accessed on 06/9/2014

[13] U.S. Energy Information Administration (EIA). 2014a. International Energy Outlook 2014. Report Number DOE/EIA-0484(2014). Washington. Available on: http://www.eia.gov/forecasts/ieo/pdf/0484(2014).pdf. Last accessed on 06/9/2014

[14] United Nations Development Programme/World Health Organisation (UNDP/WHO). 2009. The energy access situation in developing countries: A review on least developed countries and Sub-Saharan Africa. United Nations Development Programme/World Health Organization Report. New York.

[15] United Nations Economic Commission for Africa (UNECA). 2005. Report on Energy for Sustainable Development: African Regional Implementation review for the 14th Session of the Commission on Sustainable Development (CSD-14). Available on https://sustainabledevelopment.un.org/content/documents/ecaRIM_bp.pdf Last accessed on 05/02/2015

[16] Walsh, P. P. and Fletcher, P. 2008. Transient Performance. *In* Gas Turbine Performance. 2nd ed., Blackwell Science Ltd: Oxford, UK.

CHAPTER 2

2. LITERATURE REVIEW

The use of diesel fuels is less common for large-scale power generation and in gas turbines, except for start-up and as emergency back-up fuel in dual-fuel engines. In certain countries, diesel fuels are widely used for electricity generation; nearly accounting for 88% of the energy mix in Saudi Arabia [Kost et al. 2013]. In Nigeria, diesel has become the predominant fuel for power generation, especially for local businesses and industries. Over 75% of this diesel fuel is a by-product of importation. HTADC [2012] reported a diesel demand of 12 million barrel per day (MLPD) in Nigeria, of which the local refineries have the capacity to generate up to 9 MLPD along with refined product "swap"[3] arrangement from crude lifting foreign companies and off-shore processing agreement (OPA) from nearby overseas refineries. However, local refineries can only meet about 22% of the diesel fuel demand with the remaining portion being met by importation [NNPC, 2012]. These local conditions promote fuel scarcity and energy shortage while the delivery of the diesel from foreign refineries increases the cost and the environmental burden of these fuels.

In such instances, biodiesel fuels could be a valuable and renewable substitute, provided they can ensure the power plant has a competitive techno-economic and environmental performance as fossil-fired engines. Supported by local conditions such as unavailability of other fuels, local abundance of resources or initiatives, these fuels could be major players in power generation, especially in communities that lack modern energy supply.

Biodiesels are described as "fuels composed of fatty acid methyl or ethyl esters and obtained from vegetable oils or animal fats" [Demirbas, 2008]. They are produced by thermochemical conversion of triglycerides to fatty acid methyl or ethyl esters using an alcohol-catalyst dependent reaction, known as transesterification [Leung et al. 2005]. They have been derived from a wide range of sources including common and readily available feedstock such as soybean [Xin and Xhong, 2005], palm oil [Kalam, and Masjuki, 2002], rapeseed [Sheng et al. 2004], animal fats [Andersen and Weinbach, 2010] and other non-edible feedstock such as Jatropha [Lu et al. 2009], and microalgae [Christi, 2007].

[3] Swap refers to an exchange of crude oil for refined products. This arrangement is between the Nigerian National Petroleum Corporation (NNPC) and crude lifting foreign companies in Nigeria.

Some of the perceived benefits of the use of biodiesel in internal combustion engines and for energy generation include: a) similar properties to diesel fuel would not necessitate engine modification, b) renewable nature enhances biodegradability, which could minimize greenhouse gas (GHG) emissions and environmental degradation, c) fuel characteristics and oxygenated properties could improve engine performance, durability and net energy output, as well as reduce emissions and wear and tear of engine. The use of biodiesels in engines is also identified as a source of diversifying the world's energy mix, reducing fossil fuel dependence, emissions and energy cost while bringing about other economic benefits such as rural development for communities involved in its production [Demirbas, 2009, Gokalp and Lebas, 2004, Agarwal, 2007, Hill et al. 2006].

The above-mentioned potentials have given biodiesel fuels an advantage over conventional diesel fuels. However, there are debates regarding their sustainability and use in engines [Naylor et al. 2007; Wilkinson and Herrera, 2010; Zilberman et al. 2012]. These include concerns that biodiesel production could trigger a food crisis, especially in developing nations, since farmers would prefer to plant fuel crops for profit than food crops [De Fraiture et al. 2008; Piesse and Thirtle, 2009]. Also, because biodiesels are largely derived from plant oils, land is another competing element. Large scale production of biodiesels could result in land use conflicts and associated problems [Fargione et al. 2008; Lapola et al. 2010; Havlík et al. 2011]. Seasonal production can affect availability and wide locations and distances of bio-refineries, and farm sites could increase the environmental burden of the fuels, especially when transported by fossil fuel powered vehicles. In internal combustion engines including gas turbines, there are concerns that high viscous and oxygen content of biodiesel fuels could negatively affect engine performance, emissions and durability [Monyem and Van Gerpen, 2001; Canakci and Sanli, 2008; Xue et al. 2011]. Some of such effects include: interference with atomization and evaporation, difficult cold start operation, nozzle and injector soiling, all of which affect combustion performance. Other added effects include damage to hot end components of the engine and contamination of lubricating oil which could reduce cooling efficiency of fuel oils.

There are also indications that microbial growth in fuel could affect the chemistry of fuels, wherewith engine performance and emissions could be significantly affected. Although, fuel biodegradability is of environmental advantage for biofuels, its intrinsic biodegradable characteristics increase the risk of contamination of the fuels [Pattamaprom et al. 2010]. Furthermore, the continual use of biocides and anti-icing additives could exert further microbial resistance, in biofilm and spore forming

microorganisms. This could be enhanced by increasing variability and the use of biodiesels as blends [Hill and Hill, 2008; Das and Chandran, 2011, Okoh, 2006; Passman and Dobranic, 2005, Pasqualino et al, 2006, Mariano et al. 2008; Lee, 2010, Dodos et al. 2012].

2.1 Case Study Location: Nigeria

According to IEA 2014, “more than 90 million people in Nigeria (55% of the population), do not have access to (grid) electricity.” Although, Nigeria ranked as the fourth largest energy consuming country in Africa after South-Africa, Egypt and Algeria in 2012 [EIA 2014b], the primary energy sources were obtained from traditional woody biomass combusted in exposed stoves and from largely imported fossil derived fuels used in individual back-up generators.

Of the 6 GW installed capacity of power generating units, only 2 to 3.5 GW of electricity is produced at a time [FMP, 2015], such that the grid only meet 20% of the country's energy demand [Oyedepo, 2012]. Oyedepo, [2012] showed an availability range of 9% [Afam power station] to 87% [Omoku power station] for Nigerian power stations. This is attributed to failing power generation, transmission and distribution sectors of the country. Another instance is described at Olorunsogo Phase II, a power station located in South West, Nigeria, and equipped with four (126 MW) gas turbines that can either operate as an open cycle to generate 500 MW power or as a combined cycle to generate about 750 MW power. The station currently operates only as an open cycle with facilities working far below their installed capacity. For several months, the power station was not in operation due to insufficient gas and this is a familiar occurrence in many power stations in Nigeria. Some of these events were caused by ageing infrastructure, poor maintenance of the limited gas networks and power plants, vandalization of pipelines or widespread shortage of natural gas. Consequently, the country suffers from severe and forced power outages, epileptic power supply and persistent black out while residents and industries are forced to depend on self-generated electricity. The large imbalance between demand and supply of energy is therefore, Nigeria's greatest economic bane and calls for emergency solutions with platform for long term development.

Apart from the energy crisis, fuel is a luxurious commodity in Nigeria. Although, Nigeria is one of the largest producers and exporters of crude, fourth leading exporter of LNG in 2012, accounts for two-thirds of Africa's crude oil reserve with Libya and holds the largest natural gas reserve [Oyedepo, 2012; EIA, 2013b]; shortage of fuel across the country is a common occurrence. The rural population are left with no alternative than traditional woody biomass including agricultural residues for cooking while kerosene is sourced for lighting. According to a report by National Bureau of Statistics [2011], about 88% of the rural population and 42% of the urban population use wood for cooking while 58% of the Nigerian population use kerosene for lighting.

Hence, this study is tailored towards Nigerian power plants considering the above-described energy and fuel situations and applicable to similar developing countries. This enables engine simulation at ambient conditions typical to the chosen engine location and modelling of local conditions for site-specific studies. Nigeria is a developing economy with warm tropical climate and this differ from the European average.

2.2 Choice of Biofuels: Jatropha and Microalgae Biodiesel

Two biodiesel fuels derived from Jatropha and microalgae (*Chlorella vulgaris*) have been carefully selected based on the following criteria: a) non-food (edible) crop, b) classified as energy crop or with energy content, c) promising fuel for gas turbines, d) can be grown or cultivated locally and e) have other economic benefits. The Jatropha *curcas* plant meets these criteria because it is a promising energy, non-food crop that grows naturally in Nigeria. It is capable of growing on poor soil with low nutrient and water requirement. The fuel has been used in a number of internal combustion engines and considered a promising fuel. Similarly, microalgae, a microscopic unicellular organism can grow rapidly in fresh, marine or waste water. It gives rise to fuel with relatively high energy content. Both energy sources are of considerable environmental advantage because they are non-edible, can be grown locally and should not contribute to food and land crisis when grown on wasteland. They also have other economic benefits including fertilizer and medicinal use.

2.3 Choice of Engines: Heavy Duty and Aero-derivative Gas Turbine

Based on study location (Nigeria), two gas turbines have been selected and assumed to be co-located at Olorunsogo power plant in Ogun state, Nigeria. Olorunsogo power station has been selected due to the anomalies in operating hours versus the installed capacity at the facility and would adequately fit the biodiesel production and use structure presented in this thesis. As mentioned above, the power station is equipped with four 126 MW (GE 9E frame gas turbines) with combined cycle capability. Hence, a 126 MW gas turbine was selected to model a GE 9E unit with an open and combined cycle configuration and a 22.4 MW gas turbine was selected to examine a smaller capacity engine, both for base load operation. The base load operation was required for the engines because of the current energy situation in Nigeria, where energy demand is more than supply.

2.4 Relevant Literatures

A review is provided in the next section to summarize research advances in biodiesel fuels and gas turbines, and specifically for Jatropha and microalgae biodiesels where available under the following themes: a) gas turbine performance, b) gas turbine emissions, c) environmental impact of biodiesels, d) economic performance of biodiesel-fired power plants, e) microbial fuel degradation in gas turbine fuels and fuel system.

2.4.1 Biodiesels and Gas Turbine Performance

A number of studies have evaluated the performance of biodiesels in internal combustion engines with extensive reviews by [Xue et al. 2011; Dwivedi et al. 2011]. However, only a few studies are directed towards industrial gas turbines [Campbell et al. 2008; Moliere et al. 2007; Bolszo and McDonell, 2007; Chiang et al. 2007; Hashimoto et al. 2008]. A summary of the relevant studies in gas turbines and involving the use of biodiesel fuels is provided below.

Hashimoto et al. [2008] investigated the combustion characteristics of palm biodiesel in comparison to conventional diesel fuel and observed a similar range of adiabatic flame temperatures over a wide range of excess air ratios. Also both fuels had similar ignition and combustion performance, but palm biodiesel had lesser tendency to form luminous flame and soot. Another study by Liu et al. [2009] showed that the biodiesel derived from recycled cooking oil had higher dynamic viscosity and caused bigger fuel droplet size, particularly at lower pressure. The study also showed that this biodiesel had a lower flame temperature and combustor pressure drop. Overall, the biodiesel had good ignition

performance but this was dependent on the choice of air-assist pressure selected for ignition. Sallevet et al. [2014] suggest the importance of preheating biofuels to improve spray quality and combustion performance, especially for highly viscous fuels. Relatively poor atomization quality and longer evaporation rates were observed by Bolszo and McDonell [2007] during the use of soy biodiesel in a 30kW gas turbine engine. Recommendations were made to optimize the soy biodiesel atomization, one of which includes the adjustment of the fuel injection system. Many studies agree to the potentials of biodiesels to replace conventional diesels in internal combustion engines [Gupta et al. 2010. Hashimoto et al. 2008; Sallevet et al. 2014]; however, the approach of injecting fuel during gas turbine operation differs and is largely dependent on fuel source and property.

A few other studies by Hashimoto et al. [2014] and Fan et al. [2014] examined the combustion and spray characteristics of high viscous Jatropha oils, while Rehman et al. [2011] and Badami et al. [2014] examined the use of Jatropha oils. Rehman et al. [2011] carried out a study on the technical feasibility of using Jatropha oils, Jatropha biodiesels and blends on a Rover gas turbine test rig with maximum power of 44 kW to observe the effect on specific fuel consumption and emissions of the engine. It was concluded that Jatropha oil had similar characteristics to diesel oil and can be blended successfully. The fuel consumption of the engine increased initially due to the low volatility, high viscosity and low calorific value of the fuel, but this improved at higher load. Badami et al. [2014] observed the performance of a small turbo-jet engine using Jet-A, Jatropha biodiesel, gas-to-liquid kerosene and a blend of Jatropha biodiesel and Jet-A fuel. The blended fuel had higher dynamic viscosity and lower LHV than the Jet-A fuel. It was observed that the engine had similar performance as a result of the use of the fuels, however a small difference in fuel flow rates which was consistent and proportional to the reduction in LHV of the blended fuel.

None of the above studies has examined the performance of Jatropha and/or microalgae biodiesel in a simple and combined cycle configuration and for power generation.

2.4.2 Biodiesels and Gas Turbine Emissions

There are a large number of experimental studies that have evaluated the impact of biodiesel fuels on emissions of engines, with reviews by Xue et al. [2011] and Dwivedi et al. [2011]. These are however limited to diesel engines, with varying applications ranging from road transportation, heavy duty engines for farm operations to diesel powered marine engines.

For diesel engines, there are conflicting opinions about the emissions generated from biodiesels. Report by Ozsezen et al [2009] show that waste palm oil and canola oil methyl ester had reduced smoke opacity, unburned hydrocarbon and carbon monoxide (CO) emissions of 87%, 14%, 10% and 48%, 73% and 68% respectively when compared to diesel fuel. However NOx emissions increased by 22% and 7% when operating on waste palm oil and canola oil methyl ester respectively. Also, studies by Buyukkaya [2010] indicate an increase in NOx emissions using neat rapeseed oil and blends in engines while a reduction in CO emissions by 32% for 100% use of neat rapeseed biodiesel. These trends were attributed to higher oxygen mass fraction and cetane number that causes high local temperatures and shorter ignition delays, consequently promoting NOx emissions and reduced CO emissions. Other studies that reported reduced CO emissions and increased NOx emissions include [Xhu et al, 2010, Ozener et al, 2014; Banapurmatha et al. 2008]. Contrary to the above trends, Dorado et al. [2003] reports a decrease in NOx emissions in engine operating on waste olive oil methyl ester as compared to diesel fuel, but proposed further study. Also studies by Song et al. [2008] and Zheng et al. [2008] observed no significant difference in CO emissions in engines operating biodiesel blends at part load.

In industrial gas turbines, there is little information regarding the engine emissions using biofuels, particularly biodiesels. Spray characterization studies of Palm Biodiesel (PME) [Chong and Hochgreb, 2011] and Jatropha crude oil and biodiesel [Fan et al. 2014] give insight to the behaviour of biodiesels during combustion. Their behaviours are said to depend on the combustion technology and the operating conditions of the combustor. Chong and Hochgreb, [2011] reported that the Sauter Mean Diameter (SMD) and droplet velocity were higher for PME than diesel fuel, attributing these results to the effects of higher viscosity and surface tension of PME to diesel fuels. These also had effects on evaporation by elongating the spray penetration length and droplet vaporization rate. In the same study, emission results showed a decrease in NOx emissions as compared to

the diesel fuel using a swirling spray flame conditions and overall fuel lean conditions. The reduced NOx emissions were accounted to the absence or reduced fuel-bound nitrogen in the PME as compared to the diesel fuel.

Although, the studies by Fan et al. [2011] reported that emission profiles for PME were similar to diesel over a wide range of excess air ratios, there was decreasing NOx emissions for PME fuel for the same SMD or fuel kinematic viscosity as that of the diesel fuel. Also, at the same atomizing pressure using air-assist pressure swirl atomizer, NOx emissions were lower for PME than diesel fuel. Increased NOx emission trends were observed at lower atomizing pressure for both liquid fuels; hence the results demonstrate the impact of atomizing pressure on SMD, which increases droplet size and droplet numbers at lower levels. These conditions promote elongated spray penetration and formation of local regions around the droplets. Such combustion conditions occur in a diffusion flame mode and result in a near stoichiometric air-fuel ratios where high thermal NOx is formed. Further studies by the same author, Hashimoto et al. [2014], on Jatropha crude oil and biodiesel showed that NOx emission results changed significantly as a result of the air flow rate than as a function of fuel flow rate. Also, CO emissions were significantly higher for the crude oil than the biodiesel and diesel counterparts, and resulted from low evaporability of the fuel. Furthermore, study by Habib et al. [2010] found the emissions trends of CO and NO in a small-scale gas turbine using pure biodiesels to be lower than that for conventional Jet A and the NOx formation pattern was different from the Zeldovich mechanism.

Emission analysis using experimental methods supported by numerical models on an aero-derivative gas turbine engine with engine thrust of 80 N and fuel consumption of 5 g/s showed slightly higher NOx and CO emissions for gas-to-liquid kerosene than the fossil bases Jet-A kerosene. Also, studies by Bolszo and McDonell, [2009] that investigated a 30kW micro-gas turbine engine using soybean biodiesel observed NOx and CO increased emissions as load was increased from 50 to 100%. The increase in NOx emissions was demonstrated further using atomization measurement, which showed an increase in droplet sizes for soy biodiesel and higher viscosity and lower volatility than conventional diesel fuel. However, lower NOx emissions were achieved to an extent during the use of airblast atomizer assisted combustion to increase the air-to-liquid ratio. Panchasara et al. [2009] carried out combustion performance and emission studies on soy biodiesel and diesel-biodiesel oil blends and reported slightly higher CO

emissions for soy biodiesel than diesel while NOx emissions were lower for soy biodiesel than diesel in a constant heat input rate engine.

The above reports about NOx and CO emission and current focus on the environmental performance of power plants necessitate the need to better understand the emission characteristics of biodiesel fuels, in particular Jatropha and microalgae biodiesels in industrial gas turbines.

2.4.3 Economic Performance of Biodiesel-fired Plants

Despite the many benefits that are perceived with the use of biodiesels as substitute for petroleum derived fuels, if their use in power plants is not economically sustainable and quantifiable, the migration from conventional to renewable power generation could be impeded. This is why cost is a critical factor in techno-economic evaluation of power plants, most importantly, the fuel cost.

Research in economic performance of biodiesels is usually directed towards the cost of production of a kg or MJ of fuel [Wegstein et al. 2010; Christi, 2007; Hill et al. 2006; Haas et al. 2006]. Openshaw [2000] and Wegstein et al. [2010] report the production cost for Jatropha biodiesel as $0.93/L and $0.68/L respectively with price improvement over time. Sampattagul et al. [2009] carried out a life cycle costing for Jatropha biodiesel production in Thailand and observed a production cost that is relatively high for Jatropha biodiesel than the retail price of petroleum-derived diesel. A production cost of 0.6 Euro/L is reported for Jatropha biodiesel, which is equivalent to $0.75/L excluding environmental costs, considering an exchange rate of 1.24 for 2012. This cost was largely contributed by the agricultural processes of production. Parajuli et al. [2014], also estimated the trend for levelized cost of production and proposed 20% blend for successful integration of biofuels. Assuming a 20% blending rate with diesel fuel in Nepal is allowed, the levelized cost of production is expected to be $0.76/L. Also, the actual costs of production of microalgae biodiesel are yet to be established, because the commercial development of microalgae biodiesel is still in its prime stage. A range of $2/L to $350/L is however estimated. Darzins et al. [2010] estimated a production cost of $2.72/L via photobioreactor, supposing a high yield of lipid biomass and $10.74/L for race-pond production. Davis et al. [2011] also estimated the cost of microalgae biodiesel production as $9.84/gallon and $20.53/gallon for photobioreactor and race-pond production respectively. Other studies report microalgae biodiesel production cost of $2.8/L [Chisti, 2007] to $352/L [Grima et al. 2003].

In Nigeria, there are indications that the cost of production of Jatropha biodiesel might be higher than petroleum derived fuels. Analysis by Umar [not dated], indicated a benefit-cost ratio of zero due to poor or lack of seed yield as at the third-year of plantation in Kano, Nigeria, hence lack of sales. Ogunwole [2014] also report poor seed yield however high oil content for Jatropha plants grown locally. This is likely because the commercialization of Jatropha plantation in Nigeria is still at its early stages. Contrary to Umar [not dated], Ibrahim et al. [2013] estimate a positive net present value (NPV) with return on investment (ROI) for Jatropha oil production in Zaria, Nigeria.

To the author's knowledge, current economic studies are limited to biodiesel production or biomass derived energy [Eijck et al. 2012]; none of which applies to direct consumption of biodiesel fuels in gas turbines and to power generation in Nigeria.

2.4.4 Environmental Performance of Biodiesel-fired Plants

Due to the enormous dependence of life cycle assessment studies on specific site conditions and locations, there have been a number of studies on energy efficiency and environmental life cycle assessment (LCA) of Jatropha biodiesel production in the public domain. Some of these studies apply to countries such as India [Acthen et al. 2010; Pandey et al. 2011; Kumar et al. 2012], China [Ou et al. 2009; Liang et al. 2013; Wang et al. 2011], Indonesia [Nazir and Setyaningsih, 2010], Mozambique [Hagman and Nerentorp, 2011], Thailand [Prueksakorn, & Gheewala, 2008; Pruesakorn et al. 2010], Malaysia [Lam et al. 2009], Tanzania [Eshton et al. 2013] and Mali [Ndong et al. 2009]. Other studies have considered this LCA of Jatropha biodiesel from an application perspective that is, the use of Jatropha biodiesel in locomotives [Whitaker, & Heath, 2009), transportation in a small car engine [Achten et al. 2010], and electrification from a diesel fired generator set through a central PV and connected to the grid in Chhattisgarh [Gmünder et al. 2010].

Furthermore, each of the LCA analysis applies specifically to the location under study, which changes the inputs significantly. For example, Pandey et al. 2011 carried out a comparative LCA assessment for Jatropha biodiesel production to those of palm and coconut oil considering a 5 year period using primary data from a 100 acres of plantation, in Ettayapuram village of Tamil Nadu and also assuming a small case, high input system, as opposed to low input systems described in other studies. Kumar et al. [2012] examined the production of 1 tonne of Jatropha biodiesel under rain-fed and irrigated conditions with or without co-product allocation. A NER and GHG reduction range of 1.4-8.0 and 40%-107% are estimated under the consideration of co-product allocation under

rain-fed and irrigated cases, however a NER range of 1.4-1.7 without co-product allocation. The conditions described for this study do not accurately describe the Nigerian scenario.

Other studies that have evaluated Jatropha biodiesel production from a life cycle perspective include [Prueksakorn and Gheewala, 2006; Menichetti and Otto, 2008; Hoefnagels et al. 2010; Kaewcharoensombat et al. 2011 and WMJ, 2011] with review by [Janaun and Ellis 2010]. Although, these studies examined the life cycle impact of Jatropha biodiesel production, none of these investigations have examined biodiesel production in Nigeria using the standard life-cycle assessment (LCA) approach. In addition, because of the lack of available, reliable data, the reference diesel fuel used for benchmarking in these studies does not adequately represent the Nigeria case.

2.4.5 Microbial Fuel Degradation in Gas Turbines

The role of microorganisms in fuel deterioration and fouling in the gas turbine industry is well established in the literature with hundreds of incidence reports. Prior to 1952, when the incidence of microbial contamination was first reported in military gas turbine fuel systems, there were evidences of microorganisms in kerosene and aviation gasoline. For instance, some gas-producing bacteria were said to be involved in the explosion of a kerosene tank in 1939 [Thaysen, 1939], while in 1941, wide degradation of bulk-stored aviation fuels was observed [Hill and Hill, 2008].

A few of the historical instances of microbial contamination include: The contamination of JP-4 fuels in United State Air Force (USAF) Boeing B-47 and KC-97 aircraft in 1956, which led to the clogging of fuel filtering units and subsequently, impeded operation. The sudden failure of filter screens and capacitance gauges, led to extensive wing tank corrosion and presence of holes in fuel sealants, large enough to result in spillage in severely affected USAF B-52 and Boeing KC-135 Stratotanker aircraft. This is said to be caused by iced-fuel and sludge material containing loads of microbes. Furthermore, between 1956 and 1958, the US and Royal Navy reported incidences of a dark sludge material accompanied by microbes in aircraft and storage tanks. In 1960 in Australia, an extensive corrosion of the integral wings of Lockheed Hercules (C130A) and Electra (L188) aircraft occurred. Further investigations of the fuel in question (the JP-4 fuels), a number of aircraft systems, and fuel process routes led to the conclusion that microorganisms were a possible cause of fuel contamination. Similar incidences were reported in gas turbine engines in Egypt, India and North Africa, confirming this problem to be global [Hill and Hill, 2008; Brooks, 1963; Wilkes et al. 1963, London et al. 1965;

Finefrock and London, 1966; London, 1974; Pitcher, 1989; Hill, 2003; Rauch et al. 2006; Rogers and Kaplan, 1963].

In addition to aircraft fuel systems, microbial contamination has also been reported along production and distribution routes of gas turbine fuels such as in refineries and oil terminals [Pitcher, 1989, Roffey, 1989]; storage tanks for petroleum products [Hill and Hill, 1993; Gaylarde et al. 1999] and offshore oil facilities [Battersby et al. 1985]. The possibilities of a large scale impact of microbial contamination seems more likely in other gas turbine industries than aviation, though incidences are poorly reported, ignored or considered insignificant. Gaylarde et al. [1999] alluded to the fact that fuel system maintenance procedures in other industries are largely absent, poorly followed or ill-defined. Also, the wide gap in understanding between engineering and microbiology disciplines could have given rise to false reporting by field engineers [Hill, 2003].

In spite of the volume of researches, biologists and engineers have not necessarily quantified the effects of microbial contamination on gas turbine operation. Most studies are post-impact assessment, of which significant damage could have occurred prior to detection and control. Additionally, efforts to replicate fuel deterioration like real incidences have been futile and have continually led to opposing views, poor understanding of microbial fouling in fuel systems and ultimately, bias or false conclusions. Although, the application of biocides, the use of good fuel handling practices coupled with routine checks may appear to have brought the situation reasonably under control, the presence of microbes and water in fuels has not been totally eliminated in certain installations. There are indications that microbial growth in fuel could significantly affect the chemistry of fuels [Passman et al. 2001], wherewith performance and emission could be significantly affected.

With recent advances for alternative fuels, particularly liquid oil products from biofuels, increasing variability and flexibility of fuels and the use of biofuels as blends, the incidence of fuel contamination could be on the rise. Besides these, biofuels with readily available organic content, are said to have relatively higher hygroscopy, contain no sulphur, and are sourced widely with different processing and handling methods. Although, fuel biodegradability is of advantage for biofuels in terms of environmental sustainability; any degradatory effects on engine performance could limit its commercial application in gas turbine industries. Other indications that are making the concepts of fouling in gas turbine systems of particular interest include environmental concerns on the continual use of biocides and anti-icing additives, incidences of sudden recurrence

and possibility of increased microbial resistance, presence of biofilms with intrinsic ability to resist biocides, current emission limits for greenhouse and other related gases under the consideration of stricter standards.

Previous and current researches are limited to identification of the microbes responsible for fuel deterioration, qualitative examinations of engine fuel systems mainly the fuel filters and the storage tanks, and methods to control fuel deterioration and enhance fuel stability. However, there exists the gap in translating the knowledge gained from microbiological examinations to quantitative assessment of engine degradation. Hence, it is expedient to extend research beyond microorganism enumeration and qualitative engine assessment to quantitative models with indicators that can correlate microbial growth and product formation in fuels to engine degradation.

2.5 Contribution to Knowledge

Based on the identified gaps in knowledge, this thesis has contributed knowledge in the following areas.

1. Evaluated the performance of Jatropha- and microalgae-biodiesel in a typical heavy duty gas turbine (open and combined cycle application) and in an aero-derivative gas turbine at design point and site conditions and in comparison to natural gas- and conventional diesel-fired engines.

2. Highlighted the emission trends of a typical heavy duty gas turbine (open cycle application) and an aero-derivative gas turbine, both having a conventional combustor and operating on Jatropha- and microalgae-biodiesel and in comparison to natural gas- and conventional diesel-fired engines.

3. Evaluated the economic performance of Jatropha biodiesel- and microalgae biodiesel-fired engines in comparison to fossil-fired engines, using different economic measures. Proposed mechanisms for integrating Jatropha biodiesel in existing or future gas turbine power plants.

4. Determined the energy requirements and the environmental benefit that could be derived from substituting Jatropha biodiesel for diesel fuel in a typical heavy duty gas turbine using an environmental life cycle assessment approach.

5. Developed a bio-mathematical model, Bio-fAEG to simulate microbial fuel degradation in gas turbines. The use of the model has been applied to simulate microbial fuel degradation, predict biodegradation rates, estimate hydrocarbon loss and calculate the amount of water required to initiate degradation under aerobic conditions. The degraded fuels were integrated in Turbomatch (v2) to quantify the effects of microbial fuel degradation in an aero-derivative gas turbine.

2.6 References

[1] Achten, W.M., Almeida, J., Fobelets, V., Bolle, E., Mathijs, E., Singh, V.P & Muys, B. 2010. Life cycle assessment of Jatropha biodiesel as transportation fuel in rural India. *Applied Energy* 87(12): 3652-3660.

[2] Agarwal, A.K. 2007. Biofuels (alcohols and biodiesel) applications as fuels for internal combustion engines. *Progress in Energy and Combustion Science* 33(3): 233-271.

[3] Andersen, O. and Weinbach, J.-E. 2010. Residual animal fat and fish for biodiesel production: Potentials in Norway. *Biomass and Bioenergy* 34(8): 1183-1188.

[4] Badami, M., Nuccio, P. and Signoretto, A. 2013. Experimental and numerical analysis of a small-scale turbojet engine. *Energy Conversion and Management* 76: 225-233.

[5] Banapurmath, N.R. and Tewari, P.G. 2008. Performance of a low heat rejection engine fuelled with low volatile Honge oil and its methyl ester (HOME). *Journal of Power and Energy* 222(3): 323-330.

[6] Battersby, N. S., Stewart, D. J. and Sharma, A. P. 1985. Microbiological problems in the offshore oil and gas industries. *Journal of Applied Microbiology* 59: 227S-235S.

[7] Bolszo, C., McDonell, V. and Samuelsen, S. 2007. Impact of Biodiesel on Fuel Preparation and Emissions for a Liquid Fired Gas Turbine Engine. ASME Paper No. GT2007-27652, pp. 493-502

[8] Brooks, D. B. 1963. Military Research on jet fuel contamination". Paper presented at a session on Fuels during the 28th Midyear meeting of the American Petroleum Institute Division of Refining, in the Benjamin Fraklin Hotel, Philadelphia, Pennsylvania. FL 225/23

[9] Buyukkaya, E. 2010. Effects of biodiesel on a DI diesel engine performance, emission and combustion characteristics. *Fuel* 89(10): 3099-3105.

[10] Campbell, A., Goldmeer, J., Healy, T., Washam, R., Molière, M. and Citeno, J. 2008. Heavy Duty Gas Turbines Fuel Flexibility," ASME Paper No.GT2008-51368, pp. 1077-1085

[11] Canakci, M. and Sanli, H. 2008. Biodiesel production from various feedstocks and their effects on the fuel properties. *Journal of Industrial Microbiology and Biotechnology* 35(5): 431-441.

[12] Chiang, H.-W.D., Chiang, I.C. and Li, H.-L. 2007. Performance testing of microturbine generator system fueled by biodiesel. ASME Paper No. GT2007-28075, pp. 459-466

[13] Chisti, Y. 2007. Biodiesel from Microalgae. *Biotechnology Advances* 25:294–306

[14] Chong, C.T. and Hochgreb, S. 2012. Spray combustion characteristics of palm biodiesel. *Combustion Science and Technology* 184(7-8): 1093-1107.

[15] Darzins, A., Pienkos, P., & Edye, L. 2010. Current status and potential for algal biofuels production. A report to IEA Bioenergy Task, 39. Report T39-T2

[16] Das, N. and Chandran, P. 2011. Microbial Degradation of Petroleum Hydrocarbon Contaminants: An Overview. *Biotechnology Research International* Article ID 941810, 13 pages. doi:10.4061/2011/941810

[17] Davis, R., Aden, A., Pienkos, P. 2011. Techno-economic analysis of autotrophic microalgae for fuel production. *Applied Energy* (88):3524–3531

[18] de Fraiture, C., Giordano, M. and Liao, Y. 2008. Biofuels and implications for agricultural water use: blue impacts of green energy. *Water Policy* 10(Suppl. 1): 67-81

[19] Demirbas, A. 2008. Biodiesel: A Realistic Fuel Alternative for Diesel Engines, Springer London, pp 111-119.

[20] Demirbas, A. 2009. Biofuels securing the planet's future energy needs. *Energy Conversion and Management* 50(9): 2239-2249.

[21] Dodos, G.S., Konstantakos, T., Longinos, S. and Zannikos, F. 2012. Effects of microbiological contamination in the quality of biodiesel fuels. *Global NEST Journal* 14(2): 175-182.

[22] Dorado, M.P., Ballesteros, E., Arnal, J.M., Gomez, J. and Lopez, F.J. 2003. Exhaust emissions from a Diesel engine fueled with transesterified waste olive oil. *Fuel* 82(11): 1311-1315.

[23] Dwivedi, G., Jain, S. and Sharma, M.P. 2011. Impact analysis of biodiesel on engine performance - A review. *Renewable and Sustainable Energy Reviews* 15: 4633–4641

[24] Eijck, J., Smeets, E., & Faaij, A. 2012. The economic performance of Jatropha, cassava and Eucalyptus production systems for energy in an East African smallholder setting. *GCB Bioenergy 4*(6):828-845.

[25] Fan, Y., Hashimoto, N., Nishida, H. and Ozawa, Y. 2014. Spray characterization of an air-assist pressure-swirl atomizer injecting high-viscosity Jatropha oils. *Fuel* 121: 271-283.

[26] Fargione, J., Hill, J., Tilman, D., Polasky, S. and Hawthorne, P. 2008. Land clearing and the biofuel carbon debt. *Science* 319(5867): 1235-1238.

[27] Finefrock, V.H., and London, S.A., 1966. Microbial contamination of USAF JP-4 Fuels. Technical Report AFAPL-TR-66-91. Aero Propulsion Laboratory Research, Wright-Patterson Air Force Base, Ohio, USA.

[28] Gaylarde, C.C., Bento, F.M. and Kelley, J. 1999. Microbial contamination of stored hydrocarbon fuels and its control. *Revista de Microbiologia* 30: 1-10

[29] Gmünder, S.M., Zah, R., Bhatacharjee, S., Classen, M., Mukherjee, P., & Widmer, R. 2010. Life cycle assessment of village electrification based on straight Jatropha oil in Chhattisgarh, India. *Biomass and Bioenergy* 34(3): 347-355.

[30] Gökalp, I. and Lebas, E. 2004. Alternative fuels for industrial gas turbines (AFTUR). *Applied Thermal Engineering* 24(11-12): 1655-1663.

[31] Grima, E.M., Belarbia, E.H., Fernandez, F.G.A., Medina, A.R., and Chisti, Y. 2003. Recovery of microalgal biomass and metabolites: process options and economics. *Biotechnology Advances* 20:491–515

[32] Gupta, K.K., Rehman, A. and Sarviya, R.M. 2010. Bio-fuels for the gas turbine: A review. *Renewable and Sustainable Energy Reviews* 14(9): 2946–2955

[33] Haas, M. J., McAloon, A. J., Yee, W. C., & Foglia, T. A. 2006. A process model to estimate biodiesel production costs. *Bioresource technology 97*(4):671-678.

[34] Habib, Z.B., Parthasarathy, R.N. and Gollahalli, S.R. 2009. Effects of biofuel on the performance and emissions characteristics of a small scale gas turbine. *In* Proceedings of the 47th AIAA Aerospace Sciences Meeting

[35] Hashimoto, N., Ozawa, Y., Mori, N., Yuri, I. and Hisamatsu, T. 2008. Fundamental combustion characteristics of palm methyl ester (PME) as alternative fuel for gas turbines. *Fuel* 87(15-16): 3373-3378.

[36] Havlík, P., Schneider, U.A., Schmid, E., Böttcher, H., Fritz, S., Skalský, R., Aoki, K., de Cara, S., Kindermann, G., Kraxner, F., Leduc, S., McCallum, I., Mosnier, A., Sauer, T. and Obersteiner, M. 2011. Global land-use implications of first and second generation biofuel targets. *Energy Policy* 39(10): 5690-5702.

[37] Hill, E.C. and Hill, G.C. 1993. Microbiological problems in distillate fuels. *Trans. Inst. Marine Eng*. 104: 119-130

[38] Hill, E.C., and Hill, G.C. 2008. Microbial Contamination and Associated Corrosion in Fuels, during Storage, Distribution and Use. *Advanced Materials Research* 38: 257-268.

[39] Hill, J., Nelson, E., Tilman, D., Polasky, S. and Tiffany, D. 2006. Environmental, economic, and energetic costs and benefits of biodiesel and ethanol biofuels. *Proceedings of the National Academy of Sciences* 103(30): 11206-11210.

[40] Hill, T. 2003. Microbial growth in aviation fuel. *Aircraft Engineering and Aerospace Technology* 75(5): 497 – 502.

[41] Hoefnagels, R., Smeets, E., & Faaij, A. 2010. Greenhouse gas footprints of different biofuel production systems. *Renewable and Sustainable Energy Reviews* 14(7):1661-1694.

[42] Ibrahim, H. Ahmed, A.A. Bugaje, I.M. Muhammed-Dabo, I.A. 2013. Economic Evaluation of Continuous Heterogeneous Catalytic Transesterification of Jatropha oil Plant. *International Journal of Advanced Engineering Research and Technology* (*IJAERT*) 1(1):15-21

[43] International Energy Agency (IEA). 2014. World Energy Outlook 2014. IEA Publications, Paris.

[44] Janaun, J., & Ellis, N. 2010. Perspectives on biodiesel as a sustainable fuel. *Renewable and Sustainable Energy Reviews* 14(4): 1312-1320.

[45] Kaewcharoensombat, U., Prommetta, K., & Srinophakun, T. 2011. Life cycle assessment of biodiesel production from Jatropha. *Journal of the Taiwan Institute of Chemical Engineers* 42(3): 454-462.

[46] Kalam, M.A. and Masjuki, H.H. 2002. Biodiesel from palmoil - an analysis of its properties and potential. *Biomass and Bioenergy 23*(6): 471-479.

[47] Kost, C., Mayer, J. N., Thomsen, J., Hartmann, N., Senkpiel, C., Philipps, S., Nold, S., Lude, S., Saad, N. and Schlegl, T. 2013. Levelized Cost of Electricity Renewable Energy Technologies. Fraunhofer Institute for Solar Energy Systems, Freiburg, Germany.

[48] Kumar, S., Singh, J., Nanoti, S.M., & Garg, M.O. 2012. A comprehensive life cycle assessment (LCA) of Jatropha biodiesel production in India. *Bioresource Technology* 110: 723-729.

[49] Lam, M.K., Lee, K.T., & Mohamed, A.R. 2009. Life cycle assessment for the production of biodiesel: a case study in Malaysia for palm oil versus jatropha oil. Biofuels, *Bioproducts and Biorefining* 3(6): 601-612.

[50] Lapola, D.M., Schaldach, R., Alcamo, J., Bondeau, A., Koch, J., Koelking, C. and Priess, J.A. 2010. Indirect land-use changes can overcome carbon savings from biofuels in Brazil. *Proceedings of the national Academy of Sciences* 107(8): 3388-3393.

[51] Lee, J.S., Ray, R.I. and Little, B.J. 2010. An assessment of alternative diesel fuels: microbiological contamination and corrosion under storage conditions. *Biofouling: The Journal of Bioadhesion and Biofilm Research* 26(6): 623-635.

[52] Leung, D.Y.C., Wu, X. and Leung, M.K.H. 2010. A review on biodiesel production using catalyzed transesterification. *Applied Energy* 87(4): 1083-1095.

[53] Liang, S., Xu, M., & Zhang, T. 2013. Life cycle assessment of biodiesel production in China. *Bioresource Technology* 129: 72-77.

[54] Liu, A. and Weng, Y. 2009. Effects of Lower Heat Value Fuel on the Operations of Micro-Gas Turbine. *Energy and Power Engineering* 1(1): 28-37

[55] London, S. A., 1974. Microbiological evaluation of aviation fuel storage, dispensing and aircraft systems. Technical Report AFAPL-TR-74-144. Aerospace Medical Research Laboratory, Wright-Patterson Air Force Base, Ohio USA.

[56] London, S. A., Finefrock, V. H., and Killian, L. N. 1965. Microbial Activity in Air Force jet fuel systems. Technical Report AFAPL-TR-66-91. Aero Propulsion Laboratory Research, Wright-Patterson Air Force Base, Ohio, USA.

[57] Lu, H., Liu, Y., Zhou, H., Yang, Y., Chen, M. and Liang, B. 2009. Production of biodiesel from *Jatropha curcas* L. oil. *Computers and Chemical Engineering* 33(5): 1091-1096.

[58] Mariano, A.P., Tomasella, R.C., de Oliveira, L.M., Contiero, J. and de Angelis, D.F. 2008. Biodegradability of diesel and biodiesel blends. *African Journal of Biotechnology* 7(9): 1323-1328.

[59] Menichetti, E., & Otto, M. 2008. Energy balance and greenhouse gas emissions of biofuels from a life-cycle perspective. Biofuels: environmental consequences and interactions with changing land use, Proceedings of the Scientific Committee on Problems of the Environment (SCOPE) International Biofuels Project Rapid Assessment, 22-25.

[60] Molière, M., Panarotto, E., Aboujaib, M., Bisseaud, J.M., Campbell, A., Citeno, J., Mire, P.A., and Ducrest, L., 2007. Gas Turbines in Alternative Fuel Applications: Biodiesel Field Test. ASME Paper No. GT2007-27212, pp. 397-406

[61] Monyem, A. and Van Gerpen, J.H. 2001. The effect of biodiesel oxidation on engine performance and emissions. *Biomass and Bioenergy* 20(4): 317-325.

[62] National Bureau of Statistics. 2011. Annual Abstract of Statistics of the Federal Republic of Nigeria. Available on http://www.nigerianstat.gov.ng/pages/download/71 Last accessed on 06/9/2014.

[63] Naylor, R.L., Liska, A.J., Burke, M.B., Falcon, W.P., Gaskell, J.C., Rozelle, S.D. and Cassman, K.G. 2007. The Ripple Effect: biofuels, food security, and the environment. *Environment: Science and Policy for Sustainable Development* 49(9): 30-43.

[64] Nazir, N., & Setyaningsih, D. 2010. Life cycle assessment of biodiesel production from palm oil and Jatropha oil in Indonesia. In 7th Biomass Asia Workshop, 1-29.

[65] Okoh, A.I. 2006. Biodegradation alternative in the clean-up of petroleum hydrocarbon pollutants". *Biotechnology and Molecular Biology Review* 1(2): 38–50.

[66] Openshaw, K. 2000. A review of Jatropha curcas: an oil plant of unfulfilled promise. *Biomass and Bioenergy* 19:1-15

[67] Ou, X., Zhang, X., Chang, S., & Guo, Q. 2009. Energy consumption and GHG emissions of six biofuel pathways by LCA in (the) People's Republic of China. *Applied Energy* 86: S197-S208.

[68] Oyedepo, S. O. 2012. Energy and sustainable development in Nigeria: the way forward. Energy, Sustainability and Society 2:15

[69] Özener, O., Yüksek, L., Ergenç, A.T. and Özkan, M. 2014. Effects of soybean biodiesel on a DI diesel engine performance, emission and combustion characteristics. *Fuel* 115: 875-883.

[70] Ozsezen, A.N., Canakci, M., Turkcan, A. and Sayin, C. 2009. Performance and combustion characteristics of a DI diesel engine fueled with waste palm oil and canola oil methyl esters. *Fuel 88*(4): 629-636.

[71] Panchasara, H.V., Simmons, B.M., Agrawal, A.K., Spear, S.K. and Daly, D. T. 2009. Combustion performance of biodiesel and diesel-vegetable oil blends in a simulated gas turbine burner. *Journal of Engineering for Gas Turbines and Power* 131(3): 031503.

[72] Pandey, K.K., Pragya, N., & Sahoo, P.K. 2011. Life cycle assessment of small-scale high-input Jatropha biodiesel production in India. *Applied Energy* 88(12): 4831-4839.

[73] Parajuli, R. 2014. Economics of biodiesel production in the context of fulfilling 20% blending with petro-diesel in Nepal. *International Journal of Sustainable Energy 33*(2):435-447.

[74] Pasqualino, J.C., Montane, D. and Salvado, J. 2006. Synergic effects of biodiesel in the biodegradability of fossil-derived fuels". *Biomass and Bioenergy* 30: 874–879.

[75] Passman, F.J. and Dobranic, J.K. 2005. Relative biodegradability of B-100 biodiesel and conventional low sulfur diesel fuels". Paper presented at the 9th International Conference on Stability, Handling and Use of Liquid Fuels Sites, Spain, September 18-22, 2005.

[76] Passman, F.J., McFarland, B.L. and Hillyer, M.J. 2001. Oxygenated gasoline biodeterioration and its control in laboratory microcosms. *International Biodeterioration and Biodegradation* 47(2): 95-106.

[77] Pattamaprom, C., Pakdee, W. and Ngamjaroen, S. 2012. Storage degradation of palm-derived biodiesels: Its effects on chemical properties and engine performance. *Renewable Energy* 37(1): 412-418.

[78] Piesse, J. and Thirtle, C. 2009. Three bubbles and a panic: An explanatory review of recent food commodity price events. *Food Policy* 34(2): 119-129.

[79] Pitcher, D.G. 1989. Industrial case histories of microbiological fuel contamination - cause, effect and treatment. *International Biodeterioration* 25 (1-3): 207-218

[80] Prueksakorn, K., & Gheewala, S.H. 2006. Energy and greenhouse gas implications of biodiesel production from Jatropha curcas L. In Proceedings of the 2nd Joint International Conference on Sustainable Energy and Environment, 21-23.

[81] Prueksakorn, K., & Gheewala, S.H. 2008. Full chain energy analysis of biodiesel from Jatropha curcas L. in Thailand. *Environmental Science & Technology* 42(9): 3388-3393.

[82] Prueksakorn, K., Gheewala, S.H., Malakul, P., & Bonnet, S. (2010). Energy analysis of Jatropha plantation systems for biodiesel production in Thailand. *Energy for Sustainable Development* 14(1): 1-5.

[83] Rauch, M.E., Graft, H.W., Rozenzhak, S.M., Jones, S.E., Bleckmann, C.A., Kruger, R.L., Naik, R.R. and Stone, M.O. 2006. Characterization of microbial contamination in United States Air Force aviation fuel tanks. *J. Ind. Microbiol. Biotechnol*. 33: 29–36

[84] Rehman, A., Phalke, D.R. and Pandey, R. 2011. Alternative fuel for gas turbine: Esterified jatropha oil–diesel blend. *Renewable Energy 36*(10): 2635-2640.

[85] Roffey, R. 1989. Microbial problems during long-term storage of petroleum products underground in rock caverns". *International Biodeterioration* 25(1–3): 219-236.

[86] Rogers, M.R. and Kaplan, A.M., 1963. A field survey of the microbiological contamination present in JP-4 fuel and 115/145 AVGAS in a military fuel distribution system. AD410519. Defense Documentation Center for Scientific and Technical Information, Alexandria. Virginia, USA.

[87] Sallevelt, J.L.H.P., Gudde, J.E.P., Pozarlik, A.K. and Brem, G. 2014. The impact of spray quality on the combustion of a viscous biofuel in a micro gas turbine. *Applied Energy* 132: 575-585

[88] Sampattagul, S., Suttibut, C. & Kiatsiriroat, T. LCA/LCC of Jatropha Biodiesel Production in Thailand. *International Journal of Renewable Energy* 4(1):33-42

[89] Sheng, M., Wu, G.-Y., Xu, G. and Wu, M.-X. 2004. Preparation of biodiesel from rapeseed oil. *Journal of Chemical Engineering of Chinese Universities* 18(2): 231-236.

[90] Song, J.-T. and Zhang, C.-H. 2008. An experimental study on the performance and exhaust emissions of a diesel engine fuelled with soybean oil methyl ester. *Journal of Automobile Engineering* 222(12): 2487-2496.

[91] Soto I., Feto A. and Keane J. 2013. Are Jatropha and other biofuels profitable in Africa? *Jatropha Facts Series*, Issue 4, ERA-ARD.

[92] Thaysen, A.C. 1939. On the gas evolution in petrol storage-tanks caused by the activity of micro-organisms. *J. Inst. Petroleum Tech*. 25: 111-115.

[93] U.S. Energy Information Administration (EIA). 2013b. Country Analysis: Nigeria. Available on http://www.eia.gov/countries/analysisbriefs/Nigeria/nigeria.pdf. Last accessed on 06/9/2014.

[94] U.S. Energy Information Administration (EIA). 2014b. International Energy Statistics. Available on http://www.eia.gov/cfapps/ipdbproject/iedindex3.cfm?tid=44&pid=44&aid=2&cid=r6,&syid=2002&eyid=2012&unit=QBTU. Last accessed on 06/9/2014

[95] Umar, A. F. Comparative Analysis of the Costs and Benefits of Some Jatropha Curcas Renwable Energy and Other Products Enterprises in Kano State. *SCIE Journals Australian Journal of Management, Policy and Law*, 1-6

[96] Wang, Z., Calderon, M.M., & Lu, Y. 2011. Lifecycle assessment of the economic, environmental and energy performance of Jatropha curcas L. biodiesel in China. *Biomass and Bioenergy* 35(7): 2893-2902.

[97] Wegstein, M., and Adhikari, N. 2010. Financial Analysis of Jatropha Plantations, *Journal of the Institute of Engineering, Kathmandu* 8(1):1-5.

[98] Whitaker, M., & Heath, G. 2009. Life cycle assessment of the use of jatropha biodiesel in Indian locomotives (No. NREL-TP-6A2-44428). Golden, CO: National Renewable Energy Laboratory.

[99] Wilkes. C.E., Iverson, W.P., Cockey, R.R. and Hodge. H.M. 1965. Microbial Contamination of Air Force Petroleum Products". Technical Report APL-TDR-64-95, 1-53. Aero Propulsion Laboratory Research, Wright-Patterson Air Force Base, Ohio, USA.

[100] Wilkinson, J. and Herrera, S. 2010. Biofuels in Brazil: debates and impacts. *Journal of Peasant Studies* 37(4): 749-768.

[101] WMJ, A. 2011. Benchmarking the environmental performance of the Jatropha biodiesel system through a generic life cycle assessment. *Environmental Science & Technology* 45(12): 5447-5453.

[102] Xin, M. and Zhong, X. 2005. Preparation of Biodiesel from Soybean Oil by Transesterification on KF/CaO Catalyst. *Petrochemical Technology* 3: 282-286.

[103] Xue, J., Grift, T. E. and Hansen, A.C. 2011. Effect of biodiesel on engine performances and emissions. *Renewable and Sustainable Energy Reviews* 15(2): 1098-1116.

[104] Zheng, M., Mulenga, M.C., Reader, G.T., Wang, M., Ting, D.S. and Tjong, J. 2008. Biodiesel engine performance and emissions in low temperature combustion. *Fuel* 87(6): 714-722.

[105] Zhu, L., Cheung, C.S., Zhang, W.G. and Huang, Z. 2010. Emissions characteristics of a diesel engine operating on biodiesel and biodiesel blended with ethanol and methanol. *Science of the Total Environment* 408(4): 914-921.

[106] Zilberman, D., Hochman, G., Rajagopal, D., Sexton, S. and Timilsina, G. 2013. The impact of biofuels on commodity food prices: Assessment of findings. *American Journal of Agricultural Economics* 95(2): 275-281.

CHAPTER 3

3. BIODIESELS AND ENGINE PERFORMANCE ANALYSIS

This chapter presents the performance evaluation of biodiesel-fired gas turbines in comparison to fossil-fired engines. Firstly, a brief introduction is provided to appraise industrial gas turbines, fuel requirements and how they relate to engine performance. Secondly, the method of integration of the fuel properties for microalgae and Jatropha biodiesel in the current version of Turbomatch (v2.0) is described. Finally, the results of the engine performance analyses for the different fuels are discussed, with the consideration of the best choice of biodiesel fuel that could substitute fossil derived fuels in gas turbines.

3.1 Introduction

Gas turbines are established in power generation with application in on-site generation, distributed power systems, oil and gas operations, and industrial processes. The possibilities of added arrangements such as steam cycles for combined cycle power plants, heat recovery boilers for combined heat and power systems have made gas turbines indispensable for large scale power generation, district heating and mechanical drive applications. Apart from the simple cycle, gas turbines could employ advanced cycles such as recuperated, reheat and intercooled cycles as well as utilise steam or water injection to improve work output, cycle efficiency and performance or drive emissions to reliable technical limits. These engines can be applied for peak, base or intermediate loads, especially when operating as multiple units [Pilavachi, 2000; Najjar, 2001; Polullikkas, 2004; Polyzakis et al. 2008].

Their advantages over reciprocating engines include:

- Large amount of useful work from a relatively small size and weight engine
- Capability for fuel flexibility (gas and distillate oil)
- Compact size
- Relatively low capital and maintenance cost
- Fast starting and loading

3.1.1 Fuels and Engine Performance

Fuels are required to meet the following requirements at all operating conditions:

a) Ease of flow

b) Ease of ignition

c) Good combustion properties

d) High calorific value

e) Minimal negating effects on combustion components and turbine parts

f) Minimal corrosion impact on fuel systems

g) Good lubricating and conducting property for cooling requirement

h) Safe to use

i) Sufficiently high combustion efficiency

This is because fuels are critical for reliable and efficient operation of gas turbines. They enable the expansion of the working fluid by allowing chemically stored energy to be released in the presence of heat. Depending on the quality, composition and properties of the fuel along with ambient inlet conditions such as pressure, and temperature, the performance and integrity of engines could be significantly affected while cycle efficiencies could improve or deteriorate. This could affect the engine's durability, availability, maintainability and reliability.

The common properties of fuels that are important for gas turbines include density, viscosity, and calorific value. Other important properties includes: lubricity, which prevents wears on metal surfaces and leaks around seals; flash point, a key parameter for good ignition; pour point; cloud point etc, but these are outside the scope of this study.

Table 3.1 presents the typical biodiesel fuel properties and as stated by ASTM D6751-15 for biodiesels and ASTM D2880-14a for diesel fuels.

Table 3.1: Liquid Fuel Properties & Specifications [Arbab et al. 2013; Atabani et al. 2012]

Fuel Properties	Diesel Fuel ASTM D2880	Biodiesel ASTM D6751	Typical Biodiesel[4]
Density at 15^{o}C (kg/cm^{3})	876	880	837-930
Kinematic Viscosity at 40^{o}C (cSt)	1.3[5]-2.4[6]	1.9-6.0	2.61-5.9
Calorific value (MJ/kg)	42-46	-	33-42.73
Flash point (^{o}C)	38	100-170[7]	69-259
Water and sediment content (vol. %)	0.05	0.05[6]	<0.005-0.05 [0.02-450[7]]
Sulphur content (m/m %)	0.05	0.05[6]	<0.005-0.02 [0.2-474[7]]
Lubricity (HFRR, µm)	-	-	135-280

1. **Viscosity** can be classified into dynamic and kinematic viscosity. The dynamic viscosity refers to the resistance of the fuel to move over another fluid or surface and the kinematic viscosity refers to the ratio of viscous forces to inertia [Soares, 2008]. The dynamic viscosity is most applicable to liquid fuels performance because it determines the ability of a fuel to meet pumping requirement while kinematic viscosity determines the bulk conditions. According to Soares, [2008], liquids are not pumpable with kinematic viscosity of less than 1 cSt and atomization would be unsatisfactory for fuels with kinematic viscosity of less than 10 cSt. From Table 3.1, it can be observed that diesel fuels for gas turbine application are required to have a viscosity not more than 2.4 cSt but not less than 1.3 cSt, but typical biodiesel fuel exceeds this limit. Tate et al. [2006] observed that the kinematic viscosity of three biodiesels from soy, canola and fish oil were significantly higher than that of diesel fuel and decreased with temperature. This supports the general notion that biodiesels are more viscous than conventional diesel fuels, although some biodiesel fuels are in close range with diesel fuels as shown in Table 3.1.

Viscosity directly affects fuel flow rates, spray characteristics and atomizing properties of a fuel [Arbab et al. 2013]. A highly viscous fuel reduces evaporation rate, induces poor fuel atomization, and also increases the specific fuel consumption of a fuel pump.

[4] Biodiesels from Jatropha, Palm, Coconut, Cotton seed, Sunflower, Safflower, Soybean, Canola/Rapeseed
[5] Minimum
[6] Maximum
[7] ppm

2. **Density** refers to the weight of a unit volume of fuel [Demirbas, 2008]. It is expressed as specific gravity; that is, the density of the fuel to that of water at a defined temperature. Density is very closely related to viscosity and it increases the energy concentration of a fuel [Arbab et al. 2013]. From Table 3.1, it can be observed that biodiesel fuels have a wide range of density between 830 kg/m^3 and 930 kg/m^3. The density of diesel is typically in the range of 820 kg/m^3 and 880 kg/m^3 [Soares, 2008]. A high dense fuel would have relatively high viscosity and this would bring about poor combustion performance and emission characteristics.

3. **Fuel Calorific Value** can be expressed as net, the lower heating value (LHV) or gross, the higher heating value (HHV). Unlike the HHV that incorporates latent heat of vaporization of the water generated with the combustion products, the LHV gives the net energy content. LHV is heat released under pressure in a constant volume, when the combustion products are cooled to the initial temperature of 25°C [Walsh and Fletcher, 2008]. In essence, it is the quantity of heat release during combustion. A high calorific value fuel improves combustion performance and vice versa. Usually, diesel fuels have LHV in the range of 42-46 MJ/kg, but biodiesels have much lower energy content in range of 33-42 MJ/kg while natural gas has LHV of about 47 MJ/kg [Soares, 2008].

There are concerns with the use of bio-fuels in engines because of the above described differences in fuel properties that is, relatively high viscosity, low volatility and low fuel calorific value. Properties such as viscosity and volatility induce smoking by affecting spray penetration, fuel mean droplet size and evaporation rates, which initiate local fuel rich spots [Lefebvre and Ballal, 2010]. And in order to improve such properties, crude bio-oil is often converted to biodiesel via transesterification. This form of conversion of bio-oil is said to reduce the viscosity of biodiesels by a factor of 8, molecular weight by a third while increasing volatility substantially [Gupta et al. 2010]. Rehman et al. [2011] also report a reduction in the viscosity of Jatropha biodiesel from 0.92 to 0.88, due to transesterification of crude bio-oil. Other means of reducing the viscosity of biodiesels significantly include heating, blending, dilution and emulsification [Rehman et al. 2011 and Arbab et al. 2013].

Furthermore, changing one fuel property could significantly affect another [Lefebvre et al. 1985]. Demirbas [2008] observed that the various properties of fuels are closely related. An increase in the density of a biodiesel fuel from 0.85 to 0.89 kg/L resulted in a linear increase in viscosity from 2.83 to 5.12 mm^2/s. Also, their heating value directly correlated with the physical properties of the biodiesel fuel. And, the failure of a fuel to meet fuel specification could negatively impact engine performance, emissions, engine materials and component life [Tan et al. 2013]. For instance, a decrease in specific gravity of fuel could result in less fuel flow pressure, necessitate the control system to cause a compensating volume of fuel to be released and this may lead to excessive temperature or over speeding of the engine [Soares, 2008; Lefebvre and Ballal, 2010]. There could be increase in soot formation, consequently increase in radiation and flame temperature. This increases the cooling requirement and reduces durability of rotating components.

The next section describes how the properties of microalgae and Jatropha biodiesel fuels were integrated into the engine performance model for fuel analysis.

3.2 Methodology

3.2.1 Fuel Analysis

Four fuels were examined in this study: a) Natural gas b) Conventional diesel c) Jatropha biodiesel and d) Microalgae biodiesel. Since, the current version of Turbomatch(v2.0) software has natural gas and diesel fuel included in its fuel library that has been validated [Palmer, 1967; Macmillian, 1974]; only the properties of the combustion gas products for microalgae and Jatropha biodiesel (see Table 3.2) were integrated. This integration was achieved with NASA CEA (Chemical Equilibrium with Applications), a software developed by NASA and employed in many simulation tools including PROOSIS [Sethi, 2008].

The composition and LHV of microalgae and Jatropha biodiesel fuels were obtained from the literature, which the chemical formula of both fuels were calculated from their chemical composition. These data are presented in Table 3.2.

Table 3.2: Data for Microalgae and Jatropha Biodiesel

Parameters	Biodiesel			Jatropha Biodiesel	
Common Name	**Chemical Composition**	**Molar Fraction**	**Common Name**	**Chemical Composition**	**Molar Fraction**
Tridecylic acid	$C_{13}H_{26}O_2$	0.1558	Palmitic acid	$C_{16}H_{32}O_2$	0.1420
Pentadecylic acid	$C_{15}H_{30}O_2$	0.1761	Stearic acid	$C_{18}H_{36}O_2$	0.0700
Myristoleic acid	$C_{14}H_{26}O_2$	0.2887	Oleic acid	$C_{18}H_{34}O_2$	0.4470
Palmitoleic acid	$C_{16}H_{30}O_2$	0.0319	Linoleic acid	$C_{18}H_{32}O_2$	0.3280
Palmitoleic acid	$C_{18}H_{32}O_2$	0.0218	Palmitoleic acid	$C_{16}H_{30}O_2$	0.0070
Roughanic acid	$C_{16}H_{26}O_2$	0.2709	Linolenic acid	$C_{18}H_{30}O_2$	0.0020
-	$C_{24}H_{44}O_2$	0.0345	Arachidic acid	$C_{20}H_{40}O_2$	0.0020
Tetradecatrienoic acid	$C_{24}H_{42}O_2$	0.0203	Margaric acid	$C_{17}H_{34}O_2$	0.0010
			Unit		
Energy Content (LHV)	8071.0 [a]		kcal/kg	9250.5[b]	
	33.79		MJ/kg	38.73	
Chemical Formula	$C_{17.69}H_{33.11}O_2$			$C_{17.70}H_{33.17}O_2$	
Carbon/Hydrogen Ratio	6.408			6.402	
%Carbon/%Hydrogen by Mass	86.51			86.49	
Combustion Gas Composition[d]					
N_2	73.269		%	73.193	
Ar	0.879		%	0.878	
H_2O	12.334		%	12.528	
CO_2	13.519		%	13.401	
CO, O_2, Ne	0.000		%	0.000	
$F.A.R_{STOIC}$	0.0688			0.0682	
AIR_{STOIC}	84.269			84.940	

A short description of NASA CEA and how it was used to integrate fuels in Turbomatch and Steamomatch is described in the next sub-section.

3.2.1.1 Fuel Analysis

The CEA software computes the chemical composition and properties of complex chemical mixtures, assuming chemical reactions are at equilibrium. It has been used in calculating the thermodynamic properties of different chemical mixtures on the basis of their chemical composition [McBride and Gordon, 1996; Gordon and McBride, 1994]. It allows the user to assign a problem (temperature & pressure, combustion internal energy & volume, temperature & volume) to a specific fuel and oxidant mixture (air) and to generate the transport and thermodynamic properties of the combustion products. A detailed overview of this program have been described by [McBride and Gordon, 1996; Gordon and McBride, 1994].

In order to generate the products of combustion of both fuels (microalgae and Jatropha biodiesel), an input file was created using the "Problem", "Reactant", "Only" and "Output" tabs on the graphical user interface (GUI) of the CEA software. This was achieved using the following steps:

1. "Problem" tab: Selected the "Assigned Temperature and Pressure" function and stated a temperature range between 200 and 3000 in steps of 200 and maxiumum pressure of 50 Bar, as well as equivalent ratios between 0.03 and 1.
2. "Reactant" tab: Selected air as the oxidant and specifying the properties of fuels such as fuel chemical formula and composition, and relative amount of mole fractions as indicated in Table 3.2, in the reactant table; assuming the reference temperature of fuel and oxidant are 420 K and 700 K respectively with 1:1 mixture of fuel to oxidant mole fraction. The energy and temperature units of kj/mol and K were chosen respectively.
3. "Only" tab: Selected CO_2, Ar, N_2, H_2O, and O_2 as the only products of combustion, assuming chemical equilbrum; that is no dissociation of combustion products. This tab excludes the use of other tabs such as "Omit" and "Insert" tabs and enables the calculation of the combustion products at chemical equilibrum.
4. "Output" tab: Selected the thermal transport and thermodynamic properties function for calculation of mole fractions. This include properties such as enthalpy (h), Entropy (s), specific heat (cp), gamma (gam), molecular weight (mw) at trace species value.
5. "Activity" tab: Selected the "Execute CEA2" function to generate results.

The amount of the defined chemical species (N_2, O_2, Ar, H_2O, CO_2) at a combustion temperature of 2200K and pressure of 50 Bar, as well as the stoichiometric fuel to air ratio (FAR_{STOIC}) and stoichiometric air values were obtained from the output plot file, after simulation has been achieved. The combustion gas product composition as expressed in Table 3.2 was integrated into the fuel fluid library of Turbomatch (v2.0). The FAR_{STOIC} only applies mainly to the primary zone of the combustor where turbulence is sufficient to enhance a rapid mix between the air and fuel. The procedure for the method described above is shown in figure 1.1 (a-d) —Appendix I and fundamentally applies for both fuels integrated in Turbomatch (v2.0). Also, a sample of the input and output files are presented in figures 1.2 and 1.3 –Appendix I.

In order to validate the use of the fuel properties in Table 3.2, the thermodynamic properties (isentropic coefficient, specific enthalpy, entropy function, dynamic viscosity and the universal gas constant) obtained from NASA CEA were plotted against the diesel fuel and air, since these are already contained in the database and validated for use including its use in Turbomatch software. These results are plotted in figures 1.4-1.8 —Appendix I.

These thermodynamic properties are important in gas turbine calculations because the turbine work output is a function of gas mass flow, isentropic coefficient (Cp or γ) and temperature difference between turbine inlet and outlet. The Cp is a function of temperature, fuel-to-air ratio and water- to-air ratio [Sethi, 2008] and related to specific enthalpy, entropy function, dynamic viscosity and the universal gas constant. Detailed equations representing the relationships between Cp and other thermodynamic properties and how these are applied in NASA CEA code to generate fluid properties as well as in gas turbine performance calculations can be found in [McBride and Gordon, 1996; Gordon and McBride, 1994; Sethi, 2008].

3.2.2 Engine Simulation

Two engines were examined: i) 126 MW gas turbine in open and 375 MW in combined cycle application ii) 22.4 MW gas turbine. These engines were selected to model GE 9E and LM2500 (aero-derivative) engines at base load and were assumed to be co-located at Olorunsogo power plant in Ogun state, Nigeria. As discussed in Chapter 2, a hypothetical location allows the simulation and assessment of engines under site conditions and serves as a framework for modelling power plants situated in a developing economy and warm tropical climate.

Performance analysis was carried out using Turbomatch for the open cycle gas turbine (OCGT)-GX100 (126 MW) and OCGT-GX200 (22.4 MW) engines with schematics as shown in figures 3.1 - 3.2. A short description of Turbomatch is described in sub-section 3.2.2.1. A combined cycle arrangement (GX300) involving two 126 MW gas turbines connected in parallell to two Heat Recovery Steam Generators (HRSGs) and both connected to a steam turbine as illustrated in figure 3.3 was further examined using protocols outlined in section 3.2.2.2.

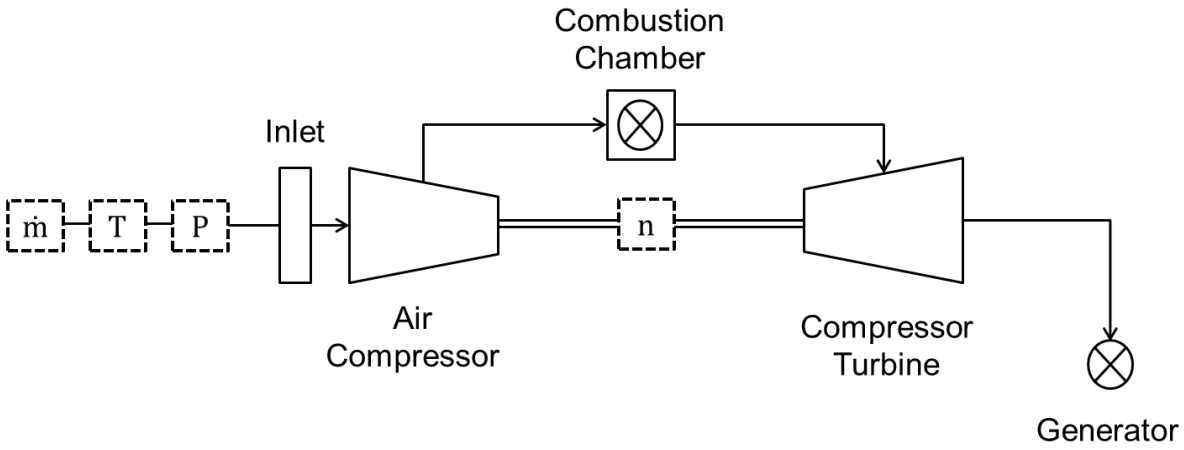

Figure 3.1: Simplified flow diagram of the OCGT-GX100 (126MW at ISO conditions)

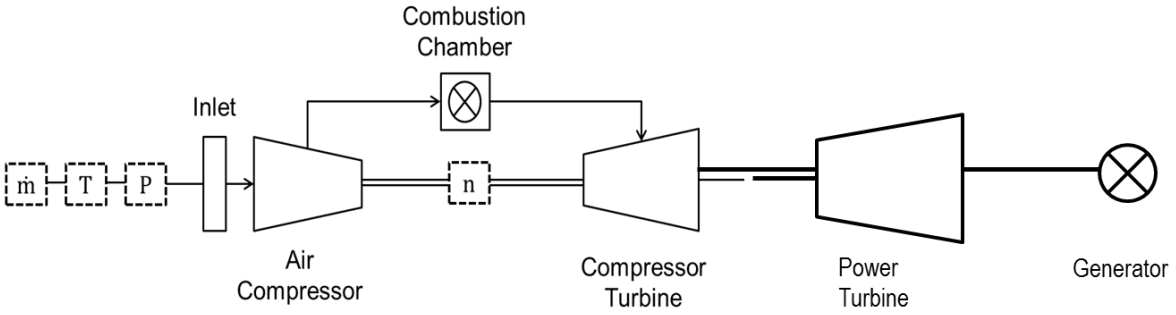

Figure 3.2: Simplified flow diagram of the OCGT-GX200 (22.4 MW at ISO conditions)

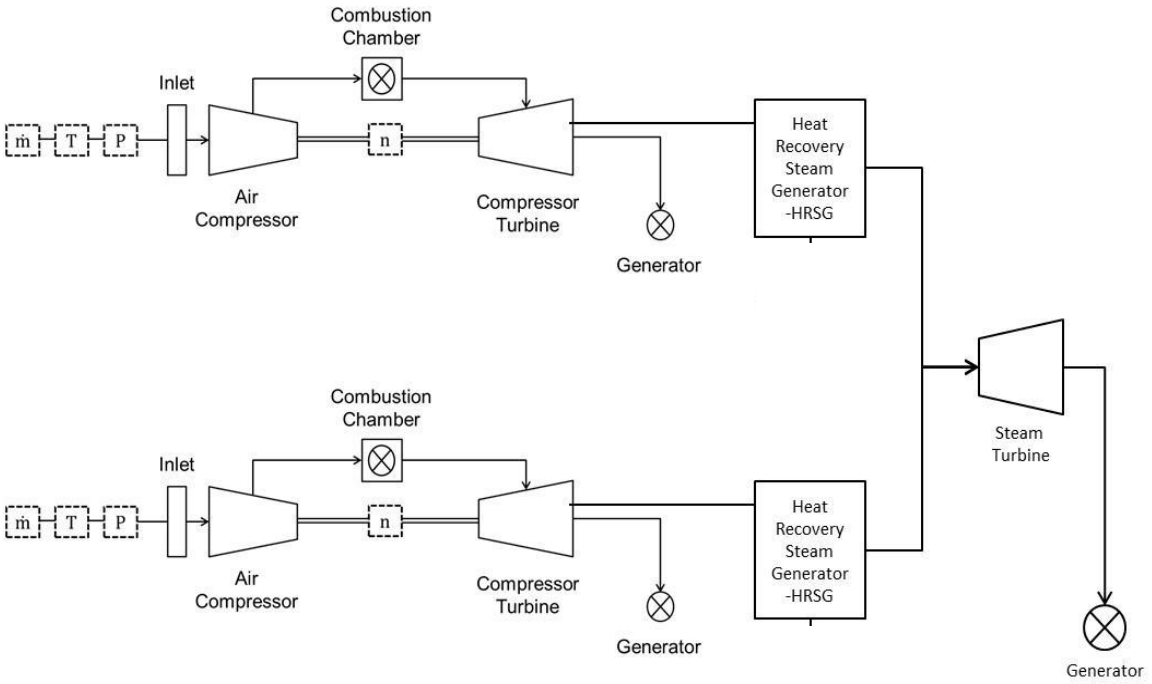

Figure 3.3: Simplified flow diagram of the CCGT-GX300 (754 MW at ISO conditions)

3.2.2.1 OCGT Simulation and Analysis using Turbomatch

Turbomatch is a 0D engine performance model developed at Cranfield University [Palmer, 1967]. It employs sets of FORTRAN routine commands capable of calculating the design point, off-design and transient performance of engines at various operating conditions using basic thermodynamics principles of mass and energy balance. It engages an integrated iterative process for matching engine components while scaling the simulated engine to typical compressor and turbine maps. The user interface allows the modeller to design any gas turbine configuration or schematics such as described in figures 3.1-3.3 with inlet station vectors items and brick data to generate engine vector results. This involve stating the components such as intake, compressor, combustor, turbine and nozzle for the engine configuration in an input file. On carrying out performance analysis, sets of engine vector results such as specific power, specific fuel consumption, and thermal efficiencies were generated. The model has been used for several performance analysis [Yin et al. 2003; Bonet et al. 2010; Nkoi et al. 2013] and validated for use [Palmer, 1967; Macmillan, 1974; Gallar et al. 2012]. A detailed overview and use of this program is described in [Gallar et al. 2012].

The GX100 and GX200 were simulated as single shaft engines in an open cycle arrangement at design point —International Standard Atmospheric (ISA), Sea Level Static condition and at off-design points —varying ambient and operating conditions. In an open cycle arrangement, the power generating unit consist of an intake component, axial compressor, annular combustor, and a compressor turbine, which drives an electric generator. The GX200 is different from GX100 because it consists of a gas generating unit that drives a free power turbine on the same shaft via the use of gearbox. The exhaust mass flow from the gas generating turbine drives the power turbine. The power turbine is then connected to an electrical generator to produce electricity. Figures 3.1-3.2 illustrate how the different components are coupled together to generate shaft power. The parameters used for simulating the engines are presented in Table 3.3.

Table 3.3: Parameters for the simulation of the GX100 and GX200 engines

Parameters	GX100	GX200
Ambient Pressure (kPa)	101.32	101.32
Ambient Temperature (K)	288.15	288.15
Relative Humidity (%)	60	60
Useful Work (MW)	126.1	22.4
Inlet Mass Flow (kg/s)	415	69.90
Pressure Ratio	12.6	18.2
TET (K)	1385	1440
Compressor Isentropic Efficiency (%)	86	86
Turbine/Power Turbine Isentropic Efficiency (%)	88	88
Combustor Efficiency (%)	99	99
Combustor Pressure Loss (%)	5	5

Model assumptions include: i) Isentropic (i.e. adiabatic and reversible) compression and expansion process ii) 100% Mechanical efficiency and negligible kinetic energy of the working fluid at the outlet of each component. iii) Mono-directional flow of the working fluid assumed constant and in an ideal state. iv) No pressure losses within the ducts connecting the components of the engine except the pressure loss that was taken into account in the combustor chamber. v) The above parameters in Table 3.3 were kept constant during the engine simulation of the different fuel types. vi) The TET was kept constant for a fixed power.

3.2.2.2 CCGT Engine Simulation and Analysis

The engine GX300 was simulated as a combined cycle power plant using the basic generating unit of engine GX100 in a 2-2-1 layout as illustrated in figure 3.3. This consists of two generating units, coupled to two heat recovery steam generators and both connected to a downstream steam turbine that drives an electric generator. Here, the waste heat from the exhaust of the gas turbine is recovered in the dual pressure heat recovery steam generator, and the resulting steam is expanded up to condenser pressure and pumped into a deaerator.

In order to calculate the power output and total energy input from the steam (bottoming cycle) of the CCGT, it was important to establish the steam-gas temperature profile. This was achieved using a combination of gas turbine exhaust gas properties, HRSG and steam turbine operating parameters, as listed in Table 3.4a-b. The International Association for the Properties of Water and Steam (IAPWS) IF-97 steam tables [Wagner and Kruse, 1998], which contain properties such as steam enthalpy, specific volume, specific density, specific heat capacity, and viscosity for water, saturated and superheated steam, were used to define the saturation temperatures at HRSG operating pressures and the temperature profile of the HRSG. The following protocols (equations 3.1-3.30) were used for calculating the performance of the GX300 engine at a single operating (simulated design) point.

Table 3.4: Parameters for the simulation of the GX300 engine operating on natural gas

Components	Parameters	GX300
Gas Turbine		
	Ambient Pressure (kPa)	1.013
	Ambient Temperature (^oC)	15
	Relative Humidity (%)	60
	Useful Work (MW)	126.1
	Inlet Mass Flow (kg/s)	415
	Pressure Ratio	12.6
	TET (K)	1385
	Compressor Isentropic Efficiency	86
	Turbine Isentropic Efficiency	88
	Combustor Efficiency	99
	Combustor Pressure Loss (%)	5
HRSG		
	Inlet Gas Temperature, T_1 (^oC)	566.52
	Inlet Gas Mass Flow Rate, M_G (kg/s)	423.1
	Inlet Feed water Temperature, T_8 (^oC)	32.88
	HP Steam Pressure, P_1 (Bar)	97
	LP Steam Pressure, P_2 (Bar)	2
	Steam Limiting Temperature, T_{17} (^oC)	560
	HRSG Pinch Point, PP	5
	HRSG Approach Point, AP	2
	Heat Effectiveness, η_{HE}	98
	Gas Specific Heat Capacity, C_p	1193
	Condenser Pressure, P_3 (Bar)	0.05
	Boiler Feed Pump Isentropic Efficiency (%)	80
Steam Turbine		
	Steam Turbine Isentropic Efficiency, η_S (%)	88
	Minimum Allowable Stack Temperature (^oC)	100
	Minimum Steam Quality (%)	88

Further model assumptions aside those made during gas turbine simulation include: a) Negligible pressure drop in HRSG, de-aerator and condenser. b) Negligible heat loss in the HRSG, turbines, condenser and de-aerator. c) Maximum temperature of steam cycle is 560^oC. d) Identical gas turbines and HRSGs and steady state process and flow through the gas turbines, HRSGs and steam turbines.

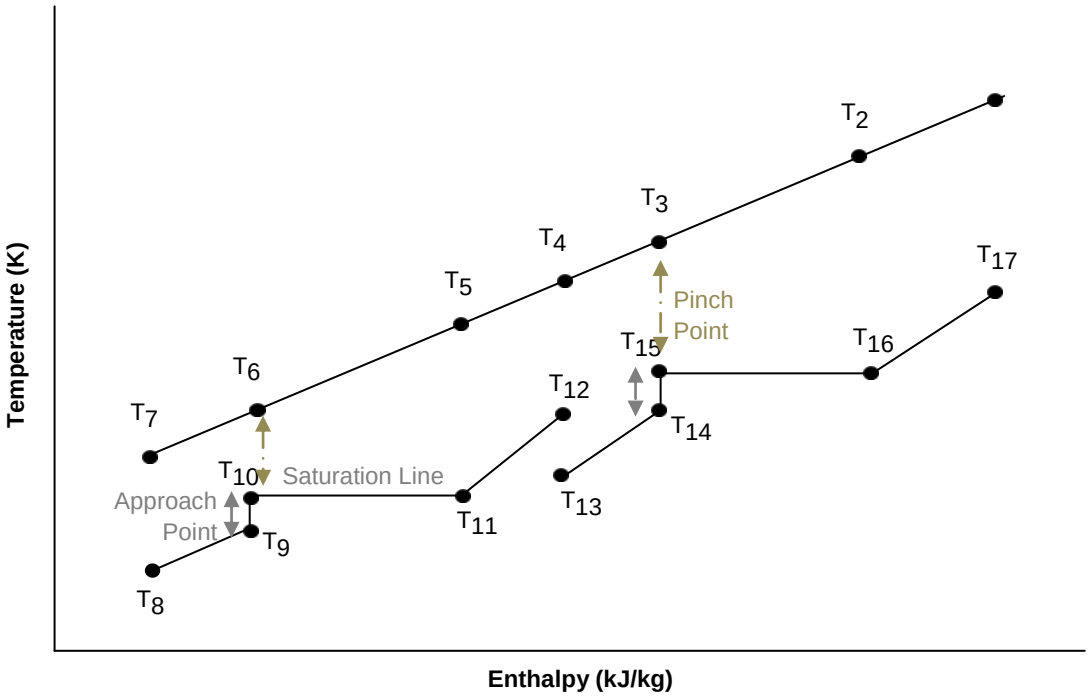

a) Temperature entropy diagram of a dual pressure HRSG

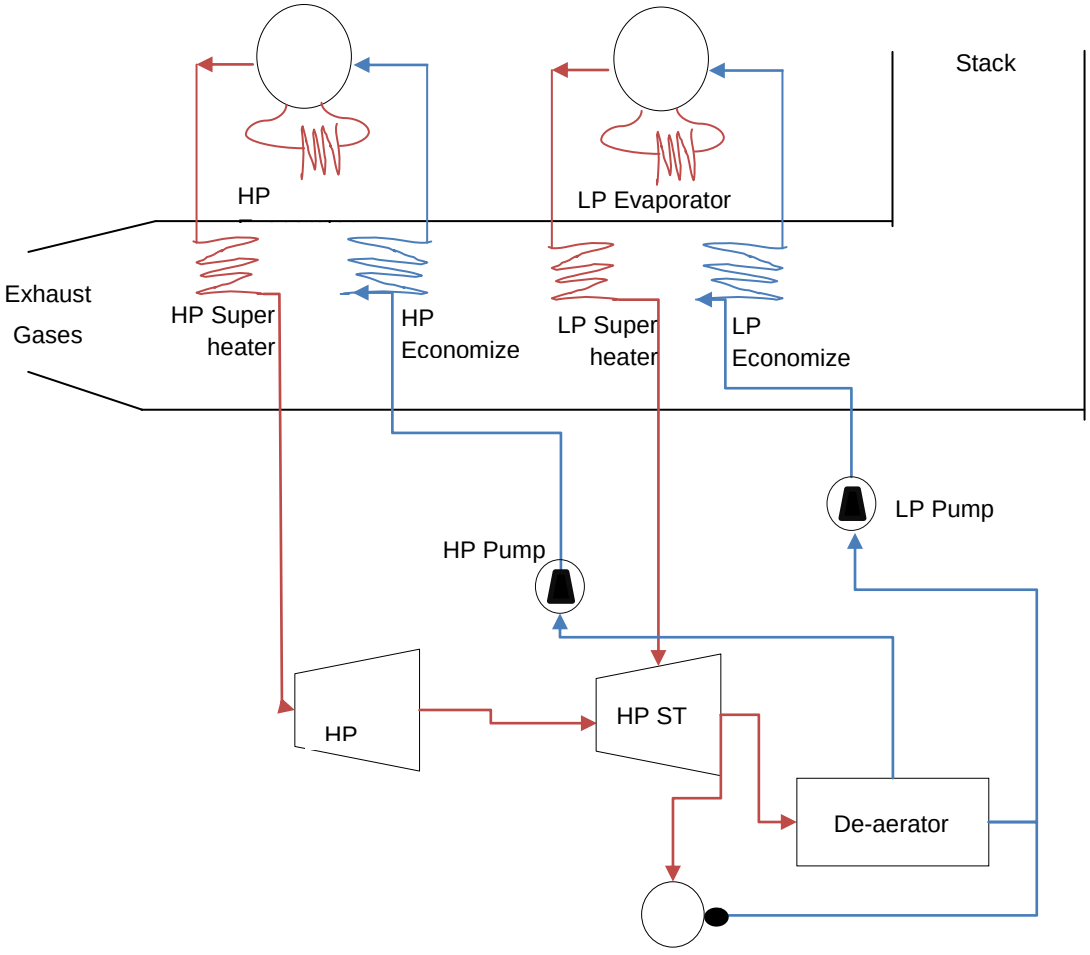

b) Schematic of a Dual Pressure HRSG

Figure 3.4: Temperature entropy diagram and a simplified flow diagram of Dual Pressure HRSG. a) Temperature entropy diagram of a dual pressure HRSG. b) Schematic of a Dual Pressure HRSG

HRSG Temperature Profile Calculations

Saturation Temperature, T_{15} @ P_1 (3.1)

Temperature of feed water entering the HP evaporator, $T_{14} = T_{15} - AP$ (3.2)

Temperature of gas leaving the HP evaporator, $T_3 = T_{15} + PP$ (3.3)

$Q_1 = M_G C_P (T_1 - T_3) \eta_{HE}$ (3.4)

$M_{S1} = Q_1 / (h_{17} - h_{14})$ (3.5)

Temperature of gas entering the HP evaporator, $T_2 = T_1 - [M_{S1} (h_{17}-h_{14}) \eta_{HE} / M_G C_P]$ (3.6)

Temperature of feed water entering the HP economizer, $T_{13} = T_{10}$ (3.7)

Temperature of steam leaving the LP super heater, $T_{12} = T_{14}$ (3.8)

Saturation Temperature, T_{10} @ P_2 (3.9)

Temperature of feed water entering the LP evaporator, $T_9 = T_{10} - AP$ (3.10)

Temperature of steam leaving the LP evaporator, $T_6 = T_{10} + PP$ (3.11)

$Q_2 = M_G C_P (T_4 - T_6) \eta_{HE}$ (3.12)

$M_{s2} = Q_2 / (h_{12} - h_9)$ (3.13)

Temperature of gas entering the LP economizer, $T_5 = T_4 - [m_{S2} (h_{12}-h_9) \eta_{HE} / M_g C_p]$ (3.14)

Temperature of gas leaving the LP economizer, $T_7 = T_6 - [m_{S2} (h_9-h_8) \eta_{HE} / M_g C_p]$ (3.15)

Heat exchanged in HP Superheater, $Q_{HPS} = m_{S1} (h_{17} - h_{16})$ (3.16)

Heat exchanged in HP Evaporator, $Q_{HPEV} = m_{S1} (h_{16} - h_{14})$ (3.17)

Heat exchanged in HP Economizer, $Q_{HPEC} = m_{S1} (h_{14} - h_{13})$ (3.18)

Heat exchanged in LP Superheater, $Q_{LPS} = m_{S2} (h_{12} - h_{11})$ (3.19)

Heat exchanged in LP Evaporator, $Q_{LPEV} = m_{S2} (h_{11} - h_9)$ (3.20)

Heat exchanged in LP Economizer, $Q_{LPEC} = (m_{S1} + m_{S2}) (h_9 - h_8)$ (3.21)

HRSG Heat Input = $Q_{HPS} + Q_{HPEV} + Q_{HPEC} + Q_{LPS} + Q_{LPEV} + Q_{LPEC}$ (3.22)

Work done by pump, $W_P = v_1 (P_2 - P_3)/n_P + v_1 (P_1 - P_2)/n_P$ (3.23)

Work of Expansion, HP Steam Turbine, $W_{HPST} = m_{S1} (h_{17} - h_{10}) \eta_{ST}$ (3.24)

Work of Expansion, LP Steam Turbine, $W_{LPST} = (m_{S1} + m_{S2}) (h_{11} - h_C) \eta_{ST}$ (3.25)

Net Steam Cycle Output, $W_{NET} = \eta_S (W_{HPST} + W_{LPST}) - W_P$ (3.26)

Steam Thermal efficiency, $\eta_{ST} = W_{ST}$/ HRSG Heat Input (3.27)

Overall Plant Heat input, $HI = M_F N_O LHV \eta_{CC}$ (3.28)

Overall Plant Output, $W_O = (W_G * N_O) + W_{NET}$ (3.29)

Overall Plant Efficiency = W_O/HI (3.30)

Where:

h_{17} is the enthalpy of superheated steam at P_1 and T_1
h_{14} is the enthalpy of feed water entering the HP evaporator at T_{14}
M_{S1} is the HP steam mass flow rate in kg/s
Q_1 is the heat energy from the gas used to heat steam in HP at or above T_{14}
h_{16} is the enthalpy of saturated vapour at pressure, P_1
h_{12} is the enthalpy of superheated steam at P_2 and T_{12}
h_9 is the enthalpy of feed water entering the LP evaporator at T_9
M_{S2} is the LP steam mass flow rate in kg/s
Q_2 is the heat energy from the gas used to heat steam in LP at or above T_9
h_{11} is the enthalpy of saturated vapour at pressure, P_2
h_8 is the enthalpy of feed water entering the economizer at T_8, condenser pressure
v_1 is specific volume of feed water
h_{18} is the enthalpy of condensation of water vapour
W_{ST} is the work of expansion through the steam turbine
M_F is gas turbine fuel flow rate
N_O is number of gas turbines
W_G is gas turbine power output
h_C is the enthalpy of evaporation

Based on the above equations, the gas-steam temperature-enthalpy profile for engine GX300 operating on natural gas at design point is summarized in Table 3.5.

Table 3.5: Gas-Steam Temperature-Enthalpy Profile for Engine GX300

Points	Parameters	Temperature (^oC)	Specific Enthalpy (kJ/kg)
T_1	Inlet Gas Temperature	566.5	3545.9
T_2	Gas entering the HP evaporator	474.4	3436.0
T_3	Gas leaving the HP evaporator	306.8	1394.8
			1273.8
T_5	Gas entering the LP evaporator	280.6	-
T_6	Gas leaving the LP evaporator	118.2	-
T_7	Gas leaving the LP economizer	100.0	1242.6
T_8	Inlet feed water Temperature	32.9	137.8
T_9	Feed water entering the LP evaporator	118.2	496.2
T_{10}	LP Saturation Temperature @ P_2	120.2	3085.8
T_{11}	Steam leaving the LP evaporator	-	2706.2
T_{12}	Steam leaving the LP super heater	306.8	3085.8
		120.2	504.7
T_{14}	Feed water entering the HP evaporator	306.8	1382.8
T_{15}	HP Saturation Temperature @ P_1	308.8	-
T_{16}	Steam entering the HP super heater	-	2730.9
T_{17}	Steam leaving the HP super heater	559.5	3528.6

Similar analyses were carried out for the different fuels using the parameters obtained from their respective gas turbine performance simulations, and assuming the following:

1. Negligible pressure drop in the HRSG, de-aerator and condenser.
2. Negligible heat loss in the HRSGs, turbines, condenser and de-aerator.
3. Maximum temperature of the steam cycle remains 560^oC.
4. Identical gas turbines and HRSGs as the natural gas case, apart from properties that changed with the use of the fuels such as inlet gas temperature, inlet gas mass flow, gas specific heat capacity etc.
5. Steady state process and flow through the gas turbines, HRSGs and steam turbines.
6. Fuel effects are only accounted for in the gas turbines. That is, only primary fuel effects on the gas turbines were considered in the HSRGs and steam cycles. This is a reasonable assumption because the primary location for combustion is in the gas turbine, and this CCGT case has no reheat capacity.

3.3 Results & Discussion

3.3.1 Validation Analysis: Engine Performance at Design Point

The engine, GX100 and GX200 were modelled after the GE Frame 9E Heavy Duty and LM2500 Base (Aero-derivative) gas turbines respectively. Thus, the performance results as shown in Table 3.6 to 3.8 for GX100, GX200 and GX300 engines are compared with public data [GE 2014 a, b)].

Table 3.6: Comparison between GX100 and Reference Engine GE 9E

Parameters	GE 9E (Power Generation)	Simulated Engine GX100	Standard Error (S.E) %
Mass Flow (kg/s)	418	423.1	+1.2
Exhaust Gas Temperature (K)	816	839.5	+2.8
η_{th} -Thermal efficiency (%)	34	34.1	+0.3
Heat Rate (kJ/kWh)	10653	10928	+2.5

[a] Thermal Efficiency: above 34%; Performance @ISO nominal rating: Temperature-15°C, Sea Level Static, Relative humidity-60%; Negligible exhaust and inlet pressure losses; Negligible accessory losses; Natural gas with LHV = 47.141 MJ/kg; TET – 1385 K; Useful Work -126.1 MW; Pressure Ratio-12.6

Table 3.7: Comparison between GX200 and Reference Engine LM2500 (Base)

Parameters	LM2500 (Power Generation)	Simulated Engine GX200	Standard Error (S.E) %
Mass Flow (kg/s)	69.8	71.2	-2.0
Exhaust Gas Temperature (K)	811	812.7	-0.2
η_{th} -Thermal efficiency (%)	35[b]	36.6	-4.4
Heat Rate (kJ/kWh)	10146	10172	-0.3

[b] Thermal Efficiency range: 34-36% (average of 35%); Performance @ISO nominal rating: Temperature -15°C, Sea Level Static, Relative humidity -60%; Negligible exhaust and inlet pressure losses; Negligible accessory losses; Natural gas with LHV = 47.141 MJ/kg; TET – 1440 K; Useful Work -22.4 MW; Pressure Ratio-18.2

Table 3.8: Comparison between GX300 and Reference Engine GE 9E CCGT (2-2-1)

Parameters	GE 9E (Power Generation)	Simulated Engine GX300	Standard Error (S.E) %
Net Plant Output (MW)	391.40	380.57	-2.77
Net Plant Efficiency (%)	52.70	50.21	-3.44

The performance results for engine GX100, as shown in Table 3.6 have a standard error of less than 3% for exhaust mass flow, exhaust gas temperature (EGT), heat rate and thermal efficiency. The results for engine GX200 —Table 3.7, have a standard error (S.E.) of less than 2% for all parameters except thermal efficiency (S.E. of 4.4%) while both parameters in Table 3.8 have a S.E. of less than 3.5%.

Since, a thermal efficiency range of 34-36% is reported in literature, the thermal efficiency of engine GX200 compares favourably, when compared to a thermal efficiency of 36%. Overall, the results obtained from the performance analysis at design point for

the three engines are within the range for typical engines and validate the use of the engine models for further fuel analysis and at off-design conditions.

3.3.1.1 Engine Performance at Off-Design Conditions

The effect of ambient temperature on specific (sp.) shaft power and thermal efficiency is shown in figure 3.5.

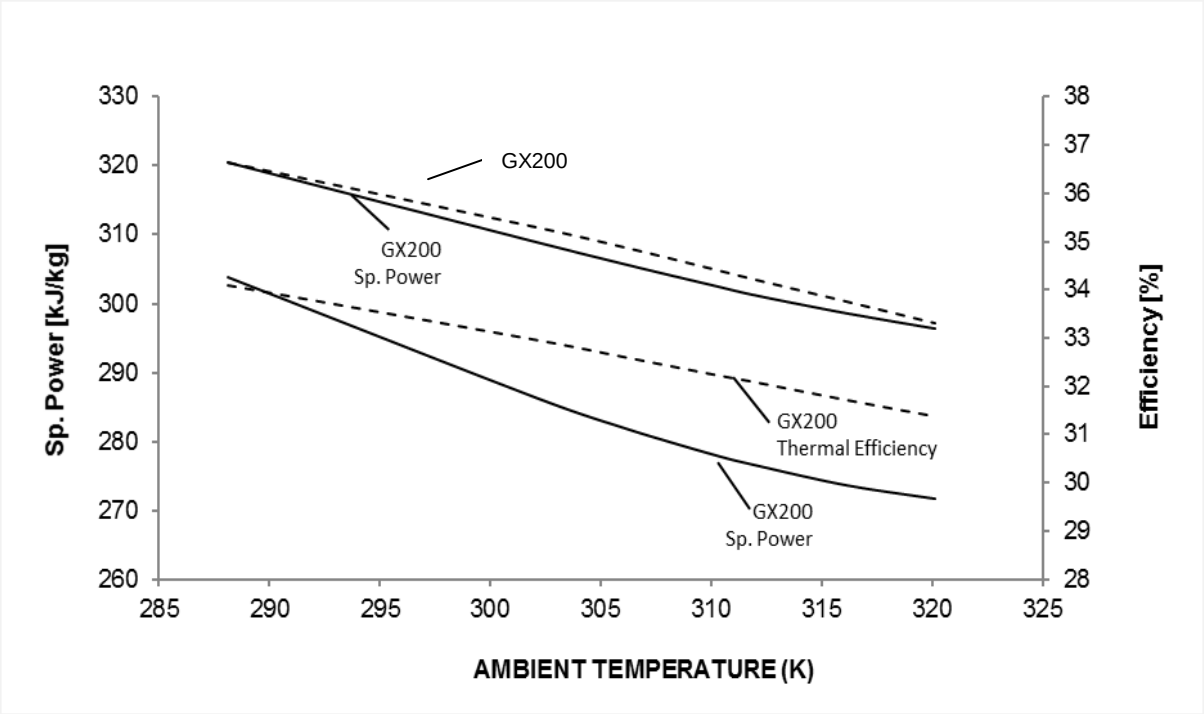

Figure 3.5: The effect of ambient temperature (K) on specific shaft power and engine thermal efficiency

The results in figure 3.5 show a trend of reduction in specific power and efficiency as ambient temperatures increase for both engine cases. These results are in agreement with what is expected of off-design performance of gas turbines in the event of changing ambient temperatures. Meher-Homji et al. [2001] reported an ideal reduction in power output between 0.3% and 0.5% for every degree Fahrenheit rise in ambient temperature. Basha et al. [2012] reported a reduction in power output of 0.5% to 0.9% drop for every 1^{o}C rise in temperature. Similar trends are reported in [Alhazmy and Najjar, 2004; Mohanty and Palaso Jr., 1995; Kakaras et al. 2006].

This analysis reports a reduction in specific power up to 0.35% for every 1^{o}C rise in ambient temperature for both engines, a resulting effect of decreasing compressor delivery pressure as the temperature of the working fluid (air) increases. Also, the density of the air flowing through the engine decreases and this reduces the rate of flow of air through the engine. Hence, the engine operates at lower pressure ratio and non-

dimensional mass flow, and thermal efficiency and specific output decreases as a result. The thermal efficiency is worsened because more fuel is consumed in order to maintain the engine's TET. On a relatively cold day, this relationship is inverted, as the engine moves along the line to a higher non-dimensional speed, hence higher pressure ratio and non-dimensional mass flow, supported by the effect of air getting colder and relatively high air density, to yield higher mass flow.

Ambient temperatures significantly affect engine performance; hence the above analysis is of importance. The range of temperature of 288 K and 318 K has been selected because the average monthly temperature in Nigeria ranges between 15^{o}C and 45^{o}C while the average monthly temperature in Ogun-state and around the case study location ranges from 23^{o}C in July to 33^{o}C in February [Akinbode et al. 2011].

The effect of altitude & ambient pressure on specific shaft power and thermal efficiency is shown in figures 3.6 and 3.7.

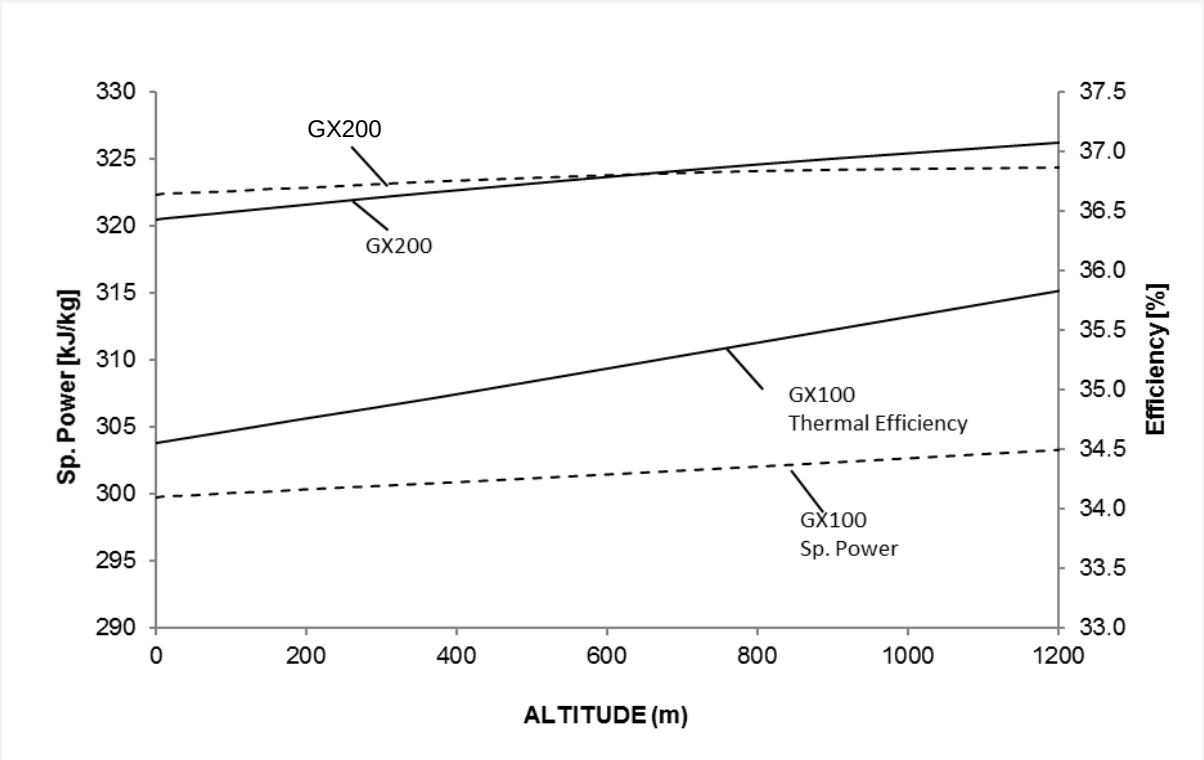

Figure 3.6: The effect of altitude (m) on specific shaft power and engine thermal efficiency

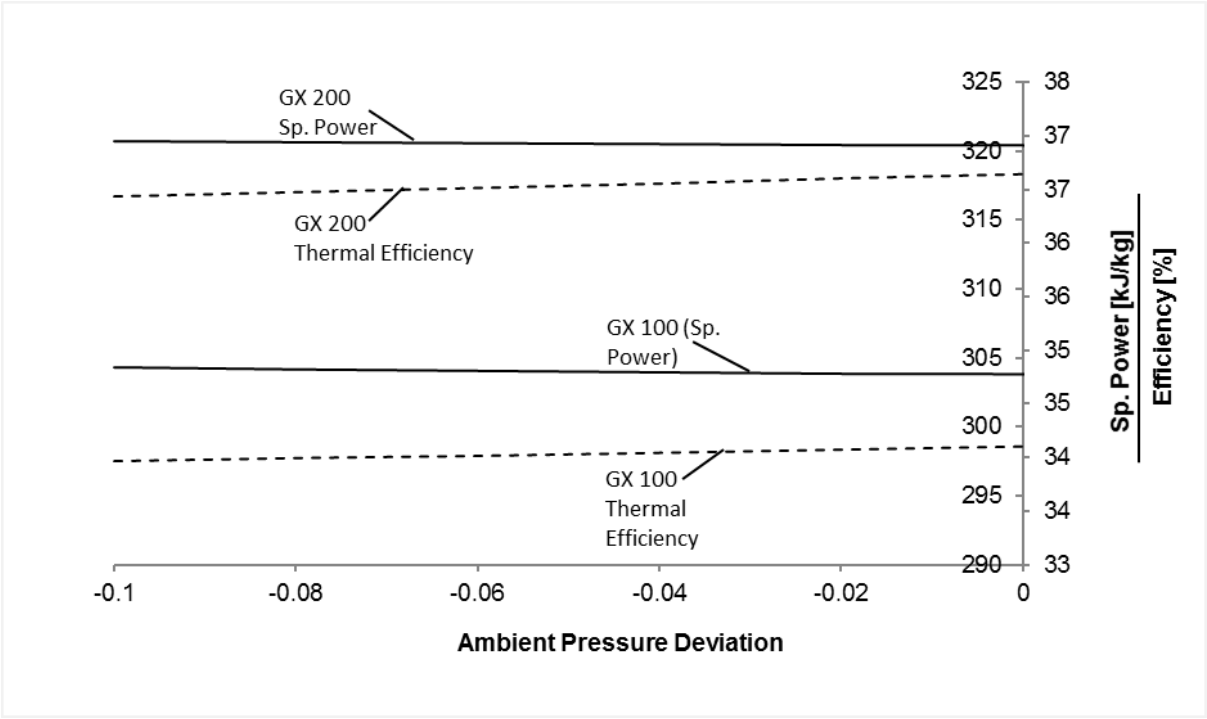

Figure 3.7: The effect of ambient pressure (Bar) on specific shaft power and engine thermal efficiency

Due to the location of interest and the country used for this study, a range of ambient pressures of 0.9 to 1 bar that correspond to a pressure altitude of 0 m to approx. 829 m were examined. The results in figure 3.6 show an increase in specific power and efficiency as site elevation increases. This is supported by a slight increase in specific power but with decrease in thermal efficiency at reduced ambient pressures (see figure 3.7). This was applicable for both engine cases.

At relatively high altitude or lower ambient pressures, the decreasing air density causes a decrease in engine shaft power; however, the increasing specific power is as a result of a non-dimensional effect of ambient conditions on the engine. At higher altitudes up to 11 km, the ambient static temperature and pressure as well as the air density falls. As a result of these decreasing ambient static pressures, there is decrease in mass flow going through the engine. This effect on mass flow is however counteracted by lower ambient temperatures. Here, the engine behaves as if $\{N/T_1\}$ is increasing with altitude because of the reduced ambient temperature [Palmers and Pachidis, 2005], consequently increasing the pressure ratio, mass flow, thermal efficiency and specific power of the system altitude. In order words, any ambient condition that promotes a decrease in the pressure of the air going through the engine would limit shaft power, and thermal efficiency, except there are dominant effects of reduced temperature as found in the case of relatively high site elevation. These results validate the use of the models at different site elevations and/or changing ambient pressures, as they are in agreement

with what is observed [Brooks, 2006]. Typically, the altitude in Nigeria is at most 1295 m [Chineke, 2009, however, the power plants are assumed to be co-located at Olorunsogo power plant in Ogun state, Nigeria with site elevation of 75 m.

The effect of relative humidity on specific shaft power and thermal efficiency is shown in figure 3.8.

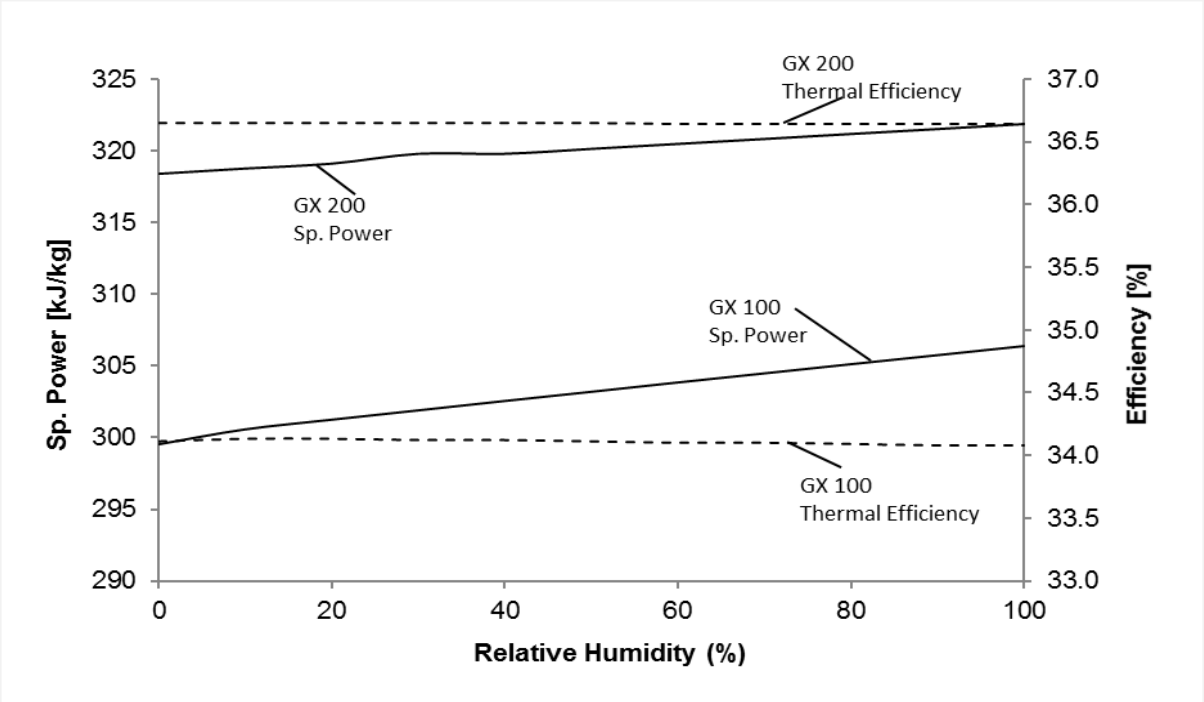

Figure 3.8: The effect of relative humidity (%) on specific shaft power and engine thermal efficiency

The results in figure 3.8 show an increase in specific power and fairly small but near negligible improvement in thermal efficiency as relative humidity increases for both engine cases. These trends are expected in the event of increasing relative humidity [Walsh and Fletcher, 1998; Brooks, 2006] for a flat rated engine or engine controlled by fixed TET, since high relative humidity directly influences the flow of air entering the engine. The cooling or condensation effect of water on air at relatively hot temperatures affect the density, gas constant and heat capacity of the air flowing through the engine. The slight increase in density and reduced temperature of the air increases the rate of flow of air through the engine, hence more power. This cooling effect could however have negative impact on performance in certain engines at low temperatures, where it forces air to reach near freezing condition. For other modes of operation or control systems, the effect of relative humidity is said to be complex and diverse [Meher-Homji et al. 2011; Brooks, 2006; Kurz and Brun 2001]. The net effect of changing relative humidity is less pronounced on thermal efficiency than for specific power because it affects the overall output of the engine rather than component efficiencies. Also, the effect of

relative humidity is considered negligible below temperatures of 0^{o}C and above 40^{o}C and of least importance among the ambient conditions that affect gas turbine performance, but greatly affect engine emission performance [Walsh and Fletcher, 1998; Lefebvre and Ballal, 2010]. Since, the average relative humidity of the location of interest varies from 40% to 90% [Eludoyin et al. 2014; Ayanda et al. 2013], the above results validate the use of the models at these conditions.

The effect of load on sp. shaft power and thermal efficiency is shown in figure 3.9.

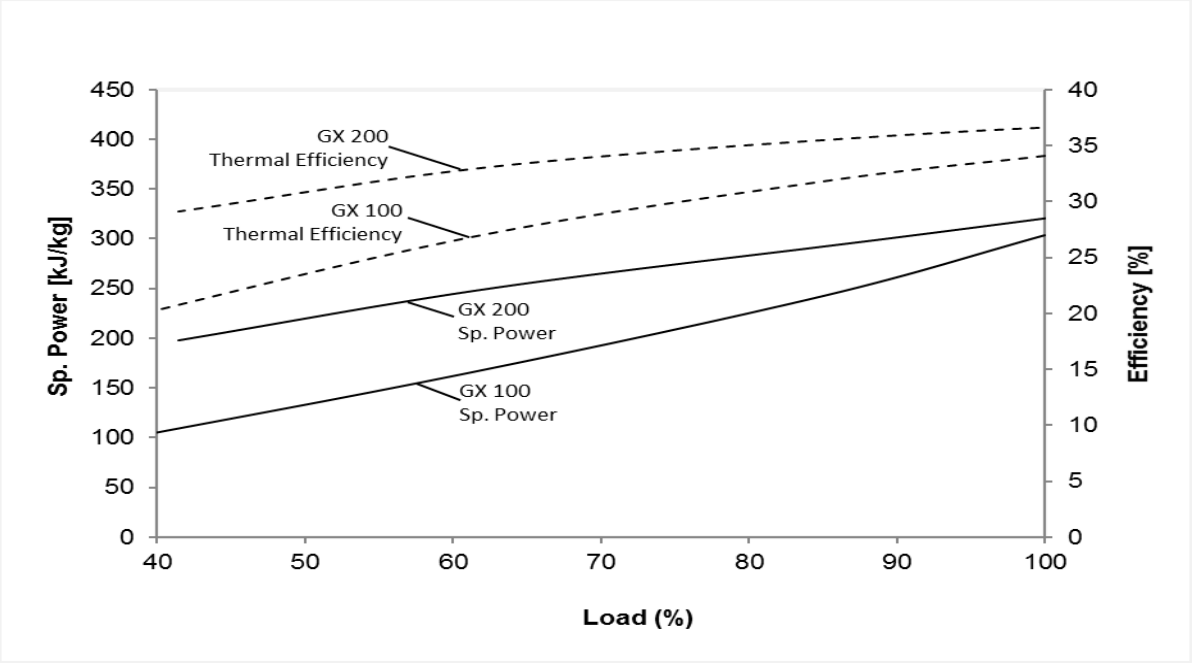

Figure 3.9: The effect of load (%) on specific shaft power and engine thermal efficiency

The effects of load on specific power and engine thermal efficiency are similar in both engine cases (see figure 3.9). The results show that there is a reduction in specific power and engine thermal efficiency as load reduces. In a single shaft engine as GX100, the engine operates at a fixed speed with the load; hence a reduction in load would trigger a reduction in fuel flow, followed by a reduction in firing temperature. Rapidly, the engine balances by moving to a new operating line on the fixed speed line with a lower compressor pressure ratio, reduced mass flow but worse component efficiency. Although fuel flow is reduced, more fuel is consumed in order to compensate for the new operating point.

3.3.2 Fuel Analysis

It can be deduced from Table 3.2 that both biodiesels used in this study have a carbon and hydrogen mass composition of about 76%, 12% and 12% and LHV that is less than 10000 kcal/kg. These are similar to values reported by Wilson et al. [2007], which showed that the carbon content of four biodiesels varied between 76.8% and 77.5% while the hydrogen content were about 12.6% to 12.8% and the oxygen content was nearly in the range of 9.4% and 9.9%. The carbon and hydrogen mass composition for natural gas and diesel fuel on the other hand are 75% and 25%, and 87% and 13%, assuming the fuel compositions are CH_4 and $C_{12.74}H_{23.8}$ respectively with LHV of above 10000 kcal/kg (see Table 3.9 footnote). With varying fuel compositions, the engine performance for engine GX100-300 is expected to vary for the different fuels. The results are presented in Table 3.9 to 3.11.

3.3.2.1 Open Cycle Application

Table 3.9: Design Point Fuel Performance Analysis of Engine GX100

Parameters	Reference Fuel Natural Gas	Conventional Diesel	Microalgae Biodiesel	Jatropha Biodiesel
Useful Work (MW)	126.1	126.1	126.1	126.1
Exhaust Mass Flow (kg/s)	423.1	423.5	425.9	424.4
Exhaust Gas Temperature (K)	839.5	832.9	841.8	837.3
η_{th} -Thermal efficiency (%)	34.10	34.71	34.28	34.47
Heat Rate (kJ/kWh)	10928.0	10426	10501	10443
Specific Equivalent Power	129.8	126.5	129.1	128.2

Performance @ISO nominal rating: Temperature-15°C, Sea Level Static, Relative humidity-60%; negligible exhaust and inlet pressure losses; negligible accessory losses; LHV-: Natural Gas-11259 kcal/kg; Diesel-10167.6 kcal/kg; Jatropha biodiesel-8071 kcal/kg; microalgae biodiesel-9250 kcal/kg; TET – 1385 K; Useful Work -126.1 MW; Pressure Ratio-12.6

At fixed TET, the results in Table 3.9 show that there is an increase in engine thermal efficiency by 0.5%, 1.1% and 1.8% for the use of microalgae biodiesel, Jatropha biodiesel and conventional diesel and in comparison to the reference fuel. These are supported with a reduction in heat rate by 3.9%, 4.4% and 4.6% using microalgae biodiesel, Jatropha biodiesel and conventional diesel fuels respectively. Similarly, the exhaust gas temperatures reduced by 0.26% and 0.79% for Jatropha biodiesel and conventional diesel respectively, however, resulted in an increase in exhaust gas temperature of 0.27% for microalgae biodiesel. The exhaust mass flow increased for all the liquid fuels with the least involving the use of conventional diesel, followed by Jatropha biodiesel, then microalgae biodiesel fuel. This is due to the differences in the LHV of the fuels that necessitated an increase in exhaust mass flow to enable the engine reach the required temperature.

Table 3.10: Design Point Fuel Performance Analysis of Engine GX200

Parameters	Reference Fuel Natural Gas	Conventional Diesel	Microalgae Biodiesel	Jatropha Biodiesel
Useful Work (MW)	22.4	22.4	22.4	22.4
Exhaust Mass Flow (kg/s)	71.2	71.3	71.7	71.5
Exhaust Gas Temperature (K)	812.7	805.0	815.3	810.1
η_{th} -Thermal efficiency (%)	36.64	37.34	36.84	37.06
Heat Rate (kJ/kWh)	10172	9642	9773	9715
Specific Equivalent Power (MW)	23.39	23.14	23.3	23.23

Performance @ISO nominal rating: Temperature-15°C, Sea Level Static, Relative humidity-60%; negligible exhaust and inlet pressure losses; negligible accessory losses; LHV-: Natural Gas-11259 kcal/kg; Diesel-10167.6 kcal/kg; Jatropha biodiesel-8071 kcal/kg; microalgae biodiesel-9250 kcal/kg; TET – 1440 K; Useful Work -22.4 MW; Pressure Ratio-18.2

Similar trends as in the case of engine GX100 were observed for engine GX200 (see Table 3.10), however with further deviations in EGTs. The was an increase in EGT by 0.32% for microalgae biodiesel when compared to the natural gas case while a reduction in EGTs of both conventional diesel and Jatropha biodiesel with values of 0.95% and 0.32% respectively. Exhaust mass flow rates increased by 0.09%, 0.31% and 0.64% for utilizing conventional diesel, Jatropha biodiesel and microalgae biodiesel respectively. And thermal efficiency increased by 0.55%, 1.15% and 1.91% when microalgae biodiesel, Jatropha biodiesel and conventional diesel fuel were utilised. In order words, the performance of the smaller (22.4 MW) gas turbine was better in terms of fuel performance than the heavy duty engine (126 MW), although this conclusion has not considered fuel economy or cost per MW produced.

Considering the engine performance results obtained above, the conventional diesel fuel had a better fuel performance among the liquid fuels and against the reference fuel in an open cycle application, since it produced the highest engine thermal efficiency and lowest heat rate. This conclusion is however incomplete without considering the equivalent power that could be derived from a kg of fuel. In this analysis, the specific equivalent shaft power that could be derived from the use of natural gas is 2.5% higher than that of conventional diesel, however, just 0.6% and 1.3% higher for engine burning microalgae and Jatropha biodiesel respectively.

Meher-homji et al. [2010] reported that gas turbines operating on natural gas will produce a range between 2% and 3% of power output more than engines using distillate oil. This higher specific output for engine burning natural gas is resulting from the much higher hydrogen-to-carbon (H/C) ratio of the natural gas. In the study, the natural gas is

assumed to be primarily composed of methane, and has a hydrogen content that is about one-third of the mixture while the hydrogen content of both biodiesels are less than one-fifth. Here, the hydrogen composition accounts for 25% in natural gas, 13.51% in microalgae biodiesel, 13.49% in Jatropha biodiesel and 13.47% in the conventional diesel fuel. These differences in the hydrogen contents explain the relatively higher specific equivalent shaft power obtained for natural gas and microalgae biodiesel in Table 3.9. And although, there is a larger amount of energy from a unit mass of fuel for natural gas than other fuels, considering the LHV of the fuels, this is counterbalanced by the relative large amount of fuel that is added into the system to compensate for the energy required from the lower LHV fuels. The LHV of both biodiesel fuels in this analysis were relatively low (range of 33-39 MJ/kg) while that of diesel fuel and natural gas are about 43 MJ/kg and 47 MJ/kg respectively. This has a major impact on fuel consumption rate. Thermal efficiency and heat rates slightly improve in both analyses in Table 3.9 and 3.10 for the biodiesels because of the chemical composition of these fuels. The biodiesel fuels are at an advantage because of their oxygen and higher carbon content. This contributes to engine fuel performance because more water vapour and CO_2 are produced, consequently, higher specific heat capacity of the combustion products, more mass flow through the engine and relatively more specific power output. Also, the oxygen content improves combustion by enhancing more conversion to CO_2. The same applies to conventional diesel fuel, although it has no additional fuel oxygen element, it is at a better advantage over the biodiesel fuels, because of its higher LHV.

In order words, the engine operating on natural gas will produce a higher specific equivalent power than other fuels. However, the biodiesels will give a better performance than natural gas due to a combination of higher carbon and oxygen content of the fuels as well as energy concentration in a mass of fuel, but much less performance to conventional diesel fuel due to their relatively lower LHV.

In summary, the performance results show that Jatropha biodiesel is a considerable alternative to conventional diesel, since it has a close performance characteristics to conventional diesel with added renewable advantage. This could imply that existing and future power plants do not require engine modifications and engine user do not necessary require operational changes to operate the fuel in the engine. In comparison to natural gas, Jatropha biodiesel could favourably substitute natural gas because it brought about a higher thermal efficiency and lower heat rate for relatively the same amount of power. The effects on engine components and durability, however requires assessment.

The microalgae biodiesel is also at advantage under fuel economy considerations, because it could yield more specific power per kg of fuel combusted than any other liquid fuel examined in this study, however at the detriment of engine health. For combined cycle applications, microalgae biodiesel could be a better choice because it gives rise to a higher exhaust mass flow and exhaust gas temperature. If the exhaust gas temperature is within the limit for the HRSGs and steam turbines, the performance loss in the gas generator could be compensated in the bottoming cycle of the power plant. This is further investigated and results presented in section 3.3.2.2.

3.3.2.2 Combined Cycle Application

Table 3.11: Design Point Fuel Performance Analysis of Engine GX300

Parameters	Reference Fuel Natural Gas	Conventional Diesel	Microalgae Biodiesel	Jatropha Biodiesel
Useful Work (MW)	380.57	383.36	380.66	378.85
Net plant efficiency (%)	50.21	53.30	52.27	52.31

The results in Table 3.11 showed that the conventional diesel fuel gave a better fuel performance that is, yielded more useful work and better net plant efficiency than all the other fuels. However, microalgae biodiesel was a better choice of renewable fuel for combined cycle application in terms of power output, but the thermal efficiency was slightly below that of the Jatropha biodiesel fuel.

There are risks associated with lower LHV fuels including biodiesels because of their tendency to move the engine running line towards higher pressure ratios, and firing temperature. Silva et al. [2013] have demonstrated the importance of employing control strategy such as air bleeds and guide vanes in the events of utilizing relatively LHV fuels. Meher-homji et al. 2010 also showed how power correction factor could be applied to engines operating on fuels with lower heating value and containing inert gases and varying carbon to hydrogen ratio. This is important to ensure safe operation of the gas turbine. This has been demonstrated with engine GX200. In this analysis, the use of both biodiesel fuels resulted in a shift in operating line and a slight reduction in surge margin for the gas turbine compressor (see figure 1.9—Appendix I). This occurs because the fuel control system forces the fuel flow rates to be significantly increased in order to compensate for the energy required to reach the engine's firing temperature.

3.3.3 Fuel Performance Analysis at Off Design Conditions

3.3.3.1 Fuel Performance Analysis at Varying Turbine Entry Temperature (TET)

To maintain a constant exit temperature and to preserve blade life, fuel control systems in actual gas turbines are designed to vary the engine's firing temperature. The effect of TET has been examined on specific power, thermal efficiency, exhaust gas temperature and exhaust mass flow using the four different fuels for engine GX100 and GX200. These are illustrated in figures 3.10-3.12 for comparison.

At reduced TET, thermal efficiency reduced and the heat rate got worse across all the fuels. There were slight differences similar to those stated in section 3.3.2 among the different fuel types. There was a loss of efficiency of nearly 30% at TET of 1220K across for engine GX100 operating on natural gas, but much improved using the liquid fuels than natural gas. Here, the percentage deviation ranged from 3.4% (Microalgae biodiesel), 5.5% (Jatropha biodiesel) to 6.4% (conventional diesel). The heat rate nearly doubled at TET of 1220K across all the fuels. The heat rate was worst in engine GX100 for utilizing natural gas. The exhaust mass flow (EMF) also followed similar trends with about 12% increase for the liquid biofuels and 14% in the natural gas fuel at TET of 1220K. In order words, there are further implications with the use of the different fuels and these were more pronounced at reduced TET. This is because there is decrease in power with decrease in turbine entry temperature, but this is not proportionate to a decrease in heat input.

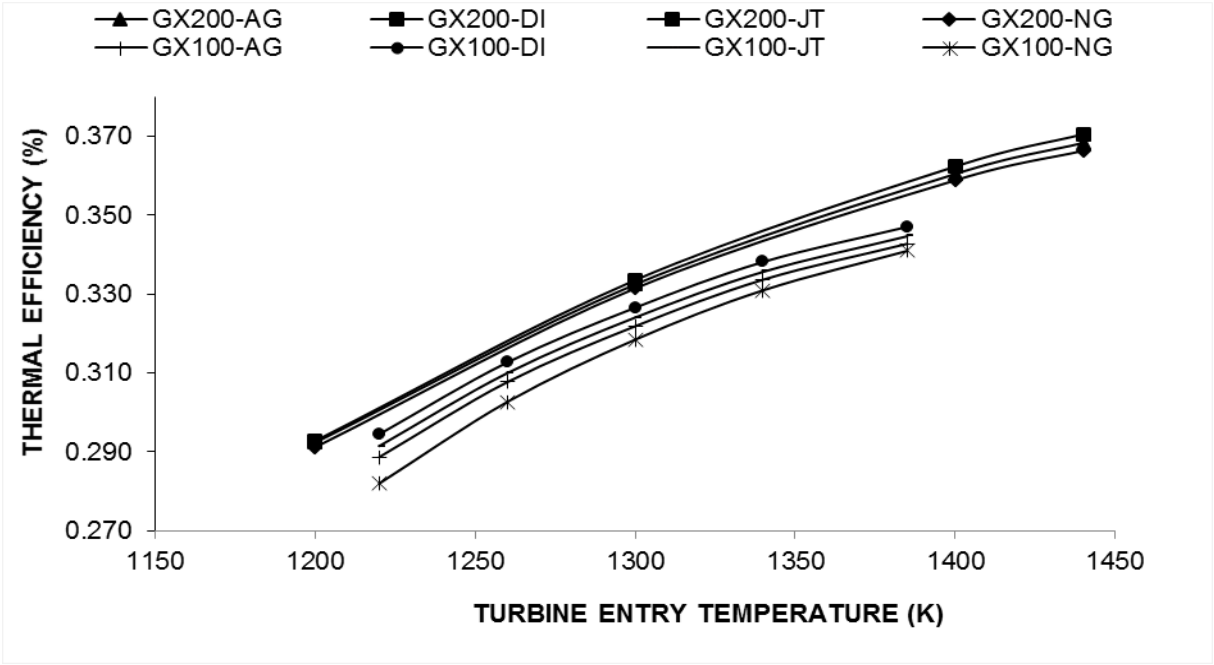

Figure 3.10: Effect of fuels on thermal efficiency of GX100 and GX200 at varying loading conditions using Natural Gas, Diesel, Jatropha biodiesel and Microalgae biodiesel fuels

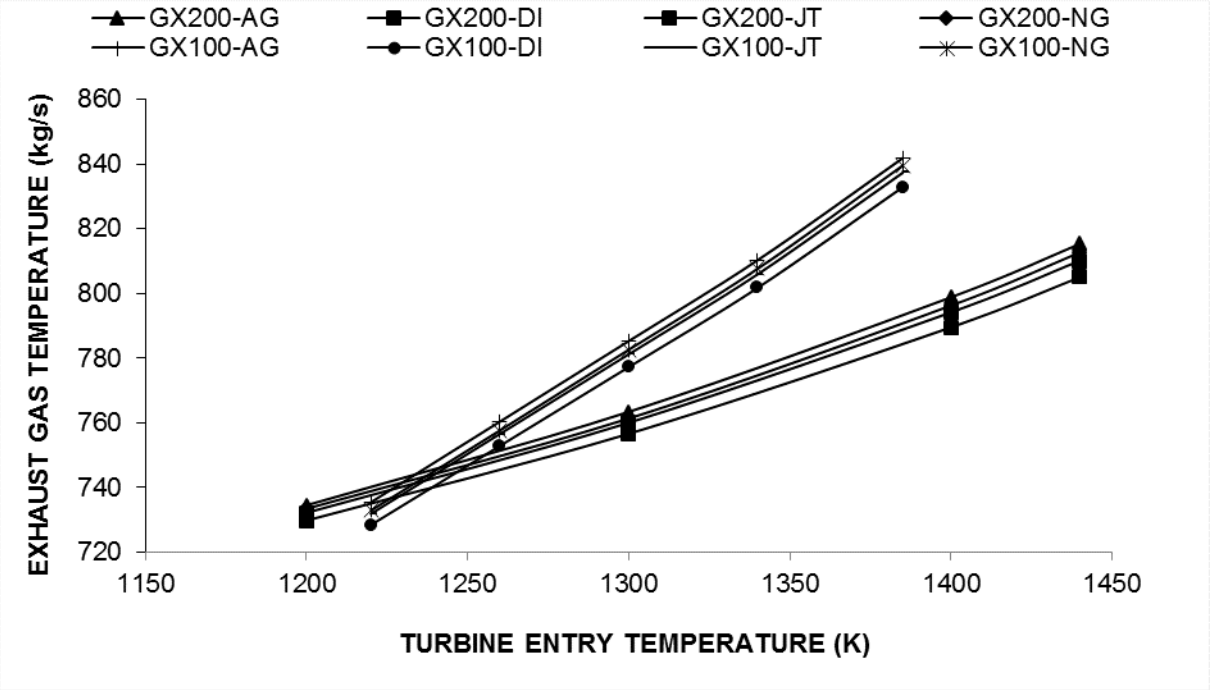

Figure 3.11: Effect of fuels on exhaust gas temperature of GX100 and GX200 at varying loading conditions using Natural Gas, Diesel, Jatropha biodiesel and Microalgae biodiesel fuels

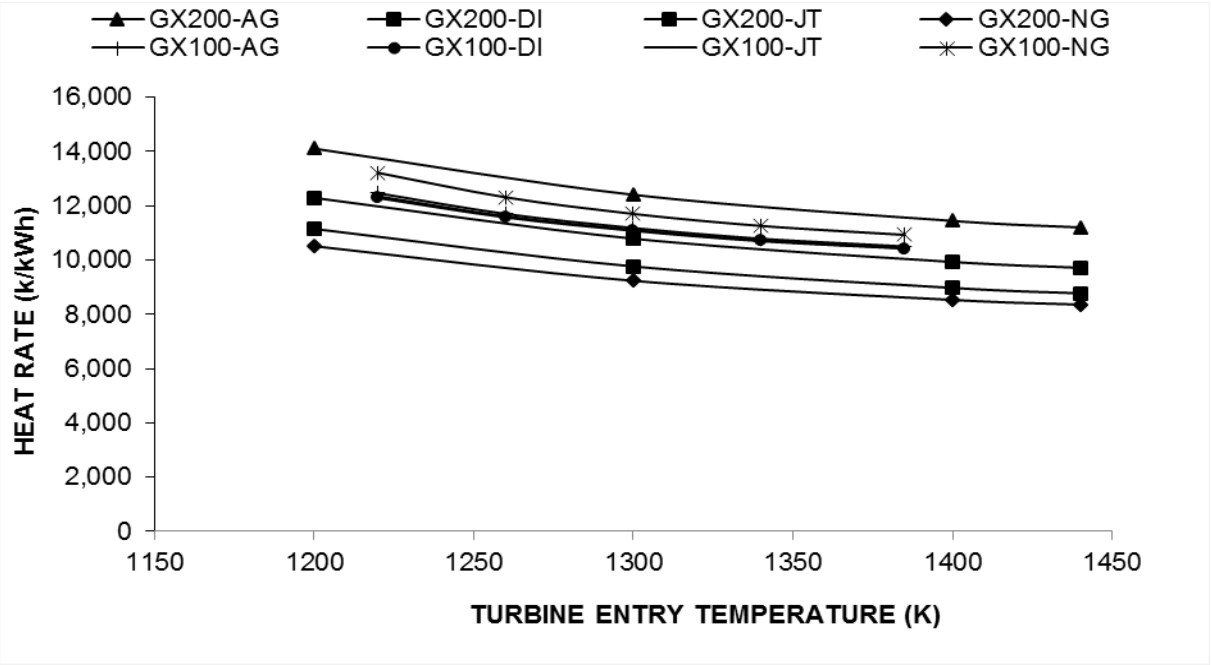

Figure 3.12: Effect of fuels on heat rate of GX100 and GX200 at varying loading conditions using Natural Gas, Diesel, Jatropha biodiesel and Microalgae biodiesel fuels

3.3.3.2 Fuel Performance Analysis at Varying Ambient Temperatures

The effect of ambient temperatures on specific power, thermal efficiency, and exhaust gas temperature using the four different fuels for engine GX100 and GX200 are illustrated in figures 3.13-3.15. Among the four engine performance parameters, there was a significant difference in the heat rate across the fuel types and with increasing ambient temperatures. With earlier observations, engine with microalgae biodiesel had the highest heat rate (about 30% higher than that of natural gas) and increasing up to 0.3% for every Celsius degree rise in ambient temperature. It was observed that there was decreasing thermal efficiencies with increasing temperatures and uniform deviation across all fuel types.

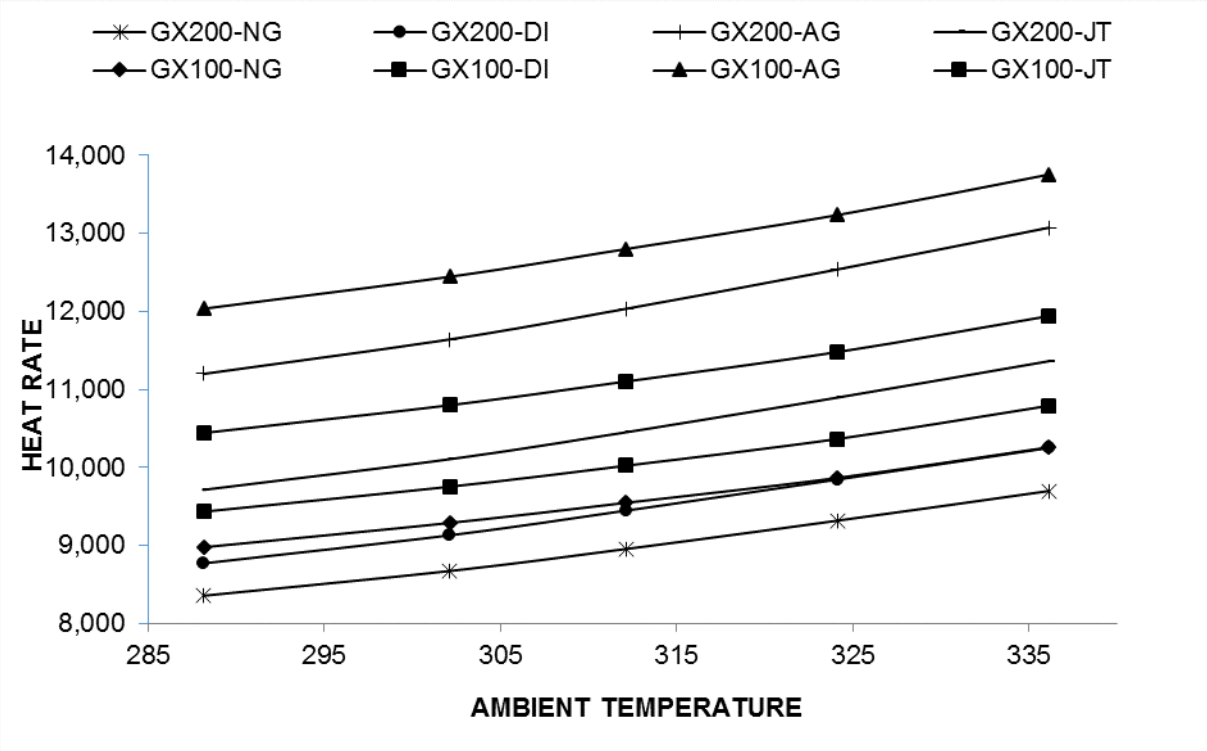

Figure 3.13: Effect of fuels on heat rate of GX100 and GX200 at varying ambient temperatures using Natural Gas, Diesel, Jatropha biodiesel and Microalgae biodiesel fuels

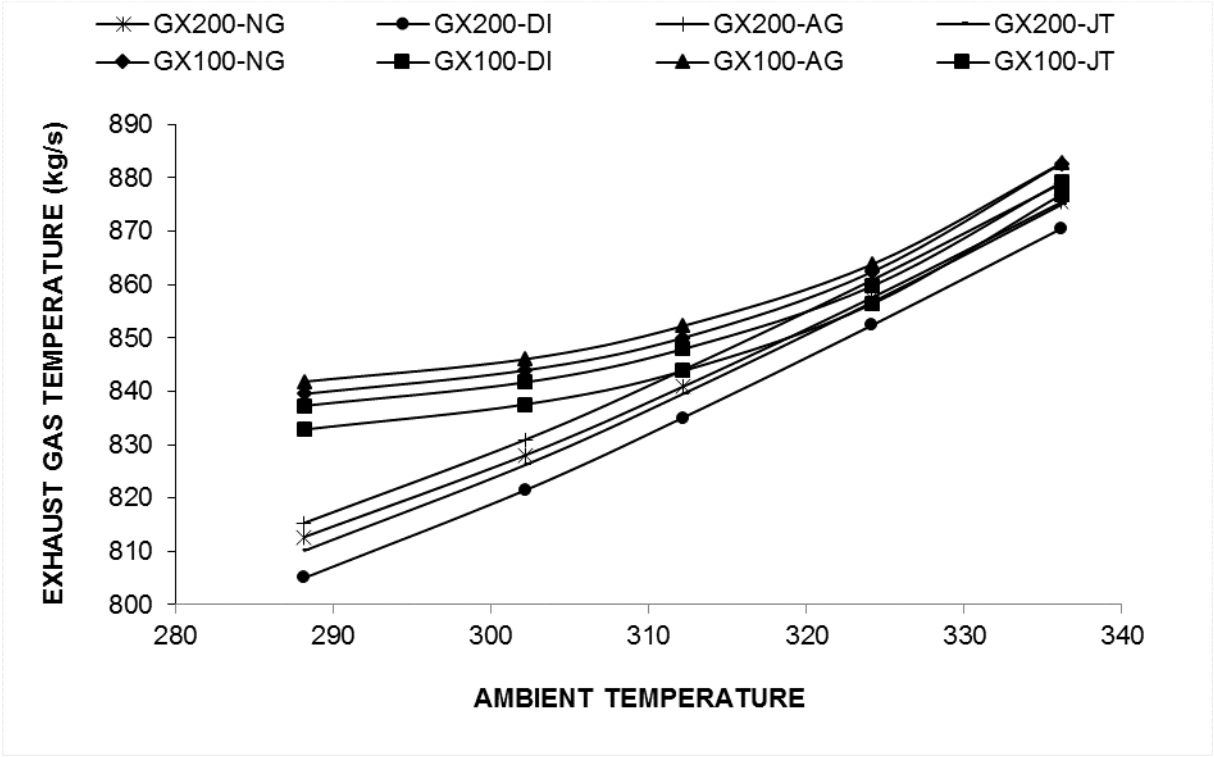

Figure 3.14: Effect of fuels on exhaust gas temperatures of GX100 and GX200 at varying ambient temperatures using Natural Gas, Diesel, Jatropha biodiesel and Microalgae biodiesel fuels

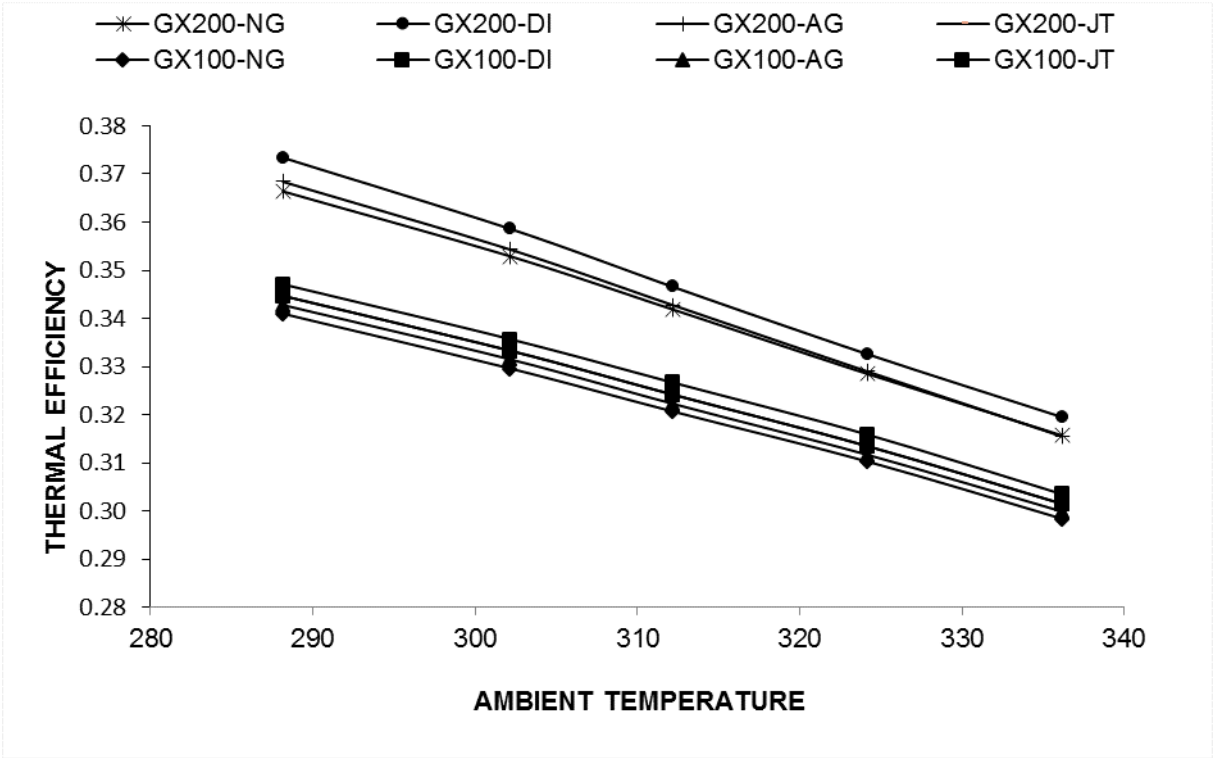

Figure 3.15: Effect of fuels on thermal efficiency of GX100 and GX200 at varying ambient temperatures using Natural Gas, Diesel, Jatropha biodiesel and Microalgae biodiesel fuels

3.3.4 Fuel Performance Analysis at Site Conditions

Ambient conditions and fuel effects factors do not affect gas turbine in isolation. Thus, fuel performance analysis was carried out for engine GX100-300 at site conditions (Altitude: 75 m; Temperature: 30^{o}C; Installation Inlet Pressure Loss: 5%; Relative humidity: 60%) and using Jatropha biodiesel, microalgae biodiesel, conventional diesel and natural gas fuels. These results are presented in Table 3.12 to 3.14.

Table 3.12: Fuel Performance Analysis of Engine GX100 at Site Conditions

Parameters	Reference Fuel Natural Gas				
	ISO Rating	Site Condition	Conventional Diesel	Microalgae Biodiesel	Jatropha Biodiesel
Useful Work (MW)	126.1	109.05	109.2	109.0	109.07
Exhaust Mass Flow (kg/s)	423.1	417.0	415.2	417.8	416.6
Exhaust Gas Temperature (K)	839.5	846.2	840.3	848.9	844.5
η_{th} -Thermal efficiency (%)	34.1	31.29	31.96	31.52	31.71
Heat Rate (kJ/kWh)	10928.0	11903.5	11335	11409	11349

Analysis carried out at Altitude-75m; Temperature-303.15K; Inlet Pressure Loss-5%; Relative humidity-60%. Fuels LHV-: Natural Gas-11259kcal/kg; Diesel- 10167.6 kcal/kg; Jatropha biodiesel- 8071kcal/kg; microalgae biodiesel- 9250 kcal/kg

At site conditions, the output of the engine, GX100 reduced by nearly 14% across all fuels. The compounding effects from the use of the fuels could be observed on thermal efficiency, heat rate, EMF and EGT (see Table 3.12). The results show that thermal efficiency of the engine operating on natural gas deviated by 8.2% at site conditions when compared to the reference point. However, with the use of other liquid fuels, with lower LHV values, the deviations were much reduced, especially with conventional diesel (6.3%) and Jatropha biodiesel (7%) at site conditions. Similarly, the EMF reduced at site conditions by 1.4% (natural gas) with more deviations in EMF for other fuels when compared to the reference point. The deviations observed were 1.9%, 1.3% and 1.6% for conventional diesel, microalgae biodiesel and Jatropha biodiesel respectively. The EGT increased by 0.8% at site conditions for the engine operating on natural gas, but only increased by 0.1% and 0.6% for conventional diesel and Jatropha biodiesel respectively and by 1.1% for microalgae biodiesel. Here, the deviations in EGT are more pronounced at site conditions with the use of other fuels. The heat rate, on the other hand increased by 3.7%, 3.9% and 4.4% in the engine operating on conventional diesel, Jatropha biodiesel and microalgae biodiesel fuel while a reduction of 5.8% is observed for natural gas. The results in Table 3.12 demonstrate that further deviations are expected in engine

performance due to the ambient effects as well as those associated with the use of the fuels.

Table 3.13: Fuel Performance Analysis at Site Conditions Engine GX200 Using Difference Fuels

Parameters	Reference Fuel Natural Gas		Conventional Diesel	Microalgae Biodiesel	Jatropha Biodiesel
	ISO Rating	Site Condition			
Useful Work (MW)	22.40	18.13	18.02	18.10	18.03
Exhaust Mass Flow (kg/s)	71.20	61.36	61.34	61.70	61.45
Exhaust Gas Temperature (K)	812.70	836.41	830.53	839.6	835.03
η_{th} -Thermal efficiency (%)	36.60	34.23	34.70	34.30	34.49
Heat Rate (kJ/kWh)	10172	10887	10372	10459	10437

Analysis carried out at Altitude-75m; Temperature-303.15K; Inlet Pressure Loss-5%; Relative humidity-60%. Fuels LHV-: Natural Gas-11259kcal/kg; Diesel- 10167.6 kcal/kg; Jatropha biodiesel- 8071kcal/kg; microalgae biodiesel- 9250 kcal/kg

Similar results were observed for the engine GX200 (see Table 3.13), however at a much larger degree. Here, the heat rate increased by 1.9%, 2.6% and 2.8% in engine operating on conventional diesel, Jatropha biodiesel and microalgae biodiesel fuel while an increase of 7.0% was observed for natural gas. The thermal efficiency of the engine operating on natural gas reduced by 6.5% at site conditions when compared to the reference point. However, with the use of liquid fuels, with lower LHV values, the deviations were not as much reduced, especially with conventional diesel (5.2%) and Jatropha biodiesel (5.8%) at site conditions.

Table 3.14: Design Point Fuel Performance Analysis of Engine GX300

Parameters	Reference Fuel Natural Gas	Conventional Diesel	Microalgae Biodiesel	Jatropha Biodiesel
Useful Work (MW)	380.57	383.36	381.60	379.77
Net plant efficiency (%)	53.70	56.81	52.40	55.80

Analysis carried out at Altitude-75m; Temperature-303.15K; Inlet Pressure Loss-5%; Relative humidity-60%. Fuels LHV-: Natural Gas-11259kcal/kg; Diesel- 10167.6 kcal/kg; Jatropha biodiesel- 8071kcal/kg; microalgae biodiesel- 9250 kcal/kg

The combined cycle engine performance results in Table 3.14 showed that conventional diesel fuel had the highest fuel performance with more useful work and net plant efficiency. Similar to the design point analysis, there is a trade-off between the two biodiesel fuels. Microalgae biodiesel had a higher useful work but reduced net plant efficiency, however, Jatropha biodiesel fuel resulted in a net plant efficiency of 55.8% with a slightly reduced useful work.

3.4 Conclusion

The performance evaluation of Jatropha biodiesel- and microalgae biodiesel-fired engines have been evaluated using appropriate engine performance simulation methodologies and results are compared with fossil-fired engines. A summary is provided below:

1. There was an increase in engine thermal efficiency by 0.5% and 1.1% for utilizing microalgae- and Jatropha biodiesel fuels when compared to the engine operating on natural gas at design point. Among the three liquid fuels, conventional diesel fuel had the highest level of thermal efficiency, a value of 34.7%, and subsequently the lowest level of heat rate.
2. The exhaust gas temperatures when compared to the reference point reduced by 0.3% and 0.8% for utilizing Jatropha biodiesel and conventional diesel fuel respectively, but increased by 0.3% with the use of microalgae biodiesel.
3. Jatropha biodiesel had a better performance than microalgae biodiesel in both engines (126 MW heavy-duty and the 22.4 MW aero-derivate gas turbine).
4. The exhaust mass flow increased for all the liquid fuels with the least involving conventional diesel, followed by Jatropha biodiesel, then microalgae biodiesel. This is due to the differences in the LHV of the fuels, which necessitated an increase in exhaust mass flow to enable the engine to reach the required temperature.
5. The biodiesels gave a better performance than natural gas due to a combination of higher carbon and oxygen content of the fuels, but lesser performance to conventional diesel fuel due to their relatively lower LHV.
6. Contrary to the above results, the use of natural gas brought about the highest level of specific equivalent shaft power, followed by the use of microalgae biodiesel, Jatropha biodiesel and conventional diesel in that order. This is because natural gas has a hydrogen composition, nearly one-third of the fuel while the biodiesels have hydrogen compositions that are less than one-fifth.
7. From this analysis, Jatropha biodiesel is a better choice of fuel, since it has performance characteristics close to those of the conventional diesel with the added advantage of being renewable. It would be applicable to existing and future power plant without necessitating engine modifications; however its effects on engine durability require assessment.
8. The microalgae biodiesel had a better advantage for the combined cycle application because of its higher exhaust mass flow and exhaust gas temperature. Also because

it yielded more specific power per kg of fuel combusted than any other liquid fuel examined in the study. Here, the performance loss in the gas generator was compensated in the bottoming cycle of the power plant with increase in net plant efficiency of 52%, as opposed to the reference point of 50% for a relatively equal amount of power output.

9. With the use of biodiesels, there is a tendency for a reduced surge margin, since the engine running line moves toward higher pressure ratios, and firing temperature, however, this was by a very slight degree.
10. At reduced load conditions, the effects of fuels on engine performance are more compounded, and at increasing ambient temperatures, the differences in engine performance were uniform and resulting from the effect of ambient temperatures only. However, when similar analyses were carried out at site conditions (Altitude -75 m; Temperature -30^{o}C (303 K); Installation Inlet Pressure Loss -5%; Relative humidity -60%), further deviations were observed and this was as a result of a combination of ambient and fuel effects.

3.5 Further Work

Biodiesel fuels have a wide range of properties that differ with origin. It would be interesting to examine Jatropha biodiesels from different countries or locations and re-examine these assessments presented here in similar engines with or without advanced cycles. This should not only increase knowledge on the use of biodiesels in gas turbines, but also enable the development of current or future advances in gas turbine cycles and fuels.

3.6 References

[1] Pilavachi, P.A. 2000. Power generation with gas turbine systems and combined heat and power. *Applied Thermal Engineering* 20 (15-16): 1421-1429.

[2] Najjar, Y.S.H. 2001. Efficient use of energy by utilizing gas turbine combined systems. *Applied Thermal Engineering* 21(4): 407–438

[3] Poullikkas, A. 2004. Parametric study for the penetration of combined cycle technologies into Cyprus power system. *Applied Thermal Engineering* 24(11-12): 1697-1707.

[4] Polyzakis A.L., Koroneos, C. and Xydis G. 2008. Optimum gas turbine cycle for combined cycle power plant. *Energy Conversion Management* 49(4): 551-563.

[5] Soares, C. 2008. Gas turbines: A Handbook of Air, Land and Sea applications. Amsterdam: Butterworth-Heinemann. London: Elsevier Inc.

[6] ASTM International. 2015. Standard Specification for Biodiesel Fuel Blend Stock (B100) for Middle Distillate Fuels. Standard Number D6751-15. ASTM International, West Conshohocken, PA. DOI: 10.1520/D6751-15

[7] ASTM International. 2014. Standard Specification for Gas Turbine Fuel Oils. Standard Number D2880-14a. ASTM International, West Conshohocken, PA. DOI: 10.1520/D2880-14A

[8] Arbab, M.I., Masjuki, H.H., Varman, M., Kalam, M. A., Imtenan, S. and Sajjad, H. 2013. Fuel properties, engine performance and emission characteristics of common biodiesels as a renewable and sustainable source of fuel. *Renewable and Sustainable Energy Reviews* 22:133-147

[9] Atabani, A.E., Silitonga, A.S., Badruddin, I.A., Mahlia, T.M.I., Masjuki, H.H. and Mekhilef, S. 2012. A comprehensive review on biodiesel as an alternative energy resource and its characteristics. *Renewable and Sustainable Energy Reviews* 16(4): 2070-2093.

[10] Rehman, A., Phalke, D.R. and Pandey, R. 2011. Alternative fuel for gas turbine: esterified Jatropha oil diesel blend. *Renewable Energy* 36(10): 2635-2640.

[11] Demirbas, A. 2008. The importance of bioethanol and biodiesel from biomass. *Energy Sources Part B: Economics, Planning, and* Policy 3(2):177–185

[12] Walsh, P.P. and Fletcher, P. 2008. Transient Performance *In* Gas Turbine Performance. 2nd ed., Blackwell Science Ltd: Oxford, UK.

[13] Lefebvre, A.H. 1985. Influence of Fuel Properties on Gas Turbine Combustion Performance. Report Number APWAL-TR-84-2104. Aero Propulsion Laboratory Research, Wright-Patterson Air Force Base, Ohio, USA.

[14] Lefebvre, A.H. and Ballal D.R. 2010. Gas Turbine Combustion: Alternative Fuels and Emissions", 3rd Ed. Philadelphia, PA. CRC Press, Taylor and Francis.

[15] Palmer, J.R. 1967. The "Turbocode" Scheme for the Programming of Thermodynamic Cycle Calculations on an Electronic Digital Computer. CoA Report Aero 198. College of Aeronautics, Cranfield Institute of Technology, UK.

[16] MacMillan, W.L. 1974. Development of a Modular Type Computer Program for the Calculation of Gas Turbine Off-Design Performance. Ph.D. Thesis, Cranfield Institute of Technology, UK.

[17] Tan, E.S., Anwar, M., Adnan, R. and Idris, M.A. 2013. Biodiesel for Gas Turbine Application - An Atomization Characteristics Study. *In* Advances in Internal Combustion Engines and Fuel Technologies. Ng, H.K (editor). INTECH Open Access Publisher. DOI: 10.5772/54154

[18] Kurz, R. and Brun, K. 2001. Degradation in gas turbine systems. *Journal of Engineering for Gas Turbines and Power* 123(1): 70-77.

[19] Sethi, V. 2008. Advanced Performance Simulation of Gas Turbine Components and Fluid Thermodynamic Properties. PhD Thesis submitted to Department of Power and Propulsion, Cranfield University, UK.

[20] Tate, R.E., Watts, K.C., Allen, C.A.W., and Wilkie, K.I. 2006. The Viscosities of Three Biodiesel Fuels at Temperature up to 300°C. *Fuel* 85(7-8): 1010–1015.

[21] McBride, B. J. and Gordon, S. 1996. Computer program for calculation of complex chemical equilibrium compositions and applications II. Report Number E-8017-1. National Aeronautics and Space Administration, OH, USA.

[22] Wilson, C., Blakey, S., Darbyshire, O., Woolley, R., Cornwell, S., Sidaway, T., and Weiss, S., 2007. Preparing the Way for Gas Turbines to Run on Alternative Fuel. Presented at "Developments in Industrial Burner Technology to Meet the Challenges of the Efficient Combustion of New and Difficult Fuels", British Flame, Birmingham, UK

[23] Gordon, S. and McBride, B.J. 1994. Computer Program for calculation of complex Chemical equilibrium compositions and applications I: Analysis. NASA RP-1311. (National Aeronautics and Space Administration, Ohio, USA.

[24] Yin, J., Li, M.S. and Huang, W. 2003. Performance analysis and diagnostics of a small gas turbine. *In* Proc. of the Int. Gas Turbine Congress, Tokyo, Japan, TS-006, November 2-7, 2003.

[25] Bonet, M., Doulgerisa, G. and Pilidis, P. 2010. Assessment of a Marine Gas Turbine Installation on a Liquefied Natural Gas Carrier. PaperID: NCH-2010-C1, Nausivios Chora 2010, Hellenic Naval Academy, Greece.

[26] Nkoi, B., Pilidis, P. and Nikolaidis, T. 2013. Performance of small-scale aero-derivative industrial gas turbines derived from helicopter engines. *Propulsion and Power Research* 2: 243-253.

[27] Gupta, K.K., Rehman, A. and Sarviya, R.M. 2010. Bio-fuels for the gas turbine: A review. *Renewable and Sustainable Energy Reviews* 14(9): 2946–2955

[28] Gallar, L., Volpe, V., Salussolia, M., Pachidis, V. and Jackson. A. 2012. Thermodynamic Gas Model Effect on Gas Turbine Performance Simulations. *Journal of Propulsion and Power* 28(4): 719-727.

[29] Wagner, W. and Kruse, A. 1998. Properties of Water and Steam. Springer, Berlin

[30] General Electric (GE) Energy, 2014a. LM2500 BASE Aeroderivative Gas Turbine Package (24 MW). Available https://www.ge-distributedpower.com/products/power-generation/15-to-35-mw/lm2500-base Last accessed on December 29, 2014

[31] General Electric (GE) Energy, 2014b. 9E Gas Turbine Proven Performance for 50 Hz Applications. Available https://powergen.gepower.com/plan-build/products/gas-turbines/9e-03-gas-turbine.html Last accessed on December 29, 2014

[32] Meher-Homji, C.B., Chaker, M.A. and Motiwala, H.M. 2001. Gas turbine performance deterioration. Proceedings of the 30th Turbomachinery Symposium, Texas, USA. pp. 139-175.

[33] Basha, M., Shaahid, S.M. and Al-Hadhrami, L. 2012. Impact of Fuels on Performance and Efficiency of Gas Turbine Power Plants. *Energy Procedia* 14: 558 – 565

[34] Alhazmy, M.M. and Najjar, Y.S.H. 2004. Augmentation of Gas Turbine, Performance Using Air Coolers. *Applied Thermal Engineering* 24 (2-3): 415-429.

[35] Mohanty, B. and Palaso Jr., G. 1995. Enhancing Gas Turbine Performance by Intake Air Cooling Using an Absorption Chiller. *Heat Recovery Systems and CHP* 15(1): 41-50

[36] Kakaras, E., Doukelis, A., Prelipceanu, A. and Karellas, S. 2005. Inlet Air Cooling Methods for Gas Turbine Based Power Plant. *J. Eng. Gas Turbines Power* 128(2): 312-317

[37] Akinbode, S.O., Dipeolu, A.O., Ibrahim, D.A. 2011. Effect of Disease Burden on Technical Efficiency among Lowland Rice Farming Households in North Central Nigeria. *World Journal of Agricultural Sciences* 7(3): 359-367.

[38] Palmer, J.R. and Pachidis, V. 2005. The Turbomatch Scheme; for Aero/Industrial Gas Turbine Engine Design Point/Off Design Performance Calculation Manual, Cranfield University, UK.

[39] Brooks F.J. 2006. GE Gas Turbine Performance Characteristics. Report Number GER-3567H GE Power Systems: Schenectafy, NY.

[40] Chineke C.T. 2009. Boosting Electricity Supply in Nigeria: Wind Energy to the Rescue? *Pacific Journal of Science and Technology* 10(2): 553-560.

[41] Walsh, P.P., and Fletcher, P. 1998. Gas Turbine Performance. 1st edition, Blackwell Science Ltd

[42] Eludoyin, O.M., Adelekan, I.O., Webster, R. and Eludoyin, A.O. 2014. Air temperature, relative humidity, climate regionalization and thermal comfort of Nigeria. *Int. J. Climatol*. 34(6): 2000–2018.

[43] Ayanda, I.F., Oyeyinka, R.A., Salau, S.A. and Ojo, F. 2013. Perceived effects of climate change on transhumance pastoralists in Ogun State, Nigeria. *Journal of Agricultural Science* 5(4):1-9

[44] Meher-Homji, C.B., Zachary, J. and Bromley, A.F. 2010. Gas Turbine Fuels-System Design Combustion and Operability. Proceedings of the 39th Turbomachinery Symposium, Texas, USA. pp. 155-186

[45] Silva, E.B., Bringhenti, C., Assato, M. and Lima, R.C. 2013. Gas Turbine Performance Analysis operating with low heating value fuels. *Engenharia Térmica (Thermal Engineering)* 12(2): 8-15.

Chapter 4

4. EMISSION ANALYSIS OF GAS TURBINE FUELS

Following the performance analysis of engines, GX100 and GX200 in Chapter 3, this chapter assesses the emission characteristics of the engines when operated on natural gas, microalgae biodiesel, Jatropha biodiesel, and conventional diesel fuel. This includes a brief introduction on the pollutants that are generated as a result of fuel combustion and how these pollutants are formed. The methods used for assessing the nitrous oxide (NOx), carbon dioxide (CO_2) and carbon monoxide (CO) emissions in both gas turbines are presented. Furthermore, the results of the emission analysis of the different fuels, including how they affect combustion performance and efficiency are discussed. The chapter ends with a summary on the best choice of biodiesel fuel that could substitute the use of fossil fuels in oil-fired gas turbines.

4.1 Introduction

The primary products of complete combustion of air and hydrocarbon fuels are carbon dioxide (CO_2) and water vapour (H_2O). Although, both by-products are not classified as pollutants, there are associated environmental and health implications. In addition to these products, sulphur dioxide (SO_2), nitrogen oxide (NOx), carbon monoxide (CO), particulate matter (PM_{10}), unburned hydrocarbons (UHC), volatile organic compounds (VOCs), soot and smoke are produced at varying levels depending on fuel type, engine operating and combustion conditions [Lefebvre and Ballal, 2010]. All these gases exit through the exhaust gas of the engine and could pollute the environment when produced in inappropriate quantities. Table 4.1 summarizes the health concerns and environmental impact associated with these emissions.

Table 4.4.1: Pollutants emitted by gas turbines and potential environmental and health impacts

Pollutant	Effects
SO_2	Acid rain (corrosive)
NOx	Ozone depletion (stratosphere), precursor of photochemical smog, contributes to acid rain and biotic damage
PM_{10}	Haziness, reduces visibility and air quality, increase asthma and respiratory diseases
UHC	Toxic, photo chemical smog in conjunction with NOx
CO	Toxic (asphyxiation or death at high concentrations),

The emissions of power plants have gained public interest in recent years, particularly CO and NOx emissions. This is due to the direct impact of exhaust emissions on air quality and their potential to cause environmental degradation and human health deterioration. There are indications that the GHGs emitted from industrial power plants are contributing to the increase in ambient temperatures across the world, a phenomenon referred to as climate change. As a result, countries are beginning to set strict limits for emissions in new and existing power plants. For instance, the power plants in the United States are said to be the largest contributor of GHG emissions with values accounting for nearly 40% of the country's total emissions and 2% of the world's emission [EIA, 2011]. The country is aiming to cut emissions from power plant by reducing the emission of GHGs including methane as well as CO_2. Similarly in the UK, power stations are said to be a major contributor of SO_2, NOx, PM_{10}, VOCs and CO [DECC, 2014]. There are concerted efforts to curb emission from these power stations across the country by decommissioning old power plants and infrastructures, introducing new technology and fuels as well as developing improved emission standards, limits and policies. Many developing countries including Nigeria are aiming to increase their energy mix in the near future through the intervention of renewable fuels. Hence, all efforts to reduce climate change involve the increasing use of clean energy. Biofuels are of peculiar advantage because they are sourced from renewable materials, and could alleviate the problems of environmental pollution while reducing world's dependency on fossil fuels.

4.1.1 Pollutants Formation in Gas Turbines

As mentioned-above, the emissions leaving the exhaust of a typical gas turbine contain CO_2, H_2O, SO_2, NOx, CO, PM_{10}, and UHC, VOCs, soot and smoke. This study however, primarily focuses on the emissions of CO, CO_2 and NOx. These emissions have been selected based on current research focus and the capability of the emission model. Currently, NOx and CO_2 are the major pollutants receiving research focus because they are important greenhouse gases that contribute to the formation of tropospheric ozone. NOx is also a precursor of photochemical smog and contributes to acidification and PM_{10} emissions. CO on the other hand is an indication of incomplete combustion of hydrocarbon fuel to CO_2.

4.1.1.1 CO Formation

In principle, CO is formed as a result of incomplete combustion of carbon based fuel. This could result from low burning rates at low power settings and in the primary zone of the combustor, insufficient or non-uniform distribution of air or oxygen to completely combust the fuel, low residence time of the fuel in the combustor or dissociation of CO_2 in slightly fuel-lean condition or at very high flame temperature.

4.1.1.2 CO_2 Formation

CO_2 is formed from complete combustion of hydrocarbon fuel. The reaction occur in the presence of sufficient air to form CO_2 and water vapour (H_2O). The amount of CO_2 formed is dependent on fuel type and concentration of oxygen in the mixture.

4.1.1.3 NOx Formation

NOx refers to both nitrogen oxide (NO) and nitrogen dioxide (NO_2). It is said to be produced in gas turbines via four mechanisms: a) thermal NOx, b) prompt NOx, c) fuel NOx and d) nitrous oxide mechanism [Lefebvre and Ballal, 2010]

a) Thermal NOx is formed as a result of oxidation of nitrogen at high temperature regions of the flame, a condition that is often promoted at fuel-lean operation. According to Lefebvre and Ballal, [2010], NOx is only significantly produced at temperatures above 1850K, where there is a competition for oxygen by carbon and nitrogen present in fuel. This result in set of reactions as shown in equation 4.1-4.4, known as Zeldovich NOx formation mechanism.

$$O_2 = 2[O] \quad (4.1)$$

$$N_2 + [O] = NO + N \quad (4.2)$$

$$[N] + O_2 = NO + [O] \quad (4.3)$$

$$[N] + [OH] = NO + [H] \quad (4.4)$$

Hence, NOx emission is said to be largely dependent on flame temperature and the operating condition of the combustor.

b) NO from Nitrous Oxide is formed from the reaction between nitrogen, oxygen and further oxidation of N_2O to NO, following the reactions stated in equation 4.5-4.6.

$$N_2 + O = N_2O \quad (4.5)$$

$$N_2O + O = NO + NO \quad (4.6)$$

c) Prompt NO occurs rarely and is formed from a complex reaction between hydrocarbon and nitrogen molecule in the flame region, following the reactions stated in equation 4.7-4.8.

$$N_2 + CH = HCN + N \quad (4.7)$$

$$HCN \longrightarrow CN \longrightarrow NCO \longrightarrow NO \quad (4.8)$$

d) Fuel NO is another prevalent source of NOx emission. Certain fuels have a high concentration of nitrogen molecules chemically bound to the fuel, referred to as fuel-bound nitrogen (FBN) such as heavy residual oil. Some of these FBN reacts with the oxidant to form fuel NO. This is also flame temperature dependent and increases with increasing residence time of the fuel in the combustor. Natural gas have very low concentration of FBN, distillate and residual fuels have up to 0.06% and 1.8% respectively while biofuels have little or insignificant quantities of FBN [Lefebvre and Ballal, 2010].

In principle, the formation of NOx and CO emissions is said to have an inverse relationship and closely related with the combustion firing temperature. That is, the concentration of CO reaches a maximum at the lowest power setting and reduces as power increases while NOx emissions reaches maximum at the highest power setting and reduces with power reduction [Lefebvre and Ballal, 2010]. This relationship is illustrated in figure 4.1.

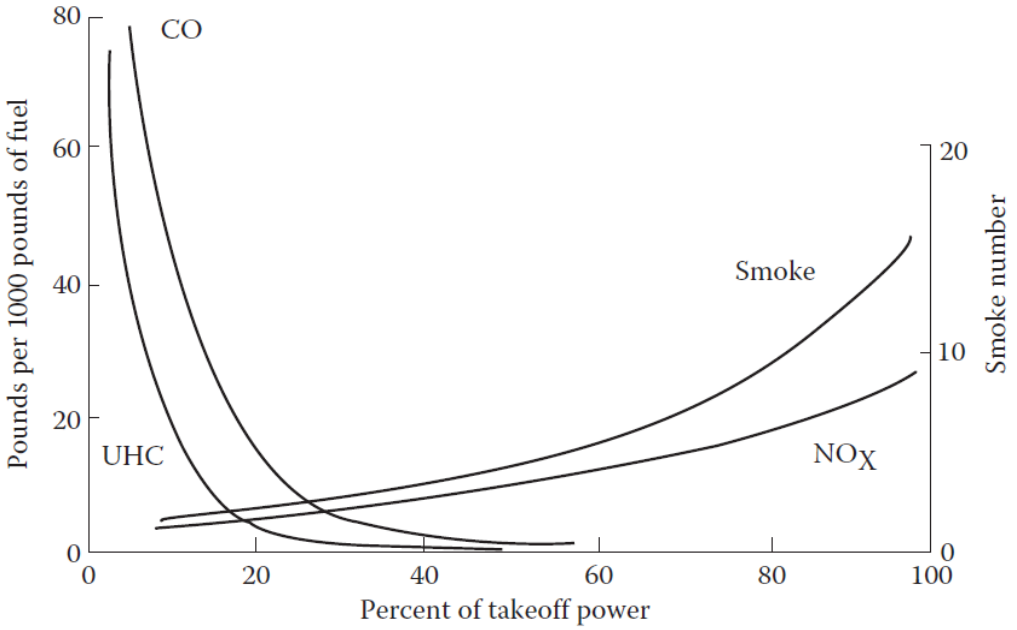

Figure 4.4.1: Emission of CO, NOx, UHC and Smoke in relation to power setting [Lefebvre and Ballal, 2010]

Furthermore these emissions have a relationship with combustor inlet temperature and pressure, primary zone equivalent ratio, residence time, operating condition of the engine and vary with combustor type.

4.1.2 Emission Regulations in Industrial Gas Turbines

Generally, the regulations of emissions in industrial gas turbines vary from country to country and depend on engine size, site conditions, fuel type, engine age and application. In the emissions standards of the Environmental Protection Agency (EPA), which is well adopted world-wide including Nigeria; the NOx emission limits for new gas turbine engines producing electricity are stated in Table 4.2.

Table 4.4.2: U.S. Environmental Protection Agency Emission NOx Limits for Power Plants

Engine Size	<3 MW	3–110 MW	> 110 MW
Natural gas	42 ppmv	25 ppmv	15 ppmv
Other fuels	96 ppmv	74 ppmv	42 ppmv

There are currently no EPA standards for CO, CO_2 and UHC emissions; however, typical CO limits are in the range of 10-40 ppm.

4.2 Methodology

4.2.1 Preliminary Emission Analysis

The CO and NOx emission analyses were carried out on both simulated engines, GX100 and GX200 using the emission model developed by [Samaras, 2011]. This is a physics-based model that predicts emission pollutants using physical quantities to describe the complex processes that occur in the combustion chamber, along with set of chemical reactions and kinetic equations. Here, four zones [flame front (FF), primary zone (PZ), intermediate zone (IZ) and dilution zone (DZ)] are represented using series of stirred reactors. These reactors consist of a) partially stirred reactor (PaSR) and b) series of perfectly stirred reactors (PSR) that represent the different levels of turbulent mixes. The PaSR and PSR represents the flame front while the series of PSR represent the PZ, IZ and DZ, and the recirculation processes around the primary zone. Figure 4.2 illustrate how the different zones are coupled together to represent a generic gas turbine combustor for emission estimation.

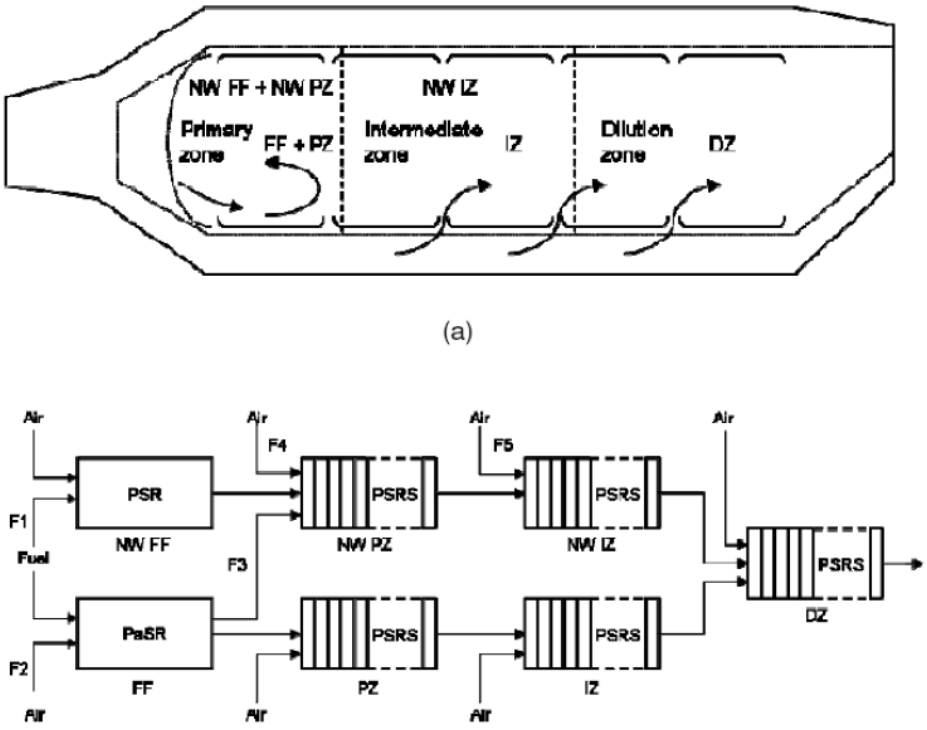

Figure 4.2: Emission of CO, NOx, UHC and Smoke in relation to power setting [Samaras, 2011]

The primary purpose of the flame front and primary zone is to anchor the flame, force recirculation of combustion gases so that sufficient turbulence and temperature is reached for combustion. The recirculation of combustion gases in the direction of the freshly mixed reactants is important because it reduces the amount of pollutants that are

generated by allowing sufficient mixing. It also sustains the ignited flame in the flame front and in the absence of external energy source. In order to model the PaSR and PSR, the model assumes that the chemical mixees are occuring at an infintely fast rate such that the flame front is perfectly mixed. It also assumes that the products that are generated in the reactors are in chemical equilibrum; hence, the NASA CEA program has been integrated in the emission model for chemical equilibrum calculations. The model allows the user to specify the combustor geometry, which takes into account the zones involved in combustion and dilution of gases, the fuel flow, air and fuel inlet conditions and distribution of air mass flow.

For this study, a generic conventional combustor was modelled according to the methods described in [Celis, 2010; Samaras, 2011]. The combustor inlet conditions were obtained from the results of the performance analysis. A sample input file used for emission analysis in engine, GX100 is presented in Appendix III. The modelled combustor describes the primary mode of operation of a DLN-1 combustor, which works in a similar fashion to those of conventional systems and where the highest levels of emissions are produced.

In principle, the early DLN combustor is capable of operating in primary, lean-lean, secondary and premix modes. In the primary mode, the combustor have a similar behaviour to conventional combustor, because it employs a diffusion flame. This is confined to the primary zone alone and applies to the low-mid load only. The lean-lean mode applies to both the primary and secondary zones and for intermediate loads. Here, fuel is introduced to the primary and secondary nozzles. The secondary mode only employs fuel and flame in the secondary zone to enable a transition of flame from the lean-lean to premix mode, while enabling the extinguishing of the flame in the primary zone. The premix mode applies to mid-full load with fuel introduction in the primary and secondary zone, however with flames in the secondary region only.

The early GE MS9001E (9E) frame engines operated on Dry Low NOx (DLN)-1 combustion system, but the later versions uses DLN 2.6 combustor and other uprated versions. The DLN-1 combustor reduces NOx emission without steam or water injection and operates a fuel staging process coupled with inlet guide vane modulation to reduce temperature rise across the combustor and NOx emission levels to about 25 ppmvd at 15% O_2 [Davis and Black, 2000].

A combustor inlet and outlet diameter of 364 mm and 346 mm while a total length of 795 mm was considered for engine, GX100. This data was interpolated from pictures of GE 9E DLN combustor and scaled accordingly assuming an engine size of 10m (length) by 5m (height) with 18 individual units arranged in a cannular configuration. These descriptions might not fit the perfect dimensions of the GE 9E DLN combustor and engine; however in the absence of combustor geometry data, it allows a platform for simulation and further scaling of emission results to that of a typical emission profile. Similar to GX100, a combustor diameter of 248 mm and length of 68 mm was used for engine, GX200. In both simulations, the combustor was modelled with the schematic in figure 4.3.

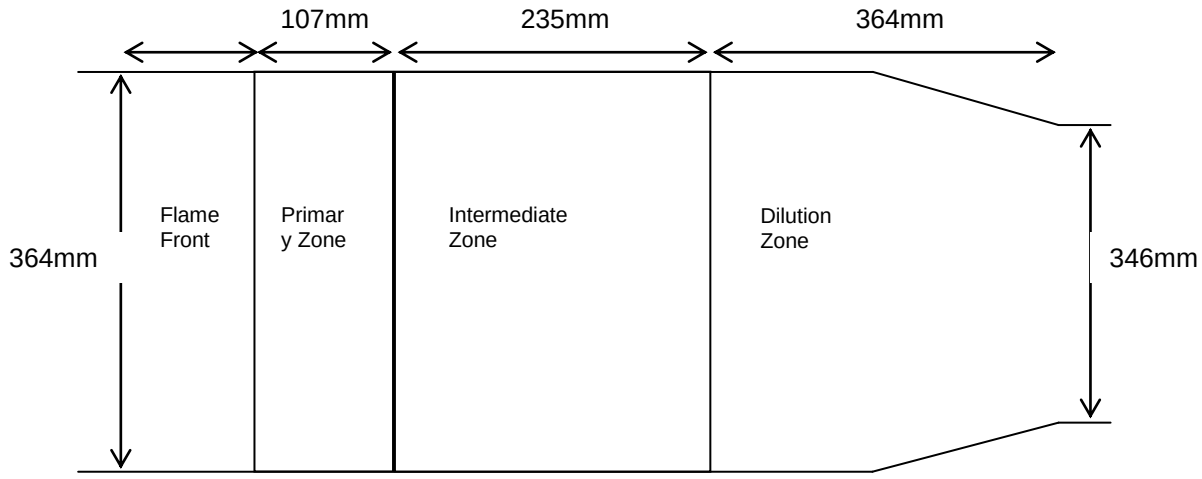

Figure 4.4.3: Simulated combustor geometry of GX100

The values used for simulating the fraction of air mass flow entering the different zones of the combustor of engines, GX100 and GX200 are presented in Table 4.3.

Table 4.4.3: Fraction of air mass flow entering the different zones of the combustor

Engine	**Combustion Zones**				
	FRAIR FF		FRAIR PZ	FRAIR IZ	FRAIR DZ
GX100	0.280		0.140	0.120	0.460
GX200	0.440		0.120	0.140	0.300
	Fuel fraction reaching FF NWR	**Air fraction going to FF core reactor**	**Comb gases fraction reaching PZ NWR**	**Fraction of FRAIR PZ going to PZ NWR**	**Fraction of FRAIR IZ going to IZ NWR**
GX100	0.17	0.60	0.15	0.20	0.20
GX200	0.15	0.60	0.20	0.20	0.20

FRAIR -Fraction of Air, FF -Flame front, PZ- Primary zone, IZ- Intermediate zone, DZ -Dilution zone, NWR -Near wall region

Fuel temperature was assumed to be 420 K to retain consistency with performance analysis; however, sensitivity analysis was carried out on a range of fuel temperatures (340-500 K).

The CO_2 emissions were calculated using equation 4.9-4.11 below and assuming a complete combustion of the fuel into CO_2 and H_2O.

$$C_xH_y + (x+ y/4)\ O_2 \rightarrow xCO_2 + y/2\ H_2O \quad (4.9)$$

Where x and y are the carbon and hydrogen compositions respectively

$$X_C = xCO_2\ (\text{mass of } CO_2 \text{ produced, that is } 44g * x \quad (4.10)$$

$$CO_2\ (\text{ppm or mg/kg fuel}) = (\text{Fuel flow rate (kg/s)} * X_C * 1000000)/\ MM \quad (4.11)$$

MM is the molecular mass of fuel derived from fuel composition

Comparative emission analysis were carried out on engine GX100 and GX200 with natural gas, conventional diesel, Jatropha biodiesel and microalgae biodiesel by inputting the chemical composition of Jatropha and microalgae biodiesel fuels (see Table 3.2 — Chapter 3) and CH_4 and $C_{12.79}H_{23.8}$ for natural gas and conventional diesel fuel. The emission model employs NASA CEA for chemical equilibrum calculations and this helps with result consistency. Analysis was carried out at fuel temperature of 420 K, ambient temperature of 288.15 K and altitude of 0 m.

4.2.2 Parametric Analysis

The NOx and CO emission results obtained from the analysis of engine GX100 were compared to typical emission profile for conventional systems, in particular MS7001EA due to lack of primary data for engine MS9001EA. This MS7001EA engine operated a conventional combustor as shown in [Davis and Black, 2000], but it is capable of operating a DLN-1 combustor similar to those of MS9001E. The results for NOx and CO emissions are presented in figures 4.4 and 4.5 respectively.

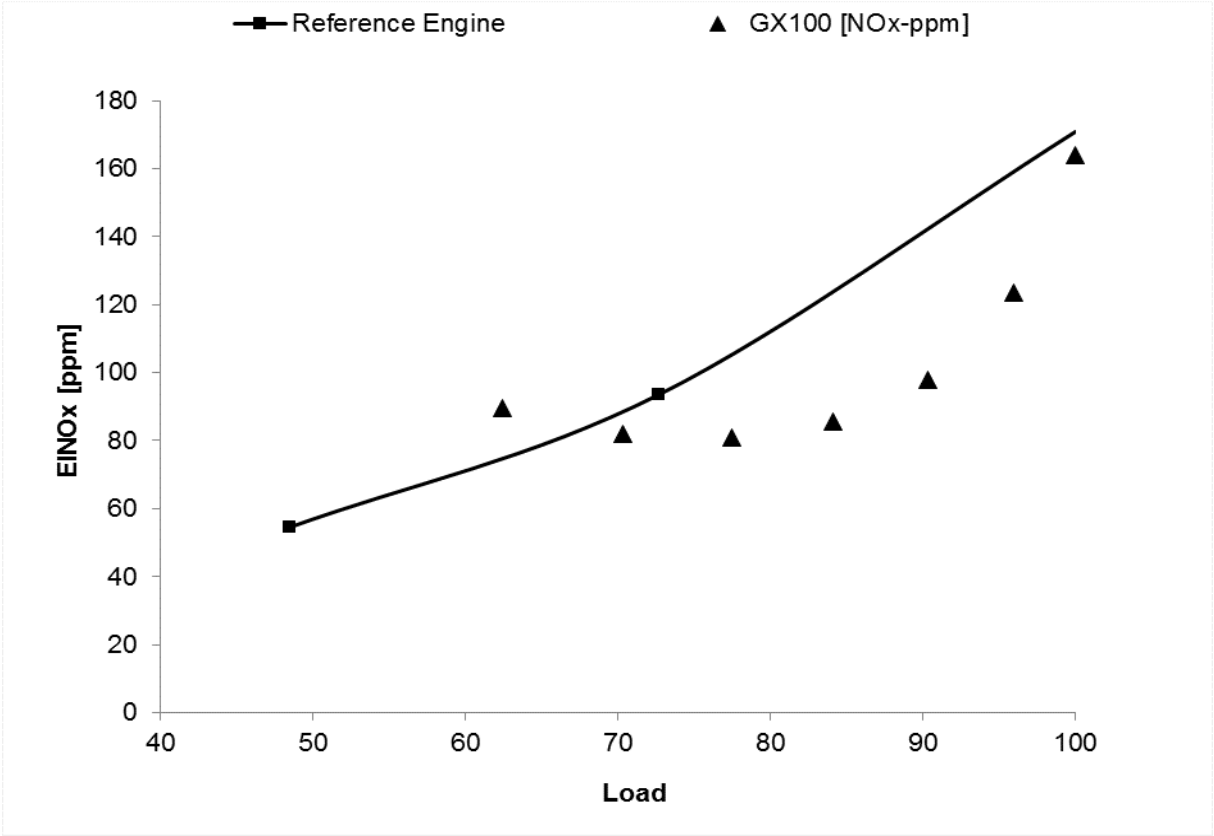

Figure 4.4: NOx emission for GX100 at vary load in comparison to the reference MS7001EA engine.

The results in figure 4.4 show that there is a decreasing trend in NOx emission of the MS7001EA (reference engine) as firing temperature reduces from 1363 K [100% load] to 813 K [25% load]. Similarly, the prediction of NOx emissions in simulated engine, GX100 show a decreasing trend as firing temperature reduces with a range of 95 ppm [54% load] to 164 ppm [100% load]. A The typical NOx emissions of MS5001P-MS9001E single shaft engines operating on natural gas and a conventional combustion without emissions control, were shown to be in the range 109 ppmvd and 162 ppmvd at 15%O_2 [Davis and Black, 2000]. The NOx results were underestimated at all load conditions and much more at certain loads than the reference engine; however, the NOx emissions are presented to compare the trends. The obvious differences in results at other load conditions asides 100% load could be attributed to the data obtained from the thermodynamic performance model, which were off-design simulations for a fixed rated engine and involves the use of generic maps in the absence of actual engine compressor and turbine maps. Since, the real combustor geometry were not used for this analysis, a correction factor of 3 has been applied to bring the results to a range similar to that of the results of MS7001EA obtained from [Davis and Black, 2000] and to allow further comparison with other fuels.

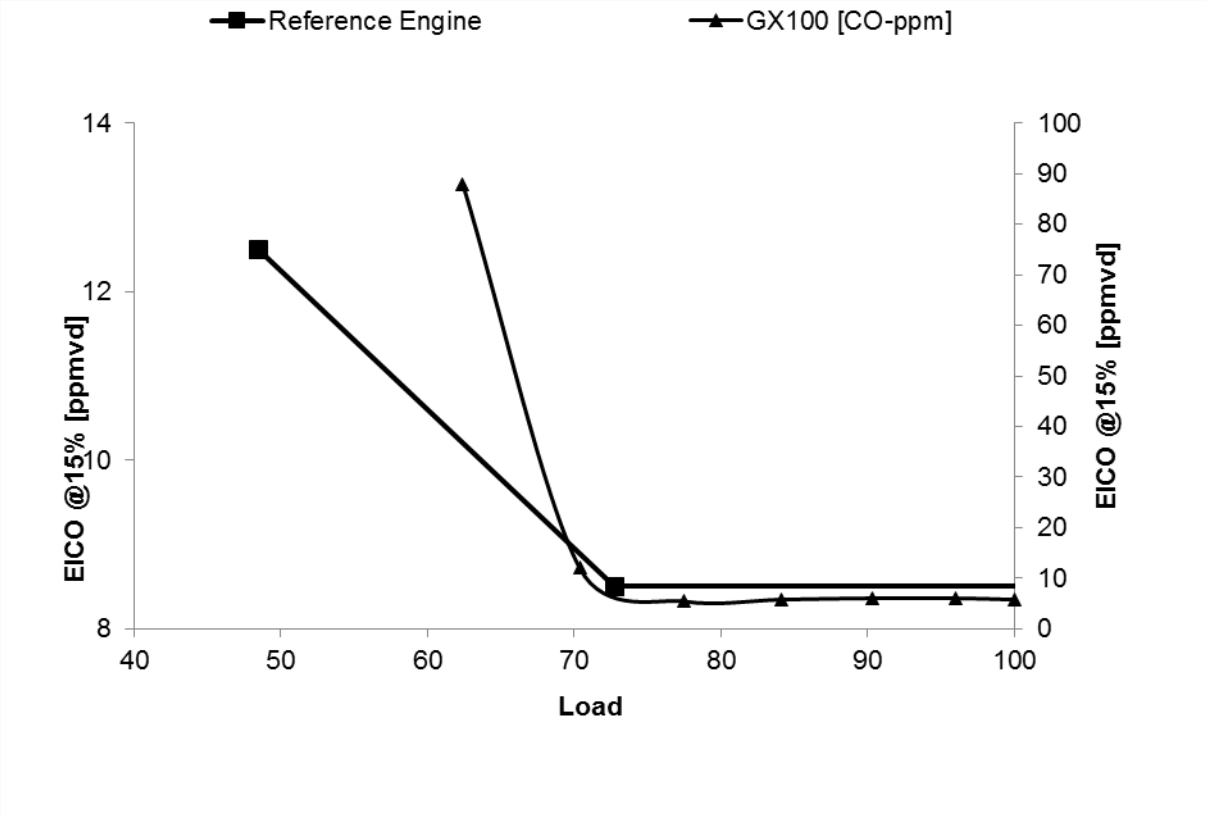

Figure 4.5: CO emission at vary firing temperature in comparison to the refernce MS7001EA engine.

Similarly, the CO emission results for engine MS7001EA show an increasing trend with values ranging from 8 ppmv [100% load] to 124 ppmv [25% load]. The CO emission of engine GX100 also increased with reduction in firing temperature. A correction factor of 0.45 was also applied to all results to obtain a range similar to that of the results of MS7001EA obtained from [Davis and Black, 2000]. This is because the results were highly overestimated. The differences in results could be attributed to the input obtained from the performance model, which is constrained by lack of availability of data of firing temperature and compressor maps.

Further NOx and CO emission analysis at fuel temperatures of 380 K to 500 K were carried out to test for sensitivity of emissions to selected parameters. The results are presented in figure 4.6 to show the variations in NOx and CO emissions.

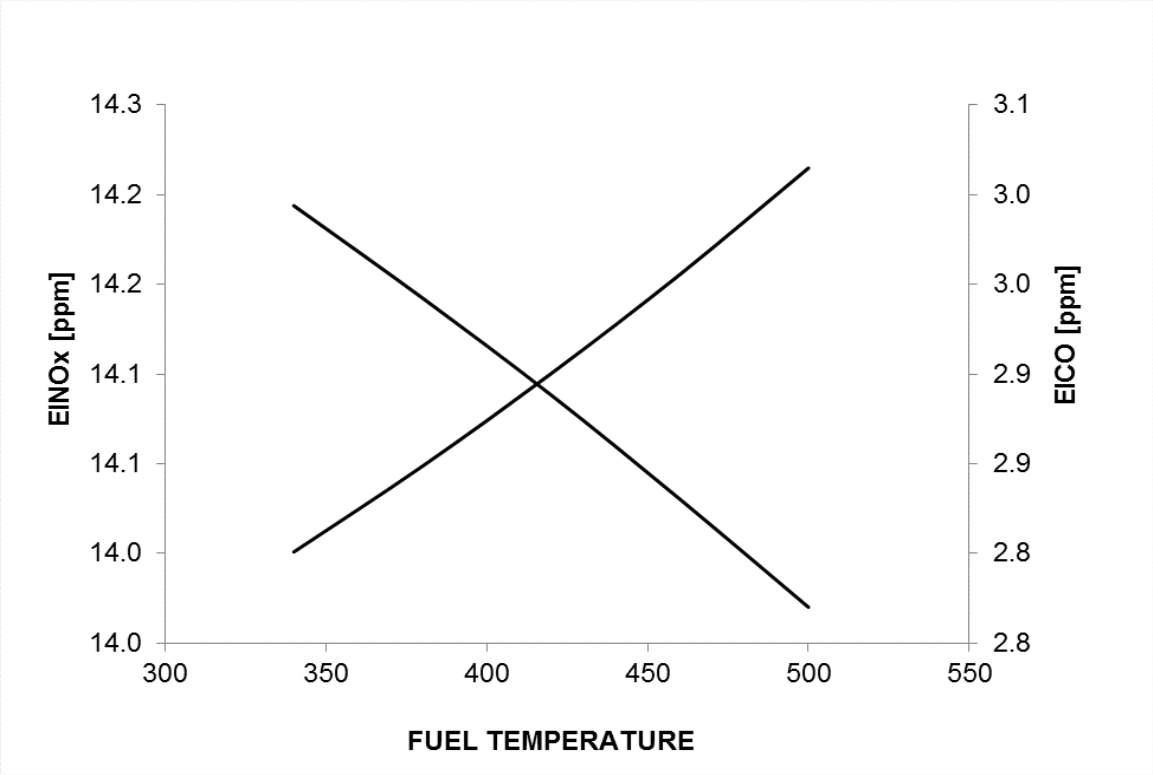

Figure 4.6: Emission analysis at varying fuel temperatures

The results shown in figure 4.6 demonstrate a decrease of about 2% in CO emission and increase of about 0.1% in NOx emission for every 40 K rise in fuel temperature. Such trends are expected, because at hotter fuel temperatures, fuels gain more energy to burn quickly. This increases the burning rate in the primary zone, reduces residence time, consequently, and reduces the emission of CO. However, this is at the detriment of NOx emission, because flame temperatures are relatively higher under such conditions. Hashimoto et al. 2009 have shown a relationship between kinematic viscosity (KV) and fuel temperature, which involves a reduction in KV as fuel temperature increases. This is particularly important to liquid fuels, which require a form of vaporization for complete combustion to take place.

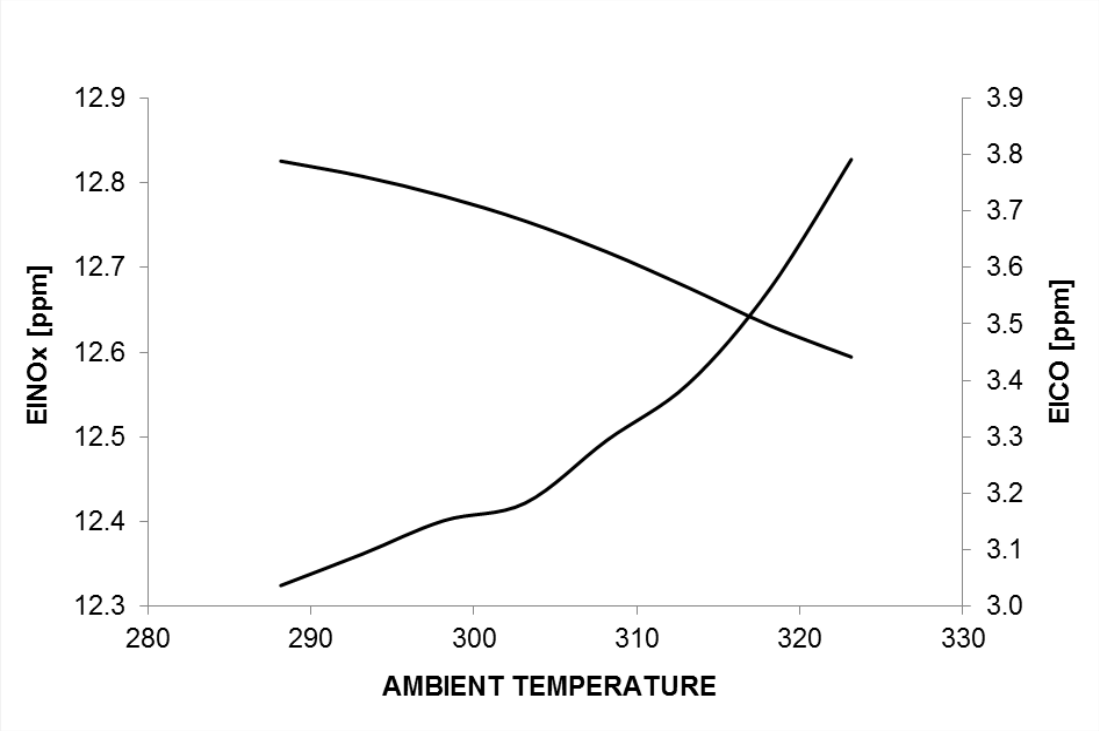

Figure 4.7: Emission Analysis at Varying Ambient Temperatures

The NOx and CO emission analysis at varying ambient temperatures of 288 K (15^{o}C) to 323 K (50^{o}C) were carried out to test for sensitivity of emissions to ambient temperatures. The results are presented in figure 4.7 to show the variations in NOx and CO emissions. There is a slight decrease and increase in CO and NOx emission as ambient temperatures increases. Such trends are also expected, because it increases the flame temperatures of the combustor. This increases the burning rate in the primary zone, reduces residence time, consequently, relatively higher NOx emissions but reduced CO emissions. Similar studies have been carried out on engine GX200 and results are presented in Appendix III.

These sort of comparisons are required to determine the boundary of the model for further fuel, engine and changing ambient condition analysis. Although, this is not adequate for model validation; it guides the simulation and analysis in the right direction. Further parametric studies using varying combustor diameter of 158 to 558 mm, length of 312 to 1112 mm, combustor air inlet temperatures, and relative humidity for similar engine with power output of 260 MW and air mass flow of 641 kg/s have been carried out by [Samaras et al. 2011].

4.3 Fuel Analysis

The results for NOx and CO emissions are presented in figures 4.8 and 4.9 respectively, while that of CO_2 emissions are presented in Figure 4.10.

4.3.1 NOx Emission

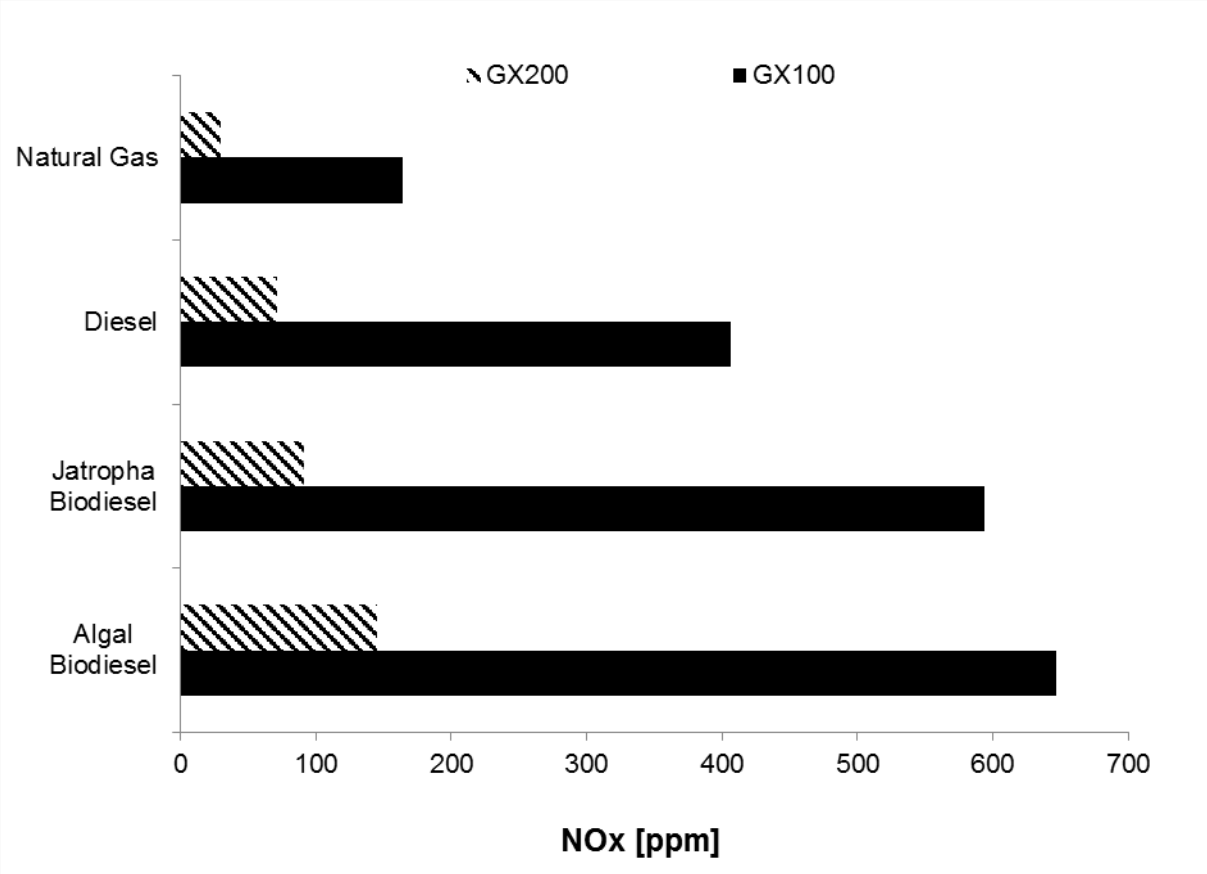

Figure 4.8: NOx emissions for the different fuels [conventional diesel, Jatropha biodiesel, algal biodiesel and natural gas]

Assuming constant air composition, equilibrium reaction, no dissociation of products and uncontrolled combustion, the results in figure 4.7 indicate increase in NOx emissions by 164 ppm for natural gas, 406 ppm for conventional diesel fuel, 594 ppm and 646 ppm for Jatropha and microalgae biodiesel fuels respectively. Alne, (2007) reports a NOx range of 229 ppm for gas fired-and 346 ppm for 29 MW distillate fired gas turbine. Same report suggest NOx emissions are within the range of 180 ppm and 400 ppm for conventional combustion of liquid fuels in gas turbines, assuming no emission control. Here, the NOx emissions of the liquid fuels varied between 250 ppm [diesel] and 480 ppm [algal biodiesel], provided the NOx emissions for the natural gas is 164 ppm. These results are overestimated when compared to the NOx emission range of 165 ppm to 279 ppm in [Davis and Black, 2000] for gas turbines operating on distillate fuel without abatement.

The differences in NOx emissions can be attributed to varying carbon content of the fuels. The carbon compositions of the fuels are in the increasing order of natural gas, conventional diesel fuel, Jatropha- and microalgae-biodiesel. This relatively high carbon composition of biodiesel fuels increases the products of combustion —mainly CO_2 and in turn, this increases the flame temperature, hence increased NOx emissions. Assuming the carbon composition of the conventional diesel fuel was similar to those of the biodiesel fuels, the NOx emission of the conventional diesel fuel could have been higher, but this is not the case. Lefebvre and Ballal, [2010] made note of operating conditions other than flame temperature, when thermal NOx emissions could significantly increase and this involve the combustor residence time. Residence time increases NOx emissions in fuel-air mixtures with ϕ equals to or above 0.4. Liquid fuels would also tend to promote the formation of envelope flames and fuel drops in the combustion zone and this initiate NOx formation. The higher tendency for biodiesel fuels to yield higher NOx emissions also involve properties such as LHV of fuel, in which higher quantity of fuel (fuel flow) brings about increased combustion temperature and NOx emissions. The chemical properties of the liquid fuels which are primarily composed of unsaturated carbon-carbon double bonds could increase adiabatic flame temperatures, thus increasing NOx emissions.

Later heavy duty engines, particularly GE engines are equipped with technologies to abate increasing NOx emissions using the advanced DLN combustion. Other methods of reducing NOx emissions include: a) steam injection, ii) water injection iii) selective catalytic reduction (SCR). These engines are equipped with capacity to limit NOx emissions to 15 ppm over a wide range of load from 50 to 100%. However, these are outside the scope of this study.

4.3.2 CO Emission

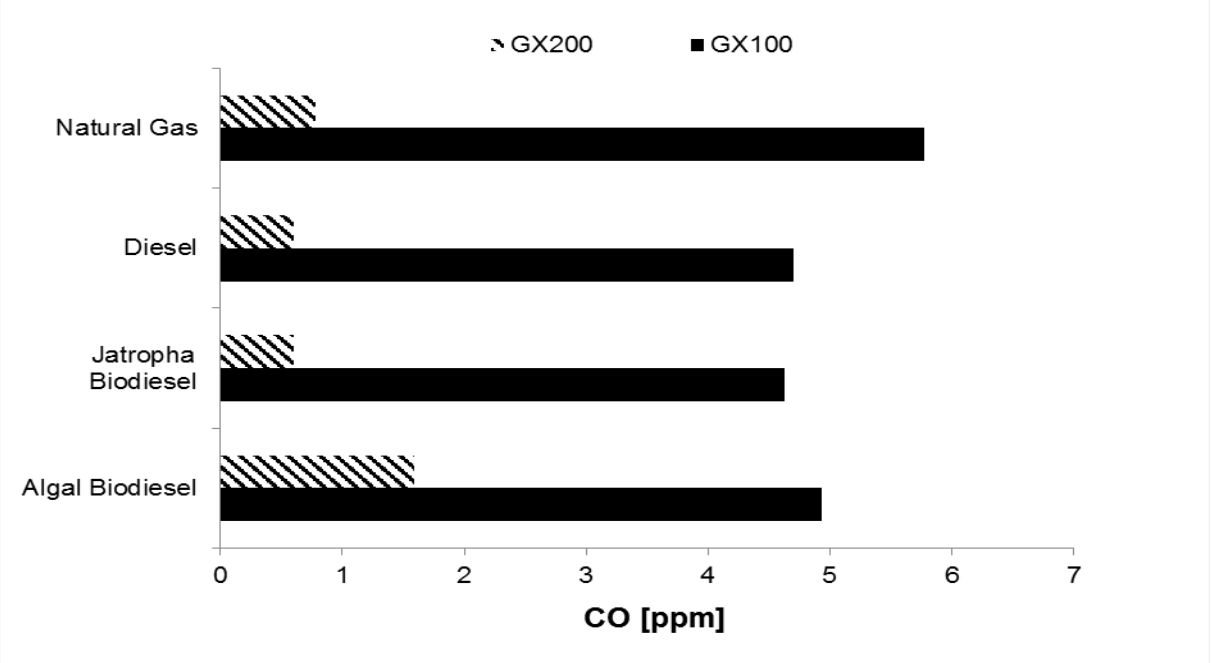

Figure 4.9: NOx emissions for the different fuels [conventional diesel, Jatropha biodiesel, algal biodiesel and natural gas]

As mentioned earlier, CO is formed as a result of incomplete combustion of carbon based fuel. Although, the carbon content of the fuel plays a role, the operating conditions of the combustor have a large effect on CO emissions. In this study, combustion is modelled as a diffusion flame combustor, a process that forces air to mix vigorously with simultaneous combustion. This condition causes a near stoichiometric gas mixture that promote conversion of CO to CO_2, but increases NOx emissions. For engine GX100, the use of Jatropha biodiesel brought about the lowest CO emission with value reducing by 1.1 ppm as compared to the natural gas case, followed by conventional diesel fuel and then algal biodiesel, all in the range of 5 ppm. These results [see figure 4.9] are similar to those reported in [Davis and Black, 2000] and less than 10 ppm as suggested by [Alne, 2007] for conventional combustion. This diffusion flame combustor type could account for the low CO emission range observed in this study, however the differences among the fuel types can be accounted to the effect of residence time. The total mean time for each of the combustion reaction are 2.020 ms, 2.162 ms, 2.171 ms and 2.172 ms. The low residence time for the microalgae biodiesel with very high fuel flow rates would result in insufficient combustion of CO to CO_2. It is also possible that the fuel-lean condition in the natural gas case, which had a high air-fuel-ratio brought about a dissociation of CO_2 but this does not apply to all the other fuels.

4.3.3 CO_2 Emission

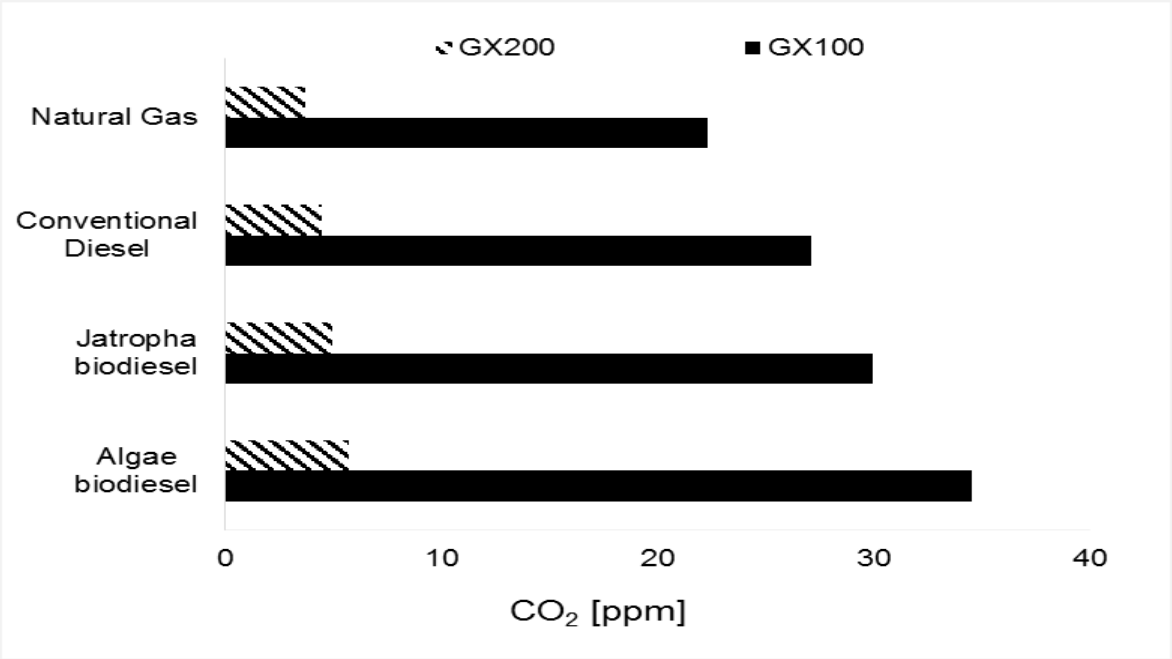

Figure 4.10: CO_2 emissions for the different fuels [conventional diesel, Jatropha biodiesel, algal biodiesel and natural gas]

The CO_2 emissions have been estimated from the carbon composition of the fuels, assuming there is complete combustion. This is the maximum theoretical carbon emission that could be reached. For engine GX100, the use of natural gas brought about the lowest CO_2 emission of 22.3 x 10^6 ppm, followed by conventional diesel fuel and Jatropha biodiesel and the highest CO_2 emission was from microalgae biodiesel with a value of 34.5 x 10^6 ppm. The differences among the fuel types can only be attributed to the carbon content the fuels, but more importantly to the fuel flow rates. Here, the fuel flow rates were 8.12 kg/s, 8.53 kg/s, 9.45 kg/s and 10.89 kg/s for natural gas, conventional diesel fuel, Jatropha biodiesel and microalgae biodiesel respectively. This implies that the high carbon-containing fuel with higher fuel flow rate would bring about the highest level of CO_2 emissions. Similar results were observed in engine GX200, however at a lower degree. Here, the fuel flow rates were in the range of 1.34 kg/s [natural gas] to 1.80 kg/s [microalgae biodiesel] and CO_2 emissions in the range of 3.69 x 10^6 ppm [natural gas] to 5.71 x 10^6 ppm [microalgae biodiesel]. The biodiesels are of advantage over the fossil fuels because the CO_2 emissions are biogenic, that is sequestered from the atmosphere by plant via photosynthesis, a natural carbon source or from a carbon based material. In environmental life cycle assessments, this type of carbon released during fuel combustion is considered neutral and of no environmental consequence.

4.4 Conclusion

The CO and NOx emission characteristics of engines, GX100 and GX200 operating natural gas, microalgae biodiesel, Jatropha biodiesel, and conventional diesel fuel have been evaluated using a physics-based emission model. Also, CO_2 emissions have been estimated from stoichiometric mass balance oxidation reaction of the fuels, assuming complete fuel combustion. A summary is provided below:

1. The NOx emissions for natural gas, conventional diesel fuel Jatropha and microalgae biodiesel fuels were 164 ppm, 406 ppm, 594 ppm and 646 ppm respectively. The differences in NOx emissions can be attributed to varying carbon content of the fuels, which increases the products of combustion, subsequently the flame temperature. The higher tendency for biodiesel fuels to yield higher NOx emissions also involve fuel properties such as LHV, in which the higher quantity of fuel (fuel flow rate) increases the combustion temperature; hence increased NOx emissions.

2. The CO emissions which is formed as a result of incomplete combustion were higher for microalgae biodiesel. Apart from the high carbon content of this fuel, operating conditions of the combustor could also have complemented the relatively high CO emissions. Here, the mean time for reaction was at its minimum, leading to insufficient combustion of CO to CO_2. It is also possible that the fuel-lean condition in the natural gas case could have resulted in the dissociation of CO_2.

3. The use of natural gas brought about the lowest CO_2 emission, followed by conventional diesel fuel and Jatropha biodiesel and the highest CO_2 emission was observed with microalgae biodiesel. The differences among the fuel types can only be attributed to the carbon content the fuels and the fuel flow rates. Here, the fuel flow rates were 8.12 kg/s, 8.53 kg/s, 9.45 kg/s and 10.89 kg/s for natural gas, conventional diesel fuel, Jatropha biodiesel and microalgae biodiesel respectively.

4. Among the two biodiesel cases, the use of Jatropha biodiesel is recommended as lower NOx and CO emissions are observed.

5. The biodiesels are of advantage over the fossil fuels because the CO_2 emissions are biogenic. This type of carbon released during fuel combustion is considered neutral and of no environmental consequence from a life cycle perspective.

4.5 Further Work

The emission analysis in this study has been conducted on a conventional combustor type technology. Recent combustor technology employs advanced combustor type that can abate increasing NOx emissions even with increasing firing temperatures. These are outside the scope of this study, however, it would be interested to upgrade the emission model for this capability and to examine these fuels under varying operating conditions. The current model would also require further development and validation to include other important GHG emissions and fuel types including oxygenated fuels.

4.6 References

[1] Alne, K. S. 2007. Reduction of NO_x Emissions from the Gas Turbines for Skarv Idun. MSc Thesis Submitted to the Department of Energy and Process Engineering, Norwegian University of Science and Technology. Available on http://www.diva-portal.org/smash/get/diva2:536427/FULLTEXT01.pdf

[2] Davis, L.B. and Black, S.H. 2000. Dry Low NO_x Combustion Systems for GE Heavy-Duty Gas Turbines. GE Power Systems GER-3568G

[3] Department of Energy and Climate Change (DECC). 2014. 2013 UK Greenhouse Gas Emissions, Provisional Figures and 2012 UK Greenhouse Gas Emissions, Final Figures by Fuel Type and End-User. Available on https://www.gov.uk/government/uploads/system/uploads/attachment_data/file/295968/20140327_2013_UK_Greenhouse_Gas_Emissions_Provisional_Figures.pdf Last accessed on 05/02/2015

[4] Glaude, P.A., Fournet, R., Bounaceur, R. and Molière, M. 2010. Adiabatic flame temperature from biofuels and fossil fuels and derived effect on NOx emissions. *Fuel Processing Technology* 91(2): 229-235.

[5] Glaude, P.A., Sirjean, B., Fournet, R., Bounaceur, R., Vierling, M., Montagne, P. and Moliere, M. 2014. Combustion and oxidation kinetics of alternative gas turbines fuels. *Proceedings of ASME* Paper No. GT2014-25070, pp. V03AT03A001

[6] Lefebvre, A.H. and Ballal D.R. 2010. Gas Turbine Combustion: Alternative Fuels and Emissions. 3rd Ed. Philadelphia, PA: Taylor and Francis.

[7] Razak, A. M. Y. 2007. *Industrial Gas Turbines: Performance and Operability.* Woodhead Publishing Limited

[8] Samaras, C., Di Lorenzo, G., Kalfas, A.and Pilidis, P. 2011. An Emissions Model for NOx and CO Emission Trends from Industrial Gas Turbines. *In* International Gas Turbine Congress, Vol. 10. , Osaka, Japan.

[9] United States Energy Information Administration (EIA). 2011. Emissions of greenhouse gases in the United States 2009. rgy Information Administration, Report Number: DOE/EIA-0573(2009). Available on http://www.eia.gov/environment/emissions/ghg_report/pdf/0573(2009).pdf Last accessed on 05/02/2015

Chapter 5

5. ECONOMIC ANALYSIS OF BIODIESEL FIRED POWER PLANTS

The focus of this chapter is to examine the economic performance of microalgae biodiesel- and Jatropha biodiesel-fired power plants, in comparison to natural gas- and conventional diesel-fired plants, using a wide range of economic indicators. The chapter begins with an overview on the economics and other aspects of cost that affect the use of biodiesels in power plant. The method of assessing the economics of power plants for the different fuels is described. Analyses are carried out to examine the economic performance of power plants as it relates to fuel utilization. These are examined under a current and future possible cost situation for base load operation in Nigeria. The results of the economic assessment of the different fuels are presented, with the view of proposing a mechanism by which biodiesels can be integrated in power plants and for power generation in Nigeria or similar developing countries. Further sensitivity analysis is carried out to evaluate alternative scenarios and how they affect the overall economic performance, in comparison to the baseline study.

5.1 Introduction

There are many benefits that countries, especially developing ones can gain from renewable fuels like Jatropha and microalgae biodiesels. Apart from the possibilities that opens for economic growth and development across the country, especially for rural communities; opportunities are available for independent power producers to generate power to off-grid users and local businesses. This is only achievable from engines and fuels with good economic performance.

The economics of any power plant depends on the capital costs, but much more on the operational and maintenance (O&M) costs. The O&M cost is largely constituted by fuel cost, which in turn is a function of fuel market price, engine's specific fuel consumption and the residual energy per kg of fuel. Furthermore, the economic performance of power plants depends greatly on specific site and other local conditions such energy demand, upfront capital cost of alternatives, carbon costs, electricity prices and fossil fuel prices. Broadly speaking, the cost of production of biodiesel fuels is said to be much higher than that of conventional diesel fuel [Wegstein et al. 2010; Christi, 2007]. These costs have limited the use of biodiesels in gas turbines and for power generation, as they increase

the cost of the energy generated. However, a simple comparison of power plants based on market fuel prices or capital costs and without the consideration of engine and fuel characteristics, engine operating conditions, emissions, fuel economy and other techno-economic parameters, is misleading.

Thus, this study aims at examining the techno-economic performance of microalgae and Jatropha biodiesel fired gas turbine power plants, in comparison to natural gas and conventional diesel fired plants, using a wide range of economic indicators. The average costs of electricity for a typical homeowner in Africa, in particular, Nigeria and for businesses are estimated. The cost of electricity and the economic performance of the power plants are compared under local conditions. Furthermore, mechanisms are proposed to enable the integration of biodiesels in existing or new power plants and to achieve good economic performance. It is expected that the outcome of this study would further broaden the perspectives on the use of biofuels in gas turbines, and much more, create additional knowledge on the cost implications of the use of biodiesel fuels in Nigeria and/or other developing countries. This information could assist policy makers, end-users, investors, financiers, plant operators and equipment manufacturers. More importantly, some of the economic measures can be used to reject, accept or estimate the risk associated with biodiesel-fired power plant projects.

5.2 Methodology

The economic assessment of natural gas-, diesel-, microalgae biodiesel- and Jatropha biodiesel–fired power plants were carried out using a series of integrated modules as illustrated in figure 5.1. These include: i) performance module, ii) fuel module iii) blade geometry module coupled with lifing module and iv) emission module, and all modules integrated in an economic model. Figure 5.1 illustrate how the different sub-modules were coupled together in an economic model.

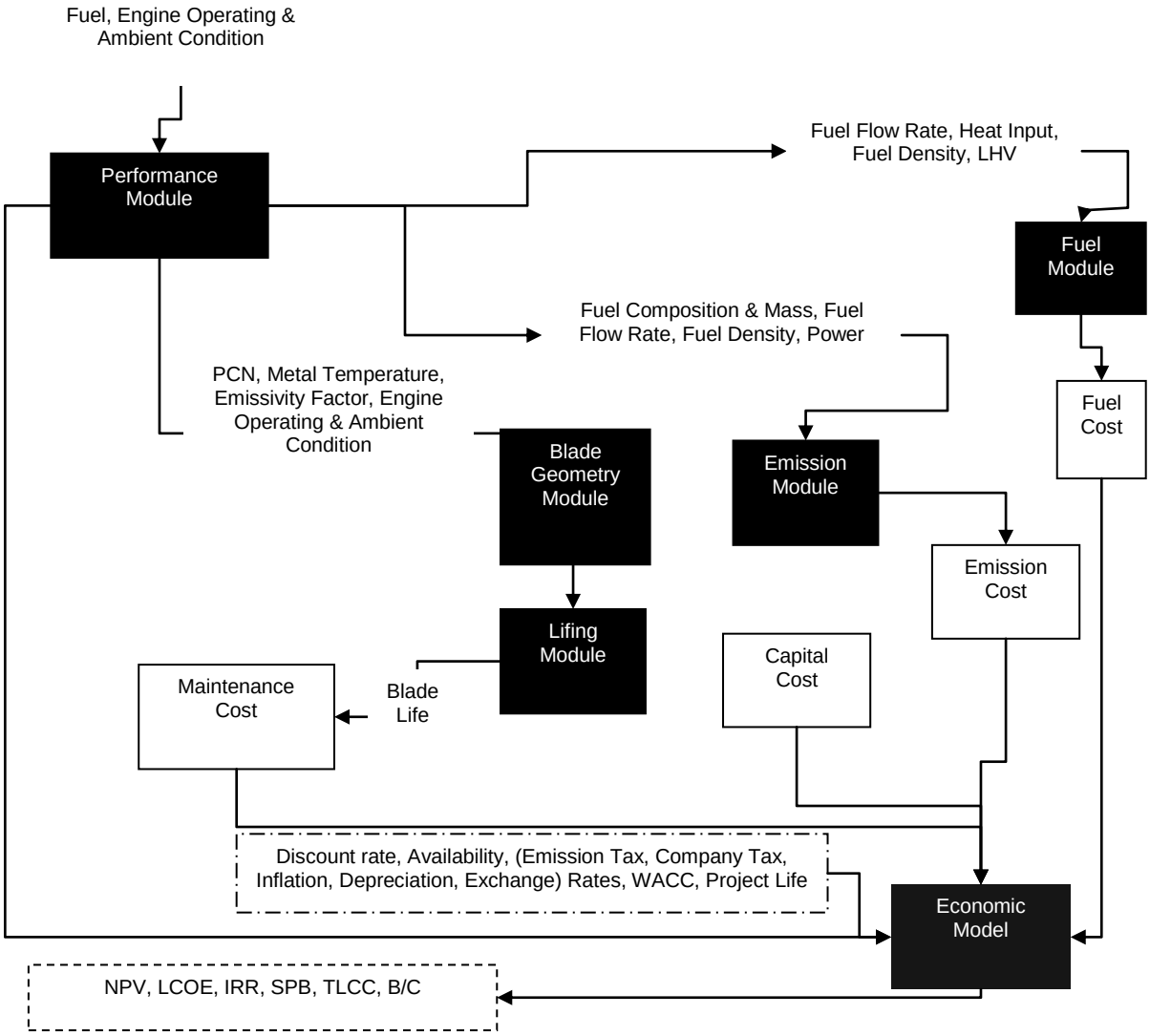

Figure 5.1: Simplified flow diagram of the economic model

The outcome of the economic model was translated to the following economic measures: i) Levelized Cost of Electricity (LCOE), ii) Net Present Value (NPV) iii) Total Life Cycle Cost (TLCC), iv) Internal Rate of Return (IRR), v) Simple Payback Period (SPB), vi) Benefit-to-Cost Ratio (B/C) vii) Revenue Requirements (RR). These measures were employed for economic analysis by [Kost et al. 2013; Leme et al. 2014, Strogen et al. 2013], but a detailed overview of these economic measures and application in energy technologies is described in [Short et al. 1995].

Three engines as simulated and validated in Chapter 3 were used in assessing the economic performance of fuels for base load operation in a current situation and future cost analysis. Hence, some of the inputs used in this chapter were obtained from performance and emission analyses in previous chapters but are listed with others in Tables 5.1 to 5.4. The economic analysis was carried out using a scenario based approach and embrace factors such as capital cost, emission cost, deficit energy cost, maintenance cost (fixed and variable) and fuel cost. The following sub-sections describe how the modules were used for estimating the cost associated to fuel utilization.

Table 5.1: Inputs and Outputs for Lifing Module

Parameters	Units	Values
A- Compressor		
Compressor inlet mass flow, m_C	kg/s	415.00
Compressor inlet stagnation temperature, T_2	K	288.15
Compressor inlet stagnation pressure, P_2	Pa	101325.00
Compressor outlet stagnation temperature, T_3	K	637.67
Compressor outlet stagnation pressure, P_3	Pa	1263928.05
Compressor efficiency $_{isentrophic}$	%	86
Coolant mass flow, m_{CO}	%	1
Coolant stagnation temperature, T_{CO}	K	637.67
Gas Constant, R	J/kg.K	287
Universal Gas Constant	J/mol.K	8.31
B-Turbine		
Mass flow, m_T after NGV	kg/s	423.12
NGV inlet stagnation temperature, T_{34}	K	1378
NGV inlet stagnation pressure, P_{34}	Pa	1200731.65
Rotor outlet stagnation temperature, T_4	K	839.52
Rotor outlet stagnation pressure, P_4	Pa	105522.89
Turbine efficiency, η_T	%	88
C- Thermodynamic Properties		
Gamma, γ_H	J/kg.K	1.32
Cp_H		1193.37
Gamma, γ_C	J/kg.K	1.39
Cp_C		1013.70
Temperature drop, ΔT_{34}	K	538.87
Turbine power	MW	272.10
Compressor, ΔT_{23}	K	349.52
Mach No, M		0.30
V/sqrt(T)		5.791
T/t		1.0142
P/p		1.0606
1000q		20.464
Velocity Coefficient		1.069
Flow Coefficient		1.148
g_{GC}		0.093
A_{NN}		0.123
D. Blade geometry		
Tip, average radius, r_T	m	0.723
Hub, average radius, r_H	m	0.605
mid shaft-mid blade distance, r_{MB}	m	0.664
Blade Height, mid-root blade section, h_{MR}	m	0.059
Distance from CG (rotation axis for root-mid sec) d_{CGMR}	m	0.634
Cross section area for root-mid blade, A_{SECMR}	m^2	0.403
Hub to tip ratio, HTR		0.840
HPT RPM		11250
Emissivity factor, ε		0.50
Blade density, ρ_H	kg/m^3	8518
shroud parameter	m	1.2
T_B	K	1008.03
ω		1178.10
Centrifugal force (root-mid blade), CF	N	178.8
σ	mpa	405.4
LMP		24.70
T_F	hours	31860
L_C	years	3.0

5.2.1 Lifing Module

The inputs for this module are presented in section A and B (Table 5.1). These were obtained from previous performance analysis and include inlet mass flow, inlet temperatures and pressures, isentropic efficiencies at the compressor inlet and outlet, as well as the NGV inlet and rotor outlet at the turbine section. Other parameters include coolant mass flow, temperatures and gas constants. These were used to calculate the thermodynamic properties of the gas, in particular specific heat ratio (ɣ), specific heat capacity (c_P), and the turbine temperature drop using equations 5.1-5.4.

$$\Delta T_{34} = T_{34}\text{-}T_4 \quad (5.1)$$

$$\text{Specific heat ratio, } \gamma = \frac{\ln\left(\frac{P_4}{P_{34}}\right)}{ln\left(\frac{P_4}{P_{34}}\right) - ln\left(1-\left(\frac{\Delta T_{34}}{\eta T * T_{34}}\right)\right)} \quad (5.2)$$

$$C_p = \frac{\gamma R}{(\gamma - 1)} \quad (5.3)$$

$$\text{Turbine Power (MW)} = m_T * C_P * \Delta T_{34} \quad (5.4)$$

Where: R is Gas Constant, 287 J/kg.K

Furthermore, annulus area (A_{NN}), the velocity and flow coefficients were deduced using equations 5.5-5.13, assuming axial inlet flow with Mach number of 0.3, constant axial velocity and mean diameter and, 50% reaction at the blade mid-height. The outcomes of these calculations are presented in Section C (Table 5.1).

$$\frac{T}{t} = 1 + \left(0.5 * (\gamma - 1)\right)M^2 \quad (5.5)$$

$$\frac{V}{\sqrt{T}} = M * \sqrt{R\gamma)} * \sqrt{1/\left(\frac{T}{t}\right)} \quad (5.6)$$

$$\frac{p}{p} = \frac{T}{t}^{\left(\frac{\gamma}{\gamma-1}\right)} \quad (5.7)$$

$$1000Q = 1000 * M * \sqrt{\left(\frac{\gamma}{R}\right)} * \left(\frac{T}{t}^{\left(-0.5\left(\frac{\gamma+1}{\gamma-1}\right)\right)}\right) \quad (5.8)$$

$$1000q = \frac{p}{p} * 1000Q \quad (5.9)$$

$$\text{Velocity Coefficient, } \psi = \sqrt{\left(\frac{1}{\left(1+\left(\left(\frac{\gamma-1}{2}\right)M^2\right)\right)*\left(1-\frac{\gamma-1}{\gamma+1}\right)}\right)} \quad (5.10)$$

$$\text{Flow Coefficient, } \varphi = \left(\left(\psi\left(\frac{\gamma+1}{2}\right)\right)^{\frac{1}{\gamma-1}}\right) * \left(\left(1-\left(\frac{\gamma-1}{\gamma+1}\psi^2\right)\right)^{\frac{1}{\gamma-1}}\right) \quad (5.11)$$

$$\text{Gas dynamic constant, } g_{GC} = \left(\sqrt{\left(\left(\frac{2}{\gamma+1}\right)^{\frac{\gamma+1}{\gamma-1}}\right)\left(\frac{\gamma}{R}\right)}\right.$$

(5.12)

$$A_{NN} = \frac{m_T\sqrt{T_{34}}}{P_{34} * g_{gc} * \psi} \quad (5.13)$$

5.2.2 Blade Geometry Module

The hub to tip ratio (HTR) used to define the geometry of the blade was deduced from [Hong et al. 2005], and applies to the first stages of the high pressure turbine blades. Other parameters such as hub, tip and mean radius, as well as the blade height and cross sectional area for root-mid blade section, were derived using equations 5.14 to 5.19 and the outcome are presented in section D (Table 5.1). These parameters as well as those obtained from the lifing module were used for hot end gas path sizing.

$$\text{Tip diameter, } r_T = \sqrt{\left(\left(\frac{4Ann}{\pi(1-HTr^2)}\right)\right)} \quad (5.14)$$

$$\text{Hub diameter, } r_H = r_T * HTR \quad (5.15)$$

$$\text{Mid-shaft-to-mid blade distance, } r_M = 0.5\,[r_T + r_H] \quad (5.16)$$

Blade Height, mid-root blade section, $h_{MR} = r_M - r_H$ (5.17)

Distance from CG (rotation axis for root-mid sec), $d_{CGMR} = r_H + 0.5\, h_{MR}$ (5.18)

Cross section area for root-mid blade, $A_{SECMR} = 0.5\, [r_M^2 + r_H^2]$ (5.19)

Since, the first stage of the rotor blade for GE 9E class engines uses directionally solidified (DS) GTD111, a nickel alloy material that can withstand high firing temperatures, stresses and varying operating conditions [Schilke, 2004]; the blade density was calculated using equation 5.20 with material composition in Table 4.1 (Appendix IV). This equation is said to be insensitive to Cobalt (Co) and Chromium (Cr) and has been validated by comparing measured densities of the sample casting to the calculated densities, [Biondo et al. 2010].

Density of Turbine Blade Material (GTD 111):

[0.307667639+ (% Mo * 0.000452137) + (% W * 0.001737591) - (% Al * 0.004497133) - (% Ti * 0.001240936) + (% Ta * 0.002133375)] * 27679.9047 (5.20)

Where: 27679.9047 is a conversion factor from lb/in3 to kg/m3, % Mo is the percentage by Weight of Molybdenum, % W is the percentage by Weight of Tungsten, % Al is the percentage by Weight of Aluminum, % Ti is the percentage by Weight of Titanium, % Ta is the percentage by Weight of Tantalum.

The blade life was deduced using equations 5.21-5.26. Here, a reference blade life was set at 26280 hours for the baseline study, while further analyses were deduced in relation to the reference point. Assumptions include emissivity factor of 0.5, design point rotational speed of 11250 rpm, carefully selected to develop a reference point for the engine blade. Typically, the GTD111 DS blade material is coupled with advanced cooling technologies and protective coatings for effective cooling and to extend the blade creep life and tensile strength while increasing its capacity to endure substantial level of stress. Since, the emissivity factor of 0.5 was assumed; further analyses were carried out to assess the sensitivity of the study to increasing or decreasing emissivity factor.

Using emissivity factor and rotational speed, the metal blade temperature was estimated with equation 5.21 while the estimation of the centrifugal force acting on the blade at the mid-root section was achieved with equation 5.23.

$T_b = T_{34} - \varepsilon^*(T_{34} - T_3)$ (5.21)

$$\omega = \frac{2\pi N}{60} \quad (5.22)$$

Centrifugal force (root-mid blade), $CF_{mr} = \frac{\rho\ hmr\ \omega^2\ dCGmr\ Asecmr}{1000000}$ (5.23)

$$\sigma = \frac{CF_{mr}}{r_m{}^2} \quad (5.24)$$

$$t_f = 10^{\left(\frac{1000LMP}{Tb}\right)-20} \quad (5.25)$$

The Larson Miller Parameter (LMP) was extrapolated from figure 5.2 using the value of centrifugal stress obtained from equation 5.23-24.

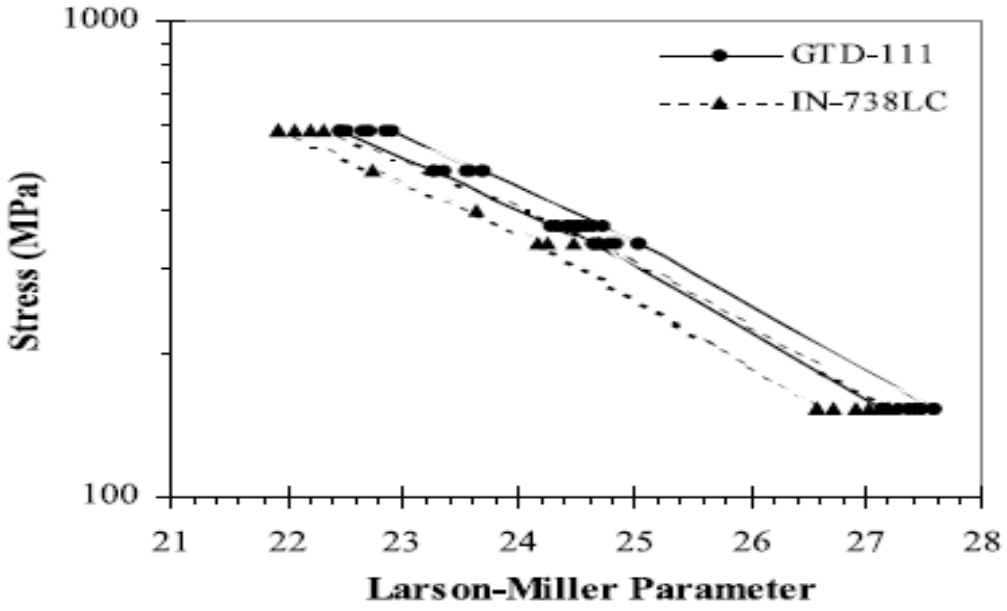

Figure 5.2: Larson–Miller parameter diagram for GTD-111 and other superalloys [Sajjadi et al. 2002]

The total blade life was then calculated from the time to failure (t_f) with application of a safety factor (S_f) of 1.21, a value selected to achieve a design reference point for analysis (equation 5.26).

$$L_{cn} = \frac{tf}{Sf} \quad (5.26)$$

Thus, blade life for baseline study is 3 years (see Table 5.1).

For further fuel analysis and to allow a comparison among the different fuels and to the baseline, creep factor, which is a ratio of the nominal blade life to the reference state (design or a reference point), was obtained using equation 5.27.

$$\text{Creep Factor, CF} = \frac{L_{cn}}{L_{cref}} \quad (5.27)$$

This creep factor was used to estimate a maintenance schedule using equation 20.

Maintenance Schedule = Plant Life (PL)/(AOH*Creep Factor) (20)

Thus, the baseline study has a creep factor of 1. This means the nominal creep life is equal to the creep life at the reference or design point (ISO condition) and applies to a single operating point. Outside the reference design condition, the creep factor reduces below 1, due to the operation and exposure of the engine to thermal stress and mechanical load. Hence, at condition other than the reference point, creep factor would be less or above 1. A creep factor above 1 indicate that the engine is operated optimally such that there is increase in component life as compared to the reference point while a creep factor below 1 mean that the engine is operated under conditions that would minimize the life of the engine components, as in this case, the HPT blades. This information is important to determine the hours and remaining life of component parts and to determine the possible maintenance cost that could be incurred. In typical plants, this is also used develop a maintenance plan for reduced operation and maintenance costs.

6.1.1.1. Maintenance Cost

The maintenance cost is estimated from the remaining blade life, an output of the lifing model and using equations 5.28-5.35.

Maintenance (M) Cost/annum= M Cost $_{\text{variable/annum}}$ + M Cost $_{\text{fixed/annum}}$ (5.28)

M Cost $_{\text{fixed/annum}}$ = MF_F * Installed capacity (5.29)

M Cost $_{\text{variable/annum}}$ = (Unplanned M Cost + Planned M Cost) per annum (5.30)

Planned M Cost = (MF_V * Installed capacity * AOH * NPMS)/PL (5.31)

Unplanned M Cost = (MF_V * Installed capacity * AOH * NUMS)/PL (5.32)

Where:

MF_F - fixed maintenance factor ($/kW)

MF_V - variable maintenance factor ($/kWh/schedule)

AOH - annual operating hours (hours)

NUMS, number of unplanned maintenance schedule per annum = MS - NPMS

NPMS, number of planned maintenance schedule per annum

PL - project/engine life (years)

$MS = (PL/ (L_{CREF} * C_F))$ ` (5.33)

When:

$C_F = 1$, NUMS = 0, because MS = NPMS (5.34)

$C_F <$ OR > 1, NUMS = MS – NPMS (5.35)

The fixed M cost should account for planned maintenance services over the life time of the engine while the variable M cost should account for unplanned maintenance services resulting from operation and over the life time of the engine. Both fixed and variable M cost factors are adopted from [Nigerian Electricity Regulatory Commissio (NERC), 2012]. Further analyses were carried out to assess the sensitivity of the study to increasing or decreasing M cost factor. In other words,

M cost ($) = Fixed + (Unplanned variable cost + Planned variable cost) (5.36)

5.2.3 Emission Module

The emission module employs parameters such as fuel composition and mass, fuel flow rate, fuel density from performance analysis as stated in Table 5.2.

Table 5.2: Inputs and Outputs for Emission Module

Parameters	Unit	NG	DI	AG	JT
Carbon Number	-	1	12.79	17.69	17.70
Hydrogen Number	-	4	23.80	33.11	33.17
Molecular Mass	gm	16	174	245	246
Carbon Mass	gm	12	150	212	212
Carbon Generated	kgC/MWh	201	296	317	293
LHV	MJ/kg	47.14	42.79	33.79	38.73
LHV	kcal/kg	11259	10168	8071	9250.5
Fuel Density	kg/L	0.864	0.82	0.98	0.92
Fuel Flow	kg/s	8.12	8.53	10.89	9.45
-	kg/h	29232	30718.8	39186.72	34002
Heat Rate	kJ/kWh	10928	11986	12137	12071

5.2.3.1 Emission Cost ($)

The CO_2 emissions can be estimated from the carbon content of the fuels, assuming complete combustion of fuels and in the presence of sufficient air for oxidation. This is estimated using the equation 5.37-5.38 below.

Mass of C emitted in kg/MWh =

$$\frac{\left(\frac{mass\ of\ carbon\ in\ fuel}{\frac{mass\ of\ fuel}{fuel\ density}}\right) * fuel\ flow\ rate}{Installed\ capacity * Capacity\ Factor} \qquad (5.37)$$

Hence,

Carbon tax = carbon tax rate ($/tC) * mass of C (kg/MWh) * installed capacity * AOH * 0.001` (5.38)

Where: 0.001 is the conversion factor from kgC to tC

In the baseline study, zero carbon tax rate was assumed while $44/tC was used to examine scenarios with carbon tax or carbon credits. Further analyses were carried out to assess the sensitivity of the study to increasing or decreasing carbon tax rates.

5.2.4 Fuel Module

The fuel module employs parameters such as fuel flow rate, heat rate, fuel density and LHV, hence, for the baseline study; the inputs stated in Table 5.3 were used.

5.2.4.1 Fuel Cost

The fuel cost was estimated using equations 5.39-5.41 below, with a fixed (specific) fuel cost, a value adopted from [NERC, 2012] for natural gas in the baseline study, assuming, that is there is no change in market price of fuel cost in the base year (2012). A fixed fuel price ($/gallon) is also assumed for the biodiesels and conventional diesel fuel based on the understanding that fuel prices of biodiesels would have to be competitive for successful adoption.

Fuel Cost = F_C * AOH * Fuel flow rate * 3600 ` (5.39)

F_C – specific fuel cost [$/kg]

Specific fuel cost [$/MMBTU (natural gas)] to $/kg = $/MMBTU * MMBTU / 293.07kWh * LHV [MJ/kg] * Heat rate [kJ/kWh] * 1000[MJ/kJ] ` (5.40)

Specific fuel cost [$/gallon (liquid fuel)] to $/kg = [$/gallon * gallon / 4.54609 Litres] / fuel density ` (5.41)

Further analyses were carried out to assess the sensitivity of the study to increasing or decreasing specific fuel cost.

5.2.5 Capital Cost

The capital cost accounts for cost of equipment, installation and any initial investment related to acquiring of the asset. This cost was estimated using equation 5.42, assuming a capital cost factor ($/MW), a value adopted from [NERC, 2012]. Further analyses were carried out to assess the sensitivity of the study to increasing or decreasing capital cost.

Capital Cost ($) = Capital Cost Factor * Installed capacity (5.42)

In summary, the inputs considered in the economic analysis for the baseline study are presented in Table 5.3. Further analyses were carried out to assess the sensitivity of some of the inputs.

Table 5.3: Inputs and Outputs for Economic Model

Parameters	Unit	Value
Installed Capacity	MW	126.1
Auxiliary Components	**%**	2%
Capacity Degradation	%	2%
Transmission Losses	%	11%
Capacity Factor (from Plant)	%	80%
Availability	%	98%
Annual Possible Service Hours (PH)	Hrs	8760
Operating Hours (OH)	Hrs	7008
Company Tax Rate	%	32%
Inflation Rate	%	11%
Depreciation Rate	%	5%
Exchange Rate	N-$	161
Project Life	Yrs	20
Pre-Tax Real WACC	%	11%
Discount rate (d):	%	11%
Capital Cost	$/MW	978500
Maintenance Cost (Fixed)	$/MW/Yr	15503
Maintenance Cost (variable)	$/MWh	5.6
Emission Tax Rate (kgCO_2)	$/tCO2	0.0000
\Fuel Cost	$/MMBTU	1.8
Fuel Cost (NG)	$/kg	0.026
Capital Cost	$	123388850
Fuel Cost (NG)	$	5427631
Emission Cost	$	0
Supplementary Cost	$	**0**
Planned Outage Repair Cost	$	1650829
Unplanned Outage Repair Cost	$	0
O&M (Fixed) exc. fuel cost	$	1954942
Deficit Energy Cost	$	342206
Capacity Charge	$/MW/Month	21832
Energy Charge	$/MWh	33
Contract Surplus Elecricity Price	$/MWh	77
Contract Deficit Elecricity Price	$/MWh	80
Fuel Cost (NG)	$/MWh	6.14
Energy Charge/Annum	$	25318669
Capacity Charge/Annum	$	33036634
TotalCharge/Annum	$	58355302
Electricity Charge	$/MWh	77.15
Electricity Charge	₦/kWh	12.42

5.3 Economic Measures

The economic measures considered in this study to evaluate the power plants operating on various fuels include: i) net present value (NPV), ii) total life cycle cost (TLCC), iii) Levelized cost of electricity (LCOE), iv) internal rate of return (IRR), v) simple payback period (SPB), and vi) benefit-to-cost ratios (B/C). All these economic measures have been chosen because they present different views of plant's economic performance to an engine operator, power generator, distributor, or user and to a financer. A summary is provided below:

5.3.1 Net Present Value (NPV)

NPV defines the economic viability of a project and can be used to accept or reject. A positive NPV indicate that the project is economically and potentially viable. It is a useful tool that provides information, if there would be a positive return on investment. Although, it does not entirely guarantees the best venture, it measures the present value of costs and benefits [Short et al. 1995]. In this study, this has been measured by examining the revenues and costs involved in the power plants, assuming an annual real discount rate equal to the project's weighted average cost of capital (WACC), and a constant dollar cash flow at the end of the period, 2012. The year 2012 has been chosen due to data availability.

Hence,

$$NPV = \sum_{n=0}^{N} \frac{FN}{(1+d)^N} = F0 + \frac{F1}{(1+d)^1} + \frac{F2}{(1+d)^2} + \cdots + \frac{FN}{(1+d)^N} \quad (5.43)$$

Where:

F_N = net cash flow each year, n

N = analysis period (project life time)

d = annual real discount rate

F_x = net taxable income each year, x

F_x = Revenue – [Investment cost* + M cost + Fuel cost + Emission cost + Deficit Power cost + Depreciation cost]
(5.44)

*Additional annual investment

$F_n = F_x - (F_x * \text{Income Tax Rate})$ (5.45)

And for each year aside the base year, inflation rate is applied to individual cost (M cost, Fuel cost, Emission cost, Deficit Power cost, Depreciation cost) using equation 5.46.

Annual Cost/Revenue = Cost/Revenue*(1 + Inflation Rate) (5.46)

Depreciation cost = Depreciation rate * initial investment (5.47)

Deficit power cost = Deficit energy cost ($/MWh) * [Total Outage Hours (TOH) * Installed capacity * Auxiliary components energy requirement] (5.48)

TOH = [Total Service Hours (SH) – Total Operating Hours (OH) (5.49)

SH is a function of engine's availability factor, which is 98% for the baseline study. The depreciation rate assumes the salvage value at the end of the project life is zero. Also, there are no further investments; hence the annual investment aside the base year is zero.

5.3.2 Total Life-Cycle Cost (TLCC)

This parameter defines the total cost spent per annum on an asset and could highlight the differences in cost involved in the use of the various fuels. This is only informational and cannot be used solely and directly as a decision tool for project viability, since there are no frame of reference for acceptable or non-acceptable costs, neither indicative of the benefit or returns associated [Short et al. 1995]. The TLCC has been calculated using equation 5.50. This involves a summation of all the discounted associated costs for the power plant.

$TLCC = \text{Initial investment} – PV_{OC}[1 - T] + [PV_{DEP} * T]$ (5.50)

Where:

$PV_{OC} = \sum_{n=0}^{N} \frac{CN}{(1+d)^N}$

$PV_{OC} = \sum_{n=0}^{d} \frac{Cd}{(1+d)^N}$

T = Income Tax rate

PV_{DEP} - present value of depreciation cost

PV_{OC} – present value of other cost

C_N - other cost in period n and includes m cost, fuel cost, emission cost, deficit energy cost, excluding depreciation cost

C_D – depreciation cost in period, n

5.3.3 Revenue Requirement (RR)

According to [Short et al. 1995], RR is the total revenue that must be collected from the customer to cover or adequately compensate for all the expenditure (costs, taxes, interested paid on debts to investors) associated with a project. It is appropriate for projects such as described in this study that solely depends on external regulation such as Nigerian Energy Regulatory Commission (NERC). The RR for the project of various fuels were calculated using equation 5.51 to determine if the RR is in a similar range to that of the reference fuel or overly different. A lower RR would recommend a project as a better choice than the alternatives, however as applicable to TLCC; it has no frame of reference for what is acceptable or non-acceptable, neither does is it indicates the benefits or returns expected. In other words, RR cannot be used to accept or reject the different operational options involved with fuel flexibility.

$$RR = \frac{TLCC}{(1-T)} \tag{5.51}$$

5.3.4 Levelized Cost of Electricity (LCOE)

This economic measure is the best and appropriate approach to compare assets with different operational options, as the case of flexible fuel operation. According to [Kreith, 2013], if LCOE is assigned to every unit of energy produced (or saved) by the system over the analysis period in a period, will be equal to the TLCC when discounted to the base year. This was calculated using equation 5.52 to 5.53 and results are expressed as \$/MWh and ₦/kWh LCOE is the cost, if assigned to individual energy unit produced by the power plant.

$$LCOE = \left(\frac{TLCC}{Q}\right) URCF \tag{5.52}$$

Q – Annual Energy Output (MWh)

URCF – Uniform Capital Recovery Factor, $\frac{d(1+d)^N}{(1+d)^N - 1}$ (5.53)

d – Discount rate

LCOE is an interesting metrics that provides the cost of generating one unit of electricity from a power producer and allows a comparison of various power options.

5.3.5 Internal Rate of Return (IRR)

The IRR is the rate at which the NPV equals to zero. This was achieved by iteration and estimated using equation. 5.54

$$IRR = NPV = \sum_{n=0}^{N} \frac{F_N}{(1+d)^N} = 0 \quad (5.54)$$

The above equation is applied by assuming that the annual revenues are invested at a rate equal to the IRR. If the outcome of the IRR is above the discount rate, the project is considered as economically viable.

5.3.6 Simple Payback Period (SPB)

SPB is a quick assessment measure that defines the number of years required to recover the cost of investment in the project. It is however limited because it ignores returns after payback and ignores time value of money since discount rate is not considered. This was calculated using equation 5.55.

$$SPB = \Delta I_n \leq \Delta S_n \quad (5.55)$$

ΔI_n – non-discounted investment costs

ΔS_n – non-discounted summation of annual cash flows

5.3.7 Benefit-to- Cost Ratios (B/C)

Benefit-to- Cost Ratios determines if there are benefit associated to a project and to what extent does the benefits exceed the costs. This was calculated using equation 5.56

B/C = PV (All Revenues) / PV (All Costs) (5.56)

It compares the ratio of incremental discounted benefits to costs. This places a value on a project; hence a B/C above 1 would be considered beneficial and vice versa.

5.3.8 Fuel and Engine Choice

Four fuels were examined in this study: a) Natural gas b) Conventional diesel c) Jatropha biodiesel d) Microalgae biodiesel. Two fuel cost scenarios of $1.8/MMBTU (baseline study) and $4/MMBTU were examined for natural gas. Three engines were assessed for economic performance as it relates to the use of the above fuels for base load operation, using a current situation and future cost scenario approach. This include: a) GX100 (126 MW) gas turbine, b) GX200 (22.4 MW) aero-derivative engine, both operating in an open

cycle arrangement and, c) GX300 (380 MW) combined cycle gas turbine with a 2-2-1 clustering. These engines have been simulated and validated in Chapter 3 and are assumed to be co-located at Olorunsogo power plant in Nigeria. For comparative assessment with engine GX100, only the power output from a single unit of engine GX300 is accounted for, that is 190MW of installed capacity.

5.3.9 Sensitivity Analysis

Range of values of the parameters stated in Table 5.4 was tested to determine the sensitivities of the economic performance results to ± 50% deviations.

Table 5.4: Inputs for Sensitivity Module

Parameters	Unit	Range
Investment cost	$/kWh	485 - 1470
WACC	%	5.5 - 16.5
Fuel cost	$/MWh	3 - 9
Emission cost	$/tCO2	-22 - 66
Fixed O&M Cost	$'000/GW	7.75 - 23.3
Variable O&M Cost	$/GWh	2.8 - 8.4
Utilization (Capacity Factor)	%	40 - 100
Inflation Rate	%	5.5 - 16.5
Depreciation Rate	%	1 - 5
Company Tax Rate	%	16 - 48
Transmission Losses	%	5.5 - 16.5
Exchange rate	-	80.5 - 241.5
Capacity Degradation/Availability	%	1 - 3
Auxiliary Components	%	1 - 3

5.4 Results and Discussion

5.4.1 Current Situation Analysis

The results of economic analysis for the microalgae biodiesel-, Jatropha biodiesel-, natural gas- and conventional diesel- fired power plants (FPP), using engine GX100 are presented in this section. The results highlight the current potential of a single unit that is 126 MW installed capacity, at Olorunsogo power station II with the view of integrating other fuel types (biodiesels), apart from its natural gas and diesel fuel capability.

5.4.1.1 Economic Performance of Engine GX100

Table 5.5: Economic Performance of Gas-, Diesel-, Biodiesel-fired Power Plants

Economic Measures	Unit	Baseline	GX100			
		NG	NG	DI	AG	JT
Simple Payback Period (SPB)	Years	3	3	>20	>20	>20
Internal Rate of Return (IRR)	%	35	31	0	0	0
Total Life Cycle Cost (TLCC)	$'000000	223	310	2993	3183	2955
Revenue Rate (RR)	$'000000	327	456	4401	4681	4345
Net Present Value (NPV)	$'000000	567	479	-3240	-3521	-
Benefit-to-Cost Ratio	-	2.65	2.51	-0.75	-0.77	-0.75
Levelized Cost of Electricity (LCOE)	$/MWh	37	51	497	528	491
Levelized Cost of Electricity (LCOE)	₦/kWh	6	8	80	85	79

The economic performance results (see Table 5.5) show that the NPVs for the liquid FPP are negative with zero IRR as opposed to the positive NPVs obtained for the gas fired power plants, where the IRRs are slightly above 30%. These results are as a result of high TLCC for the liquid fuels, which are in the range of $2.96 billion [Jatropha biodiesel FPP] to $3.18 billion [microalgae biodiesel FPP], values nearly ten-fold higher than that of the gas FPP. Similarly, the revenue requirements to operate a liquid FPP are in the range of $4.3 billion [Jatropha biodiesel FPP] to $4.7 billion [Microalgae biodiesel FPP], values also nearly ten times higher than that of the gas FPP. The LCOE for the liquid fired power plants are ₦79/kWh [Jatropha biodiesel], 80 ₦/kWh [Diesel], and ₦85/kWh [microalgae biodiesel] while ₦6/kWh and ₦8/kWh for gas FPP with fuel cost of $1.8/MMBTU and $4/MMBTU respectively.

The above results in Table 5.5 imply that liquid fuels including biodiesels are not economically viable for use all year round in heavy gas turbine power plants, as in the case of GX100; since the NPV were negative, there are no returns on investments, and

the SPB are beyond the life time of the project as opposed to the SPB of 3 years for both scenarios in gas FPP. Also, the cost of electricity for these power plants is nearly seven-fold higher than the electricity charge of 12.4 ₦/kWh [Table 5.3] received from the end user. In order words, there is a high risk in investment in operating power plants with liquid fuels in Nigeria. Although, these results appears to be a logical conclusion for the use of liquid fuels in power plants in Nigeria, the dynamic state and the problems associated with power generation in the country, such as fuel scarcity, shortage of natural gas to power plant stations and deficiency of power of nearly 70% across the country, give renewable fuels including biodiesels a unique opportunity for integration. Among the three liquid fuels, the economic performance of the Jatropha biodiesel-fired power plant was slightly better than that of the conventional diesel, and microalgae biodiesels.

5.4.1.2 Fuel Economy Analysis of Power Plants

The Energy Density (MJ/L) of any given fuel is the amount of energy conserved per unit volume of fuel while the Specific Energy (MJ/kg) of any given fuel is the amount of energy contained per unit mass of fuel. These densities vary for petroleum and biodiesel derived fuels. In this analysis, Jatropha biodiesel has a fuel density of 0.92 kg/L and LHV of 38.73 MJ/kg and conventional diesel fuel has fuel density of 0.82 kg/L and LHV of 42.57 MJ/kg. These differences have an effect on fuel economy of power plants. The effects of these properties have been discussed in section 3.4.3 and changes the actual fuel cost of power plants (see figure 5.3).

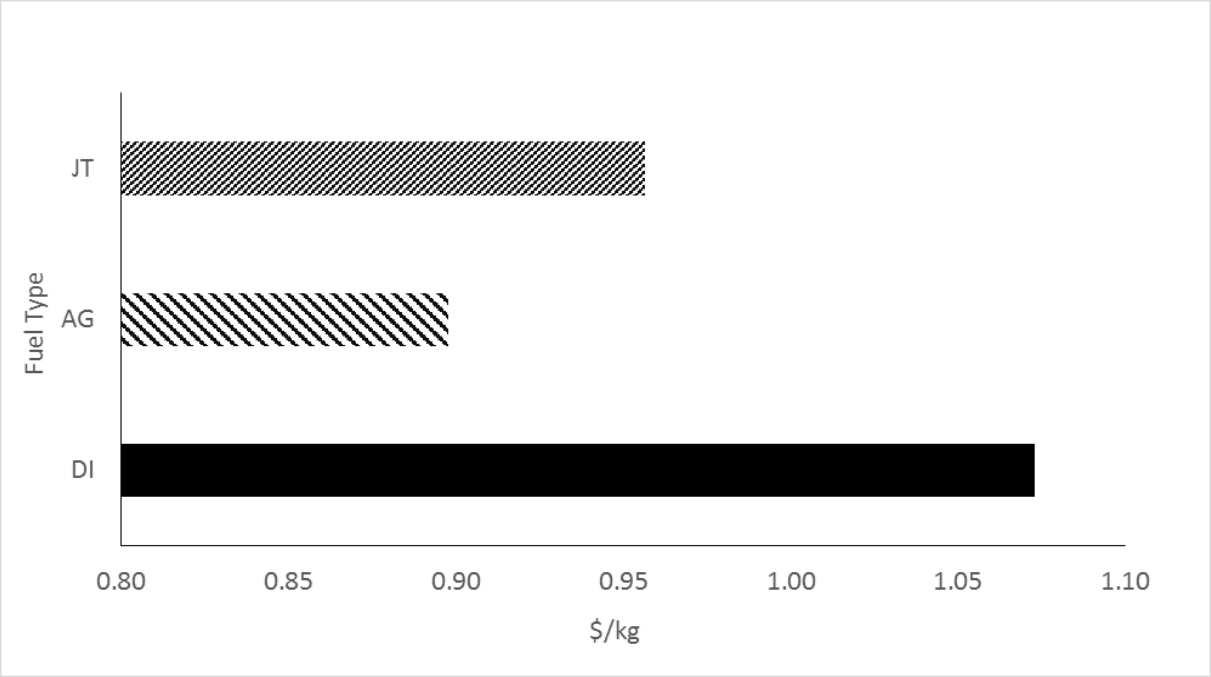

Figure 5.3: Fuel economy of liquid fired power plants

The actual fuel cost for the biodiesel FPPs are $0.96/kg [Jatropha biodiesel] and $0.898/kg [Jatropha biodiesel], as opposed to the fuel cost of conventional diesel FPP of $1.1/kg, assuming the fuel cost per gallon for all the liquid fuels at retail price are $4/gallon. This explains the differences observed in TLCC and LCOE, as well as other economic measures for the different liquid FPPs, in addition to other cost implications from the use of the fuels.

5.4.1.3 Economics of Jatropha Biodiesel-fired Power Plant (Tax incentives included)

Since, Jatropha biodiesel has remained consistent in having better performance over microalgae biodiesel and in many instances over conventional diesel fuel, this section further examines the possibility of integrating the biodiesel in power plants with the aid of government tax incentives to lower the TLCC, LCOE, and RR and improve the NPV of the power plant. Kost et al. 2013 made note of the important role diesel power plants play in electricity generation in Middle East countries, and nearly accounting for 88% of the energy mix in Saudi Arabia. This is only possible with fuel subsidization. In Nigeria, fuel subsidization is a major issue and has brought additional budgetary load on the government, but there is opportunity loss in economy growth and development, if such mechanisms were to be ignored. In the developed economies, renewable fuels have appreciably penetrated the energy mix of many countries because of government support and platforms such as production-based renewable incentives, tax credit and subsidy programs. As a result of these and in addition to advances in technology, the costs of renewable energy have been reducing consistently and penetration of renewable energy production has increased substantially. For instance, the UK operates a minimum feed-in tariff system that pays an energy generator a minimum guaranteed amount for any renewable energy generated (used or sold to the grid) over a period of years. In the U.S, the energy generator receives a tax credit and this has driven the electricity cost of production from wind and solar power very low and brought about significant economic benefits and growth. Although such platforms are mostly applicable to solar, wind and biomass derived energy, this can be adopted by developing economies to ramp up renewable energy projects.

This study has examined the minimum cost that is required to keep a biodiesel FPP in three scenarios: a) a positive NPV over the life time of the project, b) a positive PV from the first year of the project, c) the LCOE equal to that of the gas fired power plant. The results are presented in Table 5.6.

Table 5.6: Economic Analysis of Jatropha Biodiesel-fired Power Plant (Tax incentives included)

Economic Measures	Unit	Baseline	+NPV (20 Years)	+NPV (Year 1)	LCOE = Base-case
Tax/Incentives	$/MWh	0	210.5	214.6	268.2
	₦ /kWh	0	33.9	34.6	43.2
Simple Payback Period (SPB)	Years	>20	>20	15	2
Internal Rate of Return (IRR)	%	0	-	-	-
Total Life Cycle Cost (TLCC)	$'000000	2955	822.7	780.4	228.8
Revenue Rate (RR)	$'000000	4345	924.3	876.8	257.1
Net Present Value (NPV)	$'000000	-3184	0.001	62.2	873.4
Benefit-to-Cost Ratio	-	-0.75	0	0.02	0.21
Levelized Cost of Electricity (LCOE)	$/MWh	491	137	130	38
	₦/kWh	79	21.99	20.9	6.1

The results show that government incentives of up to ₦33.9/kWh could significantly change the economics of Jatropha biodiesel fired power plant. Here, the NPV changes from a negative balance to minimum value of $1080, over the life time of the project and the LCOE reduces to ₦22/kWh, a value over 70% lower than the LCOE for the baseline study, but still nearly four-fold higher than that of the gas fired power plants. Similarly, the TLCC reduced by over 70% when compared to the initial study, but nearly three-fold higher than the gas fired case. In addition, the SPB did not reduce beyond the 20 years and B/C was zero. Here, an IPP can sell electricity to off-grid users and businesses to recoup profits over the life time of the project. Consumers such as domestic users that lack electricity and depend on self-generated electricity would be willing to pay up to ₦45/kWh. An increase in government incentives by an additional 2.4% such that a value of about ₦34.6/kWh is provided to support renewable power plants, a positive NPV could be achieved from the first year of the project with $62 million over the life time of the project. Here, the SPB reduces to about 15 years while the LCOE reduces only to ₦21/kWh.

For competitiveness with natural gas FPP, government incentives of about ₦43/kWh would be necessary to support Jatropha biodiesel use in a typical gas turbine power plant. This would ensure a SPB of about 2 years and B/C of 0.21 with TLCC of $229 million/MWh. These incentives reduce the SPB period for the Jatropha biodiesel FPP to 2 years, and the risk associated with the project and this is an advantage to a financier or investor in renewable energy production. This is because the revenue is much higher with tax incentive.

5.4.1.4 Economics of Part-substitution of Diesel with Jatropha Biodiesel

Rather than all year round, 100% use of fuels over the life time of a power plant project, biodiesels could be integrated for use in power plants as part-substitution, especially when natural gas is unavailable for use. There are many instances when the Olorunsogo power station was not in operation or producing less than the installed capacity because of unavailability of natural gas supply. This was often said to result from damaged, vandalized or improperly managed gas network and pipelines.

This study has examined the maximum requirement of Jatropha biodiesel that can be substituted to keep the power plant economical under three scenarios: a) a positive NPV over the life time of the project, b) a positive PV from the first year of the project, c) to keep the LCOE equal to that of the gas fired power plant. Here, part substitution represents a fraction of the plant operating hours. The results are presented in Table 5.7 and figures 5.4 to 5.6. Table 5.7 presents the economic analysis for part-substitution of Jatropha biodiesel with natural gas at 15% and 20%, plus inclusion of government tax incentives. Figures 5.4 to 5.6 show the economic performance for a range of part-substitution of natural gas with Jatropha biodiesel.

Table 5.7: Economic Analysis of Part-substitution of Diesel with Jatropha Biodiesel

Parameters	NPV	IRR	LCOE ($/MWh)	LCOE (₦/kWh)	TLCC	SPB	B/C
JT(100)	-3184.34	0%	490.51	78.97	2954.60	20.00	-0.75
NG(100)*	560.39	35%	37.99	6.12	228.86	4.00	2.51
FM (15%)	151.53	13%	105.87	17.05	637.72	16.00	0.18
FM (20%)	13.67	0%	128.50	20.69	774.00	20.00	0.01
FM (20%) + Govt. Inc. (N33.9/kWh)	650.57	-	62.14	10.00	374.3	3	0.6

The results in Table 5.7 show that the maximum percentage of Jatropha biodiesel fuel that can substitute natural gas fuel for base load, open cycle operation of engine GX100 at Olorunsogo power station and ensure that the plant owner recovers the cost of investment without government intervention is 20%. Government intervention of ₦33.9/kWh for the period of operation of the power plants with Jatropha biodiesel fuel would significantly change the economic performance and viability of power plants operating on biodiesels. A NPV of $650 million/MWh, TLCC of $374 million and LCOE of ₦10/kWh are observed. The SPB and B/C changes from 20 years and 0.01 to 3 years and 0.6 respectively. This is supported by the reduction of TLCC by half due to

government intervention, a value that is about 60% higher than that of the gas FPP. Although, the LCOE of this case is still higher than the LCOE for the gas FPP, it is of better economic importance, if the results were to be compared to the economic loss that could ensue during the period of shut down of the power plants due to shortage of natural gas or the cost of self-generated electricity.

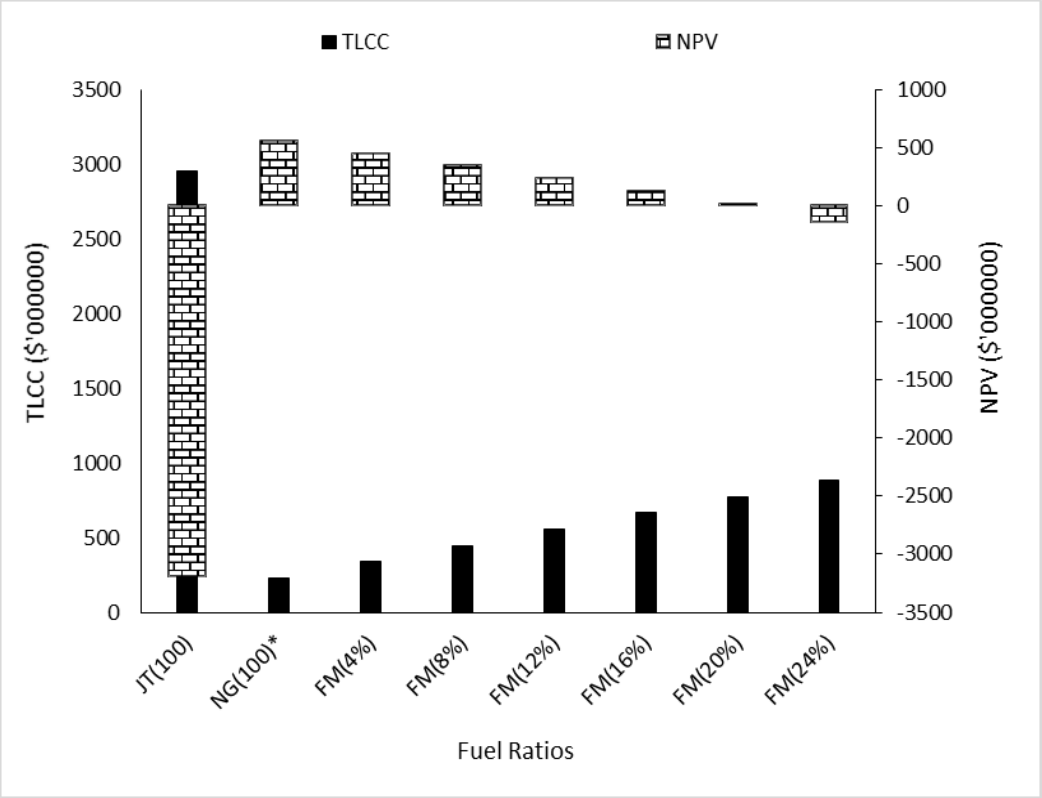

Figure 5.4: TLCC and NPV of part-substitution of Diesel with Jatropha Biodiesel

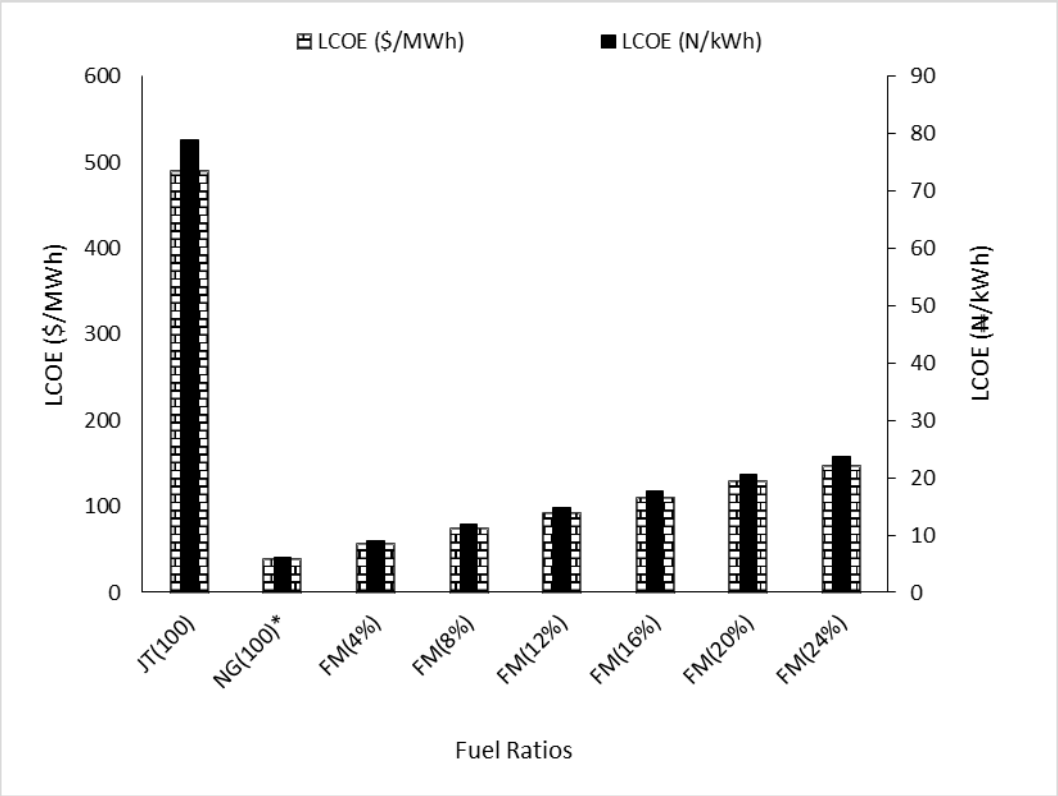

Figure 5.5: LCOE of part-substitution of Diesel with Jatropha Biodiesel

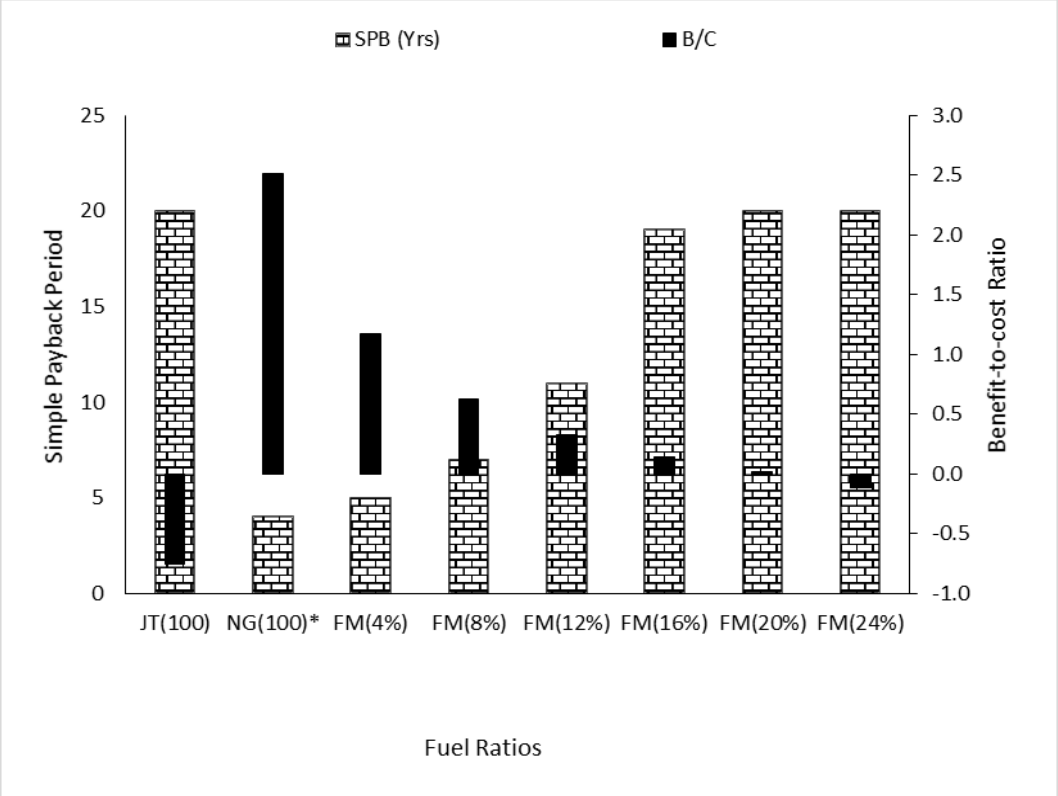

Figure 5.6: SPB and B/C of part-substitution of Diesel with Jatropha Biodiesel

The results in figure 5.4 show the change in economic performance in the power plant as Jatropha biodiesel part-substitution is progressively increased from 0-24%. Part-substitution of natural gas with Jatropha biodiesel by 20% increases the cash flow with positive PV of $14 million at the end of the project life, and as compared to the negative balance in the baseline study for Jatropha biodiesel FPP. The TLCC increased by three-fold when compared to the gas FPP. Furthermore, this 80% natural gas and 20% Jatropha biodiesel use result in a SPB of over 20 years, B/C of nearly zero while the LCOE reaches ₦21/kWh. A substitution above 20%, as observed with fuel mixture (FM) 24% would result in a negative NPV and TLCC of about $883. The 20% substitution of Jatropha biodiesel can serve up to 1402 hours (nearly 2 months of operation), assuming annual operating hours of 7008 hours per annum. The results here demonstrate that plant owners could operate power plants with Jatropha biodiesel fuel up to 15%, for customer satisfaction and other social and economic reasons, but at the expense of economic performance. Other opportunities could be sourced for increased electricity tariffs to compensate for all cost incurred during plant operation on Jatropha biodiesel fuel.

5.4.1.5 Economics of Jatropha Biodiesel-fired Power Plant (Carbon Tax Scenario)

All the above analyses have been conducted assuming zero emission tax rate. This section further examines a scenario where emission tax levies are in place for mixed fuel fired power plants that is charged based on the tC produced (see figure 5.7). The results are compared to 20% substitution with Jatropha biodiesel fuel, assuming there are government incentives and no emission tax for the fraction of the hours the power plants operate on Jatropha biodiesel fuel. This is carried out to evaluate the economic performance of power plants under carbon tax scenarios.

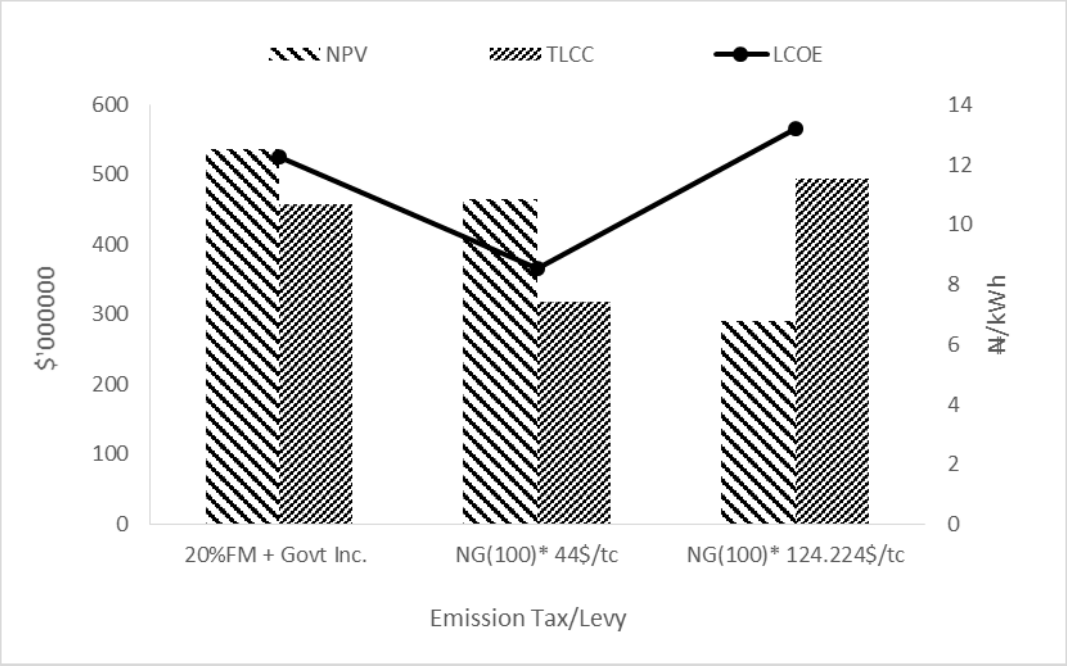

Figure 5.7: Economic performance of part-substitution of mixed fuel FPP under carbon tax scenario

The NPVs for gas fired power plants with emission tax of \$44/tCO_2 and \$124/tCO_2 are \$465 million and \$290 million respectively while the TLCCs are \$319 million and \$493 million, as opposed to the NPV of \$536 million and \$458 million for power plants operating with a mixture of 20% Jatropha biodiesel and 80% natural gas. The LCOE on the other hand indicate values of ₦9/kWh [gas fired power plants with \$44/tCO_2 levy], ₦13/kWh [gas fired power plants with \$124/tCO_2 levy] and 12 ₦/kWh [20% Jatropha biodiesel fuel mix scenario with govt. tax incentives]. These results demonstrate that the economic performance can all be encompassing and against gas fired power plants, if there is an emission tax levy up to \$124/tCO_2 generated.

5.4.2 Average Cost of Electricity in Nigeria

This section presents the summary of the energy situation in Nigeria. The data in Table 5.8 have been provided by personal communication, and represent the average energy consumption for a family of six in Nigeria, and for a business with staffing capacity of 20.

The results in Table 5.8 show that the cost of electricity generation in Nigeria is extremely high, as much as \$62/kWh for small-medium enterprise and \$15/kWh for a family of six under scenarios of minimum energy generation balanced by grid supply.

Table 5.8: The Average Cost of Electricity Use in Nigeria

Parameters		Local Businesses	
LCOE with Other Energy Cost[8]	$/kWh [N/kWh]	62.40 [10046]	14.94 [2406]
LCOE without Other Energy Cost[9]	$/kWh [N/kWh]	27.21 [4380]	9.41 [1515]
LCOE full hours[10]	$/kWh [N/kWh]	-	34.64 [5577]

Even in a worst case scenario, where residents use minimal amount of hours at the expense of power supply, that is black out condition, the average cost remains high at $27/kWh for small-medium businesses and $9.41/kWh for an average household. These costs are over 50 times higher than the LCOE from a biodiesel-fired power plant for a small-medium business and nearly 20 times higher for an average household. Assuming an average household depends on self-generated electricity throughout the day, the LCOE is $37/kWh. The results above show that although the cost of electricity generation from both Jatropha biodiesel and microalgae biodiesel FPP is nearly ten times higher than natural gas FPP, the current cost of electricity for an average family or business owner is more than that of gas FPP. This wide differences in the cost of electricity gives an opportunity for distributed and independent power generation, and the integration of renewable fuels like Jatropha- and microalgae-biodiesel. The data for this analysis are provided in Table 5.2 (Appendix IV).

5.4.3 Future Situation Analysis

As mentioned in chapter1, the power plants at Olorunsogo power stations operate as open cycles, although they have installed capacity for combined cycle operations. The results presented in this section present the economic performance of engine, GX300. For comparative assessment with engine GX100, only the power output from a single unit of engine GX300 is accounted for, since engine GX300 has a 2-2-1 configuration that is two generating units, coupled to two heat recovery steam generators and both connected to a downstream steam turbine. The results are presented in Table 5.9 for the fuel types at fuel cost of $4/MMBTU [natural gas] and $4/gallon [liquid fuels].

[8] Scenarios of minimum energy generation balanced with grid supply for the remaining hours
[9] Use of the minimal amount of hours at the expense of power supply
[10] Self-generated electricity throughout the day

5.4.3.1 Economic Performance of Engine GX300

Table 5.9: Economic Performance of Gas-, Diesel-, Biodiesel-fired Power Plants

Economic Measures	Unit	NG	DI	AG	JT
Simple Payback Period (SPB)	Years	5	>20	>20	>20
Internal Rate of Return (IRR)	%	25	0	0	0
Total Life Cycle Cost (TLCC)	$'000000	337	2946	3304	2908
Revenue Rate (RR)	$'000000	510	4332	4859	4277
Net Present Value (NPV)	$'000000	671	-2835	-3369	-3019
Benefit-to-Cost Ratio	-	2.3	-0.69	-0.72	-0.74
LCOE	$/MWh	38.14	324.07	363.49	319.93
LCOE	₦/kWh	6.14	52.17	58.52	51.51

The results in Table 5.9 show that the NPVs for the liquid FPP are also negative with zero IRR while that of the gas FPP is positive with NPV of $671 million, a value that is about 40% higher than that of the open cycle application, but with lower IRR of 25%. The TLCC for the liquid fuels are in the range of $2.91 billion [Jatropha biodiesel FPP] to $3.3 billion [microalgae biodiesel FPP]. The higher life cycle cost for the combined cycle application is as a result of increased initial investment cost, which is about 1850/kWh. Hence, the revenue requirements for liquid FPP are in the range of $4.3 billion [Jatropha biodiesel FPP] to $4.9 billion [Microalgae biodiesel FPP]. The TLCC and RR for the gas FPP are much reduced in comparison to the liquid FPP with values of $0.35 billion and $0.5 billion respectively. Most importantly, the LCOE for the liquid FPP reduced 51 ₦/kWh [Jatropha biodiesel], 52 ₦/kWh [Diesel], and 58 ₦/kWh [microalgae biodiesel] while 6 ₦/kWh for the gas FPP. This is a significant improvement when compared to the LCOE in the open cycle application, where LCOE were in the range of 79 ₦/kWh [Jatropha biodiesel] and 85 ₦/kWh [microalgae biodiesel] for liquid FPP. As opposed to the SPB of 3 years in the open cycle applications, the SPB in this combined cycle operation would require 5 years.

5.4.3.2 Economics of Jatropha Biodiesel-fired Power Plant (Tax incentives included)

Similar to previous analysis in section 5.6.1.2, the minimum cost that is required to keep a biodiesel FPP under three scenarios: a) a positive NPV over the life time of the project, b) a positive PV from the first year of the project, c) the LCOE equal to that of the gas fired power plant. The results are presented in Table 5.10.

Table 5.10: Economic Analysis of Jatropha Biodiesel-fired Power Plant (Tax incentives included)

Economic Measures	Unit	Baseline	+NPV (20 Years)	+NPV (Year 1)	LCOE = Base-case
Tax/Incentives	**$/MWh**	**0**	**132.24**	**138**	**169.15**
	₦ /kWh	**0**	**21.29**	**22.1**	**27.23**
Simple Payback Period (SPB)	Years	>20	>20	15	3
Internal Rate of Return (IRR)	%	0	-	-	-
Total Life Cycle Cost (TLCC)	$'000000	2908	918.4	844.5	345.4
Revenue Rate (RR)	$'000000	4277	1032	948.8	388.1
Net Present Value (NPV)	$'000000	-3019	0.002	108.8	842.7
Benefit-to-Cost Ratio	-	-0.74	0.00	0.03	0.21
Levelized Cost of Electricity (LCOE)	$/MWh	319.93	101	105.76	38
Levelized Cost of Electricity (LCOE)	₦/kWh	51.51	16.27	17.03	6.12

The results show that government incentives of up to ₦21.3/kWh could significantly change the economics of Jatropha biodiesel FPP. This value is reduced by 37% when compared to open cycle operation and this is resulting from the added benefit of combined cycle operation of the power plant. Here, the NPV is with minimum value of about $2000, and the LCOE has reduced to ₦16/kWh, a 25% improvement from the open cycle application, but still nearly three-fold higher than the gas FPP. Also, the TLCC reduces further to $918 million, but the SPB remains above 20 years with B/C of zero. However, an increase in government incentives up to ₦22/kWh changes the viability of the project with NPV of $108 million, a value that is about 75% higher than that of open cycle application. The SPB remains 15 years but the LCOE reduces to ₦17/kWh from ₦21/kWh in the open cycle application. For competitiveness with natural gas FPP, government incentives of about ₦27/kWh would be required to support Jatropha biodiesel use and for generating power. This would bring about a SPB of about 3 years and B/C of 0.21 with TLCC of $345 million/MWh, as opposed to $2.9 billion in the baseline study for combined cycle application.

5.4.3.3 Economics of Part-substitution of Diesel with Jatropha Biodiesel

For combined cycle operations, the maximum percentage of Jatropha fuel that can substitute natural gas fuel for base load operation at Olorunsogo power station and ensure that the plant owner recovers the cost of investment without government intervention is 25%. Here, the NPV of the plant over the life time of the project is $22.9 million, the LCOE is ₦17.5/kWh, the TLCC is $987 million, the SPB is 20 years and the B/C ratio is 0.02 (see Table 5.11).

Table 5.11: Economic Analysis of Part-substitution of Diesel with Jatropha Biodiesel

Parameters	NPV	IRR	LCOE ($/MWh)	LCOE (₦/kWh)	TLCC	SPB	B/C
JT (100)	-3019	0%	319.93	51.51	2908	>20	-0.74
NG (100)	671	35%	38.14	6.14	337	5	2.30
FM (15%)	282	13%	80.40	12.90	731	9	0.33
FM (25%)	23	-	108.60	17.48	987	20	0.02
FM (25%) **+ Govt. Inc. (₦7.41/kWh)**	**987**	**-**	**36.96**	**5.95**	**336**	**3**	**0.87**

With government intervention of ₦7.41/kWh, the LCOE can be equal to that of the gas FPP while the power plant can operate up to 1752 hours, assuming the annual operating hours is 7008 hours. The plant owner/operator as well investors also benefit, as TLCC reduces to $336 million with B/C ratio of 0.87, as against the value of 0.6 obtained in the case of the open cycle application. A 15% part-substitution without government intervention on the other hand should reduce the LCOE to ₦12.9/kWh, a value that is 25% less than the open cycle case, increase the B/C by an additional 80%, reduce SPB to 9 years and increase the NPV of the plant to $282 million, whereas the TLCC is $731 million. In both open and combined cycle cases, the IRR are about the same (13%).

5.4.3.4 Economics of Jatropha Biodiesel-fired Power Plant (Carbon Tax Scenario)

The combined cycle power plant was further analysed by considering emission tax rates of $44/t$CO_2$ and $124/t$CO_2$ in comparison to the mixed fuel option, with or without government incentives, where 20% of Jatropha biodiesel fuel substitute part of the natural gas fuel utilization. As described in section in 5.6.1.4, emission tax levies are assigned to power plants based on the tC produced from natural gas consumption and to only the fraction of the mixed fuel that operated on natural gas. That is, zero emission tax rate is applied to the fraction of the hours that the power plant operated on Jatropha biodiesel fuel. The results in Table 5.12 are also compared to those from open cycle application.

Table 5.12: Economic Analysis of Part-substitution of Diesel with Jatropha Biodiesel

Parameters	NPV	IRR	LCOE	LCOE	TLCC	SPB	B/C
FM (25%)	-184	-	125.2	20.16	1138	20	-0.12
FM (25%) + Govt. Inc. (₦7.41/kWh)	935	-	48.48	7.81	441	4	0.67
NG (100%) -$0/tCO2	671	35%	38.14	6.14	337	5	2.30
NG (100%) -$44/tCO2	575	22%	48.70	7.84	442	6	1.32
NG (100%) -$126/tCO2	401	17%	67.90	10.9	617	7	0.58

With emission tax rate of \$44/tCO_2 and \$124/tCO_2, the LCOE for the gas FPP were ₦7.8/kWh and ₦10.9/kWh respectively. These were higher than the LCOE for Jatropha biodiesel FPP that is supported by a minimum government incentive of ₦7.4/kWh. The NPVs for the gas FPPs with emission tax of \$44/tCO_2 and \$124/tCO_2 are \$575 million and \$401 million while the TLCCs are \$442 million and \$617 million respectively, as opposed to the NPV of \$935 million and TLCC of \$441 million for power plants operating with a mixture of 20% Jatropha biodiesel and 80% natural gas and supported by a minimum government incentive of ₦7.4/kWh. The SPB increased to 6 and 7 years while B/C ratio were reduced to 1.3 and 0.6 for both emission tax scenarios, as compared to the SPB and B/C values of 5 years and 2.3 observed for the non-emission tax rate case of the gas FPP. In comparison to open cycle operation of gas turbines, the analysis for combined cycle analysis demonstrate that the economic performance of mixed fuel up to 25% capacity is superior to the gas FPP if emission tax rates beyond \$44/tC are put in place.

The results in Table 5.9-5.12 illustrate that the GX100 is better operated in the combined cycle mode than as open cycle. The observable benefits include: a) additional power for relatively the same amount of fuel burn, b) better plant efficiency, c) reduced LCOE, d) higher NPV and e) better B/C: however, at the expense of increased TLCC and increased SPB. Also, the inclusion of emission levies could significantly change the economic performance of gas FPP, such that Jatropha biodiesels or similar fuels are deemed economically viable and sustainable with minimal government intervention. This calls for technological advancement in limiting emissions of carbon in power plants, if natural gas is to continual have its place in the energy mix in the near future.

5.4.4 Economic Performance of Engine GX200

Due to grid outages, a unique opportunity also emerges for power producers to generate electricity on small scale (under 25MW) and via distributed energy technologies as opposed to the centralized system of operation, where power plants generate power and

supply directly to the grid. This form of energy generation could be applicable to manufacturing hubs, off-shore processes, industrial parks, refineries, clusters of businesses and enterprises, as well as to off-grid users such as the rural population and other on-site generation requirements. This section of the report describes the result obtained from economic analysis of the GX200 power plant with installed capacity of 22.4 MW. The results are expressed in Table 5.13.

Table 5.13: Economic Performance of Gas-, Diesel-, Biodiesel-fired Power Plants

Economic Measures	Unit	GX100 Baseline	NG	DI	AG	JT
Simple Payback Period (SPB)	Years	3	3	>20	>20	>20
Internal Rate of Return (IRR)	%	35	33	0	0	0
Total Life Cycle Cost (TLCC)	$'000000	223	46.9	441	468	435
Revenue Rate (RR)	$'000000	327	69.1	648	689	640
Net Present Value (NPV)	$'000000	567	93.2	-442	-481	-433
Benefit-to-Cost Ratio	-	2.65	1.90	-0.70	-0.72	-0.70
Levelized Cost of Electricity (LCOE)	$/MWh	37	43.88	411.64	437.21	406.46
Levelized Cost of Electricity (LCOE)	₦/kWh	6	7.07	66.27	70.39	65.44

The results of the economic analysis for engine GX200 operating on natural gas indicate a positive NPV of $93 million, TLCC of $47 million, RR of $69 million, LCOE of ₦7.1/kWh with IRR and SPB of 33% and 3 years respectively. It can be observed that the LCOE of this relatively small gas turbine is higher for gas FPP than the GX100, a 126 MW power plant and the IRR is smaller, however about the same SPB. A comparison of the liquid fired power plants however indicates otherwise. Although, all the liquid fired power plant resulted in a negative NPV and B/C as found in the case of engine GX100, the LCOE is much reduced with values of ₦65.4/kWh [Jatropha biodiesel FPP], ₦66.3/kWh [conventional diesel fuel], and ₦70.4/kWh [microalgae biodiesel FPP]. Thus, the SPB were beyond 20 years and the IRR were 0%. The TLCC for the liquid fuels were in the range of $0.44 billion [Jatropha biodiesel FPP] to $0.47 billion [microalgae biodiesel FPP], values nearly ten-fold higher than that of the gas FPP. Similarly, the revenue requirements to operate a liquid FPP are in the range of $0.64 billion [Jatropha biodiesel FPP] to $0.69 billion [Microalgae biodiesel FPP], values also nearly ten times higher than that of the gas FPP. Among the three liquid fuels, Jatropha biodiesel still had a better economic performance, although close to that of the diesel fuel and found to be non-viable in such power plants without other forms of integration support and mechanisms.

The above results in section 5.6.3 demonstrate a tendency of decreasing LCOE with decreasing size of engine. Although, an increased LCOE is observed for this size of engine with the biodiesel use, the difference might not be significant when compared to the cost of self-generated electricity and opportunity loss during outages, as well as added benefits such as relative ease of installation and transportation, energy independence and reduced transmission losses and lower capital cost required.

5.5 Sensitivity Analysis

A sensitivity study was carried out to examine alternative scenarios for the inputs in Table 5.4 corresponding to the following parameters: i) investments costs, ii) WACC, iii) fuel costs, iv) emission costs, v) capacity factor, vi) inflation rate, vii) exchange rate, viii) company tax rate, ix) transmission loses, x) fixed O&M cost, xi) variable O&M cost, xii) capacity degradation, and xiii) auxiliary component energy requirements. This is to evaluate the effect of these parameters on the overall economic performance and in comparison with the baseline study (engine GX100). To achieve this, all these parameters were examined within a ±50% range to assume a pessimistic and optimistic scope. The results of the sensitivity analysis are presented in figures 5.8 to 5.10.

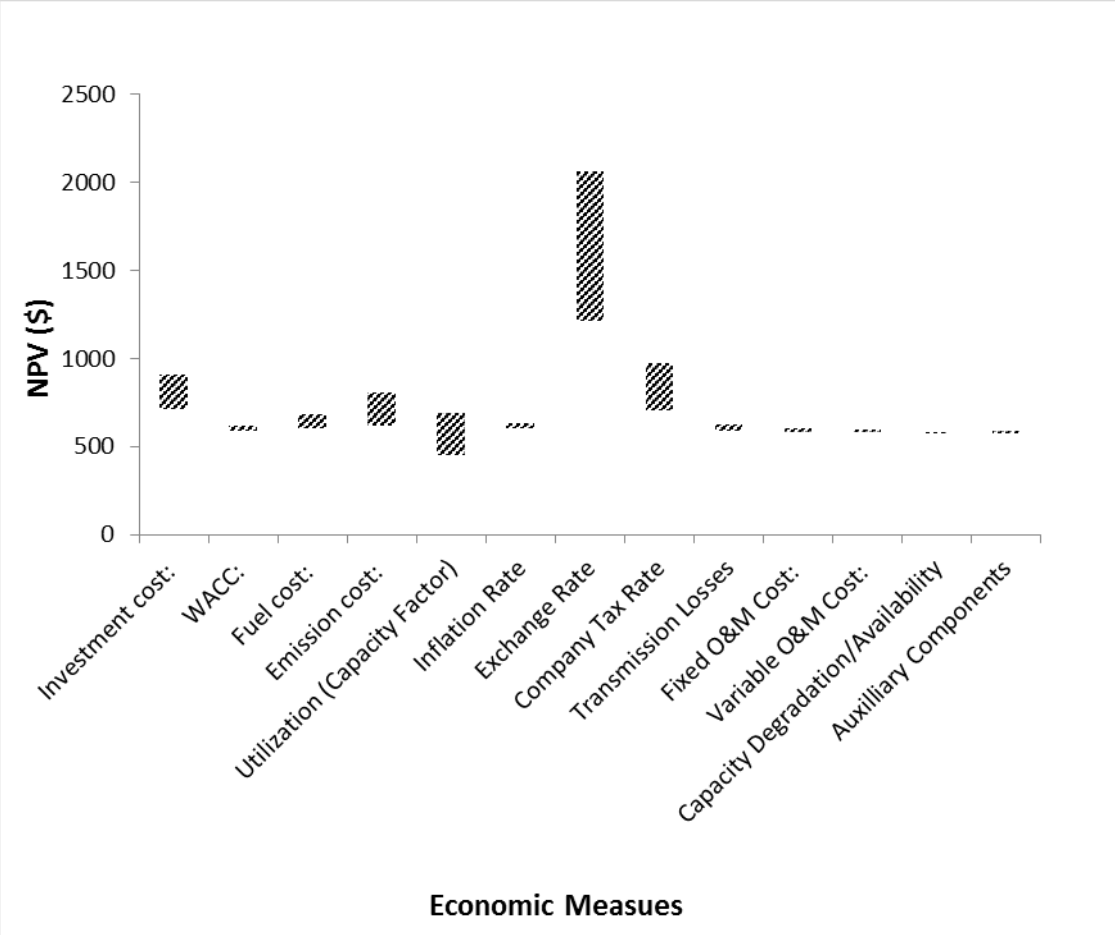

Figure 5.8: Sensitivity Analysis on NPV for Baseline Study

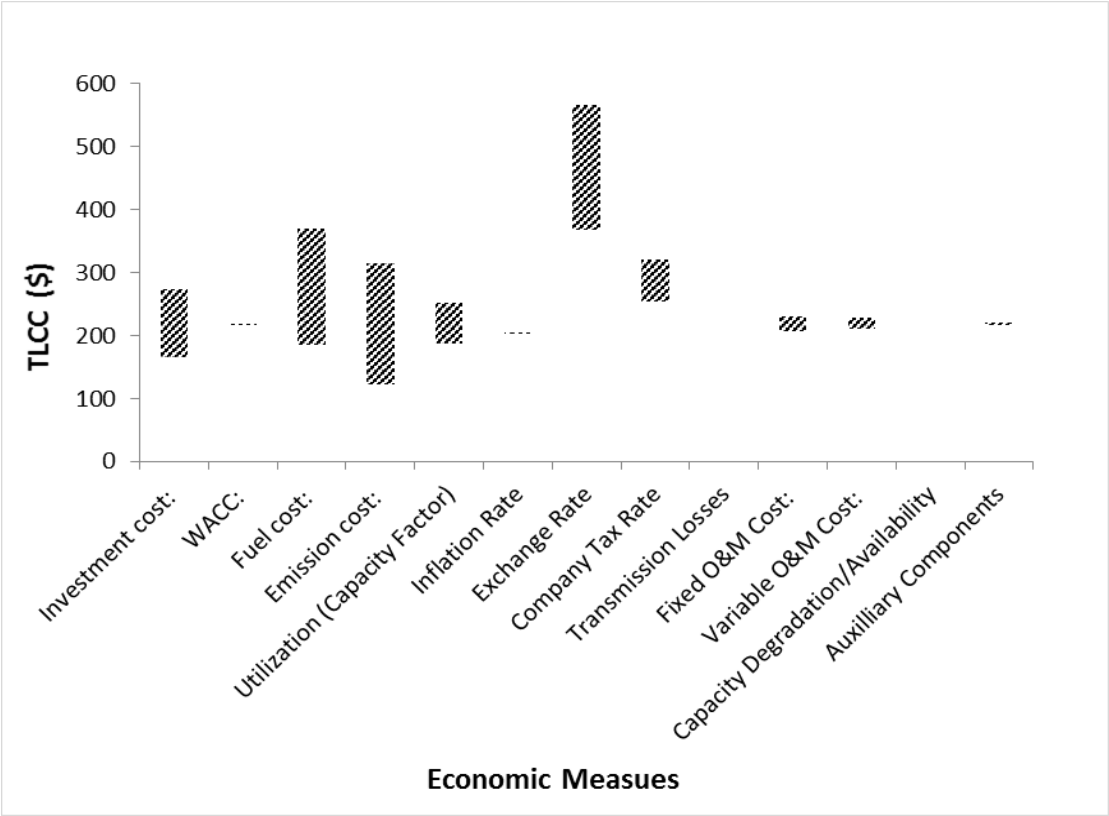

Figure 5.9: Sensitivity Analysis on TLCC for Baseline Study

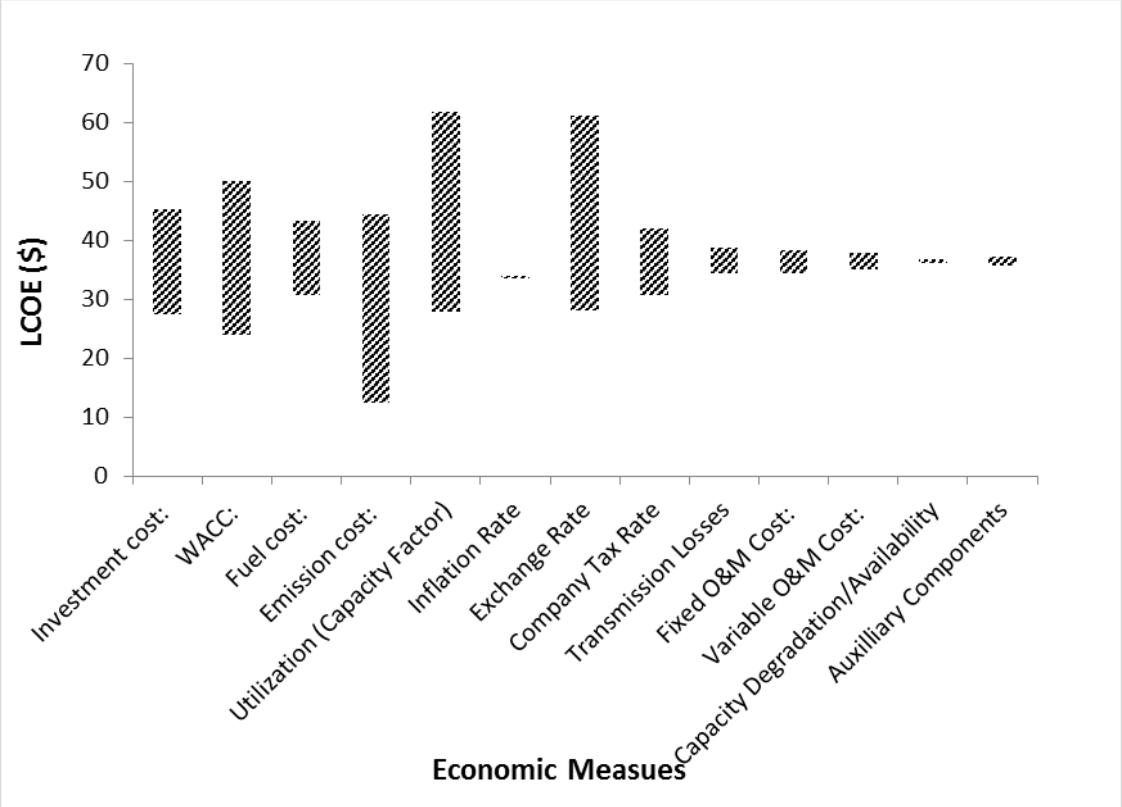

Figure 5.10: Sensitivity Analysis on LCOE for Baseline Study

Figures 5.8 to 5.10 demonstrate the effects of these variables on NPV, TLCC and LCOE. Changes in exchange rate forecasts of ±50% had significant effects on NPV, TLCC and LCOE with values between $350 million and $1211 million, $169million and $367 million, $28/MWh and $62/MWh respectively.

Typically, there are wide fluctuations in exchange rates in developing countries including Nigeria due to high forces of demand and supply, which are brought about by changes in inflation rates, interest rates, political instability, debts or relative currency strength of other currencies. The history of exchange rate in Nigeria in the public domain has a trend; as low as 9.9 in 1992, but as high as 161.5 in 2012, hence the economic value of a power plant could be understated or overstated. To an investor or financier, a significant reduction in exchange rates would mean that the NPV is understated and the LCOE is much lower. However, a significant increase in exchange rates, which is often the case, would be an overestimation of NPV and the LCOE is much higher. In the latter case the return on investment is lower than anticipated. The TLCC is also affected by exchange rates especially for developing countries, where power plant and related equipment require maintenance by expatriates and import of component parts. In this analysis, the changes in fuel cost by 50% resulted in decrease or increase in NPV by over 6% with more effects with increased fuel costs.

Other factors that are critical for TLCC are fuel cost, emission cost (when applied), and investment cost. The changes in fuel cost resulted in increase or decrease in TLCC of 15% and 19% for a 50% decrease or increase in fuel costs. Typically, fuel cost is a major fraction of operating cost, which could be as most as 75%, and depend significantly on market fuel prices. Also, depending on the quality of fuel, the operational conditions of a power plant could be affected by the use of fuels. Common effects associated with the use of fuels, in particular, liquid fuels are: heat radiation to the walls of the combustor, overheating of the combustor and transition piece walls, increased blade metal temperature, especially the early stages of the rotor blades and other thermal stresses. These could bring about additional maintenance and overhaul costs.

The emission costs also had a significant effect on plant economics in terms of TLCC, assuming a baseline emission tax scenario of \$44/tCO_2 with decreasing value of 21% and increasing value of 43% for a 50% decrease or increase in emission costs. Other factors that are sensitive to the TLCC include company tax rate and utility capacity factor. In order words, the TLCC can alter plant economics, return on investment and project benefits.

The LCOE is significantly affected by the following parameters: i) emission cost ii) capacity factor iii) exchange rate iv) WACC investment and slightly by investment cost and fuel costs. The least LCOE of 12.5\$/kWh and the highest LCOE of \$62/kWh were brought about by emission cost and utility capacity factor.

5.5.1 Effect of Ambient Temperature

A range of ambient temperature of 288.15 K [ISO] and 336 K was examined to assess its effect on blade temperature and blade life, as well as consequential effect on maintenance cost. The results are presented in figures 5.11 and 5.12.

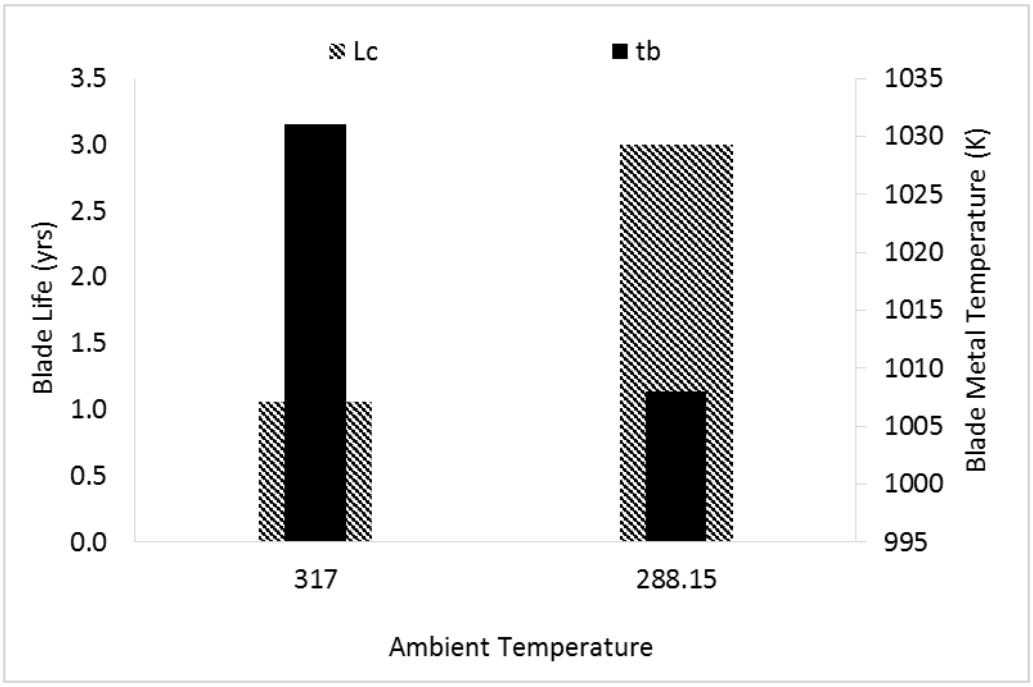

Figure 5.11: Effect of Ambient Temperature on Blade Temperature and Blade Life

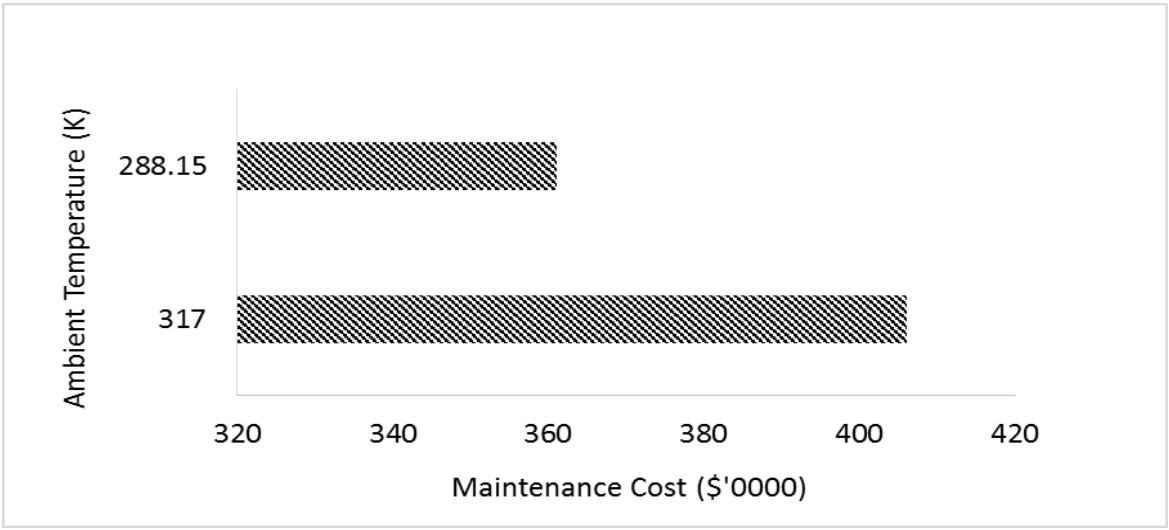

Figure 5.12: Effect of Ambient Temperature on Maintenance Cost ($'0000)

Both figures 5.11 and 5.12 show that a deviation in temperature up to 28 degrees (316 K/43^{o}C), a temperature value that is common to some parts of Nigeria, could result in increase in blade temperature by nearly 2.3% and blade life reduction of over 60%. Consequently, the variable M cost increases by 12.5%.

5.5.2 Effect of Emissivity Factor

A range of emissivity factor of 0.4 and 0.56 was examined to assess its effect on blade temperature and blade life, as well as consequential effect on maintenance cost. The results are presented in figures 5.13 and 5.14.

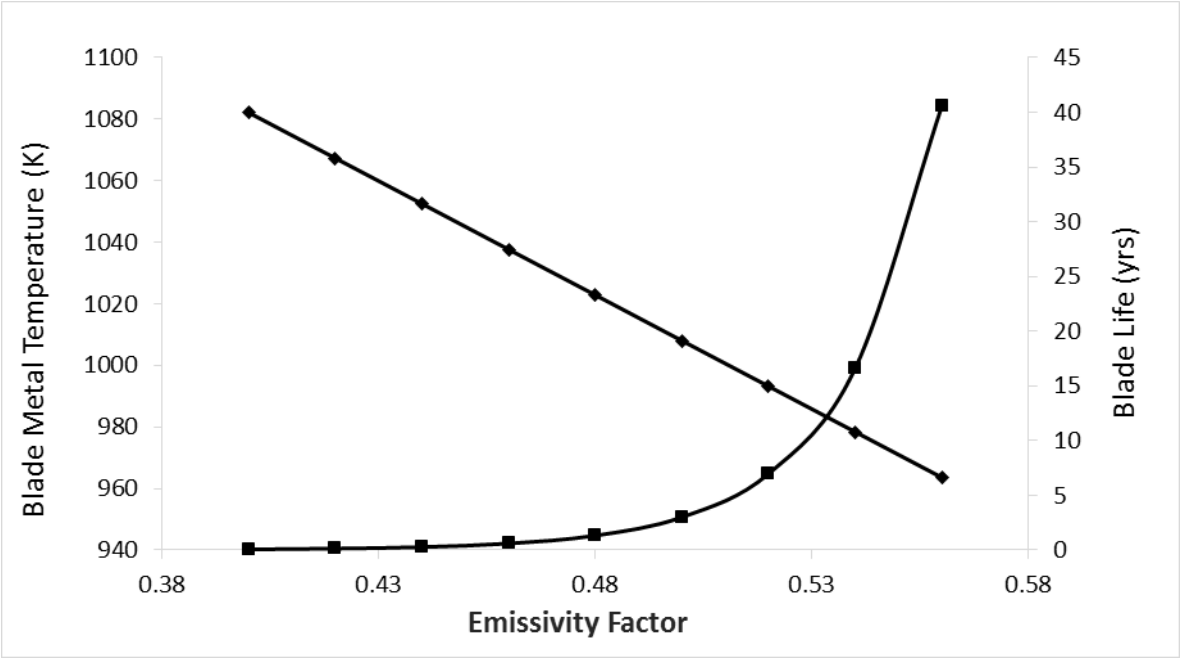

Figure 5.13: The effect of Emissivity Factor on Blade Temperature and Blade Life

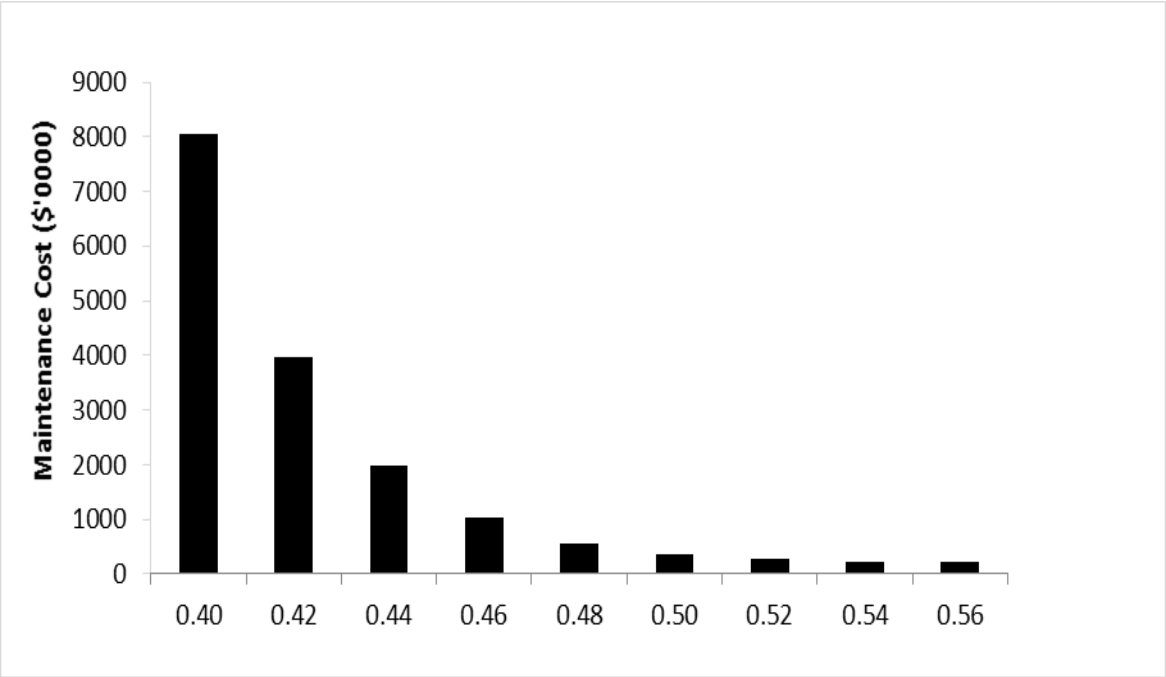

Figure 5.14: The effect of Emissivity Factor on Maintenance Cost

Figures 5.13 and 5.14 demonstrate the impact of cooling effectiveness and technologies on the life of the first stage of a HPT blade, which is constantly faced with high temperatures. Blade metal temperature reduces linearly as the emissivity factor increases, and consequently the life increases exponentially especially at emissivity factor of 0.5. Typically the emissivity factor is usually in the range of 0.4-0.6 and describes the different phenomena and technology that could be applied, such as impingement film cooling, and the effects of air bleeds. The effects on blade life are significantly felt at a relatively high emissivity factor, however at a relatively low emissivity factor below 0.44, the blade life changed only at most by 5%. Similarly there was a significant difference in the variable M cost, with largest variations observed at reduced emissivity factors. At higher emissivity factor above 0.5, the variable M cost decreased at most by 47%, compared to over tenfold increase in this cost at emissivity factor of 0.42. These results demonstrate the importance of upgrading the existing power plants with improved technology and component parts, especially for the hot-end components (combustor and turbine), as this could increase the overall life of engine components and improve the availability and reliability of the project. This is of more importance to power plant that is intended to operate above the useful life.

5.6 Conclusion

The economic performance of Jatropha biodiesel- and microalgae biodiesel-fired engines were evaluated and in comparison to fossil-fired engines, using different economic measures. The average cost of electricity for a typical household and business in Nigeria was estimated and compared to the cases above. Furthermore, other routes of integration of biodiesels were explored to achieve good economic performance in power plants. The results are summarized below:

1. The economic performance for both Jatropha biodiesel- and microalgae biodiesel-FPP were not indicative of project viability because of negative NPV, IRR of 0% and SPB of over the life time of the project. The TLCC was about ten times higher for the biodiesel fuel cases than the natural gas fuel, although slightly in the range with conventional diesel fuel.
2. For good plant economics and integration of biodiesels in existing structures, a form of production based renewable tax, incentive or other form of subsidy program would be required. A minimum amount of $0.21/kWh would be required to give the project a minimum positive balance at the end of the project life, $0.22/kWh from the end of year 1 and as much as $0.27/kWh to enable the LCOE be the same as that of natural gas fuel case. This guarantees the generator a minimum amount and covers the capital cost. The other option would require part-substitution of natural gas with the Jatropha biodiesel fuel up to a maximum of 20% to achieve a positive NPV at the end of the project life and with government incentives of $0.2/kWh to achieve similar LCOE with natural gas case.
3. A carbon tax scenario of $44/tCO2 would increase LCOE by 30%, values from N6/kWh to N9/kWh. This is lower than the part-substitution of 20% Jatropha biodiesel with natural gas that is supported by government incentives. However, a carbon tax scenario of $124/tCO2 increases the LCOE to N13/kWh, a value that is slightly higher than the 20% Jatropha biodiesel mixture with natural gas that is supported by government incentives.
4. In a worst case scenario where there are no government incentives, there are opportunities for distributed and independent power generation with the integration of renewable fuels like Jatropha-biodiesel, since the average cost of electricity is over 50 times higher for a small-medium business, and nearly 20 times higher for an average household than the gas-fired electricity generation from an OCGT.

5. Future situation analysis involving the use of CCGT shows that the LCOE reduces significantly to a range of $0.32/kWh [Jatropha-biodiesel] to $0.36/kWh [microalgae-biodiesel], although still much higher than the natural gas fired case. The use of CCGT brought about an increase in NPV due but a much higher TLCC due to additional cost of operating a bottoming cycle. Similar to the OCGT, government incentives can bring the Jatropha biodiesel application to a positive NPV and better overall plant economics, provided an amount of $0.13/kWh would be required to give the project a minimum positive balance at the end of the project life, $0.14/kWh from the end of year 1 and as much as $0.17/kWh to enable the LCOE be the same as that of natural gas fuel case. This combined cycle application will allow a maximum integration of 25% part substitution of Jatropha biodiesel with natural gas, but with additional government support of $0.05/kWh, the LCOE could be the same with that of the natural gas case.
6. Under the carbon tax scenarios, the Jatropha biodiesel part-substitution had better good plant economics than both cases requiring $44/t$CO_2$ and $124/t$CO_2$ for utilizing natural gas.
7. Comparing engine GX100 (126 MW) and GX200 (22.4 MW), the economic analysis shows that there is decreasing LCOE with decreasing size of engine, assuming the capital cost remains 978/kWh. The better advantage with engine GX200 however includes relative ease of installation and transportation, shorter installation time, energy independence plus reduced transmission losses and lower capital cost required. This opens more opportunities for renewable distributed and independent power generation.
8. The main parameters that could influence the economic performance results presented in this study include exchange rates, specific fuel cost, emission cost, WACC, capacity factor and initial investment costs.

5.7 Further Work

This study has examined the economics of Jatropha biodiesel- and microalgae biodiesel-fired engines in comparison to fossil-fired engines using ISO rated engines. It will be interesting to re-examine this analysis at site and other operating conditions such as peak load operation.

5.8 References

[1] Biondo, C., Strohl, J.P., Samuelson, J.W., Fuchs, G.E., Wlodek, S.T. and Wlodek, R.T. 2010. Nickel-base alloy for gas turbine applications. US Patent Application Number US20100080729 A1. (Patent Issued in 2010).

[2] Chisti, Y. 2007. Biodiesel from Microalgae. *Biotechnology Advanc*es: 25: 294–306

[3] Hong, C., Tran, S. and Dewey, R. 2005. Life Management System for Advanced E Class Gas Turbines: General Electric 7EA 1st Stage Bucket Analysis. EPRI, Palo Alto, CA: 2005. 1010477.

[4] Kost, C., Mayer, J. N., Thomsen, J., Hartmann, N., Senkpiel, C., Philipps, S., Nold, S., Lude, S., Saad, N. and Schlegl, T. 2013. Levelized Cost of Electricity Renewable Energy Technologies. Fraunhofer Institute for Solar Energy Systems, Freiburg, Germany.

[5] Kreith, F. and Krumdieck, S. 2013. *Principles of Sustainable Energy Systems*. CRC Press, USA

[6] Leme, M.M.V., Rocha M.H., Lora, E.E.S, Venturini, O.J., Lopes B.M. and Ferreira, C.H. 2014. Techno-economic analysis and environmental impact assessment of energy recovery from municipal solid waste (MSW) in Brazil. *Resour Conserv Recycl*. 87: 8–20

[7] Nigerian Electricity Regulatory Commission (NERC). 2012. Multi-year tariff order for the determination of the cost of electricity generation for the period 1 June 2012 to 31 May 2017. NERC, Abuja.

[8] Sajjadi, S.A. and Nategh, S. 2001. A high temperature deformation mechanism map for the high performance Ni-base superalloy GTD-111. *Mater. Sci. Eng*. 307(1): 158-164.

[9] Schilke, P.W. 2004. Advanced Gas Turbine Materials and Coatings. GE Energy, GER-3569F, Schenectady, NY

[10] Short, W., Packey, D.J. and Holt, T. 2005). *A manual for the economic evaluation of energy efficiency and renewable energy technologies*. Honolulu, Hawaii. University Press of the Pacific.

[11] Strogen, B., Horvath, A. and Zilberman, D. 2013. Energy intensity, life-cycle greenhouse gas emissions, and economic assessment of liquid biofuel pipelines. *Bioresource Technology* 150: 476–485

[12] Wegstein, M. and Adhikari, N. 2010. Financial Analysis of Jatropha Plantations. *Journal of the Institute of Engineering, Kathmandu* 8(1): 1-5.

Chapter 6

6. ENERGY BALANCE AND ENVIRONMENTAL LIFE CYCLE IMPACT ASSESSMENT

In previous chapters, Jatropha biodiesel has been considered as the next alternative to conventional diesel and should ensure good engine performance and emissions, apart from NOx penalty and economic performance provided there are supporting mechanisms to allow a successful initial integration. This chapter examines the energy requirements and environmental performance of Jatropha biodiesel production and its subsequent use in engine GX100. It begins with an introduction on sustainability issues surrounding Jatropha biodiesel and how these affect its integration in gas turbines and in power generation. This is followed by the description of the methods for assessing the energy balance and environmental life cycle impact of Jatropha biodiesel and conventional diesel fuel under a well-to-wake and well-to-wheel system boundary. A few of the comparative results that are discussed include: fossil fuel displacement, GHG savings and the effects of changing parameters on GHG and overall emissions.

6.1 Introduction

Gas turbine exhaust emissions cannot be used as the only criteria to determine the environmental burden associated with the use of fuels. As in this case of Jatropha biodiesel, there are other GHGs emitted during the production and conversion of Jatropha oil to biodiesel that negatively impact the ecosystem and cause environmental degradation. For instance, additional CO_2 is released during fertilizer application and fossil fuel consumption on farm site or in farm machineries, and this contributes to global CO_2 emissions.

Generally, first generation crops, such as sugar cane, palm oil, sweet sorghum, and Jatropha curcas, are considered to have both positive and negative impacts. Biofuels derived from these crops could improve energy security, reduce GHG emissions, improve air quality and bring about rural development [Demirbas, 2009, Gokalp and Lebas, 2004]. However, their commercial production could bring about water scarcity, ecosystem degradation, negative carbon and energy balance, increased GHG emissions, increased fuel prices, land crisis from indirect land use change, food crisis

and impact on food and energy security, as well as changes to good agricultural practices, especially those related to monocultural farming. These debating issues have limited the application of biofuels worldwide and in power generating plants, including gas turbines.

Biodiesel derived from Jatropha curcas plant has the added advantage because it is a multi-purpose plant. The oil and agricultural residue could be used for electrification, the seedcake and other agricultural residue of the plant could be used in fertilizer production and for medicinal purposes. And since the plant grows as a shrub and can reach up to a height of 10 m when grown favourably, can grow on marginal land, drought prone areas and wastelands, it provides added benefits of water conservation, fencing and erosion control. Because it is a non-edible crop, it limits the pressure on food security. These advantages place Jatropha-derived fuels in a better position than other fuels derived from energy crops, however, it's important to quantify the environmental burden associated to its production and use. And, since previous analyses have shown that the performance of Jatropha biodiesel fuel is similar to that of conventional diesel fuel, Jatropha biodiesel fuel can only demonstrate an obvious advantage over fossil derived fuels from its environmental performance.

6.2 Methodology

The environmental life cycle impact and energy balance of Jatropha biodiesel-fuel produced on a small scale and used in a typical gas turbine power plant in South-West, Nigeria was carried out in comparison with a reference diesel-fuel using LCA methodologies. This involves: i) goal and scope definition, (ii) inventory analysis, iii) impact assessment, and iv) data interpretation. Here, system boundaries, defined functional units, inventories, impact assessment methods and performance criteria are all key components. This approach has been widely employed for assessing the environmental burden associated to a system, process, product or technology and is described in detail [ISO 14040-44].

6.2.1 Goal and Scope Definition:

This study addresses the environmental aspect of the use of biofuels in gas turbines from a life cycle perspective. Following up on performance, emission and economic analyses, which have identified Jatropha biodiesel as a good substitute to petroleum diesel and natural gas fuel, the goal of this comparative LCA study is to quantify the

energy requirement and evaluate the environmental impact of small scale production of Jatropha biodiesel via the process of transesterification and its subsequent use in a typical power plant in Nigeria.

Two system boundaries are examined: a) well-to-wake and b) well-to-wheel. The “well-to-wake” boundary for Jatropha biodiesel fuel incorporate the agricultural processes of production such as cultivation & harvesting, oil extraction processes, oil conversion processes and all associated transportation. The subsequent use of the fuel in a biodiesel-fired plant (Engine, GX100), including fuel transportation to a power station further expands into a “well-to-wheel” boundary. The “well-to-wake” system boundary for the reference diesel fuel on the other hand describes the processes involved in the extraction and lifting of crude-oil from Nigerian oil wells (onshore/offshore), local refining of crude oil to diesel fuel, crude oil swaps, export of crude-oil for refining, onshore extraction of crude oil from overseas facilities and its transportation to an overseas refinery, and associated transportation processes. Similar to Jatropha biodiesel fuel, the “well-to-wheel” boundary further incorporate fuel transportation to a power station and the utilization of the fuel in a diesel-fired plant (Engine, GX100). These boundaries are illustrated in figures 6.1 and 6.2 for Jatropha biodiesel and the reference diesel fuel.

Neither boundaries have considered the impact of land use change nor, infrastructure use of recent technologies, as this was unclear and better modelled with site specific data. Also, 100% use of fuel is considered as opposed to the use of fuel blends. The functional unit for the “well-to-wake” system boundary is 1 kg of fuel produced while that of “well-to-wheel” system boundary is 1 MJ of fuel combusted in a 126 MW gas turbine power plant with multi-fuel capability, as in this case, GX100 engine.

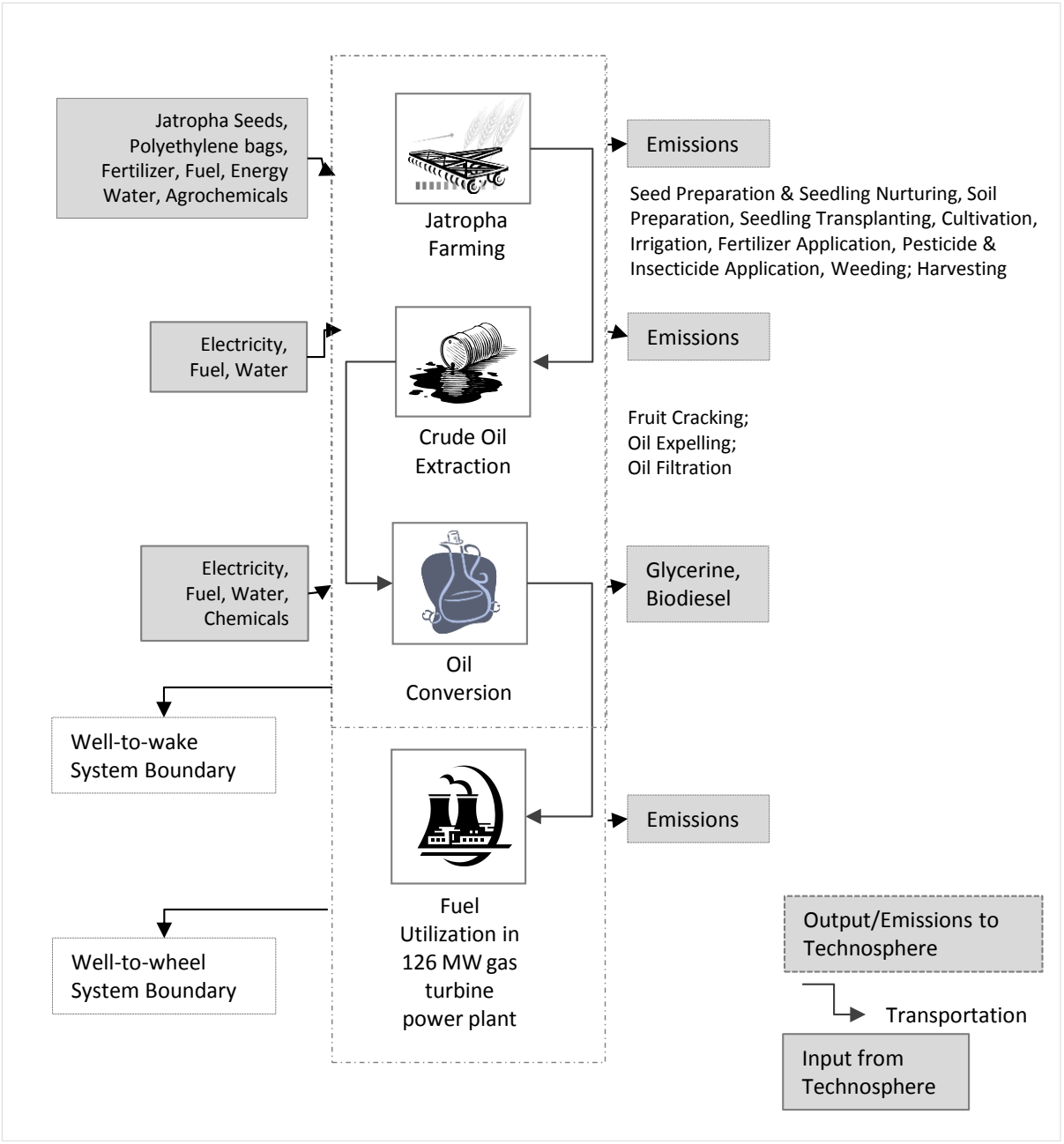

Figure 6.1: System Boundary for Jatropha biodiesel fuel

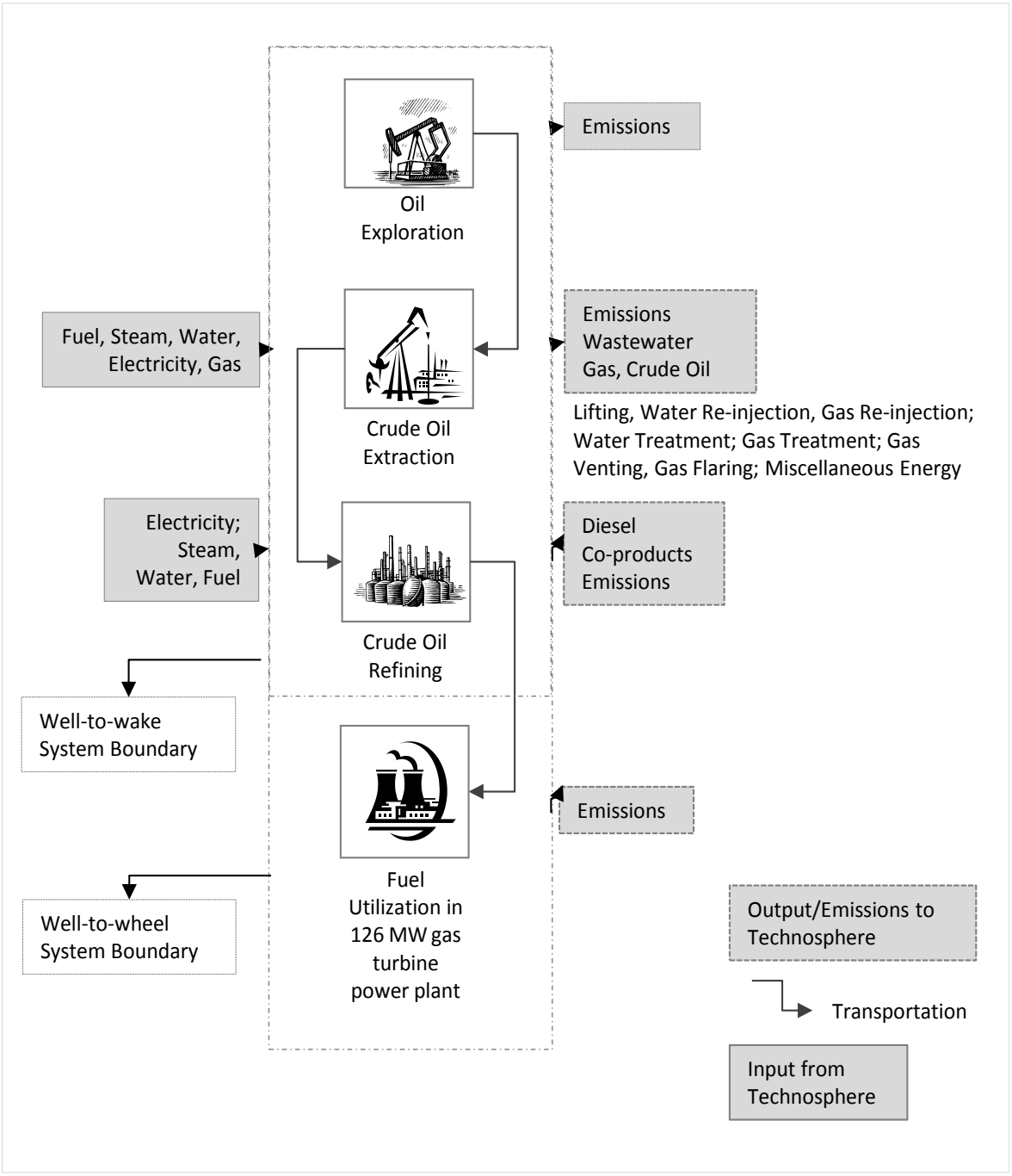

Figure 6.2: System boundary for the reference diesel fuel

6.2.2 Inventory and Life-Cycle Impact-Assessment

An inventory was developed to include material inputs, energy and fuel used as well as product, waste and emissions generated using SimaPRO 8.0.3.14 software. This software is a computational tool developed by Product Ecology Consultants [PRé, 2011], and used for assessing a number of processes and products. The software integrates a number of databases, including U.S. Life Cycle Inventory (US LCI), Agrifood Libraries, Eco-invent Libraries, European Reference Life Cycle Database (ELCD) for several processes and systems and allows the modeller to develop customized modules. Hence, inventory development and analysis were carried out for Jatropha biodiesel-fuel and the reference diesel-fuel using the Agrifood and Eco-invent libraries.

Material inputs including energy and fuels were selected based on secondary information obtained from the public domain and scientific literatures, with emphasis on local conditions and agricultural farming-systems applicable to Nigeria. In the event, where the required data were not available or absence of Jatropha or country-specific data, plausible technical assumptions and close substitutes of inputs and outputs were adopted. This was necessary because of little or no information about the commercial production and use of Jatropha biodiesel-fuel in Nigeria. Table 6.1 and 6.2 highlight the material inputs considered for Jatropha biodiesel-fuel in the well-to-wake and well-to-wheel system boundaries respectively. Other inputs in the model include product, co-products waste and emissions**.**

Because the GHG emissions associated with use of farm machinery, lorries and small transport vehicles have been taken into account in the SimaPRO software, the direct GHG emissions from fertilizer applications were only calculated using the IPCC global-warming potential (GWP) frame of 1, 25 and 298 within a 100 years' time-scale for CO_2, CH_4 and N_2O. Additional environmental impacts, such as eutrophication and acidification potential, were calculated using inorganic elements in the following categories (i) PO_4, NO_3 and NH_3 and (ii) SO_2, NOx and NH_4 respectively. Overall, the net GHG and direct and indirect discharges were expressed as kg CO_2eq and kg total emissions.

Table 6.1: The Inventory for Jatropha Biodiesel fuel Production (Well-to-Wake System Boundary)

Sub-process	Assumption/Estimate	Energy Density MJ/kg	Value kg $ha^{-1}yr^{-1}$
Jatropha Farming			
Plant Spacing	2 mx 2m [1]		-
Tree Density	2500 trees ha^{-1} [2]		-
Tractor Use for Land Preparation	25 L diesel $ha^{-1}run^{-1}$	42.79[8]	2.05
Seeds for Nursery	0.769 g $seed^{-1}$[3]	24[9]	0.13
Water for Nursery	0.2 L $plant^{-1}day^{-1}$[3]	0.0098*	1575
Polyethylene Bags (Nursery)	2 g bag^{-1}	42.6	0.35
Fertilizer, N	121.48 kg $ha^{-1}yr^{-1}$[4]	87.9[5]	36.44
Fertilizer, P_2O_5	46.49 kg $ha^{-1}yr^{-1}$[4]	26.4[5]	13.95
Fertilizer, K_2O	133.47 kg $ha^{-1}yr^{-1}$[4]	10.5[5]	40.04
Glyphosphate (Herbicide)	3 L $ha^{-1}yr^{-1}$[5]	454[10]	0.75
Paraquat (Herbicide)	2 L $ha^{-1}yr^{-1}$[5]	459.4[10]	0.50
Insecticide	0.04 g $plant^{-1}yr^{-1}$	454	0.04
Manual Weeding	5 men ha^{-1} day^{-1}	8.87[11]	5.00
Manual Harvesting	50 kg dry seed $man^{-1}day^{-1}$	8.87	70.00
Gasoline Use (Extra)	40 L $ha^{-1}yr^{-1}$	42.79	32.80
Diesel Use (Extra)	60 L $ha^{-1}yr^{-}$	43.45[8]	46.20
Transportation (To Crushing Site)	50 km @20mpg	42.79	5.79
Diesel for Irrigation	60 L $ha^{-1}day^{-1}$	42.79	49.20
Irrigation	8 L $plant^{-1}week^{-1}$[2]	0.0098	480,000
Transport for Irrigation	43 km @20 mpg	42.79	72.44
Water for Insecticide Application	100 L	0.0098	100
Oil Extraction			
Cracking Machine	2hp@100 kg hr^{-1}[5]	3.6 MJ/kWh	52.2 kWh $ha^{-1}yr$
Expeller	37.5@ 0.75 ton hr^{-1}	3.6 MJ/kWh	124.0 kWh $ha^{-1}yr$
Filtering Machine	2hp@160L hr^{-1}[5]	3.6 MJ/kWh	10.5 kWh $ha^{-1}yr$
Transportation (Crushing Site to Biodiesel Plant)	40 km@ 20 mpg	42.79 MJ/kg	4.6
Oil Conversion			
Electricity for Biodiesel Plant Use	80L/batch @4kWh/batch[5]	3.6 MJ/kWh	55.3 kWh $ha^{-1}yr$
Electricity for Pre-treatment	14kwh/t[6]	3.6 MJ/kWh	17.3 kWh $ha^{-1}yr$
Sulphuric acid	14kg/t[6]	3.1 MJ/kg	17.3 kg $ha^{-1}yr$
Methanol	110kg/t[7]	38.08 MJ/kg[7]	134.6 kg $ha^{-1}yr$
KOH	18kg/t[7]	19.87 MJ/kg[5]	22.0 kg $ha^{-1}yr$
Steam	660kg/t[7]	3.12 MJ/kg[7]	807.6 kg $ha^{-1}yr$
Transportation (Biodiesel Plant to Local Site)	50km	42.79 MJ/kg	5.8 kg $ha^{-1}yr$

[1]United Nations Department of Economic and Social Affair, 2007; [2]Gm¨under et al. 2010; [3]Brittaine and Lutaladio, 2010; [4]PrOpCom, 2012; [5]Reinhardt et al. 2007; [6]Prueksakorn et al. 2010; [7]Eshton et al. 2013; [8]Whitaker and Garvin, 2009; [9]Audsley et al. 2009; [10]Davis et al. 2014; [11]van Wesenbeeck et al. 2009

Table 6.2: The Inventory for Jatropha Biodiesel fuel Production (Well-to-Wheel System Boundary)

Sub-process	Assumption/Estimate	Energy Density MJ/kg	Value MJ/MJ
Jatropha Farming			
Plant Spacing	2 mx 2m [1]		-
Tree Density	2500 trees ha^{-1} [2]		-
Tractor Use	25 L diesel $ha^{-1}run^{-1}$	42.79[8]	2.0E-03
Seeds for Nursery	0.769 g $seed^{-1}$[3]	24[9]	7.4E-05
Water for Nursery	0.2 L $plant^{-1}day^{-1}$[3]	0.0098*	3.5E-04
Polyethylene Bags (Nursery)	2 g bag^{-1}	42.6	3.4E-04
Fertilizer, N	121.48 kg $ha^{-1}yr^{-1}$[4]	87.9[5]	7.3E-02
Fertilizer, P_2O_5	46.49 kg $ha^{-1}yr^{-1}$[4]	26.4[5]	8.4E-03
Fertilizer, K_2O	133.47 kg $ha^{-1}yr^{-1}$[4]	10.5[5]	9.6E-03
Glyphosphate (Herbicide)	3 L $ha^{-1}yr^{-1}$[5]	454[10]	7.8E-03
Paraquat (Herbicide)	2 L $ha^{-1}yr^{-1}$[5]	459.4[10]	5.2E-03
Insecticide	0.04 g $plant^{-1}yr^{-1}$	454	3.6E-04
Manual Weeding	5 men ha^{-1} day^{-1}	8.87[11]	1.0E-03
Manual Harvesting	50 kg dry seed $man^{-1}day^{-1}$	8.87	1.4E-02
Gasoline Use (Extra)	40 L $ha^{-1}yr^{-1}$	42.79	3.2E-02
Diesel Use (Extra)	60 L $ha^{-1}yr^{-}$	43.45[8]	4.6E-02
Transportation: Crushing	50 km @20mpg	42.79	5.6E-03
Diesel for Irrigation	60 L $ha^{-1}day^{-1}$	42.79	4.8E-02
Irrigation	8 L $plant^{-1}week^{-1}$[2]	0.0098	1.1E-01
Transportation: Irrigation	43 km @20 mpg	42.79	7.1E-02
Water: Insecticide Application	100 L	0.0098	2.2E-05
Oil Extraction			
Cracking Machine	2hp@100 kg hr^{-1}[5]	3.6 MJ/kWh	4.3E-03
Expeller	37.5@ 0.75 ton hr^{-1}	3.6 MJ/kWh	1.0E-02
Filtering Machine	2hp@160L hr^{-1}[5]	3.6 MJ/kWh	8.6E-04
Transportation: Biodiesel Plant	40 km@ 20 mpg	42.79 MJ/kg	4.5E-03
Oil Conversion			
Electricity for Biodiesel Plant	80L/batch @4kWh/batch[5]	3.6 MJ/kWh	4.5E-03
Electricity for Pre-treatment	14kwh/t[6]	3.6 MJ/kWh	1.4E-03
Sulphuric acid	14kg/t[6]	3.1 MJ/kg	1.2E-03
Methanol	110kg/t[7]	38.08 MJ/kg[7]	1.2E-01
KOH	18kg/t[7]	19.87 MJ/kg[5]	1.0E-02
Steam	660kg/t[7]	3.12 MJ/kg[7]	5.7E-02
Transportation: Local Site	50km	42.79 MJ/kg	5.6E-03
Oil Use			
Jatropha Biodiesel		39.65MJ/kg	1.0E-00

[1]United Nations Department of Economic and Social Affair, 2007; [2]Gm¨under et al. 2010; [3]Brittaine and Lutaladio, 2010; [4]PrOpCom, 2012; [5]Reinhardt et al. 2007; [6]Prueksakorn et al. 2010; [7]Eshton et al. 2013; [8]Whitaker and Garvin, 2009; [9]Audsley et al. 2009; [10]Davis et al. 2014; [11]van Wesenbeeck et al. 2009

The environmental life-cycle impacts were predicted using ReCiPe Midpoint methodology under twelve impact categories: i) climate change, ii) ozone depletion, iii) photochemical oxidant formation, iv) terrestrial acidification, v) freshwater eutrophication, vi) marine eutrophication, vii) terrestrial ecotoxicity, viii) freshwater ecotoxicity, ix) marine ecotoxicity, x) ionizing radiation, xi) particulate matter formation and xii) fossil depletion. The ReCiPe Midpoint methodology classifies the analysis of the inventory, mainly emissions into a limited number of indicator scores and characterizes the scores into eighteen midpoint categories, adopting a relative severity and consequential effects of emissions on human health or the ecosystem. This assessment however excluded agricultural occupation, urban occupation, natural land transformation, human toxicity and water depletion. Furthermore, an egalitarian perspective with world normalization was selected to account for a worst case scenario, assuming that these effects have a long term impact. Overall, the net GHG and direct and indirect discharges were expressed as kg CO_2eq and kg total emissions.

6.2.3 Energy Balance

The energy requirements for each system boundary was deduced using the inputs and the corresponding energy density in Table 6.1 and 6.2, and assuming a Jatropha plantation of 1 hectare (ha) over a 20-year period. The results are expressed as Net Energy Value (NEV), Net Renewable Energy Value (NREV) and Net Energy Ratio (NER) using equations 6.1, 6.2 and 6.3 respectively below [Whitaker and Heath, 2009].

NEV= Energy output $\left(\frac{MJ}{kg}\right)$ or $\left(\frac{MJ}{MJ}\right)$ of fuel - Energy input $\left(\frac{MJ}{kg}\right)$ or $\left(\frac{MJ}{MJ}\right)$ from fossil and non-fossil sources (6.1)

NREV= Energy output $\left(\frac{MJ}{kg}\right)$ or $\left(\frac{MJ}{MJ}\right)$ of fuel - Energy input $\left(\frac{MJ}{kg}\right)$ or $\left(\frac{MJ}{MJ}\right)$ from renewable sources (6.2)

$$\text{NER} = \frac{\text{Energy output } \left(\frac{MJ}{kg}\right) \text{or } \left(\frac{MJ}{MJ}\right) \text{of fuel}}{\text{Energy input } \left(\frac{MJ}{kg}\right) \text{from fossil source}} \quad (6.3)$$

The NEV, NREV and NER are similar energy performance criteria that differ in their functions. NEV reflects the energy loss or gained, while NREV determines the fossil-fuel requirement for the production and use of Jatropha biodiesel fuel and NER indicates the

energy efficiency of the system [Whitaker and Heath, 2009; Eshton et al. 2013]. These energy-performance criteria should indicate whether or not there are ecological benefits arising from the production and use of Jatropha biodiesel-fuel in Nigeria.

6.2.4 Allocation of Co-products

Beside the seed oil, there are other product yields from Jatropha biodiesel production and these include: seedcake and husks from oil pressing, fruit hulls from fruit cracking, biomass (stem and leaves), also referred to as agricultural residues and glycerol, a by-product of Jatropha crude oil conversion to biodiesel. The baseline study has not considered these other products, however, another scenario is examined that considers the local use of glycerol co-product and allocates the environmental burden on a mass basis of a 90:10 ratio for Jatropha biodiesel fuel and glycerol and assuming there is no additional energy requirement for dispensing the glycerol.

6.2.5 Jatropha Biodiesel System

The pathway for the production of 1 MJ of Jatropha biodiesel fuel is in figure 6.3

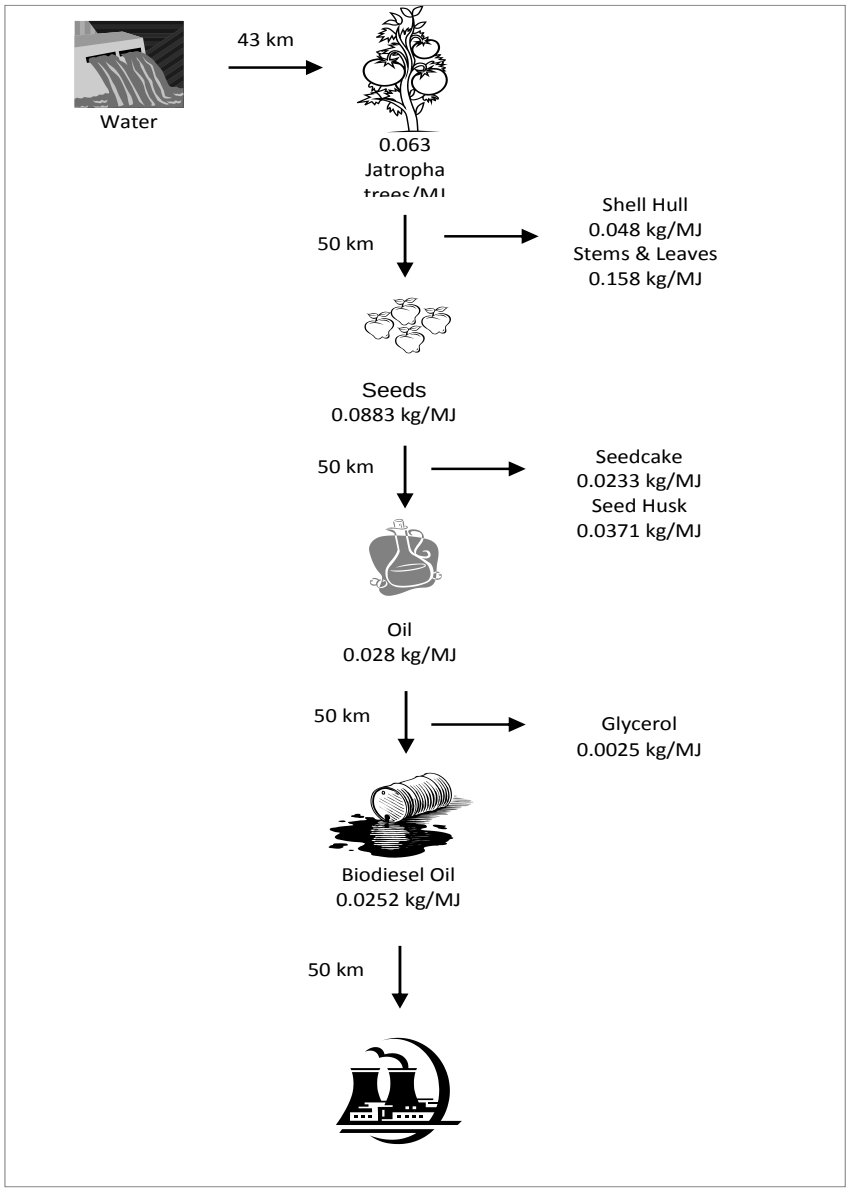

Figure 6.3: The pathway for the production of 1 MJ of Jatropha biodiesel fuel

6.2.5.1 Jatropha Farming System

Because of the absence of data concerning agricultural practices and the low commercial scale of Jatropha plant in Nigeria, a generic and hypothetical Jatropha farming system had to be developed to guide this study This assumes a multiple small-scale farming system for Jatropha in Ogun-State, Nigeria. Three scenarios have been examined which include: i) a rain-fed base-case, ii) an irrigated base-case, iii) and a large scale farming system.

Jatropha seedlings were assumed to be grown in polythene bags on nursery beds using seeds with a 80% survival rates. Field preparation in Nigeria includes activities such as tree felling, clearing, stump removal, ploughing and harrowing: these are usually achieved, by manual labour, over several days with the use of axes, hoes and cutlasses. Hence, in the base-case rain-fed scenario, manual labour involving 5 men ha^{-1} day^{-1} was assumed whereas field preparation in large-scale plantations would be undertaken by mechanized farming. Eshton et al. [2013] and Gm¨under et al. [2009; 2012] reported diesel consumptions of 12-15 litres of diesel fuel ha^{-1} for land preparation, whereas Prueksakorn and Gheewala [2008] concluded that the range is 25-40 litres of diesel fuel ha^{-1}. In Nigeria, farm machinery is rarely new and often improperly managed. There is also a tendency that farm tractors have high rates of fuel consumption. Hence, twin run of a farm tractor with diesel fuel requirement of 25 litres ha^{-1} $run^{-1}$was assumed in the present analysis.

Fertilizer application is not a common practice on small-scale farms in Nigeria due to the costs involved and because good fertilizers are rarely produced locally. This study assumes 122, 47,134 kg ha^{-1} yr^{-1} of Nitrogen (N), Phosphorus (P), Potassium (K) [Prueksakorn and Gheewala, 2008; Reinhardt et al. 2007] is applied twice per year for the first three years of the plantation, after which the residues from Jatropha plantation such as husks and seedcake are returned to the field in order to achieve a higher yield. As opposed to popular opinion about the protective insecticidal and microbicidal properties of Jatropha plant, Terren et al. [2012] reported pest and diseases to be prevalent in Jatropha farming: Jatropha plants do not appear to be protected by their insecticidal and microbicidal properties. Thus, insecticide applications of 0.04 g $plant^{-1}$ yr^{-1} of Chloropyrifos 20EC is assumed to be applied every 3 years based on local availability and herbicide application of Glyphosphate (3 litres ha^{-1} yr^{-1}) and Paraquat (2 litres ha^{-1} yr^{-1}) [Gmunder et al. 2012]. Weeding and harvesting are assumed to be

accomplished manually, twice a year for the first five years, involve 5 men ha^{-1} day^{-1} [Prueksakorn and Gheewala, 2008], and annually, with an average of 50 kg of dry seeds per $worker^{-1}$ day^{-1}.

The energy expended by manual labour was calculated using the average daily food-intake of 2120 kcal (8.9 MJ) $capita^{-1}$ day^{-1}, as estimated for a West Africa adult [van Wesenbeeck et al. 2009]. All other forms of manual labour, such as those relating to the operation of equipment were not included in the present study for both the Jatropha system and the reference diesel-fuel system. An additional gasoline consumption of 60 litres $ha^{-1}yr^{-1}$ was included in order to account for the transportation of workers in and out of the farm, as well as miscellaneous activities, such as power generation on the farm.

Irrigation is not considered in the base-case scenario because the average annual precipitation in Ogun-State exceeds 1000 mm. In the irrigated scenario, irrigation is assumed to be supplemented daily with 8 litres of water per plant per application during the dry season that lasts up to six months between October and March. For large-scale farming systems, irrigation is practised for the six months of the dry season and involved the use of farm machinery and equipment requiring 250 litres ha^{-1} of diesel fuel for all farm operations aside from miscellaneous activities, such as (power generation, transportation of workers.

Because, a yield range of 3 to14 tonnes of dry seed is reported [Jingura et al. 2011, Ogunwole, 2014] for good soil and as low as 0.7 tonnes for poor soil or wasteland [NBS, 2011], this study assumes an average yield of 3.5 tonnes of dry Jatropha seeds ha^{-1} yr^{-1} is produced over the life (~20 years) of the considered plantation. Although this is a pessimistic yield value in view of the current rapid advancements in Jatropha farming, spoilage is nevertheless likely during and after harvesting due to poor storage facilities, especially during high-humidity conditions. Also, the temperature in Nigeria is favourable for microbial growth. Other losses such as product theft could be incurred by farmers: this would result in an overall low-seed recovery. Furthermore, an oil-seed yield of 35% was assumed, although, Umaru and Aberuaba [Jingura et al. 2011] reported a yield of 53%, Aransiola et al. [2012] reported a value of 52%, whereas Ogunwole [2014] recorded a yield of 37% for Jatropha *curcas* plants grown locally.

Farming location are primarily near villages and far distant from cities. Thus, this study assumes a centralized fruit cracking and expelling facility for multiple Jatropha farming, where transportation distances are up to 50 km from the plantation field and an additional

50 km to the biodiesel production facility. Here, fruits are assumed to be transported by a farm truck of 20 tonnes capacity and a fuel consumption of 20 mpg, to the oil extraction facility.

6.2.5.2 Oil Extraction

Available power is a limiting factor in Nigeria. Thus small-scale farmers will likely choose the least expensive and readily available technology for expelling oil. Thus seeds were assumed to be sun-dried and harvested by manual labour. The technology assumed, in this study, for extracting oil from dry seed is cold pressing. The process begins with the use of a fruit cracking machine to remove the seed shells, followed by an oil expeller that ejects oil from the seeds, and finally a filtering unit is used to purify the oil. It is deduced that 3.5 tonnes of dry Jatropha seed will yield 1.11 tonnes of crude seed oil, 0.92 tonnes of seed cake and 1.42 tonnes of seed husk, with oil and husk yields of 35% and 42%. The residue (i.e. seed cake) is returned to the field to supplement the applied inorganic fertilizer. The product yields resulting from Jatropha production are presented in Table 6.3.

Table 6.3: Output for Jatropha Biodiesel Fuel Production

Product	t $ha^{-1}yr^{-1}$	MJ/kg
Seed cake	0.92	25[1]
Shell Hull	1.88	11.1[2]
Husk	1.47	16.0[2]
Glycerine	0.1	25.6[3]
Biomatter (Leaves)	2.06	3.62[28]
Biomatter (Stem)	4.19	3.93[28]
Seed	3.5	24.0[3]
Seed Oil	1.11	39.7[5]

[1]Brittaine and Lutaladio, 2010; [2]Jingura et al. 2011; [3]Prueksakorn et al. 2010; [8]Wang et al. 2011; [5]Kessom et al. 2009

6.2.5.3 Oil Conversion and Use

The crude oil obtained from extraction of Jatropha seeds is transported to a biodiesel plant located 50km away from expelling facility location. The oil is assumed to be first pre-treated to reduce the fraction of free fatty acids by reacting with methanol and sulphuric acid [Eshton et al. 2013], followed by a base-catalyzed transesterification reaction in an 80 Litre biodiesel batch–reactor, which has a 97% efficiency, where electricity requirement is 4 kWh/batch [Whitaker and Heath, 2009; Prueksakorn et al. 2008]. The mixture of glycerol and biodiesel produced is separated in the presence of excess water. The fuel produced is then transported by road over 50km to the power plant to be used. The fuel is combusted in a 109 MW sited rated gas turbine (126MW ISO rating with thermal efficiency of 34.1%). The direct GHG emissions from fertilizer application are stated in Table 6.4.

Table 6.4: Life cycle GHG Emissions from Jatropha Biodiesel Production

Process	*CO_2* *$kgCO_2\,kg^{-1}$*	*CH_4* *$kg\ CO_2\,eq.kg^{-1}$*	*N_2O* *$kg\ CO_2\,eq.\ kg^{-1}$*	*Total*
Fertilizer application	1.93	0	0.0965	2.03

Emission factor for CO_2, and N_2O per N fertilizer are 0.2 kg kg^{-1}[29] and 0.01 kg kg^{-1} for CH_4 respectively.

6.2.6 Reference Diesel System

Similar to the Jatropha biodiesel system, a generic diesel production–system, as illustrated in figure 6.4 was developed as a framework for this study. This is to simplify the diesel fuel production system in Nigeria, which is a complex mixture resulting from diverse crude types and sources, product-refinery processes and means of transportation. The reference diesel system is developed following the reported yields of fuels in Nigerian refineries in 2012 [HTADC, 2012] and public information on the export of crude oil and import of refined products into Nigeria. This information was used to calculate a mass-balance ratio of crude-oil processed and transported locally and exported, as well as the energy consumed during crude-oil and diesel fuel production. Because, the fuel density for Jatropha biodiesel is higher than that of the reference diesel fuel, a conversion factor of 1.122 was applied to the density of the reference diesel fuel to compare equal amounts of fuel density.

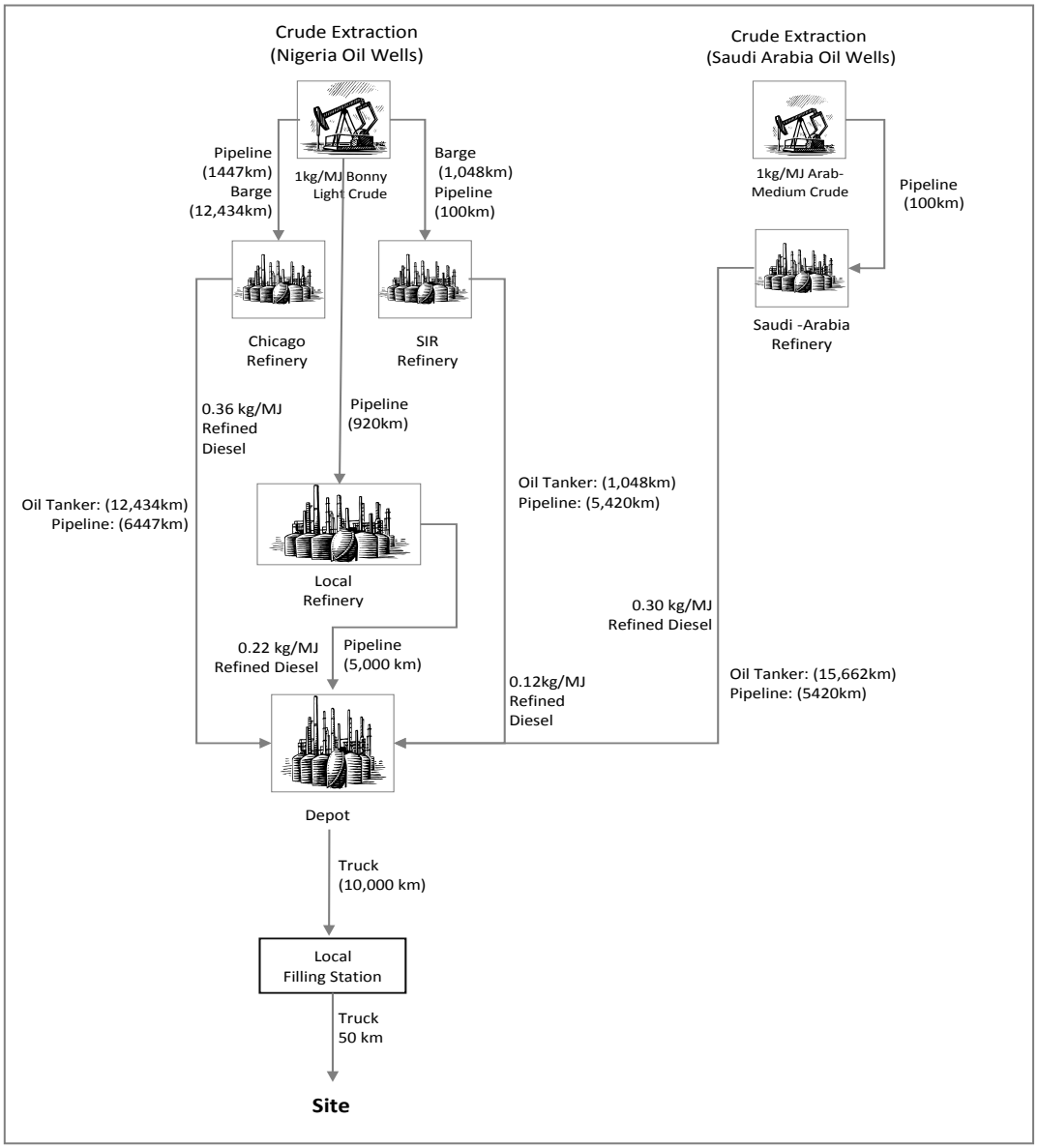

Figure 6.4: The pathway for the production of 1 MJ of conventional diesel fuel

6.2.6.1 Crude-Oil Production

Crude-oil production involves processes such as oil exploration, drilling, extraction, as well as water and/or gas re-injection. According to the NNPC Annual Statistical Bulletin, the amount of crude-oil extracted from Nigeria wells in 2012 was 8.53 billion barrels (bbl), of which 34.9 million barrels (mbl) were processed in four local-refineries, whereas 55.4 mbl and 22.7 mbl were processed overseas under a swap arrangement and off-shore processing agreement (OPA), although the exact locations of the refineries for the SWAP and OPA arrangements were not disclosed. The present analysis examines a SWAP arrangement for a refined product from a US refinery, located in Chicago, and an off-shore processing agreement from Société Ivoirienne de Raffinage (SIR) refinery in the Ivory Coast. Furthermore, importation of diesel fuel into Nigeria was assumed to be from Saudi Arabia, although there are numerous sources of importation, but of far smaller amounts, from Venezuela, India, the Middle East, neighbouring countries in Africa and many parts of the U.S.A. and Europe.

The energy requirements to produce Bonny light crude-oil from Nigeria and Arab-medium crude-oil from Saudi-Arabia were extrapolated from data in reference [Kessom et al. 2009], based on the reservoir conditions and production parameters stated in Table 6.5. The presented energy accounts for the different crude-oil types and production characteristics, as well as the processes employed, such as gas flaring, that significantly contribute to the environmental burden. For instance, a report by EIA [2013] state that the large amount of gas flared during crude production in Nigeria has values of 14.6 m^3/bbl for 2011. Kessom et al. (2009) also reported a range of 19.6 m^3/bbl and 27 m^3/bbl with energy content nearly up to 20% of the crude produced. In other words, the total energy needed for the production of Bonny light crude was extrapolated from the energy required to lift the generic crude, re-inject water and gas as well as treat the effluent and vent 0.1% of the gas flared. For example, the average GHG emission for the production of 1 MJ of conventional Bonny light crude oil is 16 gCO_2eq [Kessom et al. 2009]. If 0.1 MJ energy per MJ generic crude will yield 6.34 gCO_2eq/MJ crude, 16 gCO_2eq/MJ crude will require an energy equivalent of 0.22 energy per MJ crude (9.5 MJ/kg). A detailed illustration of the production and refining of Bonny light crude-oil and Arab-medium crude-oil with process-calculation and assumptions have been described by [Kessom et al. 2009].

Table 6.5: Reservoir Conditions and Production Parameters for Crude Production[38]

Source	Unit	Bonny light Nigeria	Arab-Medium Saudi-Arabia
Well Pressure	psi	4,300	3,000
Average Well Depth	ft	8,700	6,100
Water-to-Oil Ratio	bbl bbl^{-1}	2	2.3
Produced Gas	scf bbl^{-1}	840	650
Flared Gas Range	m3 bbl^{-1}	19.6-27	0.8-0.9
API		32.9	31.1
Sulphur Content	%wt	2.6	0.16

6.2.6.2 Crude-oil Transportation

Only 3.9% of the 8.53 bbl of crude oil that was extracted during 2012 from 129 wells scattered around the south-southern states of Nigeria was refined locally. An additional 8.7% of the crude-oil lifted was refined overseas under SWAP and OPA agreements with refined products to the local refinery for distribution [NNPC, 2012]. The rest of the crude-oil extracted was exported and not used locally. Hence, there is an environmental burden, generated locally and as well as those produced overseas, resulting from multiple transportation of crude and refined products.

In this study, crude is assumed to be produced from various sources within the south-south region of Nigeria and transported via pipeline of 320 km to terminal storage tanks located at Forcados and Escravos, as well as to Warri and Port-Harcourt refinery, before it is transported locally to Kaduna refinery via a 600 km pipeline. The crude oil exported offshore and overseas are similarly produced from various oil wells and transported from Forcados terminal via a large Very Large Crude Carriers (VLCC) oil tanker to overseas refineries. Refined diesel fuels are also transported via oil tankers and pipelines to Nigerian refineries. The transportation distances covered via pipelines and Very Large Crude Carriers (VLCC) has been calculated using sea distance calculator (ports.com) and Google map (see Table 6.7). For simplification, it was assumed that a VLCC of about 200,000 deadweight tonne (DWT) was used for transportation of crude and refined products with inputs in Table 6.6.

6.2.6.3 Crude-oil Refining and Product Yield

According to Kessom et al. (2009), product yield depends on the refinery objectives, the rate and the quality of the feed to the refinery. In 2012, local refineries produced 2.63 MLPD of diesel fuel [HTADC, 2012] with product yield of 18.2%, a value deduced from the reported 2012 annual production of 818,678 metric tonnes of diesel fuel using a conversion factor of 1177 (metric tonnes to litres). Thus, from a market diesel-fuel

demand of 12 MLPD [HTADC, 2012], it can be deduced that 2.6 MLPD of it was produced locally, 4.3 MLPD and 1.5 MLPD of diesel fuel were obtained by SWAP and OPA arrangements while 3.5 MLPD of diesel was imported into Nigeria, assuming that the product yield was 18.2% for Bonny light crude-oil and 35.4% for Arab-medium crude-oil [Kessom et al. 2009]. Analogous to crude-oil extraction, the energy requirement for refining was extrapolated [Kessom et al. 2009], as 725 MJ/bbl crude-oil for bonny light crude-oil and 785MJ/bbl crude-oil for Arab-medium crude-oil. Thus, the present analysis estimates that 3 kg of Bonny light crude-oil and 1 kg of Arab-medium crude-oil are extracted per kg of diesel fuel consumed in Nigeria. The mass balance results and energy requirements for the reference diesel fuel are presented in Table 6.7.

Table 6.6: VLCC Engine Parameters

Parameters	Units	Values
Main Engine Power Rating	kW	21,910
Fuel Consumption Rate	BTU/kWh	6,172
BSFC	g/kWh	165
CO_2 Emission	ton/day	349.6
DWT	ton	200,000
Service Speed	knots	14
Fuel LHV (Residual Oil)	BTU/gal [MJ/kg]	140,353 [39.5]
Fuel Density (Residual Oil)	g/gal	3752
Load Factor		0.83

Table 6.7: Sea and Pipeline Transportation Distances & Inputs

Parameters	Units	Values
Energy intensity via pipeline	BTU/ton mile	404
Crude Transportation via VLCC Tanker		
Sea distance (Forcados Terminal to Gulf Port)	km	12434
Forcados Terminal to Port, Abidjan	km	1048
Crude Transportation via pipeline		
Forcados Terminal to local refinery	km	920
Gulfport to Chicago Refinery	km	1447
Crude Transfer to SIR refinery	km	100
Crude Transfer to Saudi Arabia refinery	km	100
Diesel Product Transportation via VLCC Tanker		
(Jubail Port, Saudi Arabia to Forcados Terminal)	km	15662
Gulfport to Nigerian Port	km	12434
Abidjan Port to Nigerian Port	km	1048
Diesel Product Transportation via pipeline		
Local refinery to local depots	km	5000
Chicago Refinery to Gulfport	km	1447
Crude Transfer from SIR refinery to local refinery	km	300
Crude Transfer from Saudi Arabia refinery to local refinery	km	300

Table 6.8: Summary of Inputs for Reference Diesel Fuel Production

Inputs	Unit	SWAP	Local	OPA	Import	MJ/kg
kg Crude Extracted and Lifted/kg of Diesel Produced	kg/kg	1	1	1	1	171
kg Diesel Produced	kg	0.36	0.22	0.12	0.3	42.79
Diesel Energy Fraction used for Crude Production	MJ	1.73	1.73	1.73	0.5	6
Diesel Energy Fraction used for Refining	MJ	29.87	29.86	28.87	18.66	108
Energy for Transportation via Pipeline	MJ	3.5	0	0.1	1.96	6
Energy for Transportation via Sea Transport	MJ	0.79	0.89	0.13	0.1	2

6.3 Results and Discussion

6.3.1 Well-to-Wake Analysis

6.3.1.1 Energy Balance and Fossil-Fuel Displacement

Parameters such as NER, NREV and NEV have been used for defining the energy efficiency and ecological benefits of the production of Jatropha biodiesel fuel – see Table 6.9

Table 6.9: Energy Balance (Well-to-Wake System Boundary)

Parameters	Units	Reference Diesel Fuel	Jatropha biodiesel [Base-case]	Jatropha biodiesel [Irrigated]	Jatropha Biodiesel [Large Scale Farming]
Total Energy Input	MJ/kg	113	16.54	25.49	29.07
Energy Density	MJ/kg	39.65*	39.65	39.65	39.65
NER		0.35	2.40	1.56	1.36
NEV	MJ	-2.21	23.11	14.16	10.58
NREV	MJ	39.65	38.95	34.70	34.78
% Diesel Fuel Replacement	%	-	58	36	27

*Conversion factor of 0.962 was applied to the reference diesel fuel for comparing equal amounts of energy density of fuel.

The total amount of energy consumed including those derived from fossil and non-fossil energy-sources differ according to the three farming systems employed, with values of 16.5 MJ, 25.5 MJ and 29.1 MJ for the rain-fed base-case, irrigated base-case and large-scale farming respectively. These translate to NER values exceeding unity and ranging between 1.36 (large scale farming) and 2.40 (rain-fed base-case). The total energy requirement for the reference diesel fuel system was 113 MJ, resulting to a NER of less than unity.

The NER of this study cannot be compared with nominally-similar studies because of variabilities in the goal and scope definitions, model assumptions, system boundaries, site conditions and functional units. However, the NER is largely reported in the literature to be less than unity for conventional diesel fuel and exceed unity for Jatropha biodiesel. Whitaker and Heath, [2009] reported a NER of 0.79 for a conventional diesel fuel and a NER of 1.9 for 100% Jatropha biodiesel. Eshton et al. [2013] also showed that the NER is 2.3 while Achten et al. [2010] indicated a NER of 1.85±0.22 for Jatropha biodiesel fuel. The present study reports a NER as low as 0.35 for the reference diesel fuel and 2.40 for the rain-fed base-case Jatropha biodiesel fuel. These variations can be attributed to the highly intensive and 100% fossil origin in energy consumption for conventional diesel fuel production. The NER of the reference diesel system is much lower than the values

reported in the literature because of the route of production and of the diesel fuels used in Nigeria differ in quality from the well-reported European average diesel fuels.

The NEV showed that for 1 kg of Jatropha biodiesel fuel produced in Nigeria, 23 MJ, 14 MJ and 11 MJ of energy is gained for the rain-fed base-case, irrigated base-case and large-scale farming respectively whereas 2 MJ is lost in the case of the reference diesel-fuel. These predictions demonstrate that Jatropha biodiesel fuel possesses an environmental benefit and is a potential renewable fuel that could justifiably replace the use of conventional diesel fuel in Nigeria. Fuel displacement is critical and could significantly improve the available energy situation in Nigeria, because the country unfortunately depends predominantly on imported diesel fuel. In the present study, the use of Jatropha biodiesel fuel could displace the use of the reference diesel fuel by 58%, 36% and 27% for rain-fed base-case, irrigated base-case and large-scale farming respectively. Overall, this derived energy balance analysis favours the local production of Jatropha biodiesel fuel in Nigeria.

Considering of the co-product glycerol, the NEV increased to 24.8 MJ, 16.7 MJ and 13.5 MJ while the NER on the other hand increased to 2.7, 1.7 and 1.5 for rain-fed base-case, irrigated base-case and large-scale farming approaches respectively. These results demonstrate the additional benefit that could be achieved from the co-products of Jatropha plants. This study has only considered glycerol: however, other products such as agricultural residues, seedcake, seed hulls and husks that account for nearly 40% of the Jatropha plant yield could be used as fuels for producing heat and power by off-grid users. According to the National Bureau of Statistics [2011], the national grid only served 51% of the Nigeria's population in 2009, and only 40% of the rural population. About 88% of the rural population depends on wood for cooking [EIA, 2013]. Over 50% of the rural population has no access to electricity and the rest of the rural population has to supplement their electricity supplies from the grid with individual generating units. These units, usually burn inefficiently and generate much soot. They have also resulted in fire accidents, asphyxiations and deaths, especially at a cost to already poor citizens. Technologies that convert biomass, especially agricultural waste and residues to energy from large-scale farming and production of Jatropha biodiesel could significantly reduce the GHG emissions and increase the energy efficiency achieved. This would be a significant benefit for the rural population as well as small-scale businesses. There is now also a favourable financial climate driven by demand for IPPs to supply off-grid

users. This system however requires more support from the government and policies that foster support for the development of the industry.

According to Takeshima and Salau, [2010], a significant proportion of cultivation in farming is still achieve using hand tools, such as axes and hoes in Nigeria and West Africa, compared with other developing countries, because of a lack of available access to farm animals and tractors. Also, smallholder farming is predominant in the agricultural sector of Nigeria, with more than16 million families each cultivating about 1 to 2 ha under rain-fed conditions [PrOpCom, 2012]. Although, there are about 80 million hectares of land suitable for agricultural cultivation, only about 30% of this is cultivated [PrOpCom, 2012]. Nevertheless, there are current efforts to grow Jatropha on a large scale, which would drive down the cost of production, enhance product yield and raise operational effectiveness. Also, increased mechanized farming would boost production, raise profits and reduce the current trend of rural-urban migration that reduce the number of workers available for farm employment and associated activities. This could also reduce the cost of labour that is problematic in the smallholder farming system, thus bringing about additional benefits for Jatropha farming. The environmental performance of such ventures has however not previously been examined in depth.

Among the three farming systems, energy consumption increased by nearly 76% in the large-scale farming scenario and 54% in the irrigated case when compared with the rain-fed base-case, consequently reducing the net energy ratio to 57% and 65% respectively. Also, the large-scale farming system had the least favourable energy balance, due to the energy consumed through the use of heavy machinery and farm implements. These predictions lay emphasis on the adoption of less energy-intensive processes, in the farming of Jatropha system, because the farming system could significantly reduce the net energy gain and benefit that could be accrued from the production of Jatropha biodiesel fuel. The distribution of energy input according to the sub-processes for Jatropha biodiesel production is presented in figure 6.5, which shows that Jatropha farming has the largest contribution to energy consumption followed by oil conversion in all the three farming systems. Transportation also plays a significant role in energy consumption in the irrigated case base-case and large-scale farming system. These are the results of energy consumed for irrigation during the dry season, and the use of a fossil fuel for energizing farm implements instead of employing manual labour.

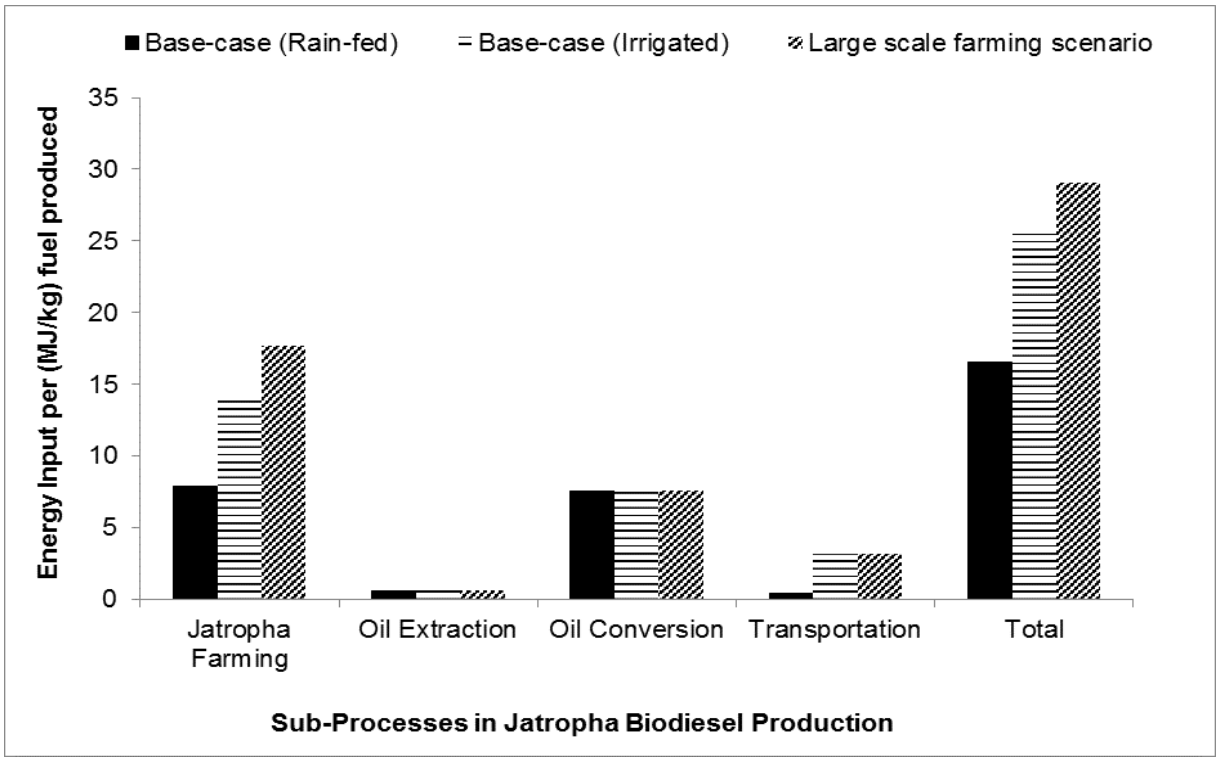

Figure 6.5: Total contributions of energy from the sub-processes of Jatropha biodiesel production. Results are presented as MJ of energy consumed per kg of Jatropha biodiesel produced.

The conclusions of this study corroborate those of studies done elsewhere [Prueksakorn and Gheewala, 2008,41]. However, Eshton et al. [2013] and Ndong et al. [2009] reported oil conversion as the most energy-intensive process in the life cycle of Jatropha biodiesel fuel production with values of 61% and 65% respectively. In comparison with analyses reported in [Eshton et al. 2013] and [Ndong et al. 2009], the present investigation shows that the sub-process with the most significant contributions to energy consumption for Jatropha biodiesel fuel production are farming with values ranging between 7.9 MJ (rain-fed base-case) and 18 MJ (large-scale farming), followed by oil conversion, then transportation. The differences in the studies can be attributed to the energy requirements for operating machinery used for oil conversion in their studies. Also, their Jatropha farming had lower energy requirements with reduced plant densities of 1250 [Eshton et al. 2013] and 1111 [Ndong et al. 2009] trees per ha, in comparison to the 2500 trees per ha used in this study. But the energy situation and costs associated with high technologies favour the use of low technologies in Nigeria. Even in large-scale farming, business owners are more likely to adopt mechanical methods with minimum fossil-energy consumptions than large industrial equipment that require large-sized diesel engines for back-up in the event of power failure. This, however, comes at a cost in efficiency of extraction and conversion.

Further analyses of the distribution of energy input for production of the reference diesel fuel are presented in figure 7.6. Product refining had the largest contribution to energy consumption, accounting for nearly 89% of the total energy input.

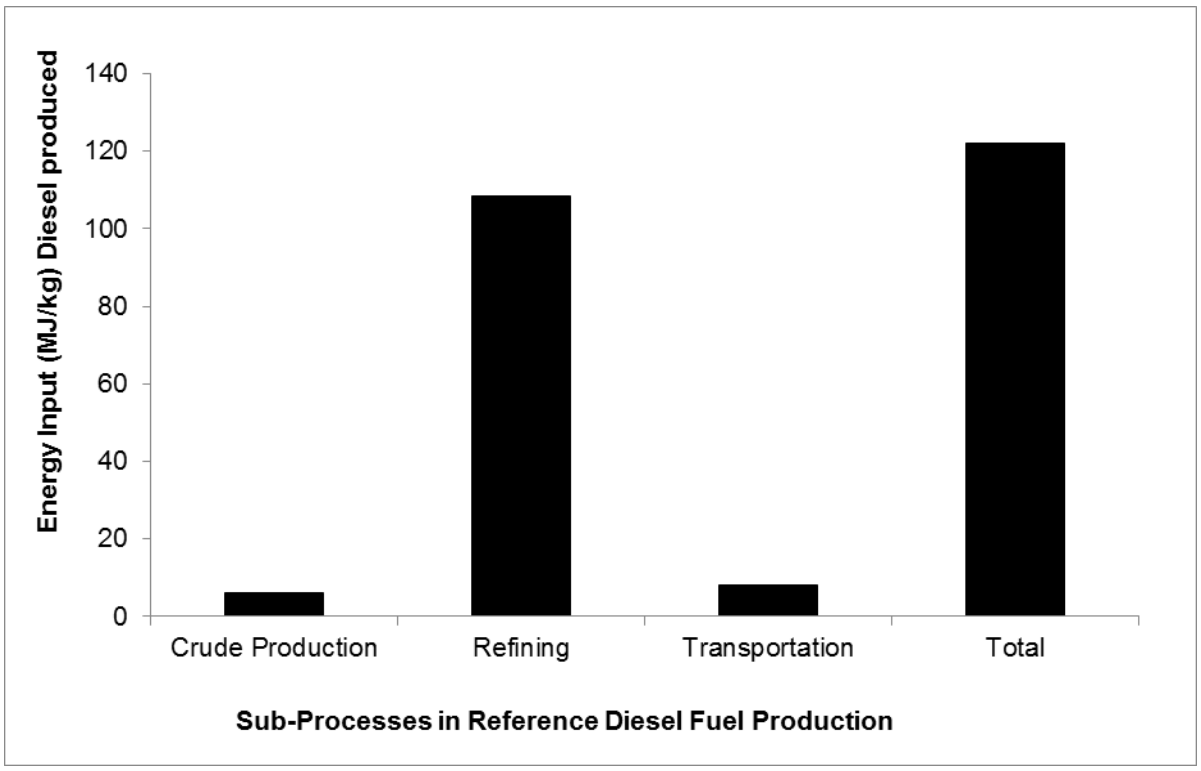

Figure 6.6: The distribution of energy input for Reference Diesel fuel System

6.3.1.2 Environmental Life Cycle Impact Assessment

The environmental impacts of the four sub-processes involved in Jatropha production were obtained from the modelled processes in SimaPRO. Their contributions to environmental impact are presented in figure 6.7. The following impact categories were considered: climate change, ozone depletion, photochemical oxidant formation, terrestrial acidification, freshwater eutrophication, marine eutrophication, terrestrial ecotoxicity, freshwater ecotoxicity, marine ecotoxicity, ionizing radiation, particulate matter formation and fossil depletion. Agricultural occupation, urban occupation and natural land transformation, human toxicity and water depletion were not considered.

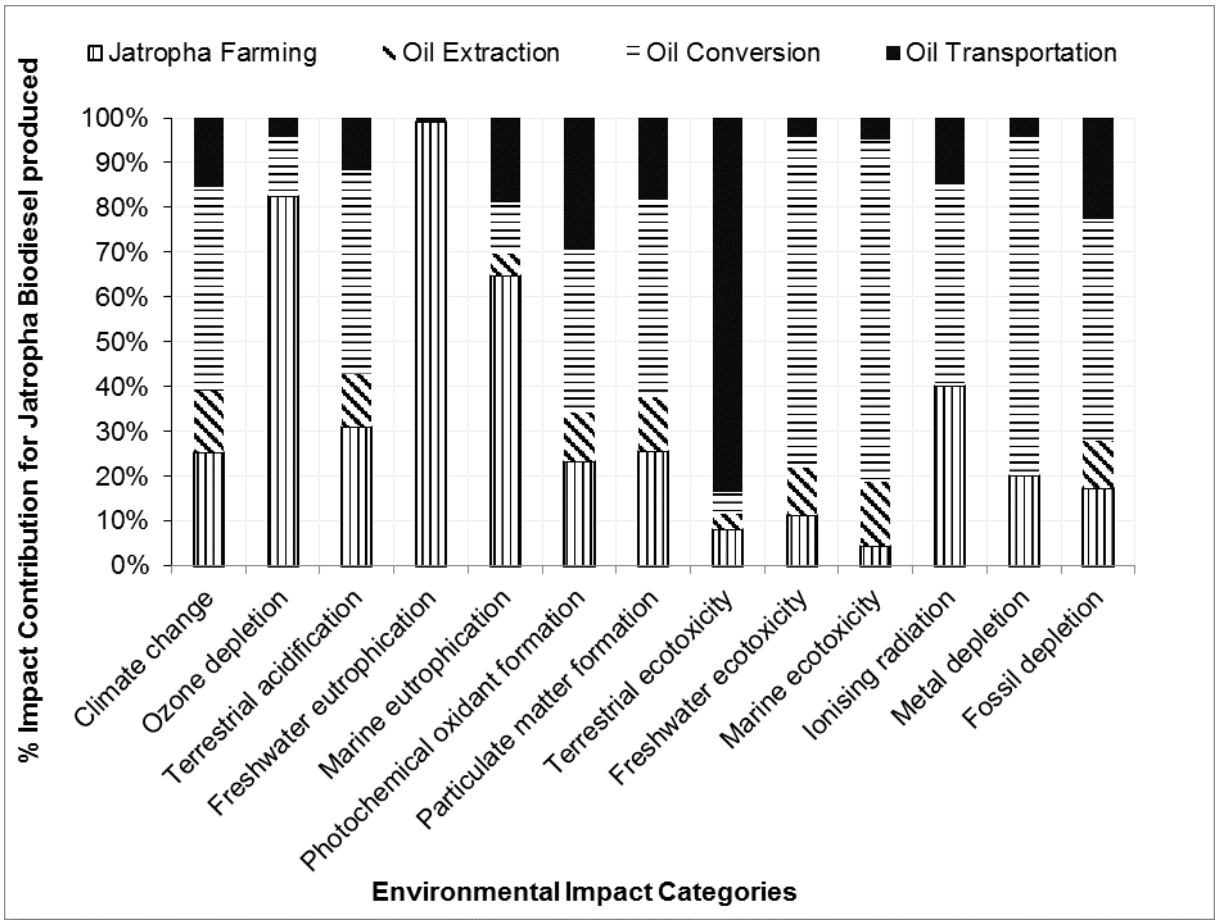

Figure 6.7: Percentage contributions to impact of the sub-processes of Jatropha biodiesel production.

In the rain-fed base-case scenario, the results in figure 6.7 show a mixture of impacts from the different categories in Jatropha biodiesel fuel production. Jatropha farming had the largest impacts on freshwater and marine eutrophication, as well as ozone depletion. This can be attributed to the effect of the production and use of nitrogen and phosphate fertilizer. These fertilizers are capable of leaking into nearby rivers and streams, and can accidentally be released into the air during application depending on the soil's properties and environmental conditions. The impact of oil-extraction processes was minimal in comparison with oil conversion because, in the rain-fed base-case scenario, there was relatively little use of energy-intensive methodologies, such as cold pressing rather than solvent extraction. Oil conversion, on the other hand, had the largest impact on fresh and marine eco-toxicity, as well as on metal and fossil depletions. It played a significant role in terrestrial acidification, particulate matter formation and climate change with significant emissions of GHGs. Transportation is a highly fossil-dependent process. Thus, transportation had a major impact on fossil depletion, photochemical oxidant formation and climate change, although not as in significant quantities as in the oil conversion process.

Although Jatropha farming involves the highest energy-demands of all the sub-processes, considering the total life-cycle impact of these processes; oil conversion contributes significantly to the environmental burden, followed by oil extraction. This is a result of the impact of electricity and chemicals used in the oil conversion. The results presented in figure 6.8 highlight the sub-processes requiring improvement and optimization.

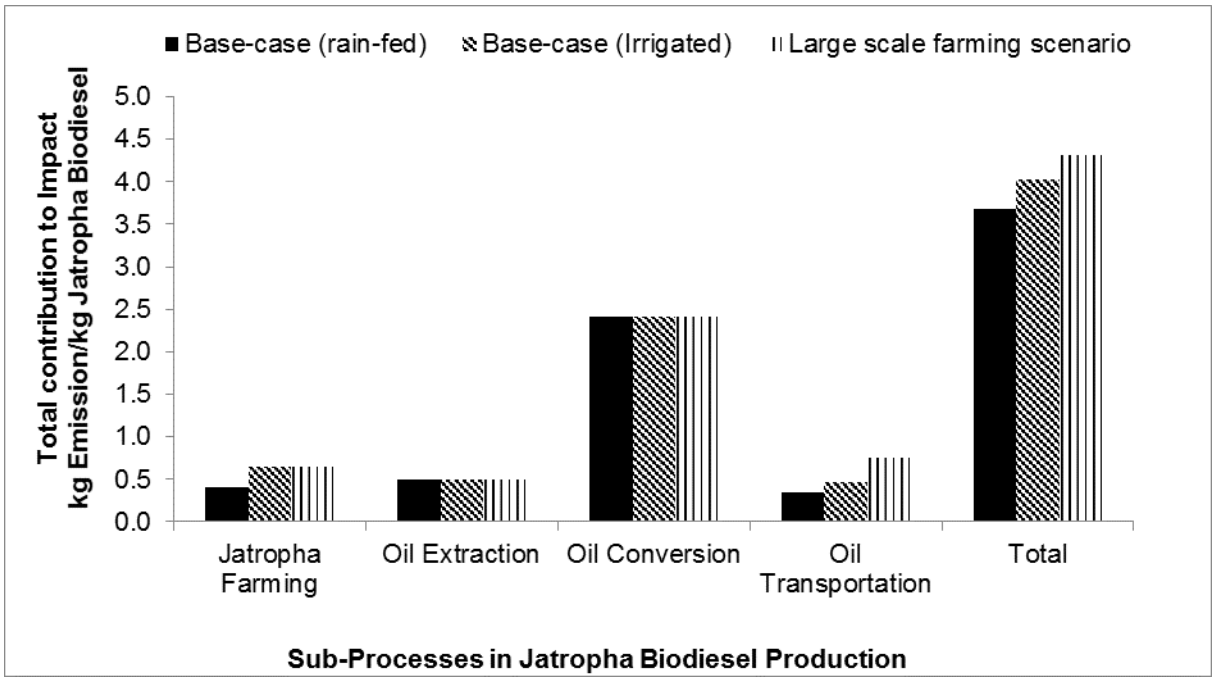

Figure 6.8: Contributions of the sub-processes to the environmental burden. Results are presented as kg total emissions for each sub-process during the production of 1kg of Jatropha biodiesel fuel.

Further examination of the different farming systems for Jatropha production, namely i) base-case rain-fed scenario ii) base-case scenario with irrigation and iii) large scale farming system, as indicated in figure 6.8 show that there is an increase in the environmental burden by nearly 10% in the irrigated scenario and by nearly 20% in the large farming scale scenario. Thus, the overall emission increased from 3.7 kg per kg fuel produced (base-case scenario) to 4.3 kg per kg fuel produced (large-scale farming scenario).

The distribution of impacts for the sub-processes of production of the reference diesel fuel show that crude exploration and production had the largest impact contribution with a value of 11.8 kg emission per kg of fuel produced, followed by transportation of crude and refined products.

6.3.1.3 Net Greenhouse Gas (GHG) Impact

With respect to GHG emissions, Jatropha biodiesel fuel production is more environmentally favourable than that for the reference diesel fuel. There are nearly 60%, 50% and 26% reductions in GHG emissions for the rain-fed base-case, irrigated base-case and large-scale farming respectively. These results (see Table 6.10) demonstrate that GHG savings could be achieved by producing Jatropha biodiesel locally to be used as a substitute for conventional diesel fuel in Nigeria.

Table 6.10: Net GHG emission and percentage reduction in GHG as compared with those for the reference diesel fuel

Impact category	*Unit*	Reference Diesel Fuel	Jatropha biodiesel	Jatropha biodiesel (Irrigated)	Jatropha biodiesel (Irrigated and Machinery Use)
Climate change	*kg CO_2 eq. per kg fuel*	2.27	0.91	1.13	1.68
	%		-59.84	-50.32	-26.29

Assuming the diesel fuel production system in Nigeria is optimized, such that 8.97 MLPD of it is produced locally while only 3.03 MLPD diesel is imported under similar transportation distances; the results as indicated in Table 6.11 show that the GHG impact of the reference diesel fuel is reduced by 4%. Consequently, the GHG savings changes for Jatropha biodiesel by 1-3% depending on the farming system employed. That is, the GHG savings reduces to 58% in the rain-fed base-case, 48% in the irrigated base-case and 23% in the large-scale farming scenario. These results demonstrate the importance of refining the crude-oil extracted from Nigerian oil-wells in local refineries. In the event of an optimized and improved diesel-fuel production system being built in Nigeria, the benefit of growing Jatropha plants and producing biodiesel fuel from an environmental standpoint would be significantly reduced. Such additional refining capacity, up to 50%, would not only be of environmental benefit to Nigeria but could bring about economic improvements and infrastructure development. However socio-economic benefits of the production and use of fuels are outside the scope of the present investigation.

Table 6.11: Net GHG emission and percentage reduction in GHG Emission as compared with those for the optimized reference diesel fuel system

Impact category	*Unit*	Reference Diesel Fuel-Optimised System	Jatropha biodiesel	Jatropha biodiesel with Irrigation	Jatropha biodiesel with Irrigation and Heavy machinery
Climate change	*kg CO2 eq. per kg fuel*	2.18	0.91	1.13	1.68
	%		-58.07	-48.13	-23.03

6.3.2 Well-to-Wheel Analysis

6.3.2.1 Energy Balance and Fossil-Fuel Savings

The energy efficiencies of the fuels produced via the three farming scenarios: i) base-case rain-fed, ii) base-case irrigated, iii) large scale farming, were quantified using parameters such as NER, NREV and NEV and compared against that of the reference diesel fuel. The results are presented in Table 6.12.

Table 6.12: Energy Balance (Well-to-Wheel System Boundary)

Parameters	Units	Reference Diesel Fuel	Base-case [rain-fed]	Base-case [Irrigated]	Large Scale Farming
Total Energy Input	MJ/MJ	2.71	0.42	0.65	0.76
Energy Density	MJ/MJ	1	1	1	1
NER		0.37	2.37	1.54	1.32
NEV	MJ	-1.71	0.58	0.35	0.24
NREV	MJ	0	0.98	0.88	0.88
% Diesel Fuel Replacement	%	-	58	35	24

The total energy inputs, expressed as MJ of energy per MJ of fuel consumed in the power plant, for Jatropha biodiesel fuels were at the least 0.42 MJ [base-case rain-fed], but at the most 0.76 MJ [large scale farming], whereas that of the reference diesel fuel was 2.71 MJ. In this work, equal amount of energy density was examined for all fuels by applying a correction factor of 0.962 to the diesel fuel to account for the differences in the energy densities or lower heating value (LHV) of Jatropha biodiesel and the reference diesel fuel. Furthermore, NERs of 2.37, 1.54 and 1.32 were obtained for base-case rain-fed, base-case irrigated and large scale farming respectively. This indicates a positive energy balance for Jatropha fuel in comparison to the fossil source, since the NER was above 1, as opposed to a value below 1 obtained for the reference diesel fuel. These

results are similar to Jatropha biodiesel production analysis in [Eshton et al. 2013] because very minimal amount of energy is required for transportation of the biodiesel fuels from oil conversion site to the power plant location. Additionally, the NEV, a parameter indicative of the energy gained or lost, was negative for the reference diesel fuel, but positive for all the Jatropha biodiesel fuels with values of 58%, 35% and 24% for base-case rain-fed, base-case irrigated and large scale farming respectively. The NREV on the other hand was 0.98, 0.88 and 0.88 for base-case rain-fed, base-case irrigated and large scale farming respectively, however, 1 for the reference diesel fuel. This demonstrate the energy gained from the use of fossil fuel. A relatively higher value indicate less amount of fossil energy input is utilised and vice versa. Consequently, this analysis demonstrate how much fossil fuel displacement that could be achieved from the use of these fuels from the three farming scenarios. A fossil fuel displacements of 58% [base-case rain-fed], 36% [base-case irrigated] and 27% large scale farming are achievable with Jatropha biodiesel fuel utilization.

Among the three farming systems, energy consumption increased by 0.23 MJ (base-case irrigated case) and 0.34 MJ (large scale farming scenario). Consequently the net energy ratio reduced to 65% and 56% respectively. Also, the large scale farming system had the least favourable energy balance and Jatropha farming had the largest contribution to energy consumption followed by oil conversion in all the three farming systems and especially for the large scale farming system. Transportation also played significant role in energy consumption in the base-case irrigated case and large scale farming system. The distribution of energy input according to the sub-processes for Jatropha biodiesel production is presented in figure 6.9.

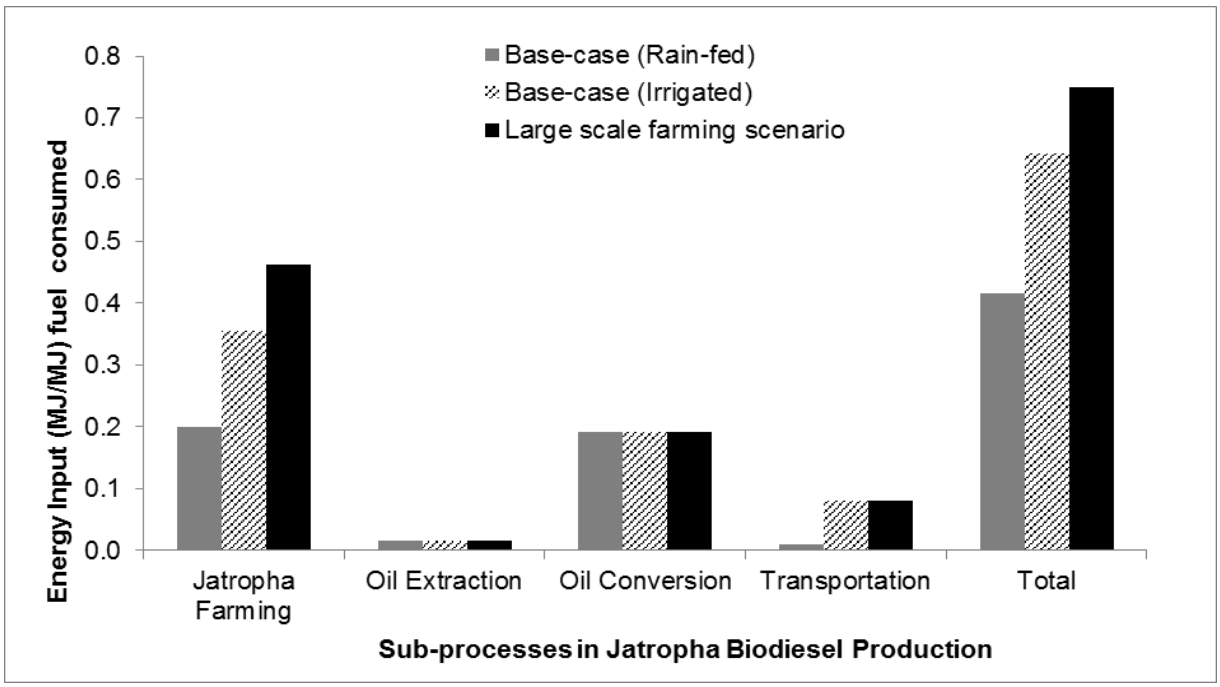

Figure 6.9: Contributions of energy input from the sub-processes of Jatropha biodiesel fuel used in a 126 MW power plant. Results are presented as MJ of energy input per MJ of Jatropha biodiesel utilised.

The above unity of the NER, and positive NEV of the biodiesel fuels derived from the three farming systems and used in the power plant indicate that the production and use of Jatropha biodiesel fuel in power generation in Nigeria is achievable and of benefit. That is, the Jatropha biodiesel fuel has higher energy efficiency and favourable to replace or substitute part of the diesel reference fuel system provided the material inputs are kept at their minimum. Furthermore, additional effort to replace the fossil fuel consumption during the production and use of the fuel, especially during transportation would change the energy balance of the system significantly.

6.3.2.2 Environmental Life Cycle Impact Assessment

The total emissions generated from the use of Jatropha biodiesel and the reference diesel fuels are expressed as kg emissions per MJ of fuel. The fraction of carbon sequestered during the growth of Jatropha plant and burnt in the engine is approximately 474 kg CO_2 per MJ fuel. The CO_2 emissions generated from the simulated 126 MW gas turbine power plant on the other hand is 1025.93 kg for Jatropha biodiesel while 1260.37 kg for the reference diesel fuel. Hence, the total emissions from Jatropha biodiesel fuel use could bring about GHG savings of about 19% across the three farming systems. These results are presented in Table 6.13.

Table 6.13: Net and percentage reductions in total emissions as compared to reference diesel

Impact category	*Unit*	Reference Diesel Fuel	Base-case [rain-fed]	Base-case [Irrigated]	Large Scale Farming
Climate change	*kg CO_2 eq. per MJ fuel*	1260.37	1025.95	1025.96	1025.97
	%		-18.61	-18.60	-18.60

Using the base-case rain-fed farming system, the Jatropha biodiesel produced as a result have varying effect on the ecology with percentage contributions to total emissions. The percentage contributions to environmental burden from each sub-process in the production and use of Jatropha biodiesel is represented in figure 6.10.

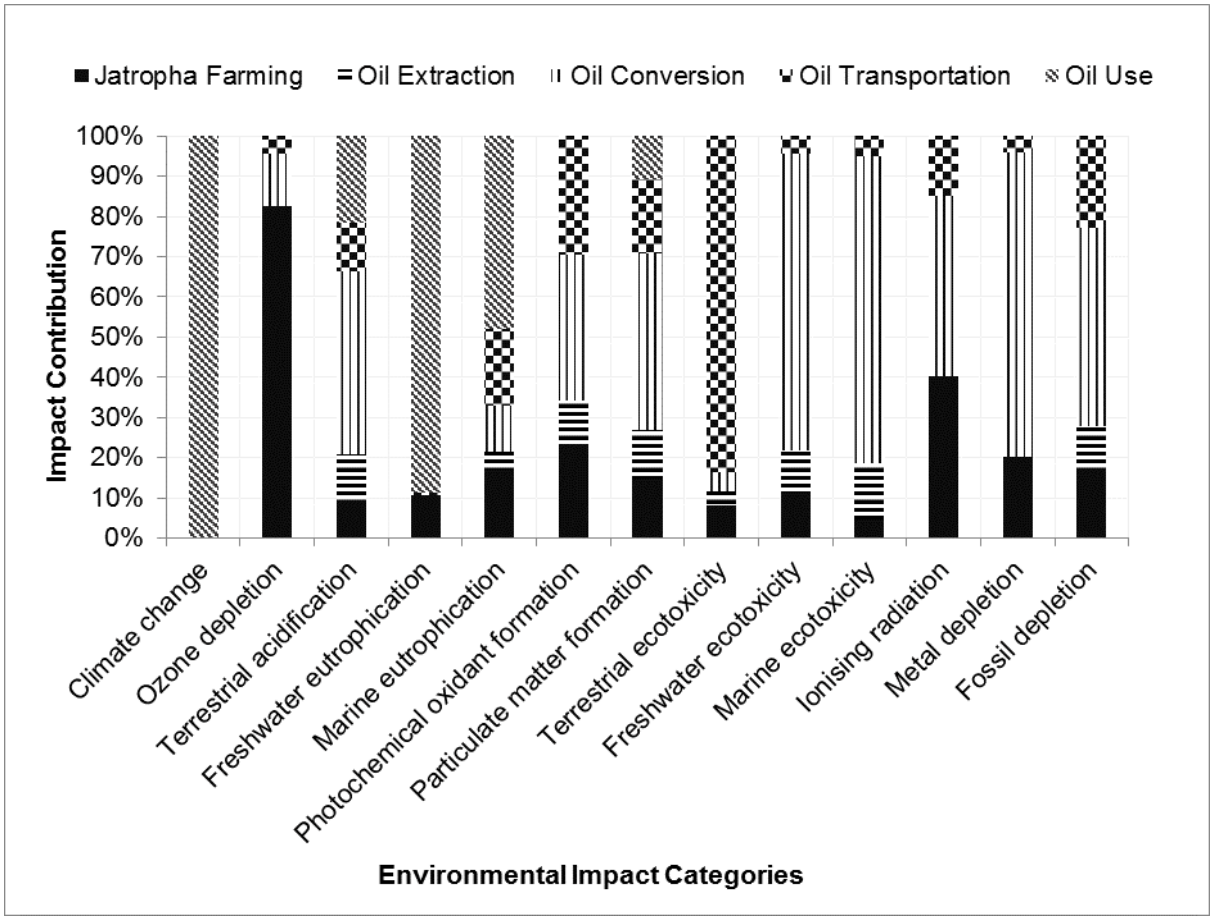

Figure 6.10: Percentage contributions to environmental burden from the sub-processes of Jatropha biodiesel production and use.

Results are presented as MJ of energy consumed per MJ of Jatropha biodiesel used in 126 MW gas turbine at ISO condition. Nearly 100% contributions to climate change is observed to result only from fuel consumption, as well as about 50% and 90%

contributions to marine and freshwater eutrophication, although in very insignificant quantities. These results are expected because carbon dioxide is one of the emissions classified with greenhouse gases that could bring about increased earth average temperature and is produced mainly as a result of combustion of fuels in engine. Emission to the atmosphere could also result in more eutrophication of fresh and water bodies by enriching its biogenic content. For instant, microscopic floating plants such as algae and water hyacinths consume carbon dioxide to increase bio-matter and uptake other dissolve nutrients such as nitrogen, phosphorus from water while using light as the energy source. This impact water quality, forces increased growth of aquatic plants, decomposition of organic matter in water bodies and depletes dissolved oxygen. Oil conversion contributes to marine ecotoxicity, freshwater ecotoxicity, metal depletion, and fossil depletion significantly by about 70%, 76%, 75% and 50% respectively. Other impacts include terrestrial acidification, photochemical oxidant formation and ionizing radiation.

Oil transportation had the largest impact on terrestrial ecotoxicity with value of about 85% and equally contributed to photochemical oxidant formation, a resulting effect on smug formation. This impact is attributed to the fossil-derived diesel fuel used during transportation of seeds, oil and refined products. The NOx and other volatile organic compounds (VOCs) produced from these diesel engines increases ozone (O_3) formation. An excessive formation of this compound at ground level could results in toxicity of plants, animals and even human health. These results indicate the importance of further reducing emissions by replacing fossil-derived fuels with renewable fuels during transportation of materials, products and co-products. Jatropha farming also had effect on several impact categories, however at relatively small quantities asides ozone depletion, in which it had a significant impact. The contributions to ozone depletion could be as a result of agrochemicals such as nitrogen and phosphate fertilizers, pesticides, insecticides or herbicides used during Jatropha farming and production. In summary, the environmental life cycle impact indicate that Jatropha oil use had largest environmental impact, followed by oil conversion, oil extraction, Jatropha farming and oil transportation, in that order but minimal contributions. Furthermore, climate change had the largest share of the impact, followed by marine ecosystem, fossil depletion, and terrestrial acidification. The rest had minimal role in the environmental burden.

However, when the results in Table 6.13 were compared to a reference diesel fuel with an European average, the result showed a negative impact for Jatropha production and

use across all farming systems (data not shown). This can be accounted to the wide differences in the reference diesel fuel system in Nigeria and that of the European average. The refining and production as described in the European average is highly efficient when compared to Nigerian production and refining process that suffers from poor production capacities, ageing infrastructures, poor maintenance with multiple transportation of materials and products.

6.4 Allocation of co-products

Considering allocation of co-product (glycerol), the NEV increases to 0.62 MJ, 0.42 MJ and 0.32 MJ while the NER on the other hand increased to 2.7, 1.7 and 1.5 for base-case rain-fed, base-case irrigated and large scale farming respectively. Similarly, the fossil fuel displacements increase to 7% [base-case rain-fed], 18% [base-case irrigated] and 32% [large scale farming]. Furthermore the total emissions reduced to 973.95 kg [base-case rain-fed] and 973.97 kg [large scale farming], thereby increasing GHG savings to 22.8%. These results demonstrate the benefit that could be obtained from harnessing further co-products such as seedcake and agricultural waste residues to generate heat and power from Jatropha. This additional energy source could be used to generate power for off-grid users, as opposed to burning of charcoal and agricultural woods in exposed units. Also, additional stream of income is available to independent power producer to generate electricity for these off-grid users, instead of generating power for the national grid using a decentralized Jatropha biodiesel production system coupled to waste to energy technologies.

6.5 Sensitivity Study

6.5.1 Sensitivity to Key Material Input

The effects of changing values of the significant inputs in Jatropha production on GHG and overall emissions have been evaluated. This was achieved by assuming a best and worst case scenario within a range of ±50%. Parameters such as transportation distances, irrigation, electricity requirement, fertilizer and steam use as well as the employment of chemicals such as methanol, sulphuric acid and sodium hydroxide were considered. For instance, the effect of a rise in the use of diesel fuel for farm equipment and machinery during Jatropha production was examined by assessing the use of 20 litres ha^{-1} and 60 litres ha^{-1} of diesel fuel. These value ranges were then compared with the rain-fed base-case scenario that assumes an additional use of 40 litres ha^{-1} of diesel fuel. The predictions for all the inputs examined are presented in figures 6.11 and 6.12 for percentage differences in GHG and overall emissions.

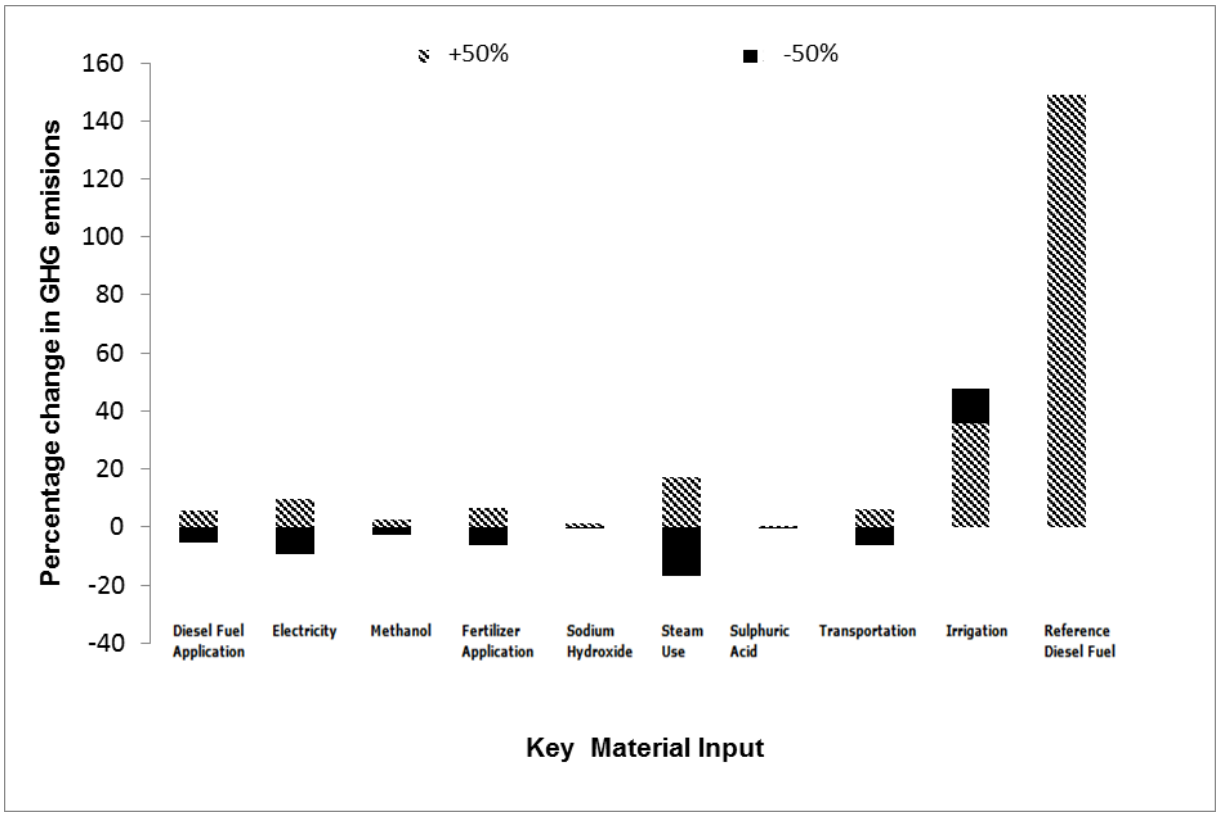

Figure 6.11: Sensitivity analysis with effects on net GHG emissions

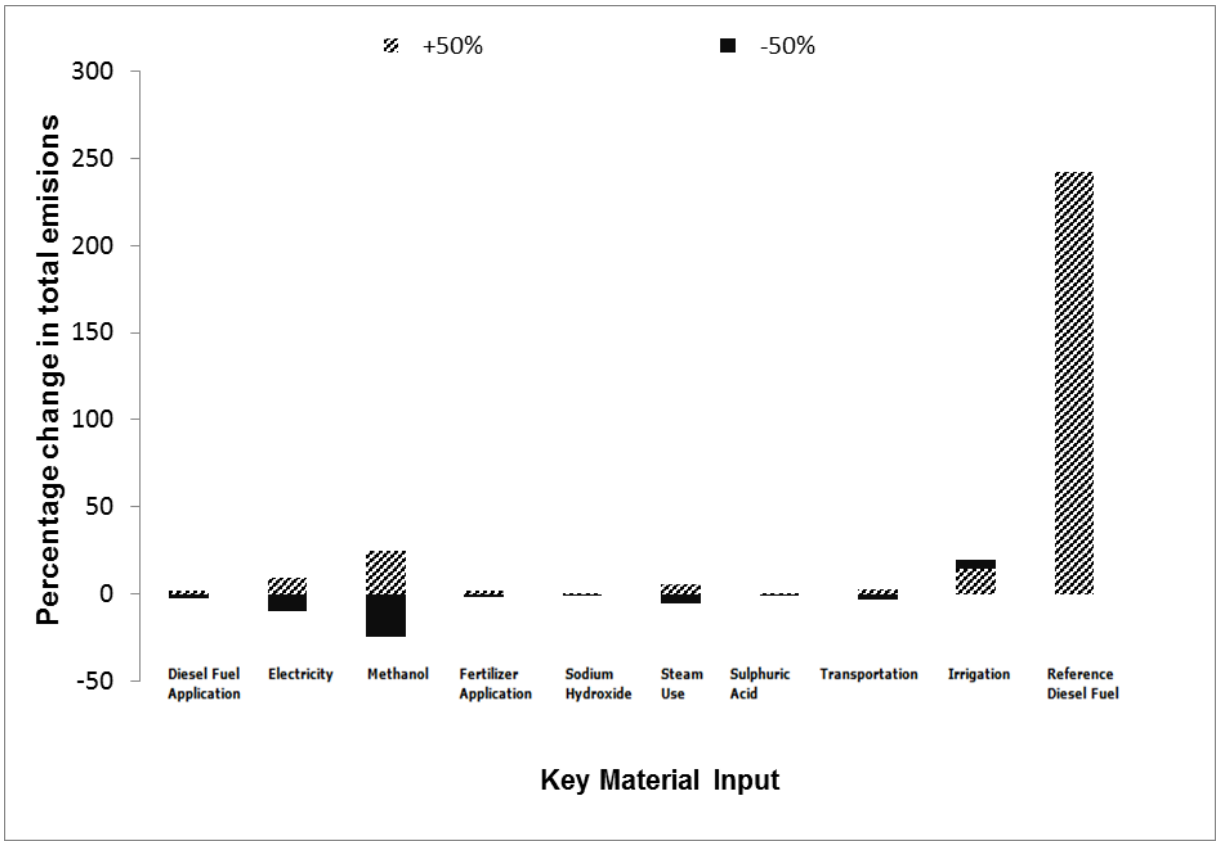

Figure 6.12: Sensitivity analysis with effects on total emissions

The parameters with the highest degree of sensitivities to GHG emissions are irrigation, steam use and electricity consumption with value ranges of 12-36%, ±17% and ±10% respectively. The application of diesel fuel, fertilizer and transportation distances also resulted in slight changes in GHG emissions with values ranging between 6% and 7%. Because all the parameters examined for a sensitivity analysis have a strong link with fossil fuels; a substitution of the respective inputs with renewable fuels or sources will significantly reduce the GHG emissions arising from Jatropha biodiesel production. The predictions also indicate that the use of irrigation is critical and can alter the environmental benefit of Jatropha production, especially when it is used in addition with other parameters such as fertilizer application and electricity use. Furthermore, the degrees of sensitivity on total emissions show that methanol use, irrigation and electricity are critical parameters in Jatropha production, with deviations up to 25%, 15% and 10% respectively. These values present a boundary scenario for a typical Jatropha farming system and demonstrate the need to limit the use of fossil fuels. For instance, farmers in Nigeria usually travel using a combination of walking, cycling and use of gasoline powered motorcycles. In the event of the use of more motorcycle transportation, increased fossil-fuel consumption could reduce the GHG savings reported in this

analysis by 5% or even more. This also applies to diesel fuel applications, irrigation, electricity use, chemical employment, fertilizer application, steam use and transportation distances.

6.5.2 Sensitivity to Seed Yield

A seed yield of 0.7 t ha^{-1} $yr^{-1}$was achieved from a four-year old Jatropha plantation with a plant spacing of 1.5 m x 1.5 m at Samaru, Nigeria [Ogunwole, 2014]. Further analysis was carried out to examine the sensitivity of Jatropha seed yield to life-cycle impact of Jatropha production by examining two worst-case scenarios (i.e. low yields of 0.6 t ha^{-1} and 1.8 t ha^{-1}). The results are presented in figure 6.13 showing the influence of seed yield on life cycle emissions. Higher yields were not examined because it would require more energy inputs from the use of fertilizers, irrigation and fossil fuels.

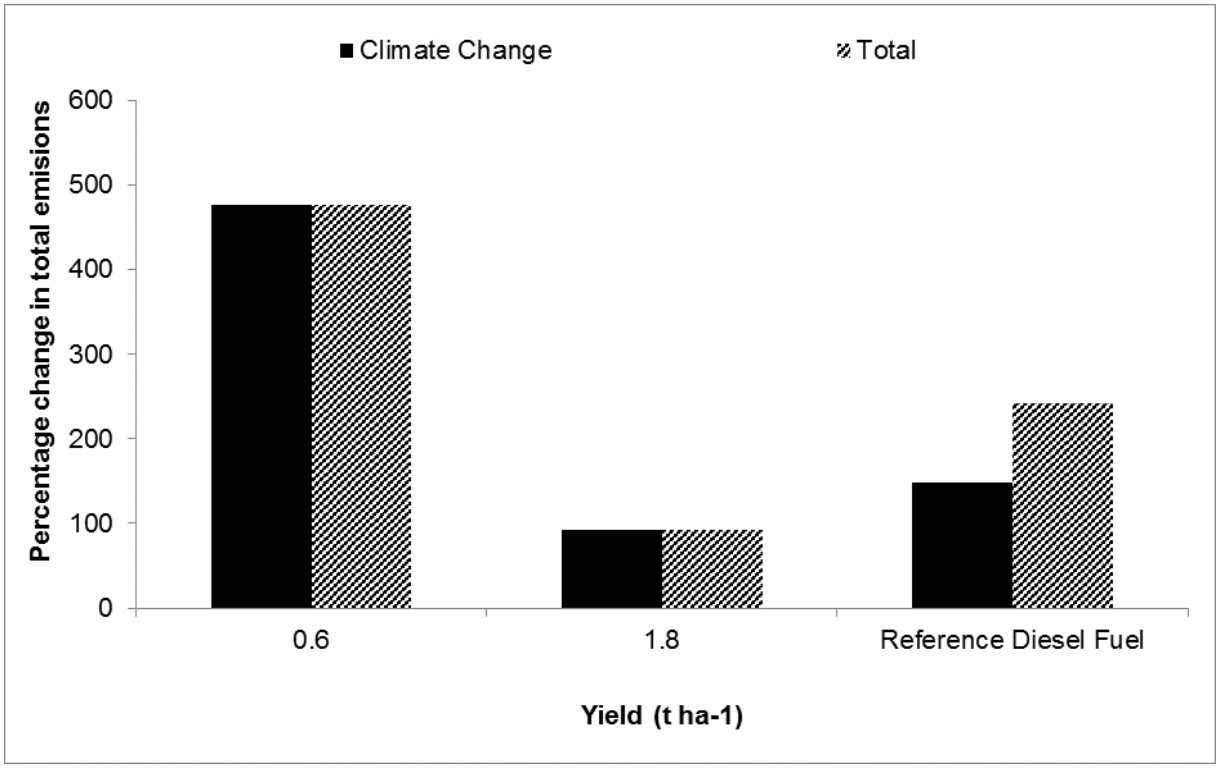

Figure 6.13: Seed yield influence on life cycle emissions

Results show that a low seed-yield of 1.8 t ha^{-1} yr^{-1} could increase GHG emissions from 0.9 kg CO_2 eq. to 1.8 kg CO_2 eq., i.e. almost a100% increase. This is however still lower than the GHG emission from the reference diesel fuel, which has a value of 2.3 kg CO_2 eq. A poor yield of 0.6 t ha^{-1} yr^{-1} on the other hand would have GHG emissions increase up to 5.3 kg CO_2 eq., with a nearly 480% increase over the base-case rain-fed scenario and 130% higher than that for the reference diesel fuel. The prediction shows that a poor yield, i.e. below 1.8 t ha^{-1} yr^{-1}, might not be viable from an environmental point–of-view,

as it could lead to more environmental degradation than if the conventional diesel fuel had been used.

6.5.3 Sensitivity to Transportation Distance

According to Kessom et al. [2009], the energy required for transportation of fuels depends on the distance covered, route for the transportation and the type of fuel used. In Nigeria, there are 21 distributed served by a pipeline network of approximately 5000 km, with fuel supplied via mainline and booster pumps. Conventional diesel oil is the most commonly used fuel in oil tankers, which also transport crude and petroleum products. Natural gas, on the other hand is used in power plants to generate power and to transport crude-oil and products via pipeline. Due to fuel shortages, pipeline vandalization, and poor maintenance that hinders effective transportation of refined products via these networks; fuels are usually transported from depots and import jetties over long distances to local filling stations using petroleum tankers usually with empty trips while imported fuels are transported over long distances using wide ranges of sea transport vessels. Katsouris and Sayne, [2013] described in detail how stolen crude-oil is shipped from Nigeria to foreign refineries for instant processing and sales through complex co-loading and along multiple routes to reduce the risk of being caught and to avoid payment of levies. This increases the total energy cost and environmental impact of diesel oil and other petroleum products in Nigeria.

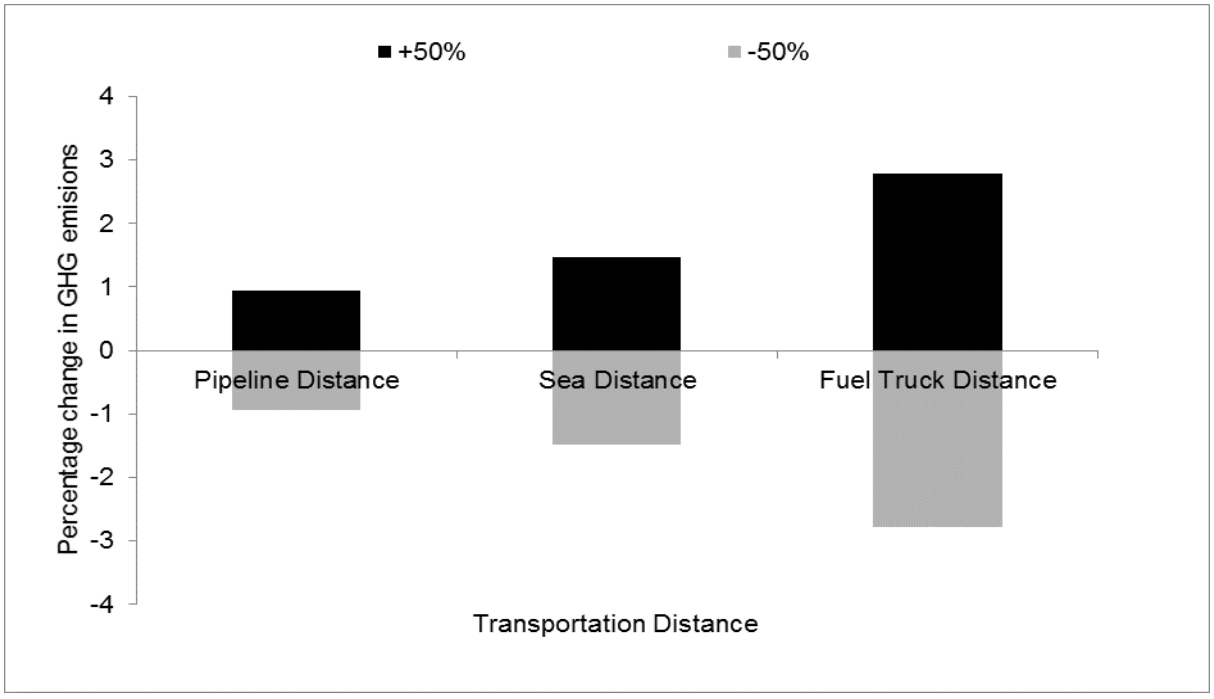

Figure 6.14: Influence of pipeline distance, sea distance and truck distance on GHG emissions

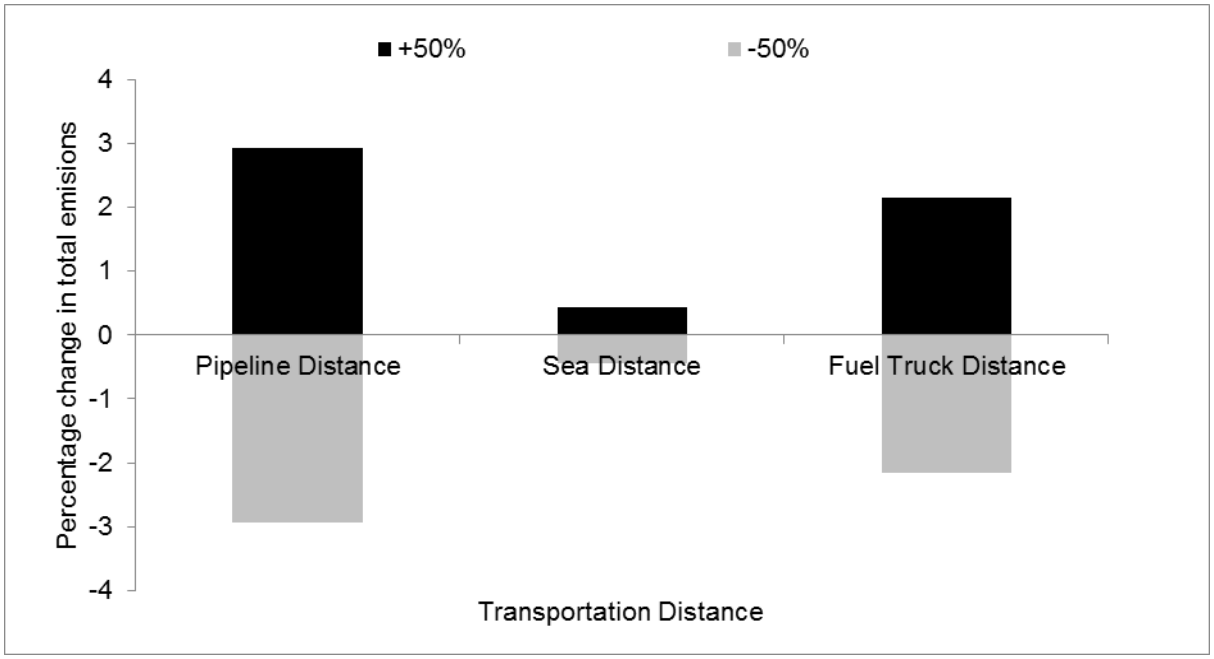

Figure 6.15: Influence of pipeline distance, sea distance and truck distance on GHG emissions

Due to these important, urgent issues, the sensitivity of transportation distance was carried out for the reference diesel-fuel. A ±50% range of sensitivities from high to low was tested on pipeline distance, sea distance and truck distance (see figure 6.14 and 6.15). Figure 6.15 shows that truck distance covered during the transportation of crude-oil and delivery of the product to a local vendor had the highest degree of influence on GHG emissions, followed by sea and pipeline distance travelled. Percentage increases and reductions in climate change were 0.94%, 1.48% and 2.78% for ± 50% changes in pipeline distance, sea distance and truck distance travelled respectively. However, when considering the change in total emissions for the transportation of crude-oil and delivery of product to a local vendor; the influence of pipeline distance on emissions was the largest, followed by truck distance covered and lastly sea distance travelled. Percentage increase and reduction in total GHG emissions were 2.94%, 0.48% and 2.17% for changes in pipeline distance, sea distance and truck distance travelled respectively.

6.6 Conclusion

The study concludes with the following:

1. Net energy ratios of 2.4, 1.6, and 1.4 and fossil-fuel savings of 58%, 36% and 27% are achievable for the production of 1 kg of Jatropha biodiesel under rain-fed base-case, base-case irrigated and large scale farming scenarios respectively. Similar results of 2.4%, 1.5% and 1.3% were obtained for the use of 1 MJ of Jatropha biodiesel used in a 126MW power plant but produced under rain-fed base-case, base-case irrigated and large scale farming scenarios respectively.

2. Jatropha biodiesel systems have a potential environmental benefit, with GHG savings of 60%, 50% and 26% for rain-fed base-case, irrigated base-case and large-scale farming respectively. However the GHG savings of nearly 19% was observed at all farming conditions using the well-to-wheel system boundary.

3. To satisfy Nigeria's energy demand, diversify the energy mix in power generation and reduce GHG emissions concurrently, Nigeria's renewable energy programme should adopt the system defined within this report, i.e. to choose a sustainable Jatropha biodiesel fuel production and use system that is of economic and environmental benefit.

6.7 Further Work

Since this study employed the use of secondary data and generic process to describe Jatropha biodiesel and diesel production in Nigeria, further work could employ primary data from established Jatropha farms to enable the use of these results as a guide and to foster policy decisions in Nigeria and similar countries. The commercial scale of Jatropha farming is yet to be established in Nigeria. Also, the impact of Jatropha biodiesel production and use can be re-examined in the light of land use change, water depletion, human toxicity and use of recent technologies with low environmental impact. There are recent assessment that examines the production, use and end-of-life of processes, products and systems, also known as well-well analysis, hence, the impacts of the end-of-life of material input and product output could be included in further work. It is also highly recommended that a comprehensive life cycle inventory database that covers the production of materials, fuels, and disposal of goods with specificity to Nigeria conditions be available for life cycle assessment study. This is because the European databases have not included the exacting conditions and inefficiencies appropriate for this kind of study. The socio-economic impact of production and use of Jatropha biodiesel would be significant and enable a holistic life cycle assessment.

6.8 References

[1.] Sambo A. S. 2008. “Matching Electricity Supply with Demand in Nigeria”, International Association of Energy Economics (IAEE), 4:32–36.

[2.] Iwayemi, A. 2008, “Nigeria’s Dual Energy Problems: Policy Issues and Challenges”, International Association for Energy Economics, pp 17–21.

[3.] Oyedepo, S. O. 2012, “Energy and sustainable development in Nigeria: the way forward”, Energy, Sustainability and Society, *2*(15):1-17.

[4.] Federal Ministry of Power (FMP), 2014, “Official Power Statistics Generated on December 23, 2012, < http://www.power.gov.ng/> (last accessed on 06/9/2014).

[5.] PHCN, 2009. “Generation and Transmission Grid Operations”, Annual Technical Report for 2008, National Control Center (NCC), Osogbo.

[6.] House of Representative Ad-Hoc Committee (HTADC) 2012. Report of the ad-hoc committee “to verify and determine the actual subsidy requirements and monitor the implementation of the subsidy regime in Nigeria‟, Resolution no. (HR.1/2012). (Last accessed on 06/9/2014).

[7.] Nigerian National Petroleum Corporation, (NNPC), 2012. “Annual Statistical Bulletin,” Corporate Planning and Strategy Division, NNPC.

[8.] Energy Commission of Nigeria (ECN), 2005. Renewable Energy Master Plan.

[9.] Energy Commission of Nigeria (ECN), 2012. Draft National Energy Master Plan

[10.] Nigerian National Petroleum Corporation, (NNPC), 2007, “Biofuels Development in Nigeria”, International Renewable Energy Conference, Abuja, March 16-19.

[11.] Chineke, T. C., Igwiro, E. C. 2008, “Urban and rural electrification: enhancing the energy sector in Nigeria using photovoltaic technology”, *African Journal Science and Technology 9*(1):102–108.

[12.] Ngala, G.M., Alkali, B., Aji, M.A. 2007, “Viability of wind energy as a power generation source in Maiduguri, Borno state, Nigeria”, *Renewable Energy*, *32* (13):2242–2246.

[13.] Akinbami, J. F. K. 2001, “Renewable Energy Resources and Technologies in Nigeria: Present Situation, Future Prospects and Policy Framework”. *Mitigation and Adaptation Strategies for Global Change*, *6*:155–181.

[14.] Idusuyi, N., Ajide. O. O., Abu, R. 2012, “Biodiesel as an Alternative Energy Resource in Southwest, Nigeria”, *International Journal of Science and Technology*, *2*(5): 323-327.

[15.] Uyigue, E. 2007. “*Renewable energy and energy efficiency and sustainable development in Nigeria*”. In: CREDC Conference on Promoting Renewable Energy and Energy Efficiency in Nigeria.

[16.] Aransiola, E. F., Daramola, M. O. Ojumu, T. V., Aremu, M. O., Layokun, S. K. Bamidele, O. S. 2012, “Nigerian Jatropha Curcas Oil Seeds: Prospect for Biodiesel Production in Nigeria”, *International Journal of Renewable Energy Research*, *2*(2): 317-325.

[17.] Jongschaap, R. E. E., Corre, W. J., Bindraban, P. S., Brandenburg, W. A. 2007. “Claims and facts on Jatropha *curcas* L.: Global Jatropha *curcas* evaluation, breeding and propagation.” *Plant Research International*, B. V., Wageningen, Report No. 158.

[18.] Brittaine, R. Lutaladio, N. 2010, “*Jatropha: A smallholder Bioenergy Crop-The Potential for Pro-Poor Development*”, Integrated Crop Management, *8*:1-114

[19.] Parawira, W. 2010, “Biodiesel production from Jatropha *curcas*: A review”, *Scientific Research and Essays*, *5*(14):1796-1808.

[20.] Jingura, R., Matengaifa, R., Musademba, D., Musiyiwa, K. 2011, “Characterisation of land types and agro-ecological conditions for production of Jatropha as a feedstock for biofuels in Zimbabwe”, Biomass and Bioenergy, *35*: 2080–6.

[21.] Umaru, M. and Aberuagba F. 2012, “Characteristics of Typical Nigerian Jatropha *curcas* oil Seeds for Biodiesel Production”, *Research Journal of Chemical Sciences*, *2*(10): 7-12.

[22.] Akande S. O. and Olorunfemi, F. B. 2009, “Research and Development Potentials in Biofuel Production in Nigeria, *African Research Review*, 3(3):34-45.

[23.] Abila, N. 2011, “Promoting Biofuels Adoption in Nigeria: A Review of Socio-economic Drivers and Incentives”, Bioenergy Technology, World Renewable Energy Congress, Linköpinh, Sweden.

[24.] Galadima, A., Garba, Z. N., Ibrahim, B. M. Almustapha, M. N., Leke, L. Adam, I. K. 2011, “Biofuels Production in Nigeria: The Policy and Public Opinions”, *Journal of Sustainable Development*, *4*(4): 22-31.

[25.] Hou, J., Zhang, P., Yuan, X., Zheng, Y. 2011, "Life cycle assessment of biodiesel from soybean, jatropha and microalgae in China conditions", Renew Sustain Energy Rev., *15*: 5081–5091.

[26.] Kaewcharoensombata, U., Prommettab, K., Srinophakun T. 2011, "Life cycle assessment of biodiesel production from Jatropha", J. Taiwan Inst. Chem. Eng., *42*: 454–462

[27.] Pandey, K. K., Pragya, N., Sahoo P. K. 2011, "Life cycle assessment of small-scale high-input Jatropha biodiesel production in India", Applied Energy, 88(12): 4831–4839

[28.] Wang, Z., Calderon, M., Lu Y. 2011, "Lifecycle assessment of the economic, environmental and energy performance of Jatropha curcas L. biodiesel in China", Biomass and Bioenergy, 35: 2893–2902

[29.] ISO (International Organization for Standardization), 2006, Environmental Management – Life Cycle Assessment – Principles and Framework, International Organization for Standardization, Geneva, Switzerland, Report No.: ISO 14040

[30.] ISO (International Organization for Standardization), 2006, Environmental management. Life cycle assessment Requirements and guidelines, International Organization for Standardization, Geneva, Switzerland, Report No.: ISO 14044

[31.] Product Ecology Consultants (PRé), 2011, “SimaPro Life cycle assessment software”, Amersfoort, the Netherlands.

[32.] Whitaker, M., Heath, H., 2009, “Life Cycle Assessment of the Use of Jatropha Biodiesel in Indian Locomotives”, Technical Report, NREL/TP-6A2-44428.

[33.] Eshton, B., Katima, J. H. Y., Kituyi, E. 2013, “Greenhouse gas emissions and energy balances of Jatropha biodiesel as an alternative fuel in Tanzania”, *Biomass and Bioenergy*, *58*:95-103.

[34.] Gm¨under, S., Singh, R., Pfister, S., Adheloya, A., Zah, R. 2012, “Environmental Impacts of Jatropha *curcas* Biodiesel in India”, *Journal of Biomedicine and Biotechnology*, pp: 1-11.

[35.] Gmu¨nder, S. M., Zah, R., Bhatacharjee, S., Classen, M., Mukherjee, P., Widmer, R. 2009, “Life cycle assessment of village electrification based on straight Jatropha oil in Chhattisgarh, India”, Biomass and Bioenergy, 1-9

[36.] Prueksakorn, K., Gheewala, S. H. 2008, “Full chain energy analysis of biodiesel from Jatropha *curcas* L. in Thailand”, *Environ Science Technology*, *42*:3388–3393.

[37.] Reinhardt, G., Gartner, S., Rettenmaier, N., Munch, J., von Falkenstein, E. 2007, “Screening Life Cycle Assessment of Jatropha Biodiesel,” Commissioned by Daimler A. G., Stuttgart, Prepared by the Institute for Energy and Environmental Research Heidelberg GmbH. December 11, 2007.

[38.] Terren, M., Mignon, J., Declerck, C., Jijakli, H., Saveri, S., Jacquet de Haveskercke, P., Winandy S. and Mergeai, G. 2012, “Principal Disease and Insect Pests of Jatropha *curcas* L. in the Lower Valley of the Senegal River”, *Tropicultura*, *30*(4):222-229.

[39.] van Wesenbeeck, C. F., Keyzer, M. A., Nubé, M. 2009, “Estimation of under nutrition and mean calorie intake in Africa: methodology, findings and implications”, *8*(37):1-18.

[40.] Ogunwole, J. O. 2014, “Development of Commercially Viable Plantations of Jatropha *Curcas* L: Case for Promotion of Its Agricultural Research”, *Advances in Plants and Agriculture Research, 1*(3): 00017

[41.] Prueksakorn, K., Gheewala, S. H., Malakul, P. and Bonnet, S. 2010, “Energy analysis of Jatropha plantation systems for biodiesel production in Thailand”, Energy for Sustainable Development, 14:1–5.

[42.] Kessom, W., Unnasch, S., Moretta, J. 2009, “Life Cycle Assessment Comparison of North American and Imported Crudes” Alberta Energy Research Institute, File No: AERI 1747, pp:1-220

[43.] Achten, W. M. J., Almeida, J., Fobelets, V., Bolle, E., Mathijs, E. Singh, V. P., Tewari, D. N., Verchot, L. V., Muys B. 2010. “Life cycle assessment of Jatropha biodiesel as transportation fuel in rural India”, Applied Energy, *87*:3652–3660

[44.] National Bureau of Statistics, 2011. Annual Abstract of Statistics of the Federal Republic of Nigeria http://www.nigerianstat.gov.ng/pages/NBS%20eLibrary. Last accessed on 06/9/2014

[45.] EIA (Energy Information Administration), 2013, Independent statistics and analysis from the United State Energy Information Administration, <http://www.eia.gov/countries/analysisbriefs/Nigeria/nigeria.pdf > (last accessed on 06/9/2014).

[46.] Takeshima, H. and Salau, S. 2010, “Agricultural Mechanization and the Smallholder Farmers in Nigeria”, International Food Policy Research Institute Policy Note No:22, pp:1-5

[47.] PrOpCom, 2012. Making tractor markets work for the poor in Nigeria: A PrOpCom case study, Abuja, Nigeria

[48.] Ndong, R., Montrejaud-Vignoles, M., Saint Girons, O., Gabrielle, B., Pirot, R., Domergue, M., Sablayrolles, C. 2009, “Life cycle assessment of biofuels from Jatropha *curcas* in West Africa: a field study. *Global Change Biology Bioenergy*, *1*:197–210.

[49.] Katsouris, C. and Sayne, A. 2013, “Nigeria’s Criminal Crude: International Options to Combat the Export of Stolen Oil”, The Royal Institute of International Affairs, pp: 1-85

[50.] United Nations Department of Economic and Social Affair, 2007, “Small-Scale Production and Use of Liquid Biofuels in Sub-Saharan Africa: Perspectives for Sustainable Development, Prepared by Energy and Transport Branch, Division for Sustainable Development (PAPER NO. 2: DESA/DSD/2007/2)

[51.] Audsley, E., Stacey, K., Parsons, D. J., Williams, A. G. 2009, “Estimation of the greenhouse gas emissions from agricultural pesticide manufacture and use”, Prepared for Crop Protection Association, pp:1-20

[52.] Davis, S. C., Diegel, S. W. & Boundy, R. G. 2014, “Transportation Energy Data Book”, Edition 33, Oak Ridge, TN: Oak Ridge National Laboratory.

CHAPTER 7

7. MICROBIAL FUEL DEGRADATION ANALYSIS

The focus of this chapter is to present the progress in modelling microbial fuel degradation in gas turbine fuels and the impact of fuel degradation on engine performance. The chapter begins by introducing bio-fouling in gas turbine fuels and fuel systems. This is followed by the description of the model, its development, and the integration of the degraded fuels in Turbomatch (v2). The results are presented with a discussion on the impact of microbial fuel degradation on engine performance.

This chapter was adapted from two articles:

1. Onabanjo, T. O.; Di Lorenzo, G.; Goodger, E. M.; Pilidis, P. 2014. The development of a model for the assessment of biofouling in gas turbine system. Journal of Engineering for Gas Turbines and Power 136 (061401):1-10. DOI: 10.1115/1.4026367

2. Onabanjo, T. O.; Di Lorenzo, G.; Goodger, E. M.; Pilidis, P. A model for simulating microbial fuel degradation in gas turbines. Submitted to International Biodeterioration & Biodegradation (Manuscript Number IBB-S-14-00425 under review)

7.1 Introduction

The gas turbine industry is under pressure to maintain high quality deliverables such as improved performance and efficiencies, as well as emission compliant, highly reliable, available, and maintainable engines. Although gas turbines are designed to achieve these potentials, they are limited by component inefficiencies [Kurz and Brun, 2001; Doering et al. 1972]. One of which is brought about by poor quality of fuel. Fuels are often compromised by unwanted materials such as rust, dust, wax, contaminated air and water droplets that enable the entry of microorganisms [Passman, 2003; Giles, 2003].

7.1.1 Bio-Fouling of Fuels & Fuel Systems in Gas Turbines

The fundamental components of gas turbine fuel systems are relatively the same with design differences varying according to the Original Equipment Manufacturer (OEM). For common gas turbines, the fuel system can be categorized into three: 1) fuel storage system, primarily the fuel tanks, 2) fuel delivery system, including the flow lines and pumps, 3) fuel injection system, most importantly the injectors [Soares, 2008, Lee et al. 2006].

The primary purpose of these sub-systems is to ensure that the fuel required for combustion is effectively stored, prepared and delivered at the right amount and pressure at all engine operations; idle conditions, low or high power requirement and during transient conditions, such as rapid acceleration or descent. They also have secondary functions, where they ensure continuous circulation of fuel for cooling fuel pumps and other hydraulic systems. Of higher consequence are secondary systems, for example, modulation of the variable area nozzles and other control systems, which depend on the operation of the fuel system. Therefore, a failure in any of these systems due to clogging has a great consequence on engine performance and ultimately could lead to damage of the entire unit.

7.1.2 Mechanisms of Bio-fouling

Generally the term “bio-fouling” refers to any biological process resulting in the accumulation of biological material on an exposed or submerged surface. The concept is well documented in the marine industry, where it increases drag on a ship’s hull [Kirchman and Mitchell, 1981, Stuart, 1995]; industrial processes where fouling reduces performance of heat exchangers and cooling units; Water and wastewater systems [Melo and Bott, 1997] with damages to filtration units, membrane systems and subsequent

treatment failures. In a typical gas turbine storage system, bio-fouling is said to exert one or more of the following effects: disappearance of certain fractions of fuel, changes in coloration, smell and clarity of fuel, changes to the physical and chemical properties of fuel, re-distribution of fuel constituents across the system, accumulation of biomass, and corrosion [Hill and Hill, 2008, Kirchman and Mitchell, 1981, Das and Chandran, 2011, Okoh, 2006].

Bio-fouling actively involves the presence of microbial biofilms. Microbial biofilm with typical illustration in figure 7.1 consists of microorganisms of one or more species, all embedded in a biological matrix [Lee et al. 2010]. It is the most complex ecological contaminant in a fuel system and involves the growth and death of microbial cells, attachment of cells to a solid support, detachment away from the biofilm, and transfer of nutrients and by-products of metabolism along a concentration gradient.

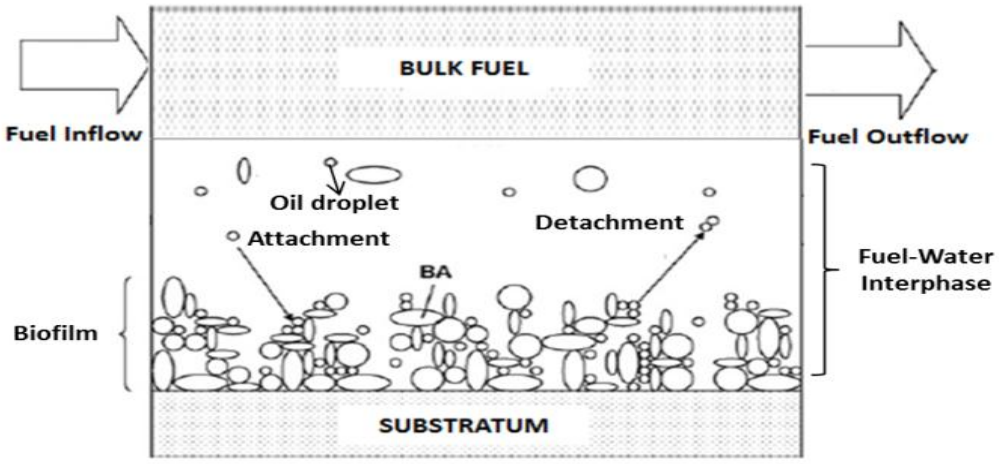

Figure 7.1: Biofilm Model System of Fouling in Gas Turbine Fuel Tanks

The fundamental developmental processes of biofilm formation are widely documented in the literature [Stuart, 1995, Sand, 1997] and involves:

a. An initial film conditioning of the supporting system e.g. metal surface of the fuel tank or pellicles at fuel-water interface, with organic polymers.

b. A subsequent attachment by microbial cells leading to colonization, production of extracellular polysaccharide (EPS) and metabolic by-products.

c. Growth

d. Maturation leading to a certain biofilm depth (BD) and age (BA),

e. A final phase of detachment and re-colonization of new conditioned surfaces.

Thus, an elaborate mathematical model of bio-fouling in fuel systems must consider mass transfer equations and transport equations—diffusion and advection terms, of all these biological processes. This involves the use of stoichiometry, mass balance and transport equations, as well as bio-energetic and kinetic considerations. This section illustrates the use of stoichiometric equations and discusses their applications.

7.1.2.1 Microbiology and Ecology of Fuels and Fuel Systems

Microorganisms found in fuel are quite enormous with over 200 genera ranging from bacteria, yeasts to moulds [Rauch et al. 2006]. Despite fuels' hostile environment, many microorganisms have adapted mechanisms for proliferating fuel to the point of fouling. They tend to concentrate at interfaces; fuel–water; fuel–air; fuel–tank wall; tank wall–air and water–tank wall interfaces, where they adhere to wall surfaces, sink into the fuel volume or stick to overhead surfaces [Passman, 2003]. On entry into the fuel storage tank, they break down complex fuel components and generate soluble degradable products that prompt further growth of new cells. After a sufficient time, which could be hours, days or weeks, cells become more unevenly dispersed in the bulk fluid with strong concentration at the so called "fuel-water interface" that is characterized by a top bulk fuel layer, a bottom water layer and a middle fuel–water phase. Survival is aided by abiotic conditions such as temperature, pH, availability of nutrients and adaptability factors such as bio-surfactants, spores and EPS. For instance, McNamara et al. [2003] found out that spore forming Bacillus subtilis survived in water bottoms containing high concentrations of Diethylene Glycol Monomethyl Ether (DiEGME). It is suggested that microorganisms assess the fuel-water interphase relatively fast and their stability on metal surfaces, either at regions close to the fuel–water interface, bottom tanks, or headspace is more rigid than at the fuel–water interface. According to Melo and Bott [1997], microbes have preferences for solid surfaces rather than live in free suspension because surfaces protect cells from unstable fluid forces and allow stability to access nutrients. This promotes high accumulation of biofilm, which subsequently creates a region of low reduction-oxidation potential and active growth of anaerobic organisms that might induce corrosion around the tank walls. Therefore, depending on the biofilm depth, there exist several ecological zones and conditions in fuel that favour the growth of different microorganisms. Haeseler et al. [2010] described four ecological zones in natural reservoirs: aerobic, nitrate-, sulphate-reducing and methanogenic conditions.

7.1.2.2 Microbial Metabolism & Growth Conditions

Different microorganisms have their energy requirements and preference for substrates, terminal electron acceptors and growth conditions. Microbial metabolism therefore describes the mechanism by which microorganisms access nutrients for growth, energy and maintenance.

Generally, hydrocarbon and ester based fuels are rich substrate media that contain sufficient amounts of carbon (C) and hydrogen (H) for microbial growth [Jones et al. 2011]. Depending on the nature of fuel, they also provide additional nutrients such as nitrogen (N) and sulphur (S). The presence of additives in fuels could provide trace amounts of essential elements. For instance, Passman et al. [2001] detected the presence of nitrate (NO_3) in microbiologically challenged fuel samples containing biocides and accounted this to the partitioning of biocides in water. Additional nutrients such as amines, amides, nitriles and nitrogen related compounds are likewise released into the environment by decayed matter and part of these are assimilated by living cells. As a result of nutrient consumption, inorganic compounds such as carbon dioxide (CO_2), nitrogen (N_2), hydrogen sulphide (H_2S) are generated [Soares, 2008].

Microbes derive their energy by converting complex organic compounds to simpler forms, and allowing the energy stored in the substrate to be accessible for growth [Das and Chandran, 2011, Okoh, 2006]. While some microbes have multiple metabolic pathways to carry out the degradation of the hydrocarbons, others are limited and depend on co-metabolism [Passman and McFarland, 1997]. They access the nutrients by: 1) interfacial uptake via diffusion or active transport, in which the fuel substrates directly penetrate the cells, 2) utilizing solubilized hydrocarbons in the aqueous phase, 3) emulsifying the hydrocarbons using bio-surfactants [Haeseler et al. 2010].

It is well established that water is significant for the growth of microorganisms in fuel [Passman, 2003]. Water exists in different forms in fuels. 1) Water exists as suspended water, which is widely dispersed within the fuel system. This accumulates and settles as “free water” at the bottom of the fuel tank. Barsness and Bertram [1959] carried out a study on JP-4 fuels to determine the limits for water saturation in fuels with temperature ranges between 4^{o}C and 30^{o}C. They concluded that solubility of water in fuel increases with temperature irrespective of the presence or absence of additives. 2) Water exists in the dissolved form and this varies with fuel types and temperature. 3) Water exists as fuel-water emulsion [Passman, 2003]. 4) If biofilms are present, some water gets locked

within the matrix and this account for over 90% [Passman, 2003, McNamara et al. 2003, and Jones et al. 2011]. Generally, fuel absorbs water and this water condenses and dissolves with temperature.

Temperature and pH have significant effects on microbial growth. While some require extreme low temperatures down to -50^{o}C, others prefer temperatures above 50^{o}C, but the most abundant bacteria in fuel thrive between 20^{o}C and 50^{o}C. They grow in a logarithmic pattern with temperature [Passman, 2003]. For pH, most microbes prefer a nearly neutral pH. However, exceptional microbes, such as sulfate reducing bacteria (SRB) prefer a strong acidic environment.

7.1.3 Modelling Biofouling in gas turbines

Based on the above described biofouling mechanisms in gas turbine fuels, an attempt was made to describe the aerobic processes of microbial fuel degradation in fuels and fuel systems using bio-mathematical modelling approach. This should provide a platform to simulate microbial fuel degradation in gas turbines when integrated with appropriate engine simulation software(s). This is the first time a gas turbine bio-fouling assessment model is being developed. It is a first step in quantifiable assessment and towards predictive condition monitoring.

The next section describes the approach for developing the model to simulate degraded fuels, predict biodegradation rates, estimate hydrocarbon loss and calculate the amount of water required to initiate degradation under aerobic conditions. This biofouling model is coined “Bio-*f*AEG” —Biofouling Assessment in Gas Turbines. Further analyses are carried out to assess the impact of fuel degradation on engine performance.

7.2 Methodology

7.2.1 Bio-*f*AEG Model Development

The Bio-*f*AEG model is based on three modules: a fuel module that defines the fuel for analysis and the relative biodegradability rates of fuel constituents, a biomass module that uses fundamental concepts of bioenergetics and thermodynamics to estimate the yield of cells for a given reaction as well as derive the microbial metabolism stoichiometry and finally, a kinetic module that `calculates the reaction rates using estimated microbial growth kinetic parameters (—see figure 7.2).

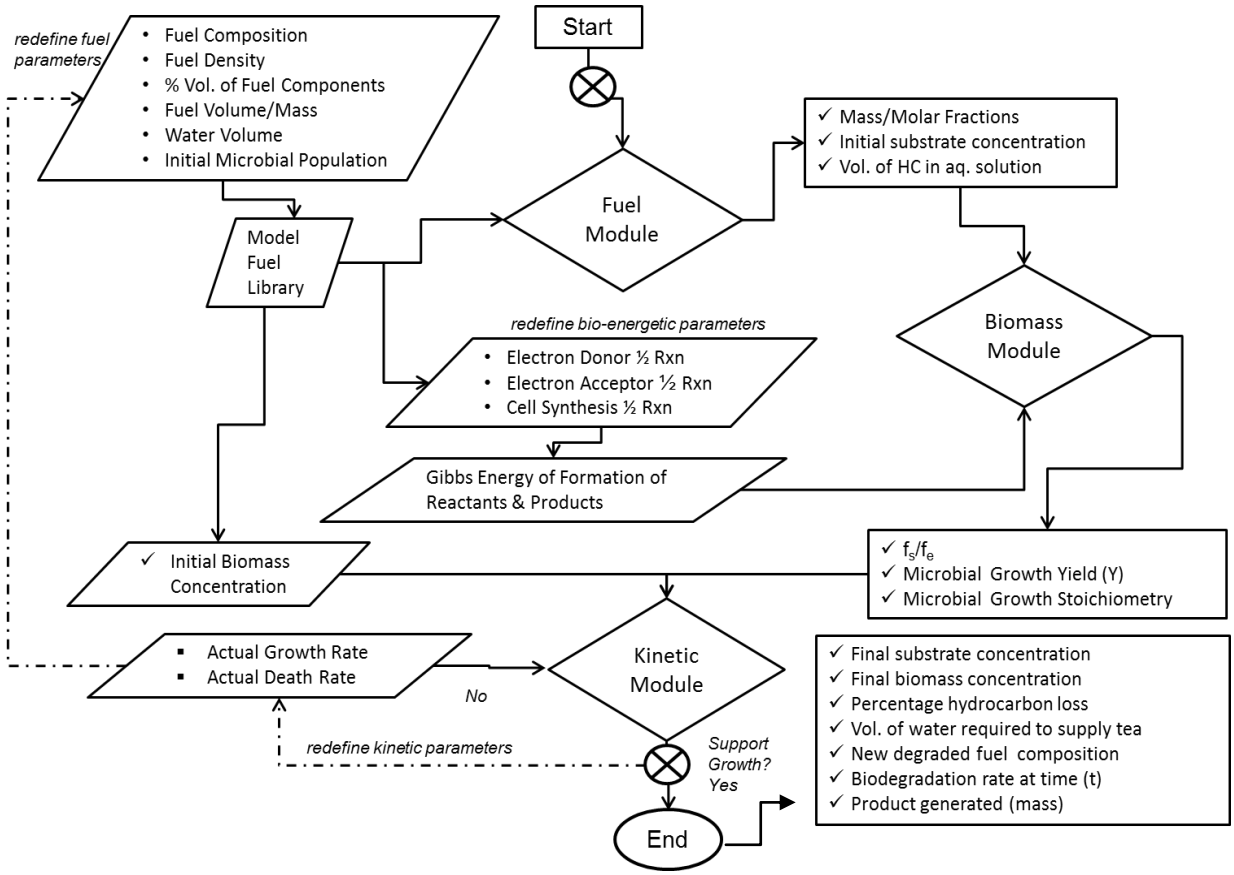

Figure 7.2: Simplified flow diagram of Bio-fAEG Model

7.2.1.1 Fuel module for defining fuels for analysis

The initial model development by Onabanjo et al. [2013] described a two-step process for defining fuels for biodegradation reaction.

1. Using a defined fuel library, which has four broad classifications based on hydrocarbon type and twelve sub-classes based on branching, number of carbon atoms and/or rings. Each fuel sub-class has an assigned relative overall biodegradability value

(X_{BIO}), a product of inherent biodegradability factor (X_{IN}) and microbial accessibility factor (X_{ACC}). This overall biodegradability values are initial estimates, relative to the most degradable fuel component and assume a limited solubility of hydrocarbons in aqueous solution with direct diffusion of oil to the microbial cell [Haeseler et al. 2010, Vandecasteele, 2008]. The fuel library classification enables a simplified representation of hydrocarbon fuels, since fuels generally contain a wide range of carbon atoms, types and biodegradability rates. For instance, a typical conventional diesel fuel contains about 2000-4000 hydrocarbons with carbon number range of 8-28 while bio-diesel fuel contain a wide range of fatty acid esters [Marchal et al. 2003, Ribeiro et al. 2007]. And unlike the recent work by [Farell et al. 2007, Pitz, et al. 2011 and Mueller et al. 2012] in developing surrogate fuels that focuses on fuel mixtures and relationship with physical properties, this model considers carbon atoms with different degradability rates. So, the fuel library is composed of a broad and a sub-classification of fuel components.

2. Choosing a biodegradation reaction, which is a stepwise reaction between a specified hydrocarbon and a given terminal electron acceptor (TEA). In this work, only aerobic degradation is presented, since it is the most reported form of hydrocarbon degradation and it involves the oxidation of hydrocarbons by oxygenases [Das and Chandran, 2011, Okoh, 2006].

Considering the limited volume of water found in practical fuel tanks, the above steps were applied, assuming partial-parallel mineralization of hydrocarbons. Partial-parallel reactions refer to complete mineralization of hydrocarbon to CO_2 at a slow progressive rate and across all fuel classes, however in preferential sequence for the most readily degradable fraction and for TEA with the highest redox potential [38]. This is supported by many fuel microbes that evolute CO_2 and preferentially utilise TEA. The assumption relate to the amount of substrate utilised and valid when hydrocarbon is the only form of carbon and energy source for the organism, with no other transformation processes occurring in the system.

Although, biodegradation reactions are complex and specific [VanBriesen, 2001], for applicable models, detailed knowledge of biochemical pathways for fuel deterioration are not necessary, hence, biodegradation reactions were expressed using simple mass balance stoichiometric equations, assuming the fuel is in contact with a given volume of water containing the essential TEA. Parameters such as percentage weight of fuel constitutent, fuel density were included.

This model was a simplified representation of progressive degradation of hydrocarbon under limited water and TEA requirements. It allowed the user to estimate the molar concentrations of TEA and products generated, as well as estimates the volume of water required to provide the essential TEA. The model was however limited because, it only considered the use of stoichiometric equations, complex to execute and did not solve the reaction mechanism from the microbial kinetics point of view, hence the concentration of biomass generated could not be estimated. The current model is a further modification of the previous model [Onabanjo et al. 2013]. Here, a biomass module and a kinetic module were further incorporated.

7.2.1.2 Biomass Module for Predicting Microbial Growth Yield (Y)

Since the organism's sole aim in the fuel environment can intuitively be said to be formation of new cell material, even in extreme environment, where maintenance and repair also take priority, Cell or Microbial Growth Yield (Y) is the fundamental parameter in the development of microbial growth stoichiometry. Cell Yield is the maximum yield of cells resulting from the consumption of a particular substrate. It can be measured experimentally, often referred to as the actual yield, or estimated through bio-energetics, also known as the theoretical yield. It is expressed in units as mole of cells per mole of substrate utilised [VanBriesen, 2002].

Generally, microorganisms require enzymes and energy in the form of ATP to carry out biodegradation reactions. The Gibbs energy required is generated from the electron transfer between an electron donor (ED) and a specified electron acceptor (EA) and is used to drive cell synthesis and the incorporation of oxidized elements into the cell. As a result of degradation, by-products such as CO_2 and H_2O are generated. Thus, the flow of Gibbs energy into cell synthesis can be monitored following a flow of electron from an electron donor to an acceptor [Xiao and VanBriesen, 2006, Xiao and VanBriesen, 2008, McCarty, 1965].

There are a number of methods described in the literature for predicting the theoretical yield of cells and some of the most widely accepted methods include: Method by Roels [1980, 1983], that is based on the empirical data of the degree of reductance of carbon in the electron donor substrate in correlation to the yield of cells, but applies to a limited set of microorganisms belonging mainy to the aerobic heterotrophic class. Another approach by Heijnen & van Dijken [1992] and Heijnen et al. [1992] is based on the assumption of a redox reaction between the electron donor and acceptor to yield biomass as the only

product. Here, the Gibbs energy of dissipation is coupled to the Gibbs energy driving catabolism and anabolism and correlates with the carbon chain length and the degree of reductance in the donor substrate. This method is restricted to short carbon chain compounds and has limited applications in complex structures and degradation pathways as found in hydrocarbon degrading reactions. The McCarty's method of yield prediction assumes that electrons in the donor substrate are partitioned between energy generation and biosynthesis [McCarty, 1965, McCarty, 2006].

VanBriesen [2001] evaluated these methods and observed similar prediction values but raised concerns about their application on different substrates, organisms and abiotic conditions. Of all these prediction models, the McCarty's method is the most simplified, consistent, widely accepted and applied in environmental technologies. It is a well applicable approach to predicting cell yield on hydrocarbon compounds, especially with six or more carbon compounds, as well as complex structures or reactions as found in bio-fouling. The McCarty's method of prediction has subsequently been modified [VanBriesen, 2002, Xiao and VanBriesen, 2006, Xiao and VanBriesen, 2008, VanBriesen, and Rittmann, 2000]. These modifications are based on the considerations of the actions of oxygenases (mono-oxygenases or di-oxygenases) as applicable in hydrocarbon degradation.

In this model, the microbial cell has been modelled as a black box using the modified McCarty's method of yield prediction, in which substrate utilization is split for catabolic (for energy production), and anabolic reactions (for biosynthesis of new cells).

According to McCarty [2006], bacterial yield prediction is governed by the following equations:

$$-f_e^0 k\Delta G_e^{01} R = f_s^0 \Delta G_{e-syn}^{01} \quad (1)$$

$$\Delta G_s = \frac{\Delta G_{fa} - \Delta G_d}{\varepsilon^m} + \frac{\Delta G_{in} - \Delta G_{fa}}{\varepsilon^n} + \frac{\Delta G_{pc}}{\varepsilon} \quad (2)$$

$$\Delta G_r = \Delta G_a - \Delta G_d - q/p\Delta G_{xy} \quad (3)$$

$$A = -\frac{\Delta G_s}{\varepsilon \Delta G_r} = -\frac{\frac{\Delta G_{fa} - \Delta G_d}{\varepsilon^m} + \frac{\Delta G_{in} - \Delta G_{fa}}{\varepsilon^n} + \frac{\Delta G_{pc}}{\varepsilon}}{\varepsilon\,[\Delta G_a - \Delta G_d - q/p\Delta G_{xy}]} \quad (4)$$

$$f_s^o = \frac{1}{1+A} \quad (5)$$

$$f_e^0 + f_s^0 = 1 \quad (6)$$

$$Y_{c/c} = \frac{\gamma_d}{\gamma_x} f_s^o \quad (7)$$

$$Y_{c/mol} = \frac{\gamma_d}{\rho} f_s^o \quad (8)$$

Overall Reaction (R) = $f_s R_c + f_e R_a - R_d$ (9)

where all the Gibbs energy (kJ/eeq) expressed are at standard temperature (T=25^{o}C) and pressure (P=1atm), and 1M of reactants and products, except (H^+) =10^7, in which the superscript ^{01} is used.

Equation 1 means that the amount of biomass (X) generated via biosynthesis can be coupled to the amount of energy accessed from the substrate (S), wherewith some energy is lost in the process. McCarty describes the fraction of the available Gibbs energy as energy efficiency (ε). This is said to account only for energy captured for cell synthesis. In essence, only a fraction of the Gibbs energy generated from catabolism is used or accessible for microbial synthesis, while the rest is dissipated as heat. Furthermore, McCarty's method assumes that for synthesis to occur, the donor substrate follows a two-step reaction, in which the substrate is first converted to an intermediate compound (pyruvate or preferably acetyl Co-A) on a common metabolic pathway and a further conversion of the intermediate product to cells, as expressed with equation 2. The equation 3 represents the energy released from the oxidation-reduction half reactions of the ED and EA. The $q/p\Delta G_{xy}$ term in equation 3 accounts for action of oxygenases.

These oxygenases catalyse the reduction of a molecule of oxygen and further insert its oxidized form into the hydrocarbon molecule without using it as an electron acceptor. *p* is the number of electrons available in a donor substrate and *q* is the number of times the oxygenase reactions take place. $\Delta G_{xy} = -219.2 \frac{kJ}{molNADH}$ represents the difference between the reduction potential of oxygen and oxidation of NADH. It is the reduction potential energy for oxidation of 1 mole of NADH, 219.2kJ/mol.

Equations 1 to 3 can be mathematically represented with equation 4 and determine the amount of electrons used for cell synthesis. Equation 5 means that the amount of electrons used for cell synthesis cannot exceed the amount of electrons available in the substrate, hence the calculation of f_s^o enables the derivation of f_e^0. This equation is coupled to cell yield equations 6 & 7 by considering the degree of reductance of the donor substrate to that of the cells, and is expressed either as mol cell C/mol substrate carbon or mol cell C/mol substrate respectively [McCarty, 2006].

VanBriesen and Rittmann [2000a] do not agree to the concept that electron donors are the same as carbon donors, since the intermediate compound is the main source of carbon while the initial hydrocarbon is the primary electron donor. It is however agreed that when the biochemical pathway of the biodegradation reaction is unknown, or when the electron donor is known to be the carbon source for the reaction, a simplification can be achieved by assuming direct relationship between energy and carbon source, and energy generation and cell synthesis. A detailed overview of this method has been described in [VanBriesen, 2001, McCarty, 2006, VanBriesen and Rittmann 2000, VanBriesen and Rittmann 1999, Yuan and VanBriesen, 2002].

When the microbial yield is known, it enables the derivation of the microbial growth stoichiometry, which is a function of mass and energy balance between the substrate utilised and the generated products. Hence, the yield of products that is expected for a given reaction and in a defined contaminated fuel system can be estimated.

7.2.1.3 Kinetic Module for Predicting Biodegradation Rates

Microbial growth stoichiometry relates with the growth yield (Y) and gives a measure of the substrate utilised. Although, this is functional to understanding how much degradation is occurring; predicting biodegradation rates or fuel changes is unachievable without defined kinetic parameters. Thus, some aspects of microbial growth kinetics were introduced into the Bio-*f*AEG model. Microbial kinetics defines the rate at which degradation is occurring by associating the processes of cell growth, survival, death, product formation and their interactions with substrate utilization. It is a widely employed approach in biological waste water treatment processes and environmental applications [Henze et al. 1987, Henze et al. 1995, Billing and Dold, 1988, Button et al. 1981, Guha et al. 1999].

The kinetic parameters employed in this model follow the Monod and Herbert model [Herbert, 1958], which state that the growth and death of an organism follows a first order kinetics in relation to biomass concentration and in a mixed order with respect to substrate concentration [Henze et al. 1987, Henze et al. 1995, Panikov, 1961]. The essential parameters are the rate of substrate utilization and biomass formation at time (t).

According to Yassine et al. [2013], the substrate concentration at time (t) can be calculated below:

$$S_{tot} = S_{tot0} - \frac{kCXo}{(YkC - kd)}\left(e^{(YkC - kd)t} - 1\right) - k_{ab}S_{sat}t \qquad (10)$$

where $C=\frac{Ssat}{Ks+Ssat}$

$$Y = \frac{dX}{-dS} \qquad (11)$$

The equation 10 determines the amount of hydrocarbon loss per time. Using the microbial growth yield, a relationship can be drawn between the substrate concentration at time (t) and the biomass formed at time (t) per substrate as in equation 11. This indicates that there is clear opposite trend between biomass formed and substrate

utilised. In essence, cell growth yield is a function of the biomass formed and in correlation to the amount of substrate consumed.

Yassine et al. [2013] examined the aerobic degradation of poorly soluble organic materials (soybean biodiesel, and conventional diesel) using a novel mechanistic approach in which experimental measurements were coupled to mathematical simulated studies. Parameters from their study follow the Monod-Herbert model [Herbert, 1968] and provided a close estimate of kinetic parameters that are likely to be observed in a typical fuel system. Their approach is based on the assumptions that microbial reaction takes place in the dissolved phase. Dissolution kinetics is faster than biodegradation kinetics. Essential nutrients including oxygen are in excess and the fuel is the only limiting substrate. Since many hydrocarbons especially alkanes have low solubility, the term S_s is said to tend towards zero (0) thus $S_s \sim S_{sat.}$ This assumption is only valid within the limit of active degradation, where dissolved substrate is considerably lower than the bulk substrate or the non-aqueous phase liquids. S_{sat} is the aqueous saturation concentration of the individual substrate (mg/L).

In the Bio-*f*AEG model, the substrate is considered biodegradable according to the said relative inherent biodegradability factor (X_{IN}), where substrate refers to the concentration of the individual hydrocarbon component. The microbes have access to the substrate according to the said relative microbial accessibility factor (X_{ACC}) where biomass refers to the active cells taking part in a given reaction while the term bio-available fraction refers to the volume of fuel in aqueous solution that is taking part in the reaction and not the entire oil. It is also assumed that the oil is uniformly dispersed in the aqueous solution and dissolution kinetics is faster than that of biodegradation kinetics [Yassine et al. 2013]. And although, Yassine et al. [2013] assumes that microbial reaction takes place in the dissolved phase, the microbial accessibility factor assumes a limited solubility of hydrocarbons in aqueous solution with direct diffusion of oil to the microbial cell [Haeseler et al. 2010]. This contrasting term is somewhat applicable because the parameters adopted in Yassine et al. [2013] applied to alkane fractions of diesel fuels and the X_{ACC} considers degradation of other hydrocarbons in relation to the n-alkanes. In essence, highly accessible and degradable hydrocarbons are more degraded than less accessible and degradable hydrocarbons.

7.2.1.4 Fuel Analysis

The demonstration of the use of the Bio-*f*AEG is presented in Appendix II using Hexadecanoic acid. Four conventional diesel-type fuels—A, B, C, and D and a biodiesel-type fuel—E with parameters and constants as stated in Appendix II (Tables I-X) were also simulated using the Bio-*f*AEG model. The total hydrocarbon loss and the amounts of water required to initiate reaction were estimated and the results are presented in section 7.3. Furthermore, the degraded fuels were applied to simulated gas turbines by integrating the thermodynamic properties and gas compositions of diesel type fuel-A in the fuel library of the current version of Turbomatch (v2). This is to simulate 1-10% fuel degradation and to examine its effects on gas turbine performance (see section 7.4 for results). The method of integrating fuels has been discussed in a previous chapter (section 3.2.1) and validation for fuel integration is presented in Appendix II (figures 4.1 to 4.5). Furthermore, the approach used to estimate the blade metal temperatures, time to failure in hours, maintenance factor and relative maintenance cost is discussed in detail in Chapter 6.

7.3 Estimation of Hydrocarbon Loss and Water Requirements

The model results presented below are based on aerobic degradation (mono-oxygenase reaction) of simulated fuels with ΔG_{IN} value of 30.9 kJeeq^{-1}, ΔG_{PC} value of 18.8 kJeeq^{-1}, empirical formula of cells of $C_5H_7O_2N$, acetyl Co-A as the intermediate and ammonia as the nitrogen source. Here, it is assumed that reactions are taking place under constant growth and environmental conditions with no abiotic losses. It is generally conceptualized that the growth of microorganisms in gas turbine fuel systems could result in significant hydrocarbon loss with preferential removal of certain substrates and possible changes to fuel properties. Some insights can be provided from the results of this model.

7.3.1 Effect of microbial growth on hydrocarbon loss

Based on the above model description, the rate of removal of hydrocarbon substrates can be determined. Thus, for a given volume of fuel (36.6 m^3) with density of 0.820 kg L^{-1} for diesel type fuels and 0.920 kg L^{-1} for biodiesel type fuel, the model predicts an initial substrate utilization rate of the bioavailable fractions of 0.37 mg day^{-1}, 0.31 mg day^{-1}, 2.77 mg day^{-1}, 1.06 mg day^{-1} and 1.48 mg day^{-1} for fuels A-E respectively, which increased with doubling capacity and residence time of the organisms. These fractions of the degraded fuel represent 1.2 x10^{-6}%, 1.1 x10^{-6}%, 9.2 x10^{-6}%, 3.5 x10^{-6}% and 5.0 x10^{-}

[6]% of the total fuel A-E respectively. On further simulations (30 days), the total hydrocarbon loss of the bioavailable fraction for fuels A-E were 84.2 mg (24%), 65.6 mg (21%), 268.8 mg (86%), 221.9 mg (71%) and 313 mg (100%) respectively, equating to 0.001% of the entire oil. The results of degradation over 60 days are shown in figure 7.3. The model predicted a near complete degradation of these fuels between 20 and 60 days. These values are within the range stated by Mariano et al. [2008]. They reported the complete degradation of pure diesels and biodiesels of 26-68 days and 3-22 days respectively, with extended degradation of 72-120 days was observed for diesel fuels.

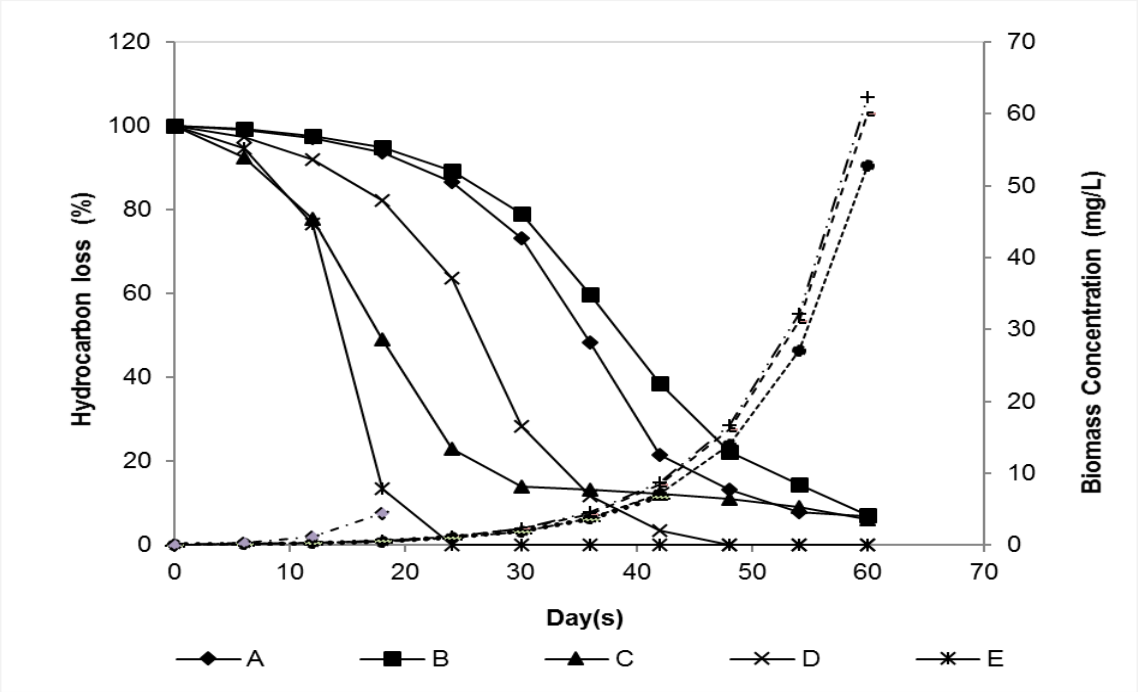

Figure 7.3: Aerobic biodegradation of diesel type fuels A, B, C, D and Biofuel type fuel E a) hydrocarbon loss over 0-60 day(s) b) biomass concentration over 0-60 day(s) [X_o=0.1mg/L: S_o=0.313mg/L]

There are many conflicting opinions on the rate of biodegradation in diesel and biodiesel fuels. In several aquatic environmental studies, the rates of degradation of biodiesel fuels were three fold higher than that of diesel fuels [Zhang et al. 1998]. Demirbas [2008] observed four-fold increase in biodegradability rates of biodiesels than conventional diesels. Their studies showed that within 30 days, a reference diesel fuel degraded by 24.5% while the counterpart biodiesel fuel degraded up to 91.2%. Studies by Tyson [1998] gave indication of degradation of 77-89% in biodiesels and 18% in diesels in 28 days. Previous work by Zhang et al. [1998] also showed similar trends with 18% and 84.4% degradation in reference diesel and biodiesels respectively. Also, blended fuels with higher concentrations of biodiesels showed higher biodegradability rates. This is

largely supported by Mariano et al. [2008], where enhanced synergistic degradation effects were observed in fuel blends. Other studies also support the above observations [Tyson, 1998, Passman and Dobranic, 1995, Pasqualino et al. 2006, Dodos et al. 2012].

However, contrasting to popular observations, Owsianiak et al. [2009] noted that such synergistic effects are only observed at biodiesel/diesel blends above 30% while DeMello [2007] observed similar degradation profiles for biodiesels and n-alkanes and more degradation for biodiesels than other hydrocarbon components.

For this analysis, the assigned inherent biodegradability factor (X_{IN}) and microbial accessibility factor (X_{ACC}) for biodiesel-type fuel were that of the n-alkane range assuming the biodegradability rates of n-alkanes and biodiesel-type fuels are the same. Results showed that the biodiesel-type fuel had the fastest rate of hydrocarbon loss with nearly 18 fold higher biomass concentration than conventional diesel fuels. This could be solely accounted to the narrow range of the fractions in the fuel being limited to methyl esters and wider spread of accessibility of substrate for microbial growth, as opposed to diesel type fuels which had wide range of fuel constituents and narrower accessibility of substrate for microbial growth.

Experimentally, examination of aerobic degradation of soybean biodiesel and conventional diesel fuel showed that there was a lag growth phase for microorganisms growing on diesel fuels while rapid growth with no lag phase was observed in FAME fuels [Yassine et al. 2013]. This can be theoretically attributed to the presence of two oxygen atoms at the hydrocarbon end of biodiesels that make it readily available for degradation. Unlike biodiesels, microbial growths in conventional diesels require a form of adaptation and enzymes such as mono-oxygenases to initiate biodegradation. This has been taken into account in the model using the biomass module, further explaining the wide differences in fuel types. Thus, the biodegradation rates among fuels A-E can be said to be a function of fuel composition, source and the percentage of the fuel constituents and would follow a sequence in accordance to their fractions of readily degradable hydrocarbons. Biodegradation rates have been shown to vary with the capabilities of different microorganisms. Nikhil et al. [2013] demonstrated biodegradation rates for different microorganisms, where 53% and 68% degradation was achieved by *Micrococcus* spp. and *Pseudomonas* spp. respectively and up to 89% when both organisms were used. Apart from the symbiotic relationships as described above or cases of co-metabolism, growth of multiple organisms on substrates could reduce

biodegradation rates significantly such as in parasitic or inhibiting conditions. This model has not taken into account the effects of co-metabolism, inhibition or competition; however, the microbial kinetic parameters could be further modified to define such conditions.

The microbial growth curve (figure 7.3) confirms the inverse relationship between biomass formation and substrate utilization. Using Fuel A as an illustration, the biomass concentration increased 20 fold within 30 days and 500 fold in 60 days. The doubling capacities of microbial populations are similar to the study by Olson et al. [2009], where a typical diesel fuel and its fractions are subjected to biodegradation by a microbial population extracted from diesel contaminated soil. Over a 35-day microbial batch culture, their biodegradation studies accounted for hydrocarbon loss of 91% (n-alkane loss of 63%, aromatic loss of 28%) and a doubling capacity of microbial population by 20-50 times the initial densities.

Preferential substrate degradation of the fuels is shown in figure 7.4. For instance, at day 60, the respective hydrocarbon loss for alkanes, aromatics, cyclic alkanes and polar fractions in Fuel A are 55%, 7%, 37% and 0.12% respectively. Preferential degradation is largely supported by Olson et al. [1999], where degradation of pure compounds was observed to be higher than their composite mixtures. It is also well agreed that during such active degradation, n-alkanes that are the most susceptible to biodegradation, constitute the largest portions of hydrocarbon loss. Olson et al. [1999] also observed that polar compounds originally thought to be non-degradable were utilised in the presence of other hydrocarbon compounds. For instance, the degradation of fluoranthene, which normally did not degrade alone, was degraded in the presence of naphthalene. Naphthalene degradation however was not enhanced in the presence or absence of fluoranthene, a phenomenon well explained with co-metabolism.

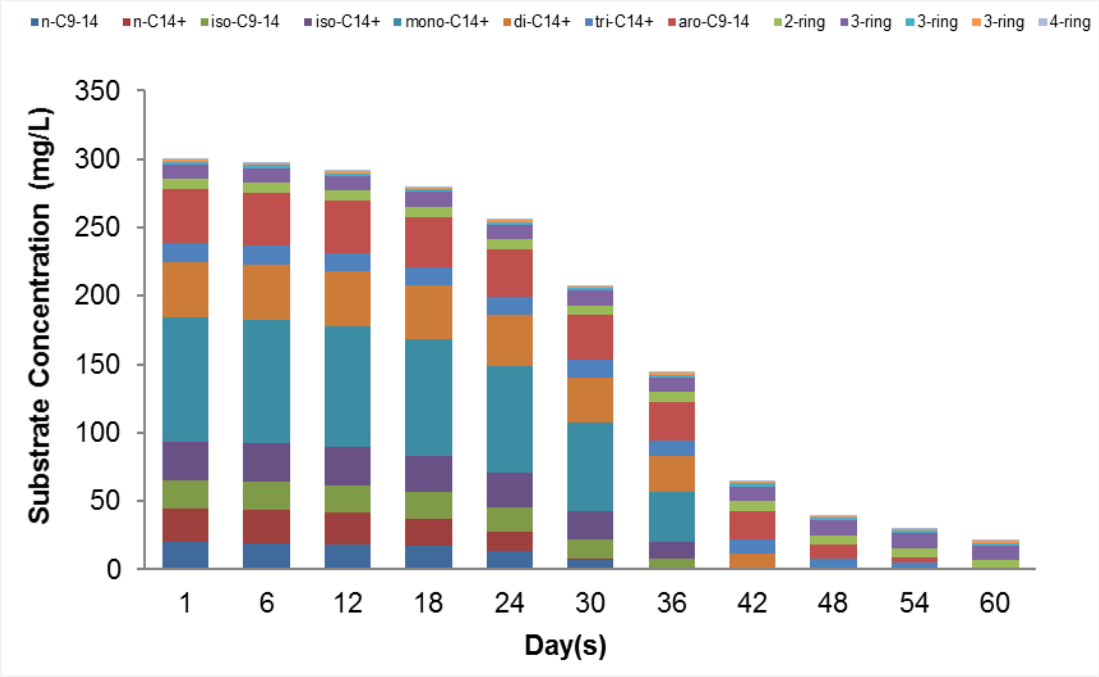

Figure 7.4: Total Hydrocarbon loss of diesel type fuel A over 0-60 day(s)

Many studies have also demonstrated that the active phase of diesel degradation is between 8-20 days [Demirbas, 2008, Olson et al. 1999, Mukherji et al. 2004], depending on the composition and type of the hydrocarbon fuel. Mukherji et al. [2004] showed that during the first 8 days of degradation, 80% were n-alkanes and 12.5% were aromatics. In this study, active degradation in Fuel A was extended up to 30 days. This could be attributed to the low initial microbial concentration; hence it was important to examine the effects of varying initial biomass concentration on hydrocarbon loss in the Bio-*f*AEG model.

7.3.2 Effect of residence time on hydrocarbon loss

The effects of microbial growth in gas turbine fuels and fuel systems are largely dependent on the residence time and degrading capabilities of the microorganisms as well as the fuel's abiotic conditions. The effect of residence time only was examined on Fuels A-E assuming that biodegradation reactions were not impeded and conditions for biodegradation remained constant. The model predicts that 81%-100% of the entire fuel will be affected in six (6) months as shown in figure 7.5. The hydrocarbon loss in fuels A, B and D appear to be significant from after the fourth month with total degradation range of 3.8-13.2% while that of fuels B and D are significant from the second and third months respectively. It is anticipated that visible effects of microbial growth in the engine fuel systems will precede this significant degradation process, as observed in many real

systems in the fuel filters. From these analyses, microbial populations of 1.54 g L^{-1}, 1.71 g L^{-1}, 1.70 g L^{-1}, 1.11 g L^{-1} and 1932 g L^{-1} are predicted in the third month for Fuels A-E respectively, all in the range of 10^8 - 10^{11} cfu ml^{-1}, assuming 1 ml of fuel-water contain 10^6 bacterial cells.

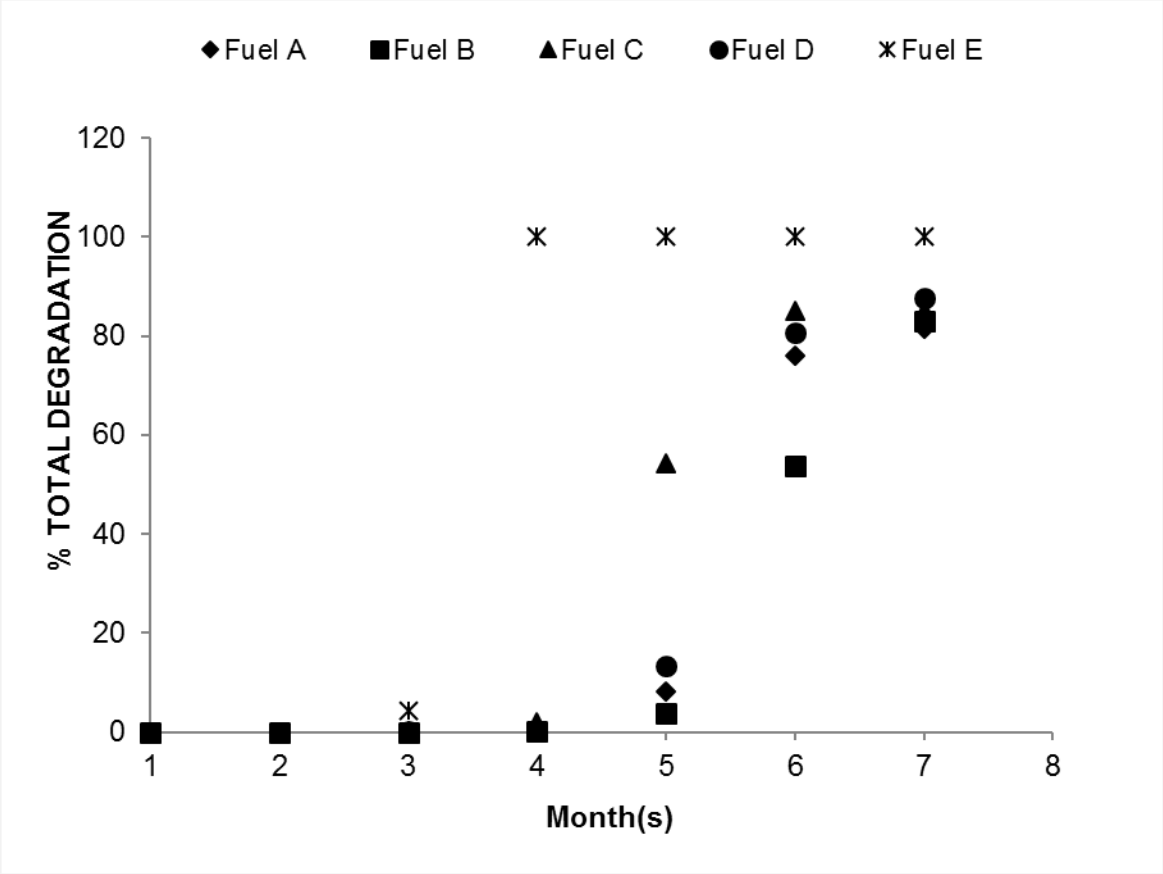

Figure 7.5: Effect of residence time on hydrocarbon loss

In a practical sense, the significance of these quantitative results is that for fuel systems that are in continuous operation, the effects of hydrocarbon loss might not be visibly evident in fuel properties. For instance, fuel quality such as density, composition and other fuel properties may not significantly change, however, accumulation of microbial biomass over time could induce secondary effects on the engine such as clogging of the fuel lines, injector soiling, induction of localized tank and metal corrosion, increased engine particulate matter emission and most importantly, damage to the fuel filter. The analyses carried out in this work are at conservative rates with low initial microbial population and minimal microbial kinetic rates, however with increased microbial populations and optimal microbial growth conditions such as availability of free water; degradation of fuel can be deleterious to engine health.

7.3.3 Estimation of water required to supply the essential TEA

It is a fundamental control strategy that free water should be removed from fuel storage systems to prevent microbial growth but there is currently no quantitative information on the minimum amount of water that could initiate such degradation reactions. Bio-*f*AEG was used to assess the volume of water sufficient to initiate microbial degradation for Fuels A-E with total volume of 36.6 m^3, assuming oxygen solubility of 10 mg L^{-1} at standard temperature and pressure. From the analysis, the volume of water required to supply oxygen concentration for initial biodegradation reactions (at time, t=1hr) for Fuels A-E are 0.97 L L^{-1} substrate, 0.82 L L^{-1} substrate, 7.38 L L^{-1} substrate, 2.75 L L^{-1} substrate and 3.16 L L^{-1} substrate respectively.

According to Siegert [2013] and Passman [2003], a standard diesel fuel is allowed to hold up to 0.1% of water. Robbins and Levy [2005] reported a ratio of hydrocarbon to water of 500-5000:1 in practical fuel tank system of 23 m^3. So, using the reported maximum allowable water content of 0.1%, the maximum volume of water acceptable for Fuels A-E in 36.6 m^3 fuel tanks in this analysis is 36.6 L while the volume of water possible in such typical fuel tank can range from 7.3 L to 73 L following Robbins and Levy's reported range. The analyses have illustrated that the maximum water acceptable in standard diesel fuels are more than sufficient to accommodate unlimited biodegradation reactions. According to Passman [2003], the volume of water normally recorded in fuel tanks is more than enough to accommodate trillions of bacterial populations, if a droplet with a diameter of 1.0 mm can hold millions of bacteria. Water could exist as suspended water; localized or widely dispersed within the fuel system as free water. It could be dissolved in the fuel, which could separate out of the fuel with temperature variance or settle on tank headspaces. It could be locked in microbial active biomass, as biofilms, of which 90% is water [Morton and Surman, 1994, McNamara et al. 2003]. Thus, there are wide sources of water available for microbial use.

7.3.4 Parametric Analysis

Quantitative information is sparse on fuel deterioration in gas turbine fuel systems. Most laboratory studies on the degradation of diesel fuels focus on wastewater management, soil and water bioremediation while studies on fuel deterioration are limited to identification and numeration studies. Hence, there is the hard challenge and uncertainties with modelling fuel deterioration in gas turbine fuel systems. Laboratory researches are required to focus on the microbial deterioration of fuels in gas turbine systems to provide sufficient data for comparison and model validation. Since, there is insignificant amount of published experimental data of microbial contamination in gas turbine fuel systems, the parameters used in this analysis was initial estimates or data derived from environmental systems, hence sensitivity analysis of key parameters was imperative.

7.3.4.1 Effects of initial biomass concentration on hydrocarbon loss

Biodegradation analysis of Fuel A for 7 days was carried out to examine the effects of initial biomass concentration on hydrocarbon loss in the Bio-*f*AEG model and the results are as illustrated in figure 7.6. Hydrocarbon loss for initial biomass concentration of 0.1-10 mg L^{-1} was quite insignificant within a 7 day period; however as the initial biomass concentration increased up to 100 mg L^{-1}, hydrocarbon loss increased by 30% and nearly 100% in two days for initial biomass concentration of 1000 mg L^{-1} (1 x 10^9 cfu ml^{-1}). This further corroborates the fact that significant hydrocarbon loss could occur in a contaminated fuel system with a large amount of microbial population, provided the environment conditions are suitable for growth. Corseuil and Weber [1994] showed the importance of initial microbial population in degradation, where 3.7 mg L^{-1} of xylene was degraded by a higher biomass concentration in 2.75 days while a lower biomass concentration utilised 2.15 mg L^{-1} and over extended days of 3.75 days. Degradation rates were 0.51mg L^{-1} per day for low biomass concentration and 1.35 mg L^{-1} per day for high biomass concentration [Corseuil and Weber, 1994].

Although, determination of biomass concentration or microbial population in fuel systems is not a standard requirement in the industry [Siegert 2013], it is generally accepted that fuel with biomass concentration of 10^4 cfu ml^{-1} is “clean”, provided the environment is not conducive for further growth. Hill and Hill [1993] highlighted that the average numbers of microbial population in slightly and highly contaminated fuels are 10^5 and 10^{6-8} cfu ml^{-1}.

Siegert [2013] classified low growth as $<10^2$ cfu ml^{-1}, slight growth as 10^2 -10^3 cfu ml^{-1}, moderate growth as 10^3-10^5 cfu ml^{-1} and massive growth as $>10^2$ cfu ml^{-1}.

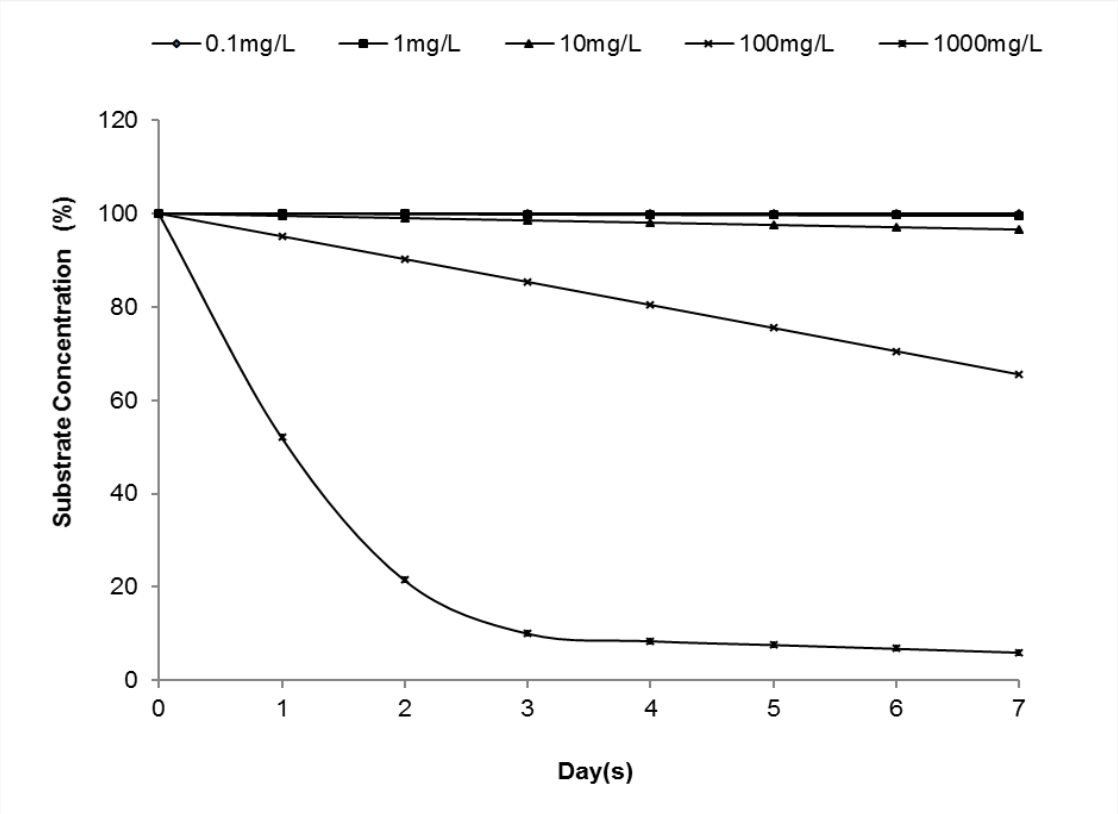

Figure 7.6: Aerobic biodegradation of diesel type fuel A at varying initial biomass concentrations

Generally, gas turbine fuels are thought to be “clean” and free of microbes once they have met the basic fuel requirement. Upstream processes such as filtration systems in the fuel delivering systems are conceived to have freed fuels from any microorganism, however, reports have consistently recorded growth of microorganisms in fuels. Rodríguez-Rodríguez et al. [2008] examined 12 refinery diesel and gas oil storage tanks for total bacterial counts and identified up to 149 bacterial strains in fuels. Microbial populations were isolated especially at the bottom of the tanks between 10^4 - 10^8 cfu ml^{-1}. Itah et al. [2009] carried out a microbial analysis in a typical aircraft tank and noted microbial count of $1.2x10^4$ - $2.2x10^4$ cfu ml^{-1}. Although within limits considered “clean”, opportunistic window and conditions promoting growth of microbes above 10^4 cfu ml^{-1} can constitute a hazard to the aircraft fuel systems especially relating to safety of aircraft, as incidentally experienced in a Nigerian aircraft and performance of the engine [Itah et al. 2009]. Hence, modelling the initial microbial population is key for good prediction and analysis. In the Bio-*f*AEG model, inputting the initial microbial population is user defined.

7.3.4.2 Effects of Specific Death Rate on hydrocarbon loss

Olson et al. [1999] observed reduction of biomass concentration after phase of degradation of 7 days and attributed this to reduction or depletion of readily degradable substrates. Other explanations include natural decay, accumulation of toxic materials, depletion of readily degradable substrate, and nutrient or oxygen limitation. This analysis assumed specific death rate of 0.008 h^{-1}, a value four fold higher than that stated in Yassine et al. [2013] but similar to Corseuil and Weber [1994] death rate value of 0.2 day^{-1} for aerobic microbial degradation of mono-aromatic hydrocarbons. The value of 0.008 h^{-1} was chosen on the basis that in a composite fuel such as diesel and in the presence of complex compounds, the death rate of any microbial specie could be much higher than expected or observed. In order to test the sensitivity of this value in the Bio-*f*AEG model, analysis at varying specific decay rates (0.002 - 0.008 h^{-1}) were carried out to examine its effect on hydrocarbon loss processes.

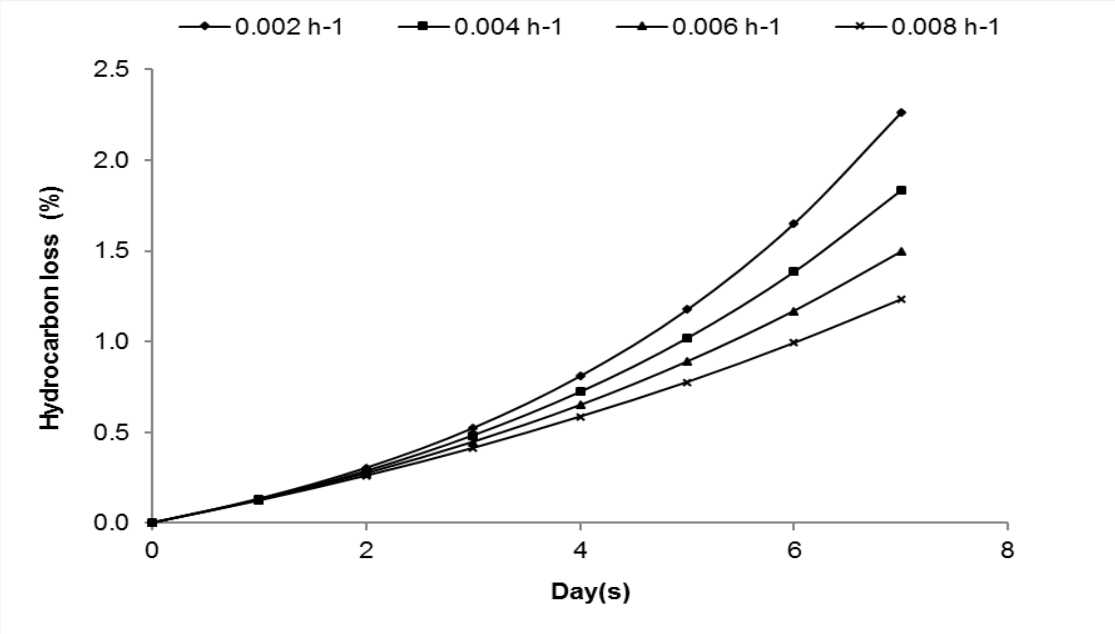

Figure 7.7: Aerobic biodegradation of diesel type fuel A at varying specific decay rates

More hydrocarbon loss was observed in systems with relatively low microbial death rate (0.002 h^{-1}) than those with higher values up to 0.008 h^{-1} (figure 7.7). This is an expected trend and can be explained to be the presence of more active cells participating in the degradation in a low microbial death rate situation than under strong decay rates. To put this information into the context of fuel biofouling, the results note that under microbial growth limiting or death promoting conditions such as the presence of biocides, or absence of nutrients, water or other major growth factors, hydrocarbon loss can be

reduced significantly. Hence, the processes of substrate inhibition can be integrated into the kinetic model or values of specific death rate adjusted by the user to define accurately the processes of natural decay, accumulation of toxic materials, depletion of readily degradable substrate, and nutrient or oxygen limitation.

7.3.4.3 Effects of microbial growth yield on hydrocarbon loss

It has been established that Y_{MAX} is the maximum growth yield achievable by a cell thermodynamically, when feeding on a specific substrate. In actual systems, these maximum values are not reached as a result of the cells requirement to repair damaged cells, or maintain cells in a harsh environment as found in hydrocarbon fuels, thus, $Y<Y_{MAX.}$ In this work, the range of for maximum growth yield is 0.76 for polyaromatics and up to 0.87 for n-alkanes. However, in the literature, there are wide ranges of yield reported for substrate degradation. Corseuil and Weber [1994] reported a cell yield of 0.65-0.67 for microbial degradation of benzene, toluene and xylene. Abuhamed et al. [2004] reported growth yield values of 0.65 - 1.2 g g^{-1}, 0.58 - 1.28 g g^{-1} and 0.44 - 0.8 g g^{-1} for microorganisms growing on benzene, toluene and phenol respectively. The effects of microbial growth yield on hydrocarbon loss were examined by considering a range of 0.8Y-1.0Y and the result are shown in figure 7.8.

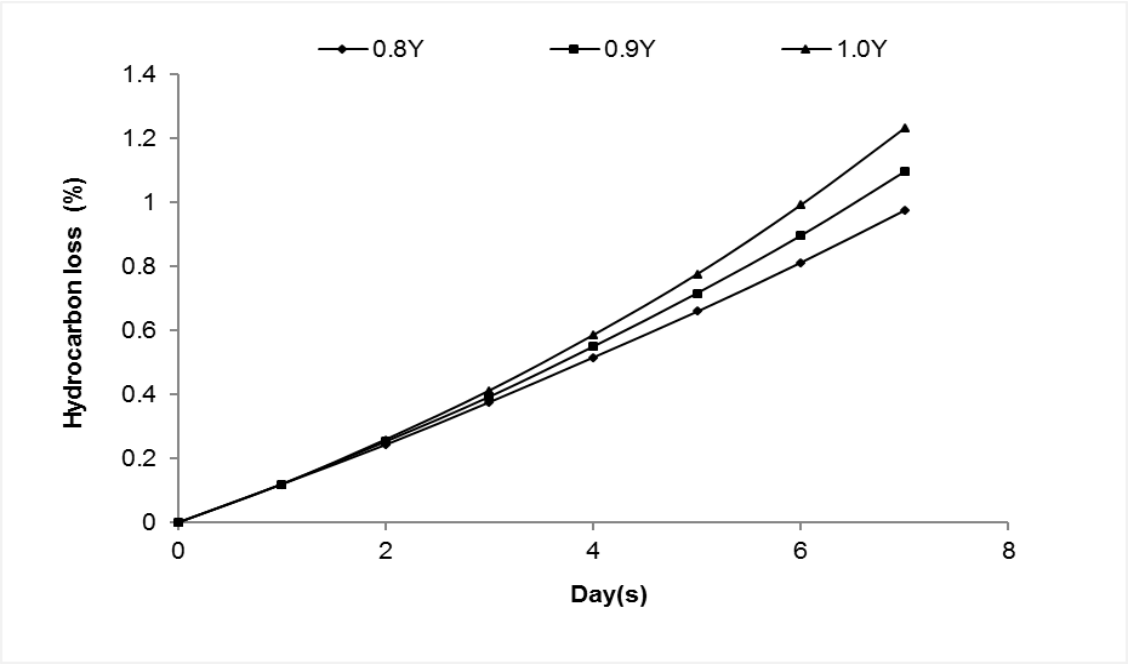

Figure 7.8: Aerobic biodegradation of diesel type fuel A at varying growth yields

In this analysis, the effect of microbial growth yield on the rate of hydrocarbon loss became prominent at increasing residence time of the organism. This can be theoretically explained that as the residence time of the organism increases, there are more cells produced, however, there is more demand for cell maintenance, repair or cell related process. Hence, part of the substrate is utilised for this purpose and fewer yields are achieved, consequently a less active cells are available for degradation of the substrates. This is a phenomenon is said to be well established in hydrocarbon fuel environment, as many toxic components are present and growth conditions are unstable. There could also be transition of ecological conditions forcing the microbes to maintain a stable cell biomass concentration rather than die-off. Therefore, it is necessary to model such a process of less cell yield by introducing a cell maintenance factor in the subsequent model modification.

7.3.4.4 Effect of energy transfer efficiency on cell yield and by-products of catabolism

With empirical formula of cells of $C_5H_7O_2N$, NH_4^+ as nitrogen source and aerobic degradation of Fuel A, the effects of energy transfer efficiency were observed on growth yield using a range of energy transfer efficiencies of 0.1 to 1.0. As energy transfer efficiency increased, there was a simultaneous increase in the yield of cells and decrease in CO_2 (figure 7.9). This result illustrates that cell synthesis, and consequently biomass accumulation, is a function of the cell's energy transfer efficiency. The contrasting patterns for yield of cells and CO_2 demonstrate the description of energy capture for cell synthesis [McCarty [2006]. McCarty [2006] stated a standard range of energy transfer efficiencies 0.2-0.3 for aerobic heterotrophs and 0.4-0.7 for anaerobic heterotrophs. Generally, an energy transfer efficiency value of 0.6 is used in environmental applications [McFarland and Sims, 1991]. For general application in Bio-*f*AEG, McCarty's optimum value of 0.37 applicable for either pure or mixed cultures of microorganisms is adopted to represent a slow biomass-producing aerobic growth system [Tyson, 1998].

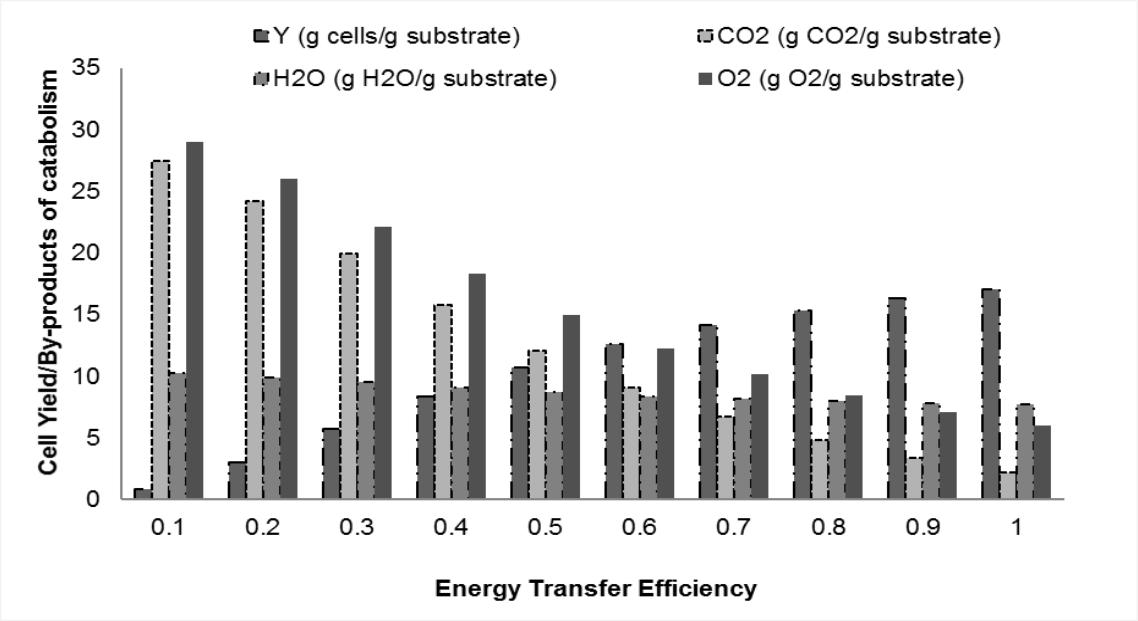

Figure 7.9: Effect of energy transfer efficiency on cell yield and by-products of catabolism

Also, using energy transfer efficiency, a classification can be drawn: efficient and inefficient microbial systems. A microbial system is considered inefficient if the substrate energy transfer efficiency is low and conversely efficient if the substrate energy transfer efficiency is considerably high. This phenomenon can be substantiated using von Stockar's theory on the driving force for microbial growth and its relationship with biomass yield [von Stocker et al. 2006]. In an efficient growth system, high biomass is observed because cell synthesis places high demand on energy transfer but growth is said to proceed at a relatively slow rate. This is because of the low overall driving force. Conversely for an inefficient growth system, small amount of biomass is produced, reaction is however said to proceed at a vigorous rate, thereby compensating for the inefficient system [von Stocker et al. 2006, Zhi-feng et al. 2007].

The implication of this result to hydrocarbon loss in fuel systems is that for highly efficient microbial systems such as anaerobes, where a large amount of biomass is produced at a relatively slow rate, there could be significant hydrocarbon loss and effect on fuel system in unmonitored/uncontrolled systems, as high levels of other by-products such as hydrogen sulphide, nitrogen and cellular metabolites are generated. In aerobic and other inefficient systems, where less amount of biomass is produced at a vigorous rate of growth, large amounts of by-products such as CO_2 are readily made available, and this could make the system more assessable to more microbial proliferation and co-metabolism.

7.3.4.5 Effect of different nitrogen sources on cell yield and by-products of catabolism

Apart from the fuel-bound nitrogen, which are relatively higher in heavy residual fuels and in minute fractions in jet fuels, there are other nitrogen sources in hydrocarbon fuels such as dead biomass, cell metabolites and fuel additives. Passman and Dobranic [2005] observed the presence of nitrate and nitrite in antimicrobial-treated samples after a week of inoculation. This is accounted to biocide partitioning in the aqueous phase. Comparing the yield estimates for microbial degradation of Fuel A under different nitrogen sources, assuming energy transfer efficiency of 0.37 and empirical formula of cells of $C_5H_7O_2N$, figure 7.10 shows that cell yield decreases in the order $NH_4^+ > N_2 > NO_2 > NO_3$ and this supports the fact that ammonium is the most preferred nitrogen source for cell synthesis [McCarty, 1965]. Using thermodynamic and energetic considerations, other nitrogen sources aside $NH4^+$ require additional electrons from the biochemical pathway to induce a reduction reaction. According to McCarty's estimation [McCarty, 1965], N_2, NO_2, NO_3 require an additional 3, 6, and 8 electrons respectively, thereby reducing the yield that could have resulted from investing electrons in the oxidized nitrogen compounds.

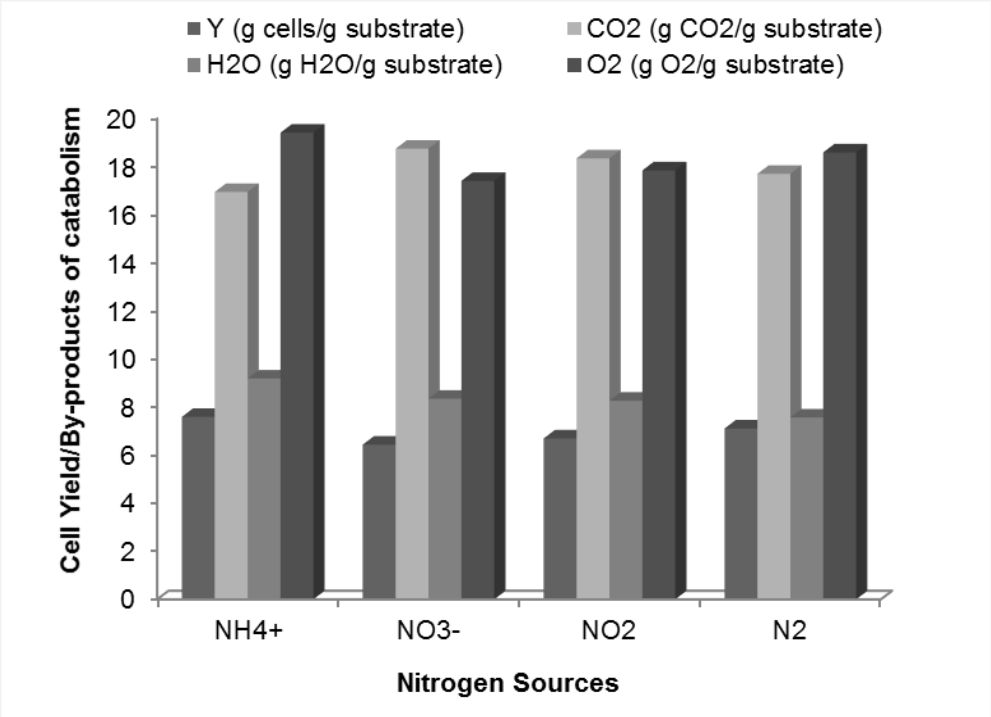

Figure 7.10: Effect of different nitrogen sources on cell yield and by-products of catabolism

7.4 Application of Bio-*f*AEG in simulating microbial fuel degradation in Gas Turbines

The diesel type fuel-A was degraded up to 10% using the Bio-*f*AEG model. The fuel composition of the 0% (clean diesel-type fuel), 1%, 5% and 10% degraded fuels are represented in Table 7.1.

Table 7.1: Fuel composition of the simulated diesel-type fuel

Fuel Composition	C	H	Clean Fuel* 0%	Simulated Degraded Fuels* 1%	5%	10%
Nonane	9	20	0.0363	0.0354	0.0313	0.0257
Dodecane	12	26	0.0300	0.0286	0.0221	0.0127
Hexadecane	16	34	0.0811	0.0799	0.0748	0.0679
3-methyldodecane	13	28	0.0695	0.0691	0.0673	0.0648
2,2,4,4,6,8,8-Heptamethylnonane	16	34	0.0960	0.0955	0.0932	0.0901
Butylcyclohexane	10	20	0.1223	0.1228	0.1251	0.1284
n-Dodecylcyclohexane	18	36	0.1800	0.1804	0.1824	0.1854
Decalin	10	18	0.1816	0.1832	0.1902	0.1999
1,2,4-Trimethylbenzene	9	12	0.1313	0.1325	0.1378	0.1452
Acenaphthene	12	10	0.0719	0.0726	0.0757	0.0799

*molar ratio

The gas compositions derived from these fuels using NASA CEA program are presented in Table 7.2.

Table 7.2: Fuel Parameters integrated in Turbomatch Model

Combustion Gas Composition	Clean Fuel 0%	Simulated Degraded Fuels 1%	5%	10%
Chemical Formula	$C_{12.75}H_{23.96}$	$C_{12.74}H_{23.91}$	$C_{12.69}H_{23.70}$	$C_{12.64}H_{23.41}$
N_2 (%)	73.108	73.167	73.188	73.204
Ar (%)	0.877	0.878	0.878	0.878
H_2O (%)	12.350	12.347	12.295	12.220
CO_2 (%)	13.072	13.238	13.270	13.315
CO, O_2, Ne (%)	0.000	0.000	0.000	0.000
F.A.R_{STOIC} (%)	0.06877	0.06879	0.06886	0.06897
AIR_{STOIC} (%)	84.257	84.235	84.142	84.010
Energy Content (LHV) kcal/kg	10217.8	10115.1	9706.7	9195.6

These gas compositions were integrated in the fuel library of the current version of Turbomatch (v2) to carry out a comparative performance analysis on the simulated GX100 at design point, ISA SLS conditions. The deviations in EGT are shown in figure 7.11 while the effects of fuel degradation on thermal efficiency (%) and heat rate (kJ/kWh) are presented in figure 7.12.

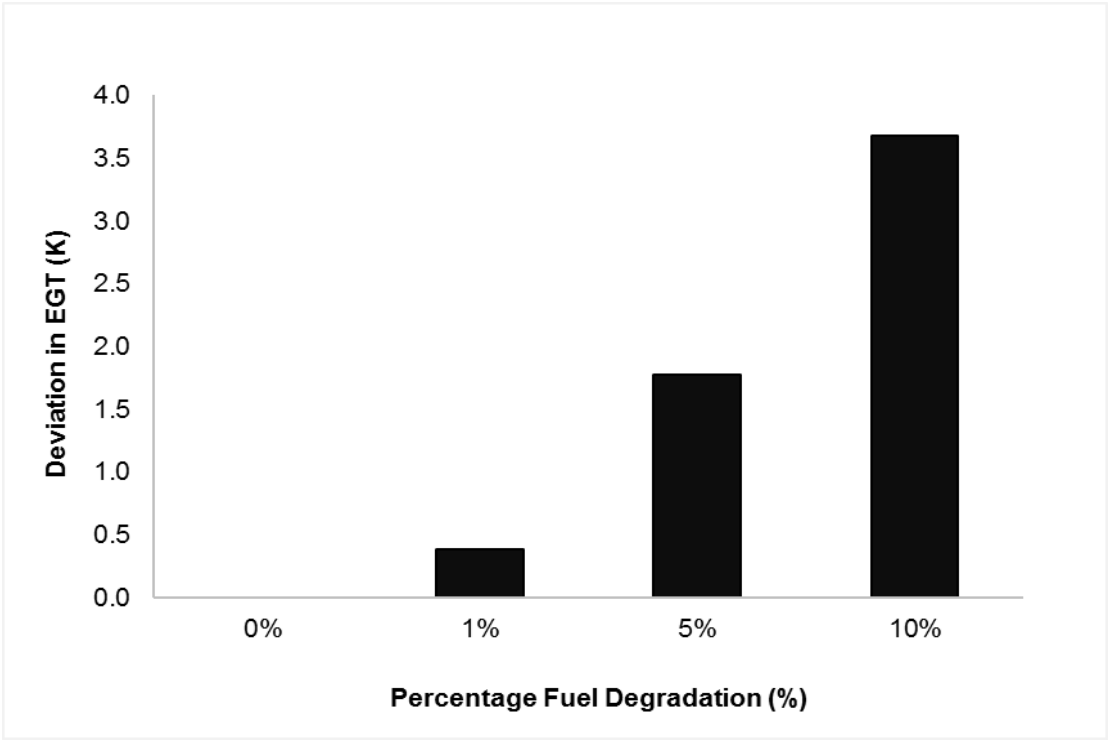

Figure 7.11: Deviation in EGTs (^{o}C) for the different grades of fuels

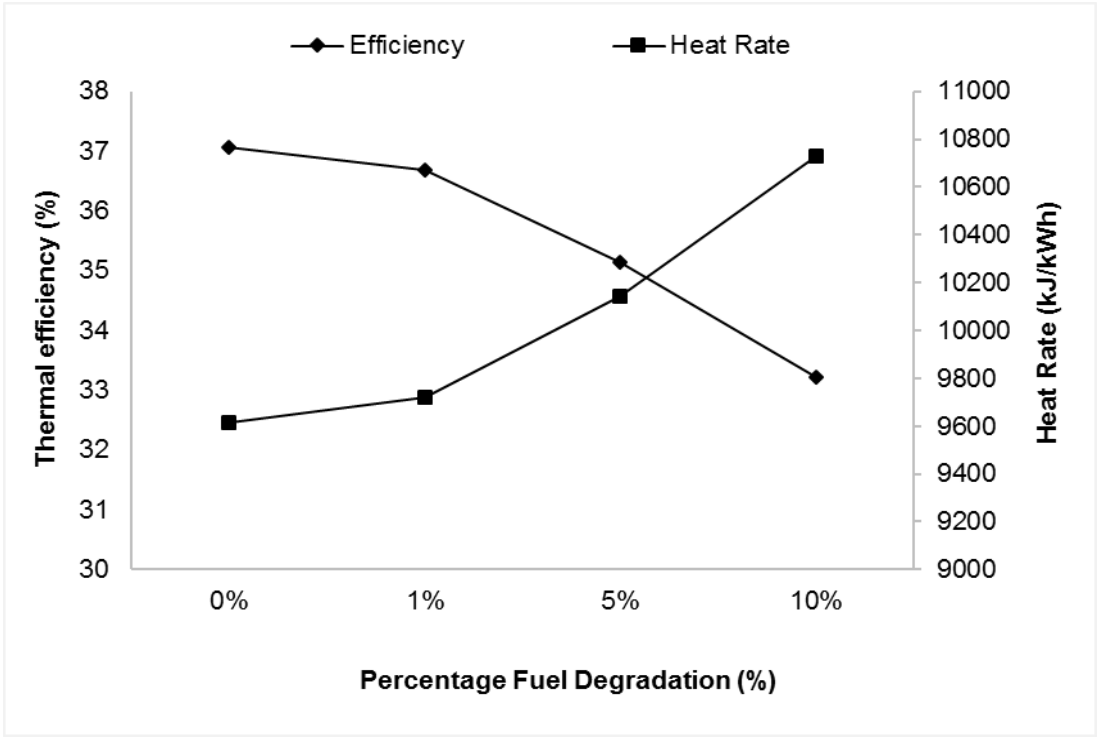

Figure 7.12: The effect on thermal efficiency (%) and heat rate (kJ/kWh) for the different grades of fuels

From the chemical composition in Table 7.1, it can be observed that there is loss of hydrocarbon fractions at each level of degradation, except with the clean fuel and at progressive rates. A decreasing trend in hydrogen-to-carbon ratio, with a range of values of 1.88 (clean) to 1.85 (10% degraded fuel) and a slight increasing trend in carbon-to-hydrogen ratio of 0.53 (clean) to 0.54 (10% degraded fuel) can be observed. This resulted in reduced water vapour but increased CO_2 concentration (see Table 7.2). These differences are due to the decreasing fractions of the fuels and the effects on performance parameters for engine, GX200 include: a) reduced thermal efficiency, b) increased heat rate, c) increased EGT.

The EGT, a parameter that depends on the engine firing temperature, increased by 0.4°C, 1.8°C and 3.7°C for engine operating on 1%, 5% and 10% degraded fuels respectively (figure 7.11). The increasing EGTs were complemented by lower thermal efficiencies and higher heat rates. Thermal efficiency of the simulated engine reduced significantly by 1%, 5% and 10% for 1%, 5% and 10% degraded fuels respectively. And since heat rate and thermal efficiency have an inverse proportional relationship, analysis shows that heat rate also increased by 1%, 5.5%, and 11.6% for engine using 1%, 5% and 10% degraded fuels respectively.

Thermal efficiency is of importance to an operator as it relates directly to specific fuel consumption of the engine. Any loss in thermal efficiencies reduces the amount of power that could be generated from the same volume of fuel. Heat rate on the other hand, is an integral parameter to gas turbine users because, it defines how efficient and cost effective a plant operates and in comparison with others. In other to reduce cost, gas turbine power plant operators pay attention to means to improve thermal efficiency, consequently, reduced heat rate of engines. Also, since fuel cost may account for over two-third of the operator's annual operational cost [Kurz et al. 2012] and in some cases, up to 90% of total operational cost; a reduction of fuel consumption by 1% is a great progress in ensuring that heat rate is significantly improved.

The EGT on the other hand is an indication of the amount of heat emitted in the exhaust system into the surroundings. Since, it is impractical to measure the firing temperature of an engine, the EGT is usually used to denote the deviations in firing temperature and engine health, therefore any increase in the EGT is an indication of deteriorating health condition and performance capacity reduction of an engine. This analysis has demonstrated an increase in EGT by nearly 4^{o}C for the engine operating on 10%

degraded fuel. Although, this value is not as much as those obtained from other degradation effects [Meher-homji and Gabrilles, 1998], it could initiate a non-uniform temperature profile along the rotor metal blades, reduce the life of hot end components and durability of the engine. Meher-homji and Gabrilles, [1998] described a scenario of an engine failure that resulted from the accumulation of heavy fuel deposits on the third stage turbine blades. This caused non-uniformity of temperature on the metal blades, thereby leading to blade fatigue failure. This effects were observed from the deviations in the EGT that increased from 500°C to 730°C.According to Cao [2010], an increase by every 10°C to 15°C rise in metal temperature can reduce blade creep life by 50%.

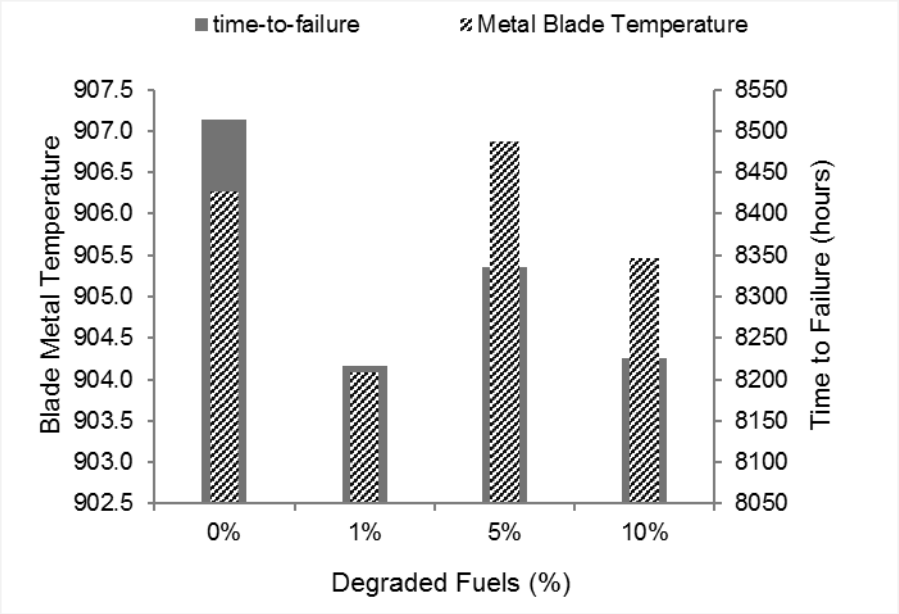

Figure 7.13: Relative effect of degraded fuels on Blade Metal Temperature and Time to Failure (hours)

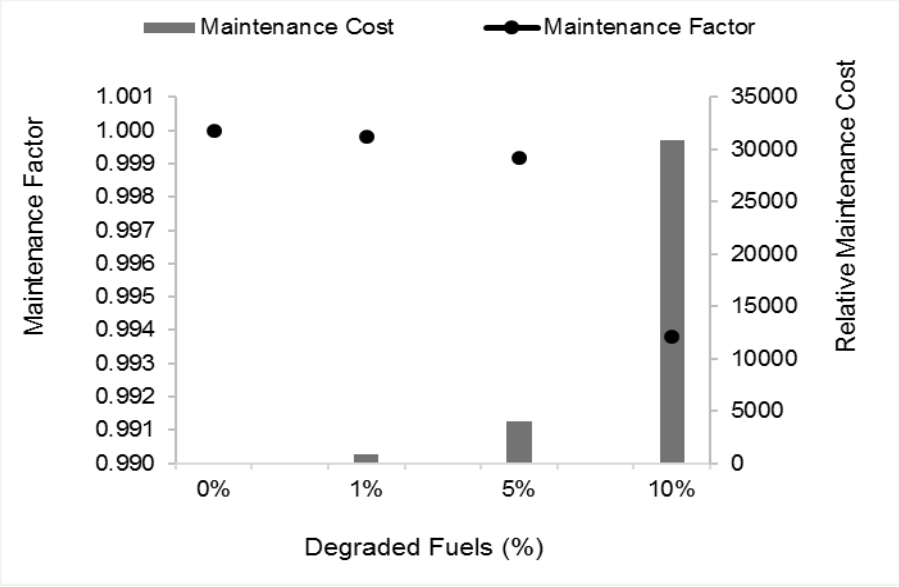

Figure 7.14: Relative effect of degraded fuels on Maintenance Factor and Cost

Further fuel degradation analysis carried out to estimate the blade metal temperatures, time to failure in hours and relative maintenance cost resulting from 10% fuel microbial degradation shows that there was an increase in blade metal temperatures by 1°C and an equivalent impact on blade life, also by 1%. Furthermore, the maintenance factor, which is in comparison to the reference point (clean state) reduced to the greatest extent when degradation was up to 10% and consequently, the annual variable maintenance costs increased by over $30000 (figures 7.13-7.14).

In order words, the impact of fuel degradation on engine performance can be explained with the turbine power output equation, where power output is a function of specific heat capacity, temperature difference across the turbine and gas mass flow—a parameter that includes both fuel and air mass flow. The 10% degraded fuel brought about a lower thermal efficiency and worse heat rate than the clean fuel because of its relatively lower LHV, even though the specific power was higher. The relatively lower LHV forces the fuel control system to increase the fuel flow rates to compensate for the energy loss in the system, and this reduces the thermal efficiency and increases the heat rate of the engine. This is worsened by the slight reduction of H/C ratio of the fuels, hence reduced water vapour concentration. The increased C/H ratio with consequential increase in CO_2 concentration was however insufficient to improve engine performance. The increased fuel flow rates as in the case of the degraded fuels could have an impact on engine health, as it moves the engine running line towards higher pressure ratios, and firing temperature, thereby reducing the surge margin for the gas turbine compressor -see figure 4.6 in Appendix II. Hence, typical flat rated units adapt fuel control systems to maintain firing temperature, compensate any loss in turbine efficiency and recover lost engine performance.

In typical engines, microbial degradation of fuels within the system is a salient energy conversion process that could affect engine performance significantly depending on the mode of deterioration. Based on the complex mechanisms of microbial degradation of hydrocarbon fuels described in section 7.1.2., the growth of microorganisms in fuels could result in accumulation of biomass and hydrocarbon loss with/without significant changes to fuel's chemical composition and properties, especially those affecting fuel combustion performance parameters, such as fuel density, calorific value and viscosity. The biomass accumulated could settle at the base of the tank or get suspended in the fuel, and deposited along the fuel systems or hot end components of the turbine. The irreversible loss of energy could bring about secondary effects such as filter clogging and

increased particulate formation. This analysis has simulated a case of degradation of fuels resulting in LHV of fuels and changes to fuel chemistry. Hence, the engine performance results would be similar to burning a LHV of fuels with added effects of hydrocarbon loss.

Microbial characteristic is a critical factor that affects the fuel degradation rates and hydrocarbon loss. The loss of lighter fractions would increase the heavier fractions of the fuel and this result in increased C/H ratio, as shown in section 7.4. Also, the relative density of the fuels reduces slightly when compared to the clean state and there is a likelihood that viscous and volatile properties of the fuel change over time. The loss of hydrocarbon could be reversal that is loss of heavy fractions to increase the lighter fractions of the fuel and this result in increased H/C ratio. This is often not the case due to preferential microbial degradation of the lighter fractions of fuel components.

Microbial fuel degradation is also time dependent as shown in figure 7.5, and to achieve 10% degradation (loss of hydrocarbon and reduced LHV) as modelled in this study, this would require a neglect of good fuel handling practices, the absence of control measures such as biocide application, elimination of water and routine fuel tank inspection, such that the microbes proliferate in the fuel systems. This analysis suggests that if such conditions exist during the operation of a power plant and biodegradation rates remained constant and unlimited, 10% degradation could be achieved within three months in Fuel A (figure 7.5). This could be worsened in the presence of a mixed culture of organisms that are capable of degrading a number of substrates at the same time by a co-metabolism phenomenon, in which one organism degrades a compound and makes it readily available for further degradation by another organism. Also, a degraded substrate could become a precursor for degradation of another compound. In essence, degradation is achieved in a relatively short period of time with mixed culture and in days as related by figure 7.6. This is opposite to pure cultures where one or more compounds are degraded over time.

Nearly all hydrocarbon fuels are susceptible to microbial degradation, although in varying degrees and depending on the availability of nutrients, terminal electron acceptors, and environmental conditions, particularly, temperature. Microbial fuel degradation is also preferential as mentioned above and depends on the molecular weight, structure of hydrocarbon bonds and the presence of readily accessible functional groups in hydrocarbon fuels, such that low molecular weight compounds and straight chain

hydrocarbons are more readily assessed than high molecular weight and polyaromatic compounds [Xiao and VanBriesen, 2006, Xiao and VanBriesen, 2008]. Therefore, microbial fuel degradation analyses are more important for biofuels, including biodiesels because of their readily available organic content and high hygroscopic nature. This is only achievable after the limitation of the current model has been addressed in further work.

7.5 Performance of Degraded Fuels on Engine at Part Load

Analysis carried out at varying loads show that heat rate increased significantly nearly by 28% and thermal efficiency reduced by 21% at part load of 41% at all fuel conditions (figure 7.15).

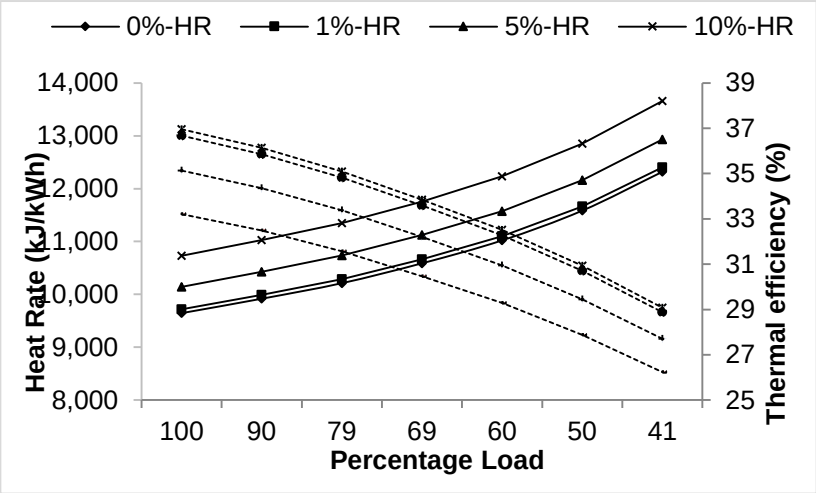

[11]*Figure 7.15: Heat rate and thermal efficiency at different load and fuel grades.*

With the use of 10% degraded fuel, thermal efficiency was at 26% rather than at 29%, as the case for the clean fuel. These results imply that combusting less energy containing fuels as in the case of degraded fuels means the engine is operating at lower thermal efficiency, higher heat rate and at relatively higher EGT. And at part load operations, these effects are more compounded.

[11] HR- Heat Rate, TE-Thermal Efficiency

7.6 Performance of Degraded Fuels on Engine at Varying Ambient Temperatures

Comparing the engine with clean fuel and 10% degraded fuel, the results in Figure 10 imply that the loss of efficiency due to fuel degradation can be compensated slightly on a relatively cold day. This means that if an engine is located in a warm climate with average ambient temperature of 34.5^{o}C, the use of a clean diesel fuel on engine GT500 would bring about a thermal efficiency of about 35%, while the use of the 10% degraded fuel would result in thermal efficiency of about 30%. On a relatively cold day (14.5^{o}C), the effect of 10% degraded fuel would be less observed with thermal efficiency of 33%. This is due to the effect of ambient temperature on engine performance as mentioned in section 3.1. Opposite trends are observed with heat rate. The engine heat rate improves at lower temperatures; hence reduced performance that is brought about by fuel degradation might be compensated slightly by the effect of lower ambient temperatures. The above results lay emphasis on engine monitoring and control of microbial fuel degradation, especially in locations with warm climate, where microbial growth and reactions are rapid and the impact on engine performance are more observed.

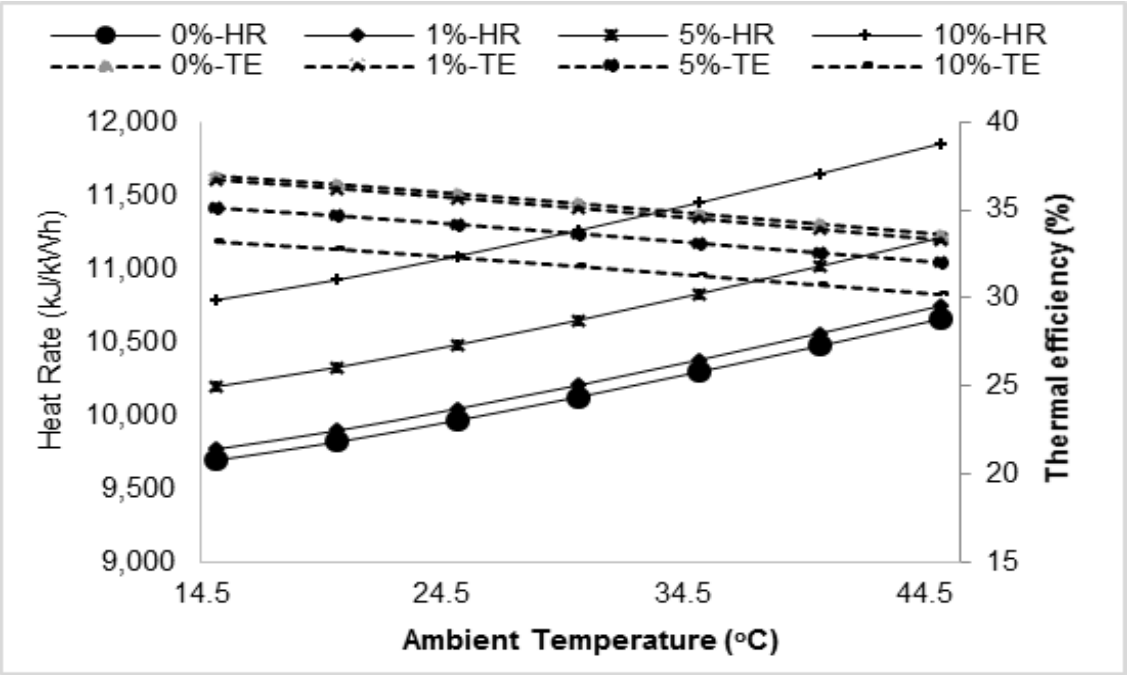

[11]*Figure 7.16: Heat rate and thermal efficiency of engine GT500 at varying loads at ambient temperatures with 0-10% degraded fuels.*

7.7 Conclusion

A bio-mathematical model, Bio-*f*AEG was developed to simulate degraded fuels, predict biodegradation rates, estimate hydrocarbon loss and calculate the amount of water required to initiate degradation under aerobic conditions. The degraded fuels were integrated in the fuel library of the current version of Turbomatch (v2) to carry out comparative performance analysis on the simulated GX100 at design point. A summary is provided below:

1. The model has demonstrated that fuel hydrocarbon loss and biodegradation rates are a function of fuel characteristics, nutrients and water availability as well as, microbial degrading capabilities, microbial load, and residence time of the organism. However, caution is required with the underlying assumptions.
2. The biodiesel-type fuel had the fastest rate of hydrocarbon loss with nearly 18 fold higher biomass concentration than conventional diesel fuels, assuming that the biodegradability rates of n-alkanes and biodiesel-type fuels are the same.
3. The maximum water acceptable in standard diesel fuels is more than sufficient to initiate unlimited biodegradation reactions.
4. Microbial degradation of fuel of up to 10% and corresponding to loss of hydrocarbons and reduced LHV could increase the engine heat rate by nearly 12% and reduce thermal efficiency by 10%. The engine health is also at the risk because EGT increases by nearly 4^{o}C, with the tendency of a reduced surge margin for the gas turbine compressor.
5. The study implies that the hydrocarbon and energy loss due to microbial fuel degradation is at a cost to the plant operator. Although, the energy loss has not been destroyed and still contained in the fuel, it has been transformed into biomass and is ultimately flushed out as waste during cleaning and maintenance. Additional maintenance cost arises as a result of these and from secondary effects on hot end components of the turbine such as turbine blade. This study estimates an additional maintenance cost of about $30,000.
6. The Bio-fAEG model has taken into account the biological processes of substrate utilization and microbial growth formation, using fundamental concepts of mass and energy balance, thermodynamics, bioenergetics and microbial kinetics, to estimate hydrocarbon loss and fuel degradation. This is the first time gas turbine bio-fouling assessment model is being developed. It has provided a platform to simulate microbial

fuel degradation in gas turbines when integrated with appropriate engine simulation software(s). This is an initial step towards predictive condition monitoring of microbial fuel degradation in gas turbines.

7.8 Further Work

Many data generated from the Bio-fAEG tool were in agreement with several cited work, however, this model is not a one-size fit all for degradation of fuels in gas turbines. The model has not taken into account the effect of abiotic losses of fuel components, abiotic factors such as temperature, pH presence of inhibitory fuel components and other ecological conditions such as sulphate reducing and nitrate reducing conditions. The microbial kinetic parameters have not considered the effects of multi-capability of microorganisms to utilise a single or multiple substrate, cell maintenance, a significant cell requirement in harsh environment such as in hydrocarbon fuels, or the effects of co-utilization of substrates by multiple organisms. Hence, further development should aim at reducing these limitations. Furthermore, the assumptions in each of the sub-modules in the Bio-*f*AEG model have been selected to enable a simplified representation of the complex biological processes occurring in the fuel system. It would be important to verify the underlying assumptions and data by carrying out mechanistic experiments for accurate description of practical systems. For instance, biomass cells do not attain their theoretical cell yield in actual systems due to presence of other organisms that compete, inhibit or initiate other processes etc. This could be further examined. Also, data for parameters such as microbial empirical formula of cells, energy transfer efficiency are not available for research in gas turbine fuels and systems; hence research could continue to examine the critical elements in this model.

It would also be interesting to extend this aspect of the work to biodiesels, since they are relatively more degradable than diesel fuels. This model has considered only aerobic conditions and monooxygenase mode of degradation; however it would be important to examine the impact of fuel degradation under various biodegradation conditions and mechanisms. It is likewise important to examine how the economics of fuel degradation could affect future application of biofuels in gas turbines, emission tax policies, fuel handling practices and management as well as other legislation scenarios. The components of fuels, especially middle distillate fuels are very large. Although, there are current work in developing surrogate fuels for experimental analysis. These studies have excluded factors such as biodegradation rates. And since, the least degradable substance might become susceptible to degradation due to co-metabolizing organisms, it would be important to further develop surrogate fuels for these types of microbial studies. Other considerable aspect of this work include the examination of the effects of fuel

degradation on gas turbine emissions, especially smoke, soot and particulate matter; evaluation of fuel deposition on fuel injectors, coking of combustor, and other secondary effects that are microbial-initiated processes. The model can be further developed by integrating advanced microbial kinetics, fuel chemical kinetics with advanced platforms for engine performance and emission analysis and predictive condition monitoring.

7.9 References

[1] Kurz, R. and Brun, K. 2001. Degradation in gas turbine systems. *Journal of Engineering for Gas Turbines and Power* 123(1): 70-77.

[2] Doering, H. von E. and Vincent. J. A. 1972. Manual on Requirements, Handling, and Quality Control of Gas Turbine Fuel". ASTM Publication 531. Florida, USA.

[3] Passman, F. 2003. Fuel and Fuel System Microbiology: Fundamentals, Diagnosis, and Contamination Control. ASTM International, PA, USA.

[4] Giles, H. N. 2003. "Methods for Assessing Stability and Cleanliness of Liquid Fuels". In Rand, S. J. (7^{th} ed.) Significance of tests for Petroleum products, pp. 108–118. ASTM International, West Conshohocken, PA

[5] Thaysen, A. C. 1939. On the gas evolution in petrol storage-tanks caused by the activity of micro-organisms". *J. Inst. Petroleum Tech*. 25: 411-415.

[6] Hill, E. C. and Hill, G. C. 2008. Microbial Contamination and Associated Corrosion in Fuels, during Storage, Distribution and Use. *Advanced Materials Research* 38: 257-268

[7] Brooks, D. B., 1963. "Military Research on jet fuel contamination. Paper presented at a session on Fuels during the 28th Midyear meeting of the American Petroleum Institute Division of Refining, in the Benjamin Franklin Hotel, Philadelphia, Pennsylvania. FL 225/23

[8] Wilkes. C. E., Iverson, W. P., Cockey, R. R., and Hodge. H. M., 1963. "Microbial Contamination of Air Force Petroleum Products". Technical Report APL-TDR-64-95, 1-53. Aero Propulsion Laboratory Research, and Technology Division, Wright-Patterson Air Force Base, Ohio, USA.

[9] London, S. A., Finefrock, V. H., and Killian, L. N. 1965. "Microbial Activity in Air Force jet fuel systems". Technical Report AFAPL-TR-66-91, 1-154. Aero Propulsion Laboratory Research, Wright-Patterson Air Force Base, Ohio, USA.

[10] Finefrock, V.H., and London, S.A., 1966. Microbial contamination of USAF JP-4 Fuels. Technical Report AFAPL-TR-66-91. Aero Propulsion Laboratory Research, Wright-Patterson Air Force Base, Ohio, USA.

[11] London, S. A., 1974. Microbiological evaluation of aviation fuel storage, dispensing and aircraft systems. Technical Report AFAPL-TR-74-144. Aerospace Medical Research Laboratory, Wright-Patterson Air Force Base, Ohio USA.

[12] Pitcher, D.G. 1989. Industrial case histories of microbiological fuel contamination - cause, effect and treatment. *International Biodeterioration* 25 (1-3): 207-218

[13] Hill, T. 2003. Microbial growth in aviation fuel. *Aircraft Engineering and Aerospace Technology* 75(5): 497 – 502.

[14] Rauch, M.E., Graft, H.W., Rozenzhak, S.M., Jones, S.E., Bleckmann, C.A., Kruger, R.L., Naik, R.R. and Stone, M.O. 2006. Characterization of microbial contamination in United States Air Force aviation fuel tanks. *J. Ind. Microbiol. Biotechnol*. 33: 29–36

[15] Rogers, M.R. and Kaplan, A.M., 1963. A field survey of the microbiological contamination present in JP-4 fuel and 115/145 AVGAS in a military fuel distribution system. AD410519. Defense Documentation Center for Scientific and Technical Information, Alexandria. Virginia, USA.

[17] Roffey, R. 1989. Microbial problems during long-term storage of petroleum products underground in rock caverns. International Biodeterioration 25(1–3): 219-236.

[18] Hill, E.C. and Hill, G.C. 1993. Microbiological problems in distillate fuels. Trans. Inst. Marine Eng. 104: 119-130

[19] Gaylarde, C.C., Bento, F.M. and Kelley, J. 1999. Microbial contamination of stored hydrocarbon fuels and its control. Revista de Microbiologia 30: 1-10

[20] Battersby, N. S., Stewart, D. J. and Sharma, A. P. 1985. Microbiological problems in the offshore oil and gas industries. Journal of Applied Microbiology 59: 227S-235S.

[21] Passman, F.J., McFarland, B.L. and Hillyer, M.J. 2001. Oxygenated gasoline biodeterioration and its control in laboratory microcosms. International Biodeterioration and Biodegradation 47(2): 95-106.

[22] Soares, C. 2008. Gas turbines: A Handbook of Air, Land and Sea applications. Amsterdam: Butterworth-Heinemann. London: Elsevier Inc.

[23] Lee, J.S., Ray, R.I. and Little, B.J., 2006. Microbiologically Influenced Corrosion in Military Environments. *In* ASM Handbook 13C, 211-219. ASM International, USA.

[24] Kirchman, D. and Mitchell, R. 1981. A Biochemical Mechanism for Marine Biofouling. Oceans 81: 537-541.

[25] Stuart, R. A., 1995. Microbial attack on ships and their equipment. Lloyd's Register Technical Association Paper No. 4, Session 1994-95. London.

[26] Melo, L.F. and Bott, T.R. 1997. Biofouling in water systems. *Experimental Thermal and Fluid Science* 14(4): 375-381.

[27] Lee, J.S., Ray, R.I. and Little, B.J. 2010. An assessment of alternative diesel fuels: microbiological contamination and corrosion under storage conditions. *Bio-fouling* 26(6): 623-635.

[28] Sand, W. 1997. Microbial mechanisms of deterioration of inorganic substrates- a general mechanistic overview". *International Biodeterioration and Biodegradation*, 40(2-4):183-190.

[29] McNamara, C. J., Perry, T. D., Wolf, N., Mitchell, R., Leard, R. and Dante, J. 2003. Corrosion of aluminium alloy 2024 by jet fuel degrading microorganisms." Paper No 51300-03568-SG. Presented at Corrosion 2003.

[30] Shekhawat, D., Berry, D.A., Haynes, D.J. and Spivey, J.J. 2009. Fuel constituent effects on fuel reforming properties for fuel cell applications. *Fuel* 88(5): 817-825.

[31] Das, N. and Chandran, P. 2011. Microbial Degradation of Petroleum Hydrocarbon Contaminants: An Overview. *Biotechnology Research Internationa*l Article ID 941810, 13 pages. doi:10.4061/2011/941810

[32] Okoh, A.I. 2006. Biodegradation alternative in the clean-up of petroleum hydrocarbon pollutants". *Biotechnology and Molecular Biology Review* 1(2): 38–50.

[33] Passmann, F.J., and McFarland, B.F. 1997. Understanding, recognizing, and controlling microbial contamination in fuels and fuel systems – a primer". FQS Limited, INC., Princeton. Report prepared for Chevron, USA.

[34] Barsness, D.A., and Bertram, N.L., 1959. Saturation limits of water in jet fuels. Wright Air Development Centre Technical Note 59-287, Ohio, USA.

[35] Morton, L.H.G. and Surman, S.B., 1994. Biofilms in Biodeterioration - a Review". *International Biodeterioration and Biodegradation*, 34(3-4): 203-221.

[36] Jones, R., Goldmeer, J. and Monetti, B. 2011. Addressing Gas Turbine Fuel Flexibility". GE Energy. GER-4601

[37] Haeseler, F., Behar, F., Garnier, D. and Chenet, P-Y. 2010. First stoichiometric model of oil biodegradation in natural petroleum systems: Part I – The BioClass 0D approach. *Organic Geochemistry* 41(10): 1156-1170.

[38] Onabanjo, T.O., Di Lorenzo, G., Goodger, E.M. and Pilidis, P. 2013. Techno-Economic Assessment of Gas Turbines with Bio-Fuels: A Fuel Bio-fouling Approach. Presented at the ASME Turbo Expo 2013/ASME International Gas Turbine Institute, on June 3-7, 2013, San Antonio Convention, Texas, USA.

[39] Vandecasteele, J.P. 2008. Petroleum Microbiology: Concepts, Environmental Implications, Industrial Applications. France: Ophrys.

[40] Marchal, R., Penet, S., Solano-Serena, F. and Vandecasteele, J.P. 2003. Gasoline and diesel oil biodegradation. *Oil and Gas Science and Technology* 58(4): 441–448.

[41] Ribeiro, N.M., Pinto, A.C., Quintella, C.M., da Rocha, G.O.; Teixeira, L.S.G.; Guarieiro, L.L.N., Rangel, M.D.; Veloso, M.C.C.; Rezende, M.J.C.; da Cruz, R.S.; de Oliveira, A.M., Torres, E. A.and de Andrade, J.B. 2007. The role of additives for diesel and diesel blended (ethanol orbiodiesel) fuels: A review. *Energy Fuels* 21(4): 2433–2445.

[42] VanBriesen, J.M. 2001. Thermodynamic yield predictions for biodegradation through oxygenase activation reactions. *Biodegradation* 12(4): 263 - 279.

[43] VanBriesen, J.M. 2002. Evaluation of methods to predict bacterial yield using thermodynamics. *Biodegradation* 13: 171–190.

[44] Xiao, J. and VanBriesen, J.M. 2006. Expanded thermodynamic model for microbial true yield prediction. *Biotechnol. Bioeng*. 93(1): 110–121.

[45] Xiao, J. and VanBriesen, J.M. 2008. Expanded thermodynamic true yield prediction model: adjustments and limitations. *Biodegradation* 19(1): 99-127.

[46] McCarty, P.L. (1965). Thermodynamics of biological synthesis and growth. *In*: Baers J. (Ed) Advances in Water Pollution Research. Proceedings of the 2nd International Conference on Water Pollution Research 2: 169–199. Pergamon Press, Inc., Oxford, England.

[47] Roels, J.A. 1980. Application of Macroscopic Principles to Microbial Metabolism. *Biotechnology and Bioengineering* 22(12): 2457-2514.

[48] Roels, J. A. 1983. Energetics and Kinetics in Biotechnology. Elsevier Biomedical Press, Amsterdam, the Netherlands.

[49] Heijnen, J.J. and van Dijken, J.P. 1992. In search of a thermodynamic description of biomass yields for the chemotrophic growth of microorganisms. *Biotechnol. Bioeng.* 39(8): 833–858.

[50] Heijnen, J.J., van Loosdrecht, M.C.M. and Tijhuis, L. 1992. A black box mathematical model to calculate auto- and heterotrophic biomass yields based on Gibbs energy dissipation. *Biotechnol. Bioeng*. 40: 1139–1154.

[51] McCarty, P.L. 2007. Thermodynamic electron equivalents model for bacterial yield prediction: modifications and comparative evaluations. *Biotechnology and Bioengineering* 97(2): 377-388.

[52] VanBriesen, J.M. and Rittmann, B.E. 2000. Mathematical Description of Microbiological Reactions Involving Intermediates. *Biotechnology and Bioengineering* 67(1): 35-52.

[53] VanBriesen, J.M. and Rittmann, B.E. 1999. Modelling speciation effects on biodegradation in mixed metal/chelate systems. *Biodegradation* 10: 315–330.

[54] Yuan, Z. and VanBriesen, J.M. 2002. Yield prediction and stoichiometry of multi-step biodegradation reactions involving oxygenation. *Biotechnology and Bioengineering* 80(1): 100–113.

[55] Henze, M., Grady, C. P. L., Gujer, W., Marais, G. V. R., Matsuo, T. (1987). Activated sludge model No. 1. IAWQ Scientific and Technical Report 3. London: IAWQ.

[56] Henze, M., Gujer, W., Mino, T., Matsuo, T., Wentzel, M.C and Marais, G.v.R. 1995. Activated sludge model No 2. IAWQ Scientific and Technical Report, No 3. London: IAWQ.

[57] Billing, A.E. and Dold, P.L. 1988. Modelling techniques for biological reaction systems (1) Mathematical description and model representation. *Water S.A*. 14(4): 185-192.

[58] Button, D.K., Schell, D.M. and Robertson, B.R. 1981. Sensitive and accurate methodology for measuring kinetics of concentration-dependent hydrocarbon metabolism rates in seawater by microbial communities. *Applied and Environmental Microbiology* 41(4): 936-941.

[59] Guha, S., Peters, C.A. and Jaffe, P.R. 1999. Multisubstrate biodegradation kinetics of naphthalene, phenanthrene, and pyrene mixtures. *Biotechnology and Bioengineering* 65(5): 491-499.

[60] Panikov, N.S. 1991. Kinetics of Microbial Growth: General Principles and Ecological Applications. Nauka Publ., Moscow.

[61] Yassine, M.H., Suidan, M.T. and Venosa, A.D. 2013. Microbial kinetic model for the degradation of poorly soluble organic materials. *Water Research* 47(4): 1585-1595.

[62] Mariano, A.P., Tomasella, R.C., de Oliveira, L.M., Contiero, J. and de Angelis, D.F. 2008. Biodegradability of diesel and biodiesel blends. *African Journal of Biotechnology* 7(9): 1323-1328.

[63] Zhang, X., Peterson, C.L., Reece, D., Haws, R. and Moller, G. 1998. Biodegradability of biodiesel in the aquatic environment. *Transactions of the ASABE* 41(5): 1423-1430.

[64] Demirbaş, A. 2008. Biodegradability of Biodiesel and Petrodiesel Fuels. *Energy Sources, Part A: Recovery, Utilization, and Environmental Effects* 31(2): 169-174.

[65] Tyson, K. S. 1998. Biodiesel Research Progress 1992-1997. National Renewable Energy Laboratory, USA. NREL/SR-580-24433.

[66] Passman, F. J. and Dobranic, J. K. 2005. Relative biodegradability of B-100 biodiesel and conventional low sulfur diesel fuels. Paper presented at the 9th International Conference on Stability, Handling and Use of Liquid Fuels Sites, Spain, September 18-22, 2005.

[67] Pasqualino, J.C., Montane, D. and Salvado, J. 2006. Synergic effects of biodiesel in the biodegradability of fossil-derived fuels. *Biomass and Bioenergy* 30(10): 874–879.

[68] Dodos, G.S., Konstantakos, T., Longinos, S. and Zannikos, F. 2012. Effects of microbiological contamination in the quality of biodiesel fuels. *Global NEST Journal* 14(2): 175-182.

[69] Owsianiak, M., Chrzanowski, L., Szulc, A., Staniewski, J., Olszanowski, A., Olejnik-Schmidt, A. and Heipieper, H. 2009. Biodegradation of diesel/biodiesel blends by a consortium of hydrocarbon degraders: effect of the type of blend and the addition of biosurfactants. *Bioresour Technol* 100: 1497–1500.

[70] DeMello, J.A., Carmichael, C.A., Peacock, E.E., Nelson, R.K., Arey, J.S. and Reddy, C.M. 2007. Biodegradation and Environmental Behaviour of Biodiesel Mixtures in the Sea: An Initial Study. *Marine Pollution Bulletin* 54(7): 894-904.

[71] Nikhil, T., Deepa, V., Rohan, G. and Satish, B. 2013. Isolation, characterization and identification of diesel engine oil-degrading bacteria from garage soil and comparison of their bioremediation potential. *International Research Journal of Environment Sciences* 2(2): 48-52.

[72] Olson, J.J., Mills, G.L., Herbert, B.E. and Morris, P.J. 1999. Biodegradation rates of separated diesel components. *Environmental Toxicology and Chemistry* 18(11): 2448-2453.

[73] Mukherji, S., Jagadevan, S., Mohopatra, G. and Vijay, A. 2004. Biodegradation of diesel oil by an Arabian Sea sediment culture isolated from the vicinity of an oil field. *Bioresource Technology* 95(3): 281–286.

[74] Siegert, W. 2013. Microbial Contamination in Diesel Fuel – Are New Problems Arising from Biodiesel Blends? *In* Proceeding of Colloquium Fuels Conventional and Future Energy for Automobiles, Stuttgart/Ostfildern, Germany.

[75] Robbins, J.A. and Levy, R. 2005. A review of the microbiological degradation of fuel. *In*: Paulus, W., (Ed.), Directory of microbicides for the protection of materials, New York, Springer, pp. 177-201.

[78] Corseuil, H.X. and Weber, W.J. 1994. Potential biomass limitations on rates of degradation of monoaromatic hydrocarbons by indigenous microbes in subsurface soils. *Water Research* 28(6): 1415 – 1423.

[79] Rodríguez-Rodríguez, C.E., Rodríguez-Cavallini, E. and Blanco, R. 2008. Bacterial contamination of automotive fuels in a tropical region: the case of Costa Rica. *Rev. Biol. Trop*. 57(3): 489-504.

[80] Itah, A.Y., Brooks, A.A., Ogar, B.O. and Okure, A.B. 2009. Biodegradation of international Jet A-1 aviation fuel by microorganisms isolated from aircraft tank and joint hydrant storage systems. *Bull. Environ. Contam. Toxicol*. 83(3): 318–327.

[81] Abuhamed, T., Bayraktar, E., Mehmetoglu, T. and Mehmetoglu, U. 2004. Kinetics model for growth of *Pseudomonas putida* F1 during benzene, toluene and phenol biodegradation. *Process Biochem* 39(8): 983–988.

[82] McFarland, M.J and Sims, R.C. 1991. Thermodynamics framework for evaluating PAH degradation in the sub-surface. *Groundwater* 29(6): 885-896.

[83] von Stockar, U., Maskow, T., Liu, J., Marison, I.W. and Patino, R. 2006. Thermodynamics of microbial growth and metabolism: An analysis of the current situation. *Journal of Biotechnology* 121(4): 517–533.

[84] Hu, Z.F., Dou, J.F., Liu, X., Zheng, X.L. and Deng, D. 2007. Anaerobic biodegradation of benzene series compounds by mixed based on optional electronic acceptors. *Journal of Environmental Sciences* 19(9): 1049-1054.

[85] Cao, Y. 2010. Miniature High-Temperature Rotating Heat Pipes and Their Applications in Gas Turbine Cooling. *Frontiers in Heat Pipes (FHP)* 1: 023002. DOI: 10.5098/fhp.v1.2.3002

[86] Meher-Homji C.B., and Gabriles G.A. (1998). Gas Turbine Blade Failures—Causes, Avoidance, and Troubleshooting. Proceedings of the 27th Turbomachinery Symposium, Texas, USA. pp. 129-180.

[87] Kurz, R., Lubomirsky, M. and Brun, K. 2012. Gas Compressor Station Economic Optimization. *International Journal of Rotating Machinery*, Article ID 715017. doi:10.1155/2012/715017.

[88] Farrell, J.T., Cernansky, N.P., Dryer, F.L., Friend, D.G, Hergart, C.A., Law, C.K., McDavid, R.M., Mueller, C.J., Patel, A.K. and Pitsch, H. 2007. Development of an experimental database and kinetic models for surrogate diesel fuels. *Society of Automotive Engineers Technical Paper* 2007-01-0201. doi: 10.4271/2007-01-0201

[89] Pitz, W.J. and Mueller, C.J. 2011. Recent progress in the development of diesel surrogate fuels. *Prog. Energy Combust Sci*. 37(3): 330-350.

[90] Mueller, C.J., Cannella, W.J., Bruno, T.J., Bunting, B., Dettman, H.D., Franz, J.A., Huber, M.L., Natarajan, M., Pitz, W.J., Ratcliff, M.A. and Wright, K. 2012, " Methodology for Formulating Diesel Surrogate Fuels with Accurate Compositional, Ignition-Quality, and Volatility Characteristics. *Energy and Fuels* 26(6): 3284–3303.

[91] Herbert, D. 1958. Some principles of continuous culture. In G. Tunevall (ed.), Recent Progress in Microbiology. Blackwell, London: 381–396

8. CONCLUSION AND RECOMMENDATION

The use of Jatropha- and microalgae-biodiesel in 22.4 MW and 126 MW —open and combined cycle configuration, industrial gas turbines have been examined for power generation using techno-economic and environmental life cycle impact assessment methodologies. Comparative fuel assessments were carried out between the biodiesel and fossil fuels (natural gas and diesel). These involve engine performance, emission and environmental analysis with economic evaluation. The concept of microbial fuel degradation was also examined in gas turbines.

8.1 Conclusion

A detailed summary have been provided under each chapter, however, an abridge conclusion that addresses each objectives underlined in this thesis is provided below:

8.1.1 Techno-economic performance of gas turbines

To satisfy energy demand in developing and least developed countries, there should be diversification in the energy mix for power generation and a reduction in GHG emissions concurrently. In such applications, Jatropha biodiesel is a worthwhile substitute for conventional diesel fuel, because it has close performance and emission characteristics to conventional diesel. For equivalent power and open cycle application, the engine thermal efficiency increased by 1.1% (heavy duty) and 1.2% (aero-derivative) with reduced EGT of 0.26% and 0.32% respectively when compared to their corresponding natural gas case. For combined cycle application, the fuel brought about a reduced useful work but increased overall plant efficiency compared to the natural gas case. For economic viability and sustainability of gas turbine operated plants, power producers require a minimum amount of $0.22/kWh for open cycle and $0.17/kWh for combined cycle application to recover the added cost of operating 100% Jatropha biodiesel. This could be provided as production based renewable tax incentive. Operators could also explore options such as part substitution of fuel during fuel shortages to avoid deficit energy cost and prevent opportunity loss during power outages. Here, a maximum of 20% fuel mix can be achieved with open cycle engine and 25% for combined cycle configuration with or without government intervention and beyond which operating on biodiesels would not be economically viable. Furthermore, the intervention of carbon tax and the use of CCGT both have the tendency to improve the economic performance of biodiesel fired plants. In worst case scenarios, where there are no government

incentives, the local conditions in Nigeria with extreme LCOE open opportunities for distributed and independent power generation from renewable fuels like Jatropha-biodiesel. The use of microalgae biodiesel is also achievable; however, considerations are required for engine health with open cycle application.

8.1.2 Environmental performance of gas turbines

The consequent displacement of conventional diesel fuel with Jatropha biodiesel could have significant environmental benefit with GHG savings of 26% in a worst case scenario, and 60% for a best case condition. Here, the magnitude of the benefits is highly dependent on the farming approach adopted for growing the Jatropha: the rain-fed scenario is recommended.

8.1.3 Impact of microbial-induced fuel degradation

The renewable nature of biodiesel fuels draws significant attention to microbial fuel biodegradation; hence the impact of fuel degradation is a critical area of research that requires multidisciplinary approach. The model developed has demonstrated that the maximum water acceptable in standard diesel fuels is more than sufficient to initiate unlimited biodegradation reactions. Microbial degradation of fuel of up to 10% and corresponding to loss of hydrocarbons and reduced LHV could increase the engine heat rate by nearly 12% and reduce thermal efficiency by 10%. The engine health is also at the risk because EGT increases by nearly 4^{o}C, with the tendency of a reduced surge margin for the gas turbine compressor. Bio-mathematical models like Bio-fAEG provide a platform to simulate and could enable a better understanding of microbial fuel degradation in gas turbines. This thesis has provided a first step in quantifiable assessment and towards predictive condition monitoring.

8.2 Recommendation

The objectives outlines in this thesis have been successfully achieved; however, there are more areas of research that can be considered as part of future work. The author recommends the following:

1. Jatropha biodiesel from different countries and origins could be explored to determine the variability in engine performance and for common standards, since this fuel is widely grown.
2. The capability of the current emission model for industrial gas turbine could be further developed to account for advanced combustion and emission control.

3. The elements of land use change, water depletion, human toxicity and use of recent technologies with low environmental impact could be further explored in environmental life cycle assessment studies of Jatropha biodiesel fuels.
4. The Bio-fAEG could be further developed to assess fuel degradation under sulphate reducing and nitrate reducing conditions and to account for abiotic factors such as temperature, pH, even presence of inhibitory fuel components and conditions. The kinetic module could be further developed to explore microorganisms with multiple capabilities and to utilize multiple substrates or co-utilize a single substrate. The microbial empirical formula of cells that is specific for fuel systems should be explored with the support of mechanistic experiments. On further validation, biofouling analysis should be extended to biodiesels, since they are relatively more degradable than diesel fuels. It is likewise important to examine how the economics of fuel degradation could affect future application of biofuels in gas turbines, emission tax policies, fuel handling practices and management as well as other legislation scenarios. Furthermore, the development of surrogate fuels that is specific for this type of microbial studies could be developed.
5. Other possible areas to be explored with this thesis include social impact of the use of biodiesels in gas turbines, well-to-well life cycle assessment, and future peak load operation of power plants under similar conditions.

APPENDIX I

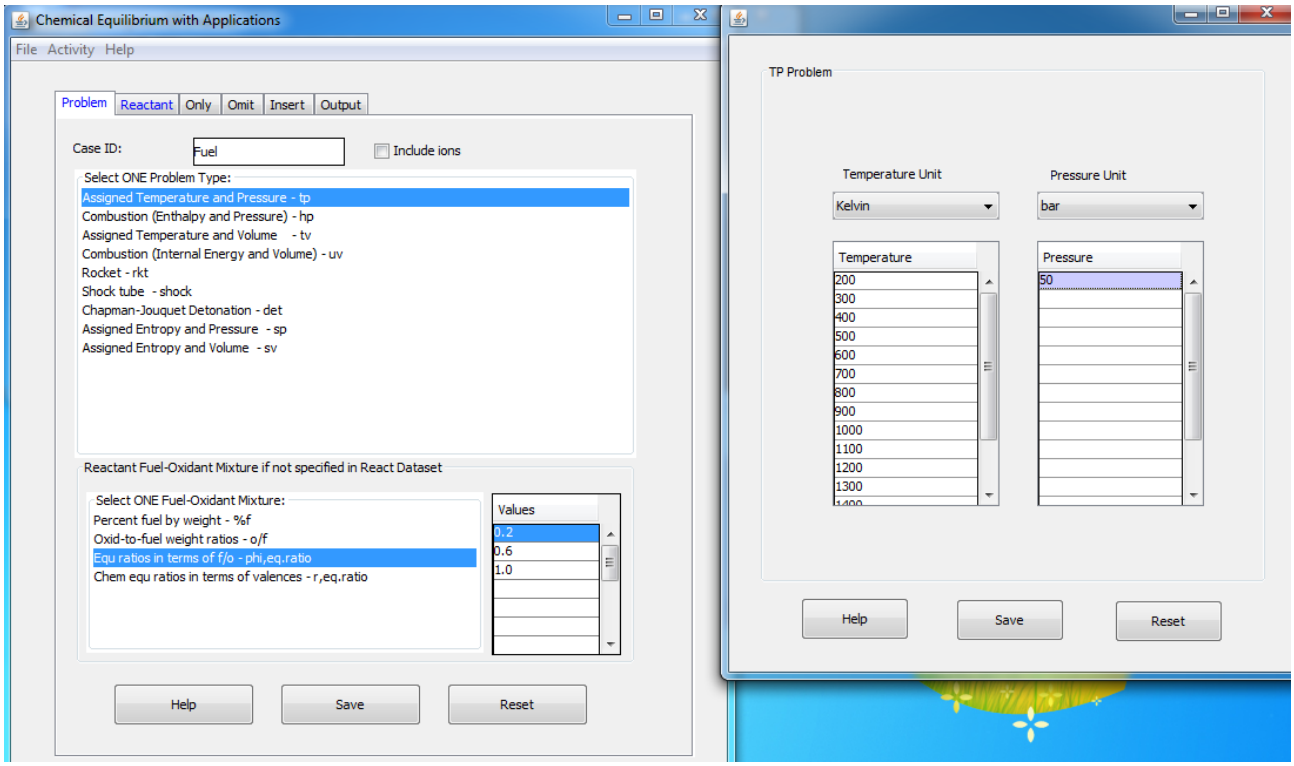

Figure a: "Problem" Tab illustration

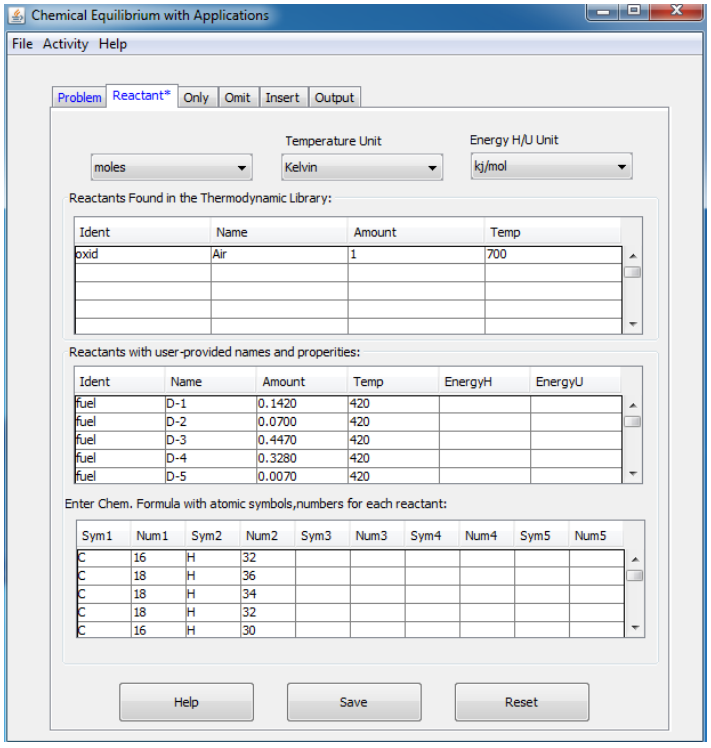

Figure b: "Reactant" Tab illustration

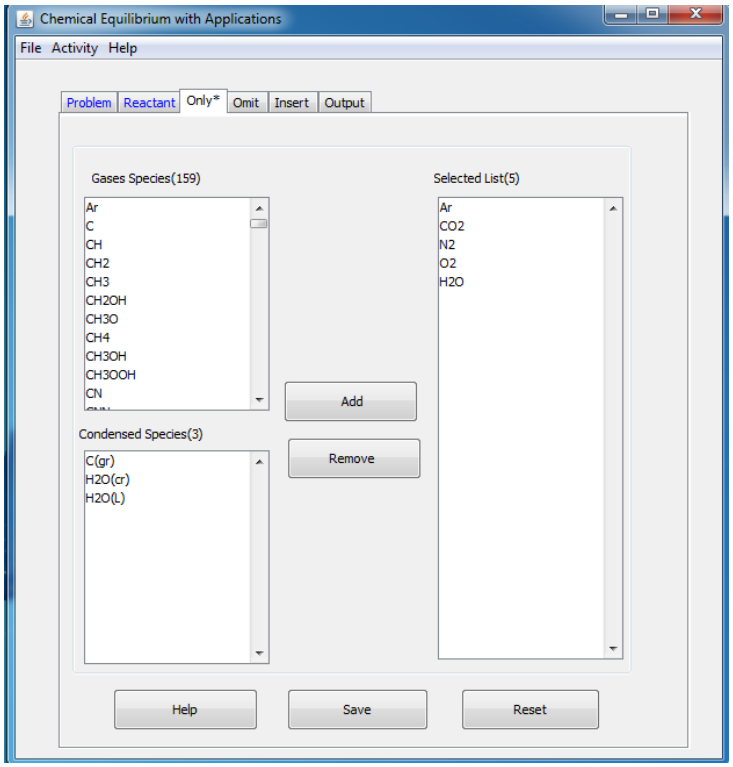

Figure c: "Only" Tab illustration*

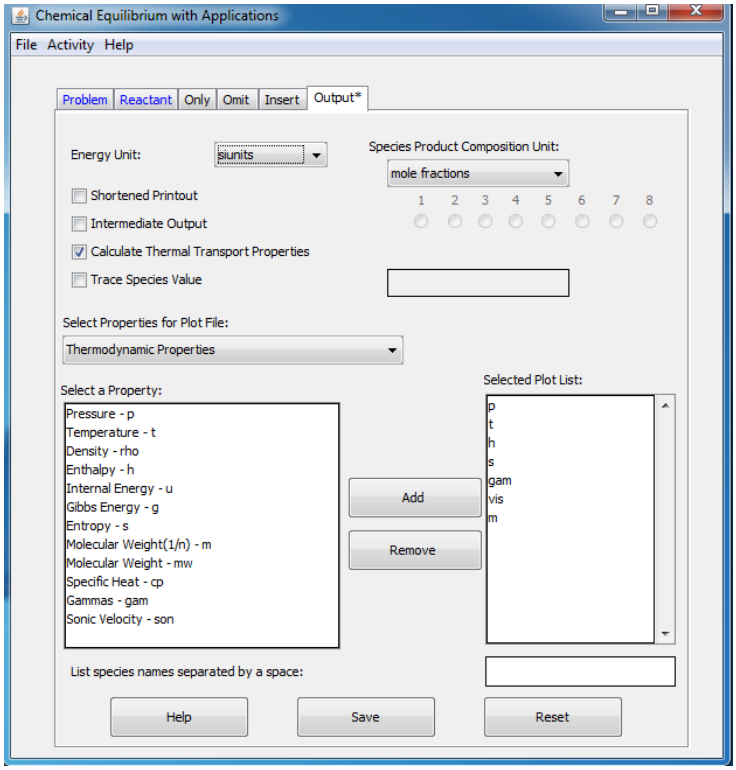

Figure d: "Output" Tab illustration

Figure 1.1 (a-d): Step-by-step procedure for use of NASA CEA GUI platform. a) "Problem" tab b) "Reactant" tab c) "Only" tab d) "Output" tab e) "Activity tab

```
problem   case=Fuel phi,eq.ratio=0.3,0.6,1.0
tp   t,k=200,300,400,500,600,700,800,900,1000,1100,1200,1300,1400,1500,1600,1700,  p,bar=50,
react
oxid=Air moles=1 t,k=700
fuel=D-1 moles=0.1558 t,k=420 C 13 H 26
fuel=D-2 moles=0.1761 t,k=420 C 15 H 30
fuel=D-3 moles=0.2887 t,k=420 C 14 H 26
fuel=D-4 moles=0.0319 t,k=420 C 16 H 30
fuel=D-5 moles=0.0218 t,k=420 C 18 H 32
fuel=D-6 moles=0.2709 t,k=420 C 16 H 26
```

Figure 1.2: Sample input file (.in) for Algae Biodiesel in NASA CEA

```
*******************************************************************************
        NASA-GLENN CHEMICAL EQUILIBRIUM PROGRAM CEA2, MAY 21, 2004
                BY  BONNIE MCBRIDE AND SANFORD GORDON
     REFS: NASA RP-1311, PART I, 1994 AND NASA RP-1311, PART II, 1996
 *******************************************************************************
OPTIONS: TP=T  HP=F  SP=F  TV=F  UV=F  SV=F  DETN=F  SHOCK=F  REFL=F  INCD=F
 RKT=F  FROZ=F  EQL=F  IONS=F  SIUNIT=T  DEBUGF=F  SHKDBG=F  DETDBG=F  TRNSPT=T

 T,K =   200.0000   300.0000   400.0000   500.0000   600.0000   700.0000   800.0000
 T,K =   900.0000  1000.0000  1100.0000  1200.0000  1300.0000  1400.0000  1500.0000
 T,K =  1600.0000  1700.0000
 TRACE= 0.00E+00  S/R= 0.000000E+00  H/R= 0.000000E+00  U/R= 0.000000E+00
 P,BAR =    50.000000

REACTANT          MOLES    (ENERGY/R),K   TEMP,K  DENSITY
EXPLODED FORMULA
 O: Air            1.000000   0.143092E+04   700.00  0.0000 N  1.56168  O  0.41959  AR 0.00937  C  0.00032
 F: D-1            0.155800   0.000000E+00   420.00  0.0000 C 13.00000  H 26.00000
 F: D-2            0.176100   0.000000E+00   420.00  0.0000 C 15.00000  H 30.00000
 F: D-3            0.288700   0.000000E+00   420.00  0.0000 C 14.00000  H 26.00000
 F: D-4            0.031900   0.000000E+00   420.00  0.0000 C 16.00000  H 30.00000
 F: D-5            0.021800   0.000000E+00   420.00  0.0000 C 18.00000  H 32.00000
 F: D-6            0.270900   0.000000E+00   420.00  0.0000 C 16.00000  H 26.00000
 F: D-7            0.034500   0.000000E+00   420.00  0.0000 C 24.00000  H 44.00000
 F: D-8            0.020300   0.000000E+00   420.00  0.0000 C 24.00000  H 42.00000

SPECIES BEING CONSIDERED IN THIS SYSTEM (CONDENSED PHASE MAY HAVE NAME LISTED SEVERAL TIMES)
LAST thermo.inp UPDATE:    9/09/04

SPECIES WITH TRANSPORT PROPERTIES
PURE SPECIES

  Ar             CO2            H2O            N2          O2

O/F =  48.479769

                 EFFECTIVE FUEL     EFFECTIVE OXIDANT       MIXTURE
```

```
……..

O/F=   48.47977  %FUEL=  2.021028  R,EQ.RATIO= 0.301064  PHI,EQ.RATIO= 0.300000

THERMODYNAMIC PROPERTIES

P, BAR          50.000   50.000   50.000   50.000   50.000   50.000   50.000   50.000
T, K           200.00   300.00   400.00   500.00   600.00   700.00   800.00   900.00
RHO, KG/CU M    8.7170 1 5.8113 1 4.3585 1 3.4868 1 2.9057 1 2.4906 1 2.1792 1 1.9371 1
H, KJ/KG       -1000.61  -898.98  -796.23  -691.79  -585.13  -475.92  -364.06  -249.68
U, KJ/KG       -1057.97  -985.02  -910.95  -835.19  -757.21  -676.67  -593.50  -507.80
G, KJ/KG       -2078.95 -2640.07 -3235.89 -3857.84 -4501.03 -5162.28 -5839.36 -6530.62
S, KJ/(KG)(K)    5.3917   5.8036   6.0991   6.3321   6.5265   6.6948   6.8441   6.9788

M, (1/n)        28.991   28.991   28.991   28.991   28.991   28.991   28.991   28.991
(dLV/dLP)t     -1.00000 -1.00000 -1.00000 -1.00000 -1.00000 -1.00000 -1.00000 -1.00000
(dLV/dLT)p      1.0000   1.0000   1.0000   1.0000   1.0000   1.0000   1.0000   1.0000
Cp, KJ/(KG)(K)   1.0119   1.0211   1.0349   1.0547   1.0790   1.1054   1.1315   1.1559
GAMMAs          1.3955   1.3905   1.3833   1.3735   1.3620   1.3504   1.3395   1.3300
SON VEL,M/SEC    282.9    345.9    398.4    443.8    484.1    520.7    554.4    585.9

TRANSPORT PROPERTIES (GASES ONLY)
```

Figure 1.3: Sample output file (.out) for Algae Biodiesel in NASA CEA

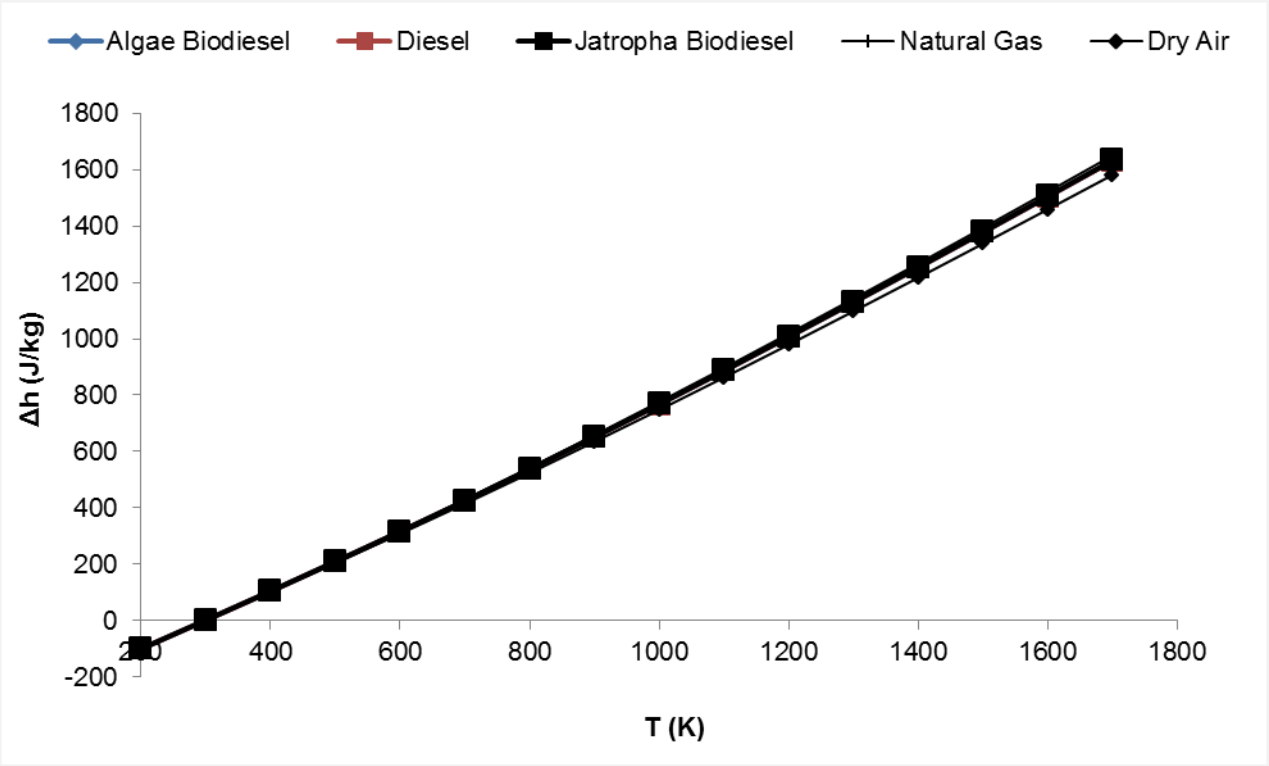

Figure 1.4: Comparison of Sp. Enthalpy (h) as a function of Temperature for the Various Fuels for GX Engines (Chemical Equilibrium, Φ=1, P=50 Bar)

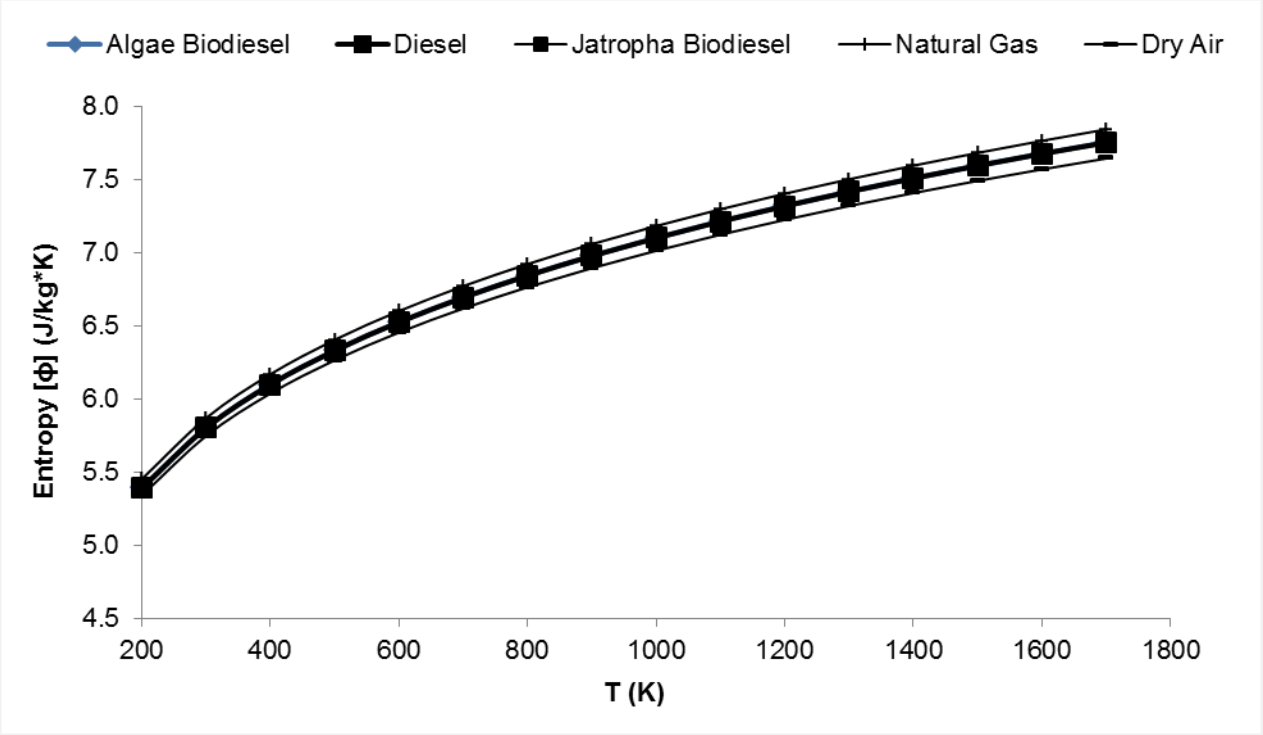

Figure 1.5: Comparison of Entropy (φ) as a function of Temperature for the Various Fuels for GX Engines (Chemical Equilibrium, Φ=1, P=50 Bar)

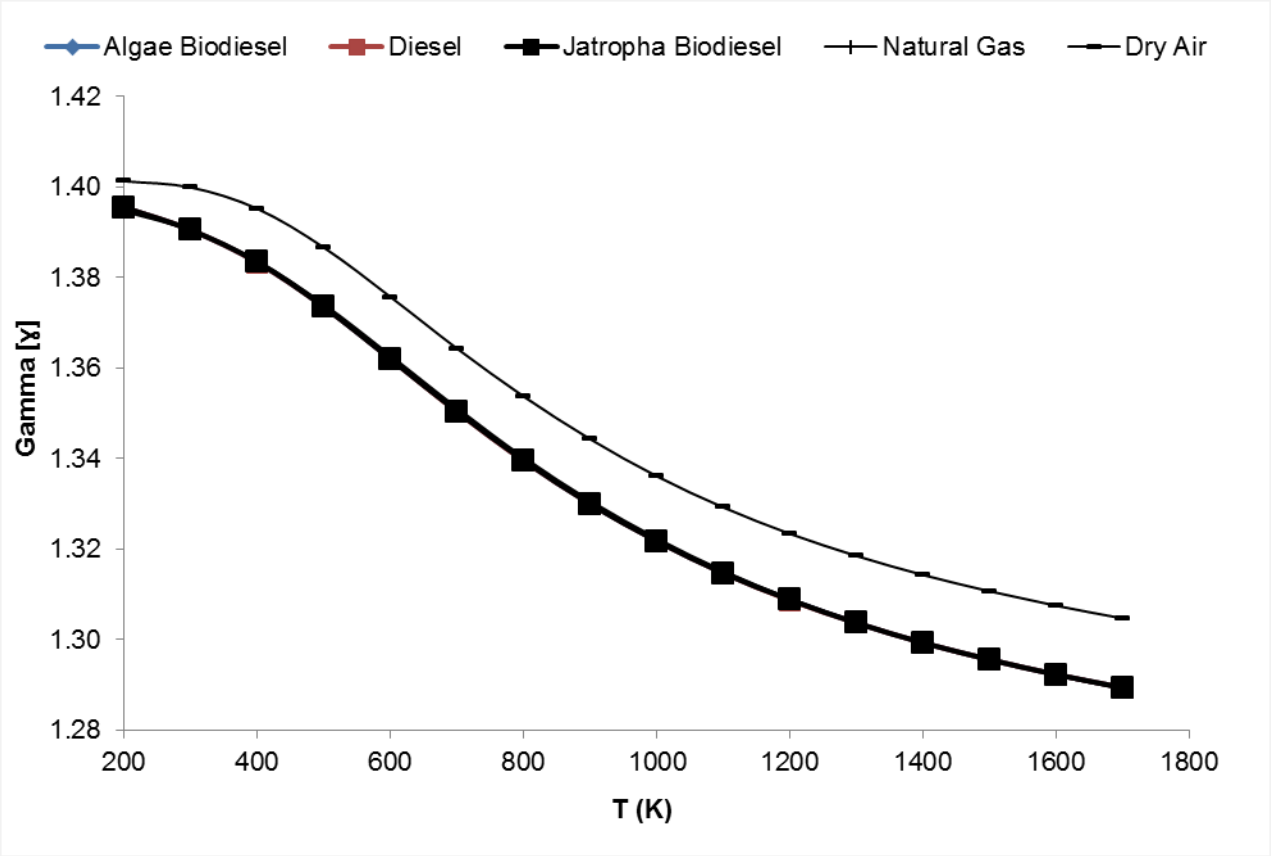

Figure 1.6: Comparison of Gamma (γ) as a function of Temperature for the Various Fuels for GX Engines (Chemical Equilibrium, Φ=1, P=50 Bar)

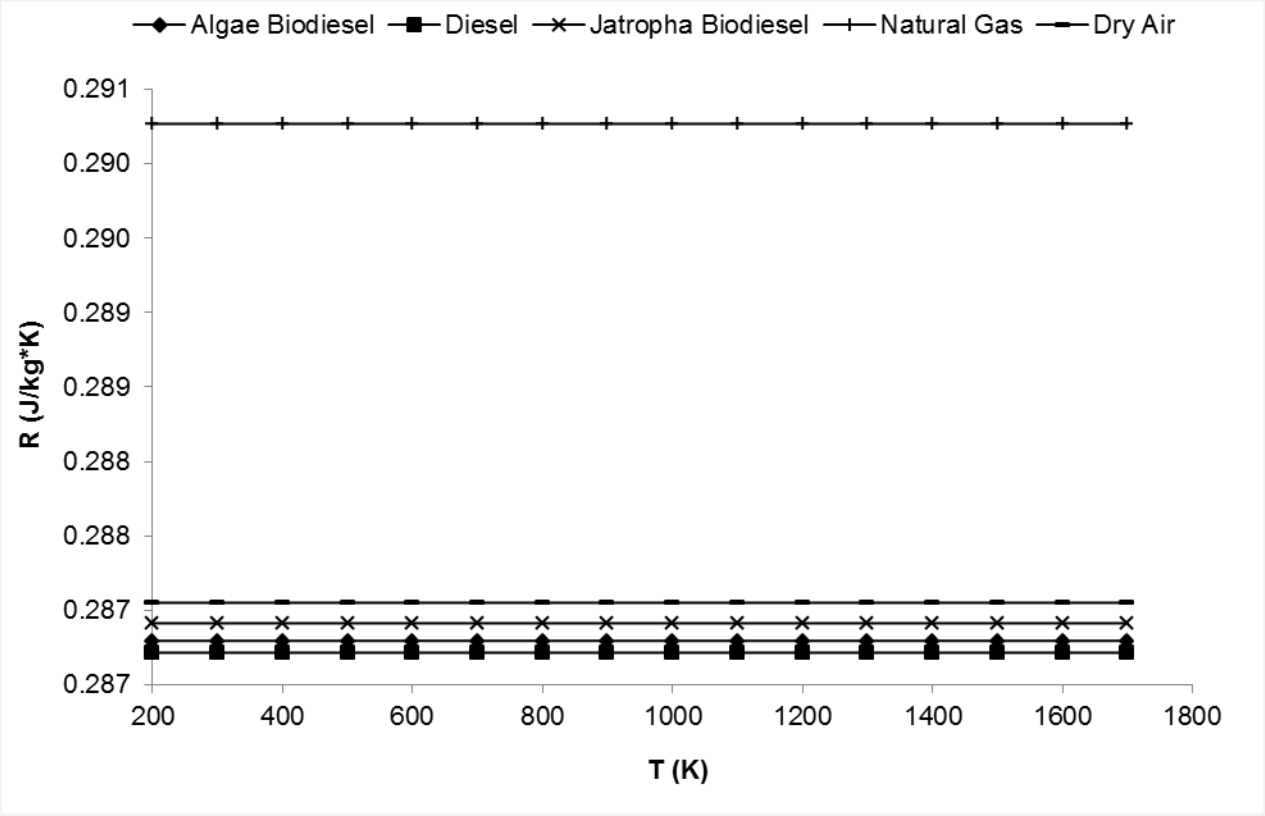

Figure 1.7: Comparison of Gas Constant (R) as a function of Temperature for the Various Fuels for GX Engines (Chemical Equilibrium, Φ=1, P=50 Bar)

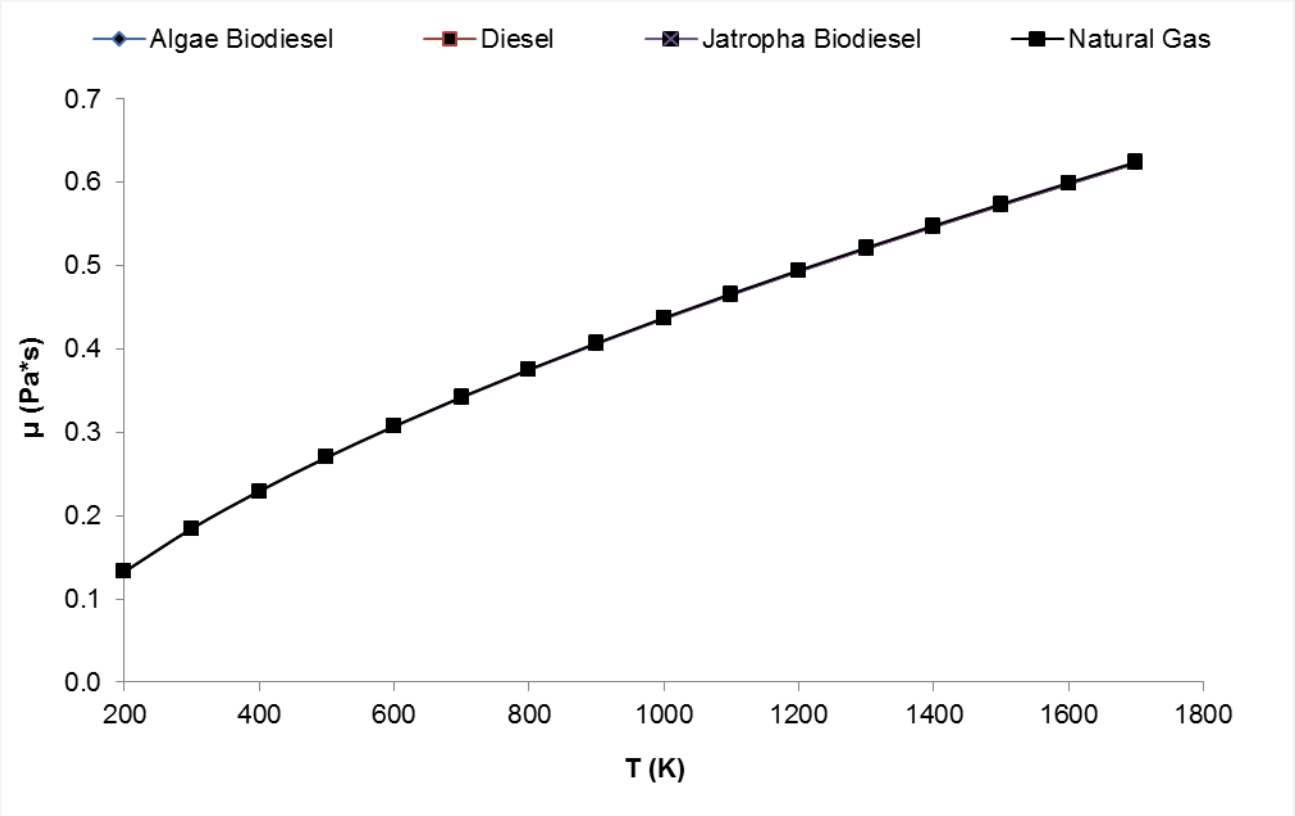

Figure 1.8: Comparison of Viscosity (φ) as a function of Temperature for the Various Fuels for GX Engines (Chemical Equilibrium, Φ=1, P=50 Bar)

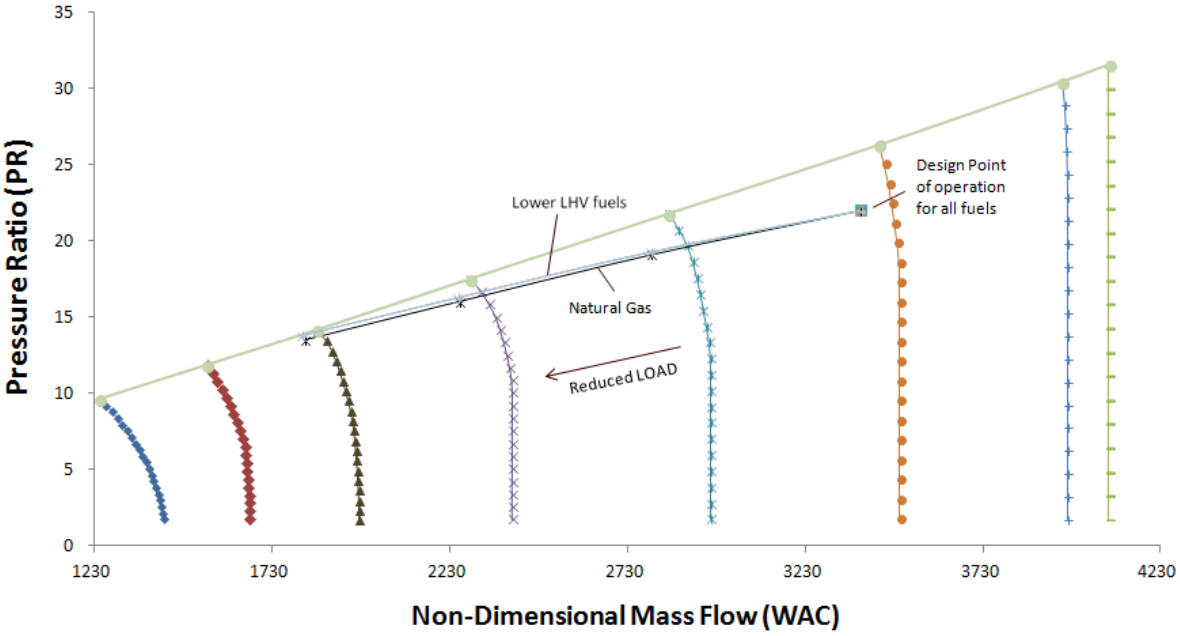

Figure 1.9: Compressor map characteristics showing the effects of reduced load on engine operating line

APPENDIX II

DEMONSTRATION OF Bio-*f*AEG

Assuming aerobic degradation of Hexadecanoic acid, where ε=0.37, the cell yield and overall growth stoichiometry is as follows:

Electron Donor (Hexadecanoic acid)

Half Reaction (R_d):

$$\frac{1}{98}C_{16}H_{34} + \frac{16}{49}H_2O \rightarrow \frac{8}{49}CO_2 + H^+ + e^- \qquad \Delta G_d^o = -27.66 \text{ KJ/eeq}$$

Electron Acceptor (Oxygen)

Half Reaction (R_a):

$$\frac{1}{4}O_2 + H^+ + e^- \rightarrow \frac{1}{2}H_2O \qquad \Delta G_a^o = -78.72 \text{ KJ/eeq}$$

Half Reaction (R_c): ***Cell Synthesis ($C_5H_7O_2N$) with NH_4^+ as nitrogen source***

$$\frac{1}{5}CO_2 + \frac{1}{20}NH_4^+ + \frac{1}{20}HCO_3^- + H^+ + e^- \rightarrow \frac{1}{20}C_5H_7O_2N + \frac{9}{20}H_2O$$

$\gamma_d = \rho_{donor}/C_{cells}$ = 98/16 =6.125

$\gamma_x = \rho_{cells}/C_{cells}$ = 20/4 =5

f_s and Y

$$-A = \frac{\frac{0-27.66}{0.37^1} + \frac{30.9-0}{0.37^1} + \frac{18.8}{0.37}}{0.37(-78.72 - 27.66) - \frac{8.0}{98} * -219.2}$$

A=1.819

$f_s^o = \frac{1}{1+A}$ =0.355

f_e^o = 1 - 0.355 = 0.645

$Y_{c/c} = \frac{\gamma_d}{\gamma_x} f_s^o = \frac{6.125}{4} * 0.355 = 0.544$ molCcell/molCacetate

$Y_{c/c} = \frac{p}{Y_x} f_s^o = \frac{98}{4} * 0.355 = 8.70$ molCcell/mol acetate

Overall Reaction (R): $f_sR_c + f_eR_a - R_d$

$f_s^o R_c = 0.355 \left(\frac{1}{5} CO_2 + \frac{1}{20} NH_4^+ + \frac{1}{20} HCO_3^- + H^+ + e^- \rightarrow \frac{1}{20} C_5H_7O_2N + \frac{9}{20} H_2O\right)$

$f_e^o R_a = 0.645 \left(\frac{1}{4} O_2 + H^+ + e^- \rightarrow \frac{1}{2} H_2O\right)$

$R_d = \frac{1}{98} C_{16}H_{34} + \frac{16}{49} H_2O \rightarrow \frac{8}{49} CO_2 + H^+ + e^-$

$= \frac{1}{98} C_{16}H_{34} + \frac{13}{733} NH_4^+ + \frac{13}{733} HCO_3^- + \frac{5}{31} O_2 \rightarrow \frac{13}{733} C_5H_7O_2N + \frac{19}{122} H_2O + \frac{6}{65} CO_2$

Simplified Overall Reaction (R):

$= C_{16}H_{34} + 1.738\ NH_4^+ + 1.738\ HCO_3^- + 15.81 \rightarrow 1.738\ C_5H_7O_2N + 15.26\ H_2O + 9.05\ CO_2$

$= -\frac{1}{8.69} C_{16}H_{34} - 0.2\ NH_4^+ - 0.2\ HCO_3^- - 1.82\ O_2 + C_1H_{1.4}O_{0.4}N_{0.2} + 1.76\ H_2O + 1.04\ CO_2$

Y= 0.869 g cells/g substrate

Using equation 10, and assuming initial substrate concentration of Hexadecanoic acid of 0.313 mg/l, actual growth rate (*k*C) of 0.0145, death rate (k_d) of 0.008 and initial microbial population (X_0)of 0.0134 mg/l where abiotic factor (k_{ab}) is zero (0).

$S_{tot} = S_{tot0} - \frac{kCXo}{(YkC - kd)} \left(e^{(YkC - kd)t} - 1\right) - k_{ab}S_{sat}t$

At time (t)=0hr, S_{tot} =0.313

At time (t)=24hrs: S_{tot} =0.3118, X_0=0.0150, Hydrocarbon loss of 0.38% and microbial population increased by 3.45%.

Table I: Model Parameters & Constants for simulation of conventional diesel-type fuel A [S_o=0.3125mg/L, kC=0.015, k_d=0.008]

FUEL A		Assigned Hydrocarbon Substrate	WT%	mol	C	H	MM	X_{acc}	X_{in}	X_{bio}	X_o mg/L	kCX_o	Y	YkC	YkC-k_d	$S_{tot(t)}$
Paraffin	n-C_{9-14}	Nonane	6.63	0.155	9	20	128	0.136	0.173	0.240	0.014	0.00020	0.872	0.013	0.005	0.000034
	n-C_{14}^{+}	Hexadecane	8.11	0.108	16	34	226	0.134	0.134	0.184	0.013	0.00019	0.958	0.014	0.006	0.000026
	iso-C_{9-14}	2,2,3 trimethylpentane	6.95	0.163	9	20	128	0.068	0.173	0.120	0.007	0.00010	0.872	0.013	0.005	0.000017
	iso-C_{14}^{+}	3-methylpentadecane	9.60	0.127	16	34	226	0.078	0.134	0.106	0.008	0.00011	0.869	0.013	0.005	0.000015
Cyclic Alkanes	mono-C_{14}^{+}	n-Nonylcyclopentane	30.23	0.463	14	28	196	0.078	0.110	0.087	0.008	0.00011	0.898	0.013	0.005	0.000012
	di-C_{14}^{+}	1-Butyl Decalin	13.62	0.211	14	26	194	0.078	0.086	0.068	0.008	0.00011	0.872	0.013	0.005	0.000010
	tri-C_{14}^{+}	Trinaphthenes	4.54	0.071	14	24	192	0.039	0.077	0.030	0.004	0.00006	0.845	0.012	0.004	0.000004
Aromatics	aro-C_{9-14}	Benzene	13.13	0.505	6	6	78	0.156	0.094	0.149	0.016	0.00023	0.763	0.011	0.003	0.000021
	2-ring	Naphthalenes	2.47	0.058	10	8	128	0.078	0.019	0.015	0.008	0.00011	0.729	0.011	0.003	0.000002
	3-ring	Acenaphthene	3.55	0.069	12	10	154	0.039	0.000	0.000	0.004	0.00006	0.000	0.000	0.000	0.000000
PAH	3-ring	Fluorenes	0.67	0.012	13	10	166	0.039	0.000	0.000	0.004	0.00006	0.000	0.000	0.000	0.000000
	3-ring	Anthracenes	0.47	0.008	14	10	178	0.039	0.000	0.000	0.004	0.00006	0.000	0.000	0.000	0.000000
	4-ring	Pyrenes	0.03	0.000	16	10	202	0.039	0.000	0.000	0.004	0.00006	0.000	0.000	0.000	0.000000
Total			**100**	**1.000**				**1.000**	**1.000**	**1.000**	**0.100**					

FUEL B		Assigned Hydrocarbon Substrate	WT%	mol	C	H	MM	X_{acc}	X_{in}	X_{bio}	X_o mg/L	kCX_o	Y	YkC	YkC-k_d	$S_{tot(t)}$
Paraffin	n-C_{9-14}	Nonane	3.63	0.085	9	20	128	0.145	0.147	0.193	0.014	0.00021	0.872	0.0126	0.0046	0.000031
	n-C_{14}^{+}	Dodecane	3.00	0.053	12	26	170	0.145	0.147	0.193	0.014	0.00021	0.885	0.0126	0.0048	0.000031
	n-C_{14}^{+}	Hexadecane	8.11	0.108	16	34	226	0.143	0.114	0.148	0.014	0.00021	0.869	0.0126	0.0046	0.000024
	iso-C_{9-14}	3-methyldodecane	6.95	0.113	13	28	184	0.072	0.147	0.096	0.007	0.0001	0.869	0.0126	0.0046	0.000015
	iso-C_{14}+	2,2,4,4,6,8,8-heptamethylnonane	9.60	0.127	16	34	226	0.083	0.114	0.086	0.008	0.00012	0.871	0.0130	0.0046	0.000014
Cyclic Alkanes	mono-C_{14}^{+}	butylcyclohexane	12.23	0.262	10	20	140	0.083	0.094	0.070	0.008	0.00012	0.851	0.0126	0.0043	0.000011
	mono-C_{14}^{+}	n-dodecylcyclohexane	18.00	0.214	18	36	252	0.083	0.094	0.070	0.008	0.00012	0.858	0.0123	0.0044	0.000011
	tri-C_{14}^{+}	Decalin	18.16	0.395	10	18	138	0.041	0.065	0.024	0.004	6E-05	0.833	0.0111	0.0041	0.000004
Aromatics	aro-C_{9-14}	1,2,4-Trimethylbenzene	13.13	0.328	9	12	120	0.165	0.080	0.120	0.017	0.00024	0.776	0.0106	0.0032	0.000019
PAH	4-ring	Acenaphthene	7.19	0.140	12	10	154	0.041	0.000	0.000	0.004	6E-05	0.766	0.0000	0.0031	0.000000
Total			**100**	**1.000**				**1.000**	**1.000**	**1.000**	**0.100**					

Table II: Parameters for simulation of conventional diesel-type fuel B [S_o=0.3125mg/L, kC=0.015, k_d=0.008]

FUEL C		Assigned Substrate	Hydrocarbon	WT%	mol	C	H	MM	X_{acc}	X_{in}	X_{bio}	X_o mg/L	kCX_o	Y	YkC	YkC-k_d	$S_{tot(t)}$
Paraffin	n-C_{14}^+	n-dodecane		43	0.76	12	26	170	0.31	0.377	0.46	0.031	0.00045	0.885	0.0128	0.0048	0.000170
	iso-$C_{9\text{-}14}$	isocetane		27	0.36	16	34	226	0.16	0.377	0.23	0.016	0.00023	0.869	0.0126	0.0046	0.000090
Aromatics	mono-C_{14}^+	methylcyclohexane		15	0.46	7	14	98	0.36	0.205	0.28	0.036	0.00052	0.842	0.0122	0.0042	0.000110
PAH	2-ring	1-methyl naphthalene		15	0.32	11	10	142	0.18	0.042	0.03	0.018	0.00026	0.736	0.0107	0.0027	0.000010
Total				**100**	**1.000**				**1.000**	**1.000**	**1.000**						

Table III: Model Parameters & Constants for simulation of conventional diesel-type fuel C [S_o=0.3125mg/L, kC=0.015, k_d=0.008]

FUEL D		Assigned Substrate	Hydrocarbon	WT%	mol	C	H	MM	X_{acc}	X_{in}	X_{bio}	X_o mg/L	kCX_o	Y	YkC	YkC-k_d	$S_{tot(t)}$
Paraffin	n-$C_{9\text{-}14}$	n-dodecane		30	0.53	12	26	170	0.17	0.227	0.23	0.017	0.00024	0.87	0.0126	0.0046	0.000055
	n-$C_{9\text{-}14}$	tetradecane		20	0.3	14	30	198	0.17	0.227	0.23	0.017	0.00024	0.87	0.0126	0.0046	0.000055
	iso-C_{14}^+	isocetane		10	0.13	16	34	226	0.1	0.176	0.1	0.01	0.00014	0.869	0.0126	0.0046	0.000024
Aromatics	mono-C_{14}^+	methylcyclohexane		20	0.61	7	14	98	0.19	0.123	0.14	0.019	0.00028	0.842	0.0122	0.0042	0.000034
	mono-C_{14}^+	o-xylene		15	0.42	8	10	106	0.19	0.123	0.14	0.019	0.00028	0.773	0.0112	0.0032	0.000034
	mono-C_{14}^+	tetralin		5	0.11	10	12	132	0.19	0.123	0.14	0.019	0.00028	0.772	0.0112	0.0032	0.000034

Table IV: Model Parameters & Constants for simulation of conventional diesel-type fuel D [S_o=0.3125mg/L, kC=0.015, k_d=0.008]

Total				**100**	**1.000**				**1.000**	**1.000**	**1.000**	**0.100**				

Table V: Model Parameters & Constants for simulation of biodiesel-type fuel E [S_o=0.3125mg/L, kC=0.015, k_d=0.008]

FUEL E		**Assigned Substrate**	**Hydrocarbon**	**WT%**	**mol**	**C**	**H**	**MM**	**X_{acc}**	**X_{in}**	**X_{bio}**	**X_o mg/L**	**kCX_o**	**Y**	**YkC**	**YkC-k_d**	**$S_{tot(t)}$**
Fatty Esters	Fatty Esters	Methyl Palmitate		12.8	0.14	17	34	270	0.200	0.200	0.8	0.02	0.00029	0.725	0.0111	0.0085	0.000233
		Methyl Stearate		7.8	0.08	19	38	298	0.200	0.200	0.8	0.02	0.00029	0.734	0.0111	0.0086	0.000233
		Methyl Oleate		44.8	0.45	19	36	296	0.200	0.200	0.8	0.02	0.00029	0.718	0.0106	0.0084	0.000233
		Methyl Linoleate		34	0.35	19	34	294	0.200	0.200	0.8	0.02	0.00029	0.702	0.0103	0.0082	0.000233
		Erucic		0.6	0.01	22	42	338	0.200	0.200	0.8	0.02	0.00029	0.731	0.0114	0.0086	0.000233
Total				**100**	**1.000**				**1.000**	**1.000**	**1.000**	**0.100**					

Table VI: Microbial growth stoichiometry & generated products of aerobic degradation of conventional diesel-type fuel A [S_o=0.3125mg/L, kC=0.015, k_d=0.008, t=1]

A	**$S_{tot(0)}$g-$S_{tot(1)}$g C_xH_y (mol)**	**O_2 (mol)**	**C_xH_y (g)**	**O_2 (g)**	**CO_2 (g)**	**H_2O (g)**	**NH_4 (g)**	**HCO_3- (g)**	**$C_5H_7O_2N$ (g)**
	1.7E-05	1.7E-05	2.2E-03	3.0E-04	1.7E-05	4.9E-03	1.7E-05	1.0E-03	1.5E-04
	9.0E-06	1.7E-05	2.0E-03	3.1E-04	1.7E-05	4.3E-03	1.7E-05	1.1E-03	1.3E-04
	8.9E-06	8.8E-06	1.1E-03	1.6E-04	8.8E-06	2.6E-03	8.8E-06	5.4E-04	8.1E-05
	6.2E-06	1.1E-05	1.4E-03	1.9E-04	1.1E-05	3.1E-03	1.1E-05	6.6E-04	9.8E-05
	1.8E-05	2.9E-05	3.6E-03	5.2E-04	2.9E-05	7.8E-03	2.9E-05	1.8E-03	2.4E-04
	6.6E-06	9.8E-06	1.3E-03	1.8E-04	9.8E-06	2.7E-03	9.8E-06	6.0E-04	8.6E-05
	9.8E-07	1.4E-06	1.9E-04	2.5E-05	1.4E-06	4.0E-04	1.4E-06	8.6E-05	1.3E-05
	3.4E-05	1.8E-05	2.7E-03	3.3E-04	1.8E-05	5.3E-03	1.8E-05	1.1E-03	1.7E-04
	4.0E-07	3.3E-07	5.1E-05	6.0E-06	3.3E-07	1.0E-04	3.3E-07	2.0E-05	3.2E-06
	0.0E+00	0.0E+00	0.0E+00	0.0E+00	0.0E+00	0.0E+00	0.0E+00	0.0E+00	0.0E+00
	0.0E+00	0.0E+00	0.0E+00	0.0E+00	0.0E+00	0.0E+00	0.0E+00	0.0E+00	0.0E+00
	0.0E+00	0.0E+00	0.0E+00	0.0E+00	0.0E+00	0.0E+00	0.0E+00	0.0E+00	0.0E+00
	0.0E+00	0.0E+00	0.0E+00	0.0E+00	0.0E+00	0.0E+00	0.0E+00	0.0E+00	0.0E+00
Total	**0.0001**	**0.0001**	**0.0146**	**0.0020**	**0.0001**	**0.0313**	**0.0001**	**0.0068**	**0.0010**
mol/mol		**1.10033**							
g/kg		**0.01195**							
l/l subs		**0.9803**							

Table VII: Microbial growth stoichiometry & generated products of aerobic degradation of conventional diesel-type fuel B [S_o=0.3125mg/L, kC=0.015, k_d=0.008, t=1]

B	**$S_{tot(0)}$g-$S_{tot(1)}$g C_xH_y (mol)**	**O_2 (mol)**	**C_xH_y (g)**	**O_2 (g)**	**CO_2 (g)**	**H_2O (g)**	**NH_4 (g)**	**HCO_3- (g)**	**$C_5H_7O_2N$ (g)**
	8.4E-06	8.3E-06	1.1E-03	1.5E-04	8.3E-06	2.4E-03	8.3E-06	5.1E-04	7.6E-05
	5.2E-06	6.9E-06	8.9E-04	1.3E-04	6.9E-06	2.0E-03	6.9E-06	4.2E-04	6.2E-05
	8.1E-06	1.4E-05	1.8E-03	2.5E-04	1.4E-05	4.1E-03	1.4E-05	8.6E-04	1.3E-04
	5.6E-06	7.9E-06	1.0E-03	1.4E-04	7.9E-06	2.3E-03	7.9E-06	4.8E-04	7.2E-05
	5.6E-06	9.7E-06	1.3E-03	1.8E-04	9.7E-06	2.8E-03	9.7E-06	5.9E-04	8.8E-05
	9.4E-06	9.9E-06	1.3E-03	1.8E-04	9.9E-06	2.9E-03	9.9E-06	6.1E-04	9.2E-05
	7.7E-06	1.5E-05	1.9E-03	2.7E-04	1.5E-05	4.3E-03	1.5E-05	9.0E-04	1.3E-04
	4.9E-06	5.0E-06	6.8E-04	9.0E-05	5.0E-06	1.5E-03	5.0E-06	3.1E-04	4.7E-05
	2.0E-05	1.7E-05	2.4E-03	3.0E-04	1.7E-05	5.1E-03	1.7E-05	1.0E-03	1.6E-04
	0.0E+00	0.0E+00	0.0E+00	0.0E+00	0.0E+00	0.0E+00	0.0E+00	0.0E+00	0.0E+00
Total	**0.0001**	**0.0001**	**0.0125**	**0.0017**	**0.0001**	**0.0275**	**0.0001**	**0.0057**	**0.0009**
mol/mol		**1.24201**							
g/kg		**0.00995**							
l/l subs		**0.81611**							

Table VIII: Microbial growth stoichiometry & generated products of aerobic degradation of conventional diesel-type fuel C [S_o=0.3125mg/L, kC=0.015, k_d=0.008, t=1]

C	**$S_{tot(0)}$g-$S_{tot(1)}$g C_xH_y (mol)**	**O_2 (mol)**	**C_xH_y (g)**	**O_2 (g)**	**CO_2 (g)**	**H_2O (g)**	**NH_4 (g)**	**HCO_3- (g)**	**$C_5H_7O_2N$ (g)**
	4.1E-04	5.5E-04	7.0E-02	9.9E-03	5.5E-04	1.6E-01	5.5E-04	3.4E-02	4.9E-03
	9.8E-05	1.7E-04	2.2E-02	3.1E-03	1.7E-04	4.9E-02	1.7E-04	1.0E-02	1.5E-03
	1.6E-04	1.1E-04	1.5E-02	2.0E-03	1.1E-04	3.4E-02	1.1E-04	6.9E-03	1.1E-03
	1.1E-05	1.0E-05	1.6E-03	1.8E-04	1.0E-05	3.1E-03	1.0E-05	6.2E-04	9.7E-05
Total	**0.0007**	**0.0008**	**0.1092**	**0.0152**	**0.0008**	**0.2434**	**0.0008**	**0.0515**	**0.0076**
mol/mol		**1.24509**							
g/kg		**0.09001**							
l/l subs		**7.38066**							

Table IX: Microbial growth stoichiometry & generated products of aerobic degradation of conventional diesel-type fuel D [S_o=0.3125mg/L, kC=0.015, k_d=0.008, t=1]

D	$S_{tot(0)}g$-$S_{tot(1)}g$ C_xH_y (mol)	O_2 (mol)	C_xH_y (g)	O_2 (g)	CO_2 (g)	H_2O (g)	NH_4 (g)	HCO_3-(g)	$C_5H_7O_2N$ (g)
	9.3E-05	1.2E-04	1.6E-02	2.2E-03	1.2E-04	3.6E-02	1.2E-04	7.4E-03	1.1E-03
	5.3E-05	8.1E-05	1.1E-02	1.5E-03	8.1E-05	2.4E-02	8.1E-05	4.9E-03	7.4E-04
	1.0E-05	1.8E-05	2.3E-03	3.2E-04	1.8E-05	5.2E-03	1.8E-05	1.1E-03	1.6E-04
	6.7E-05	4.9E-05	6.6E-03	8.8E-04	4.9E-05	1.5E-02	4.9E-05	3.0E-03	4.6E-04
	4.6E-05	3.4E-05	4.9E-03	6.1E-04	3.4E-05	1.0E-02	3.4E-05	2.1E-03	3.2E-04
	1.2E-05	1.1E-05	1.6E-03	2.0E-04	1.1E-05	3.4E-03	1.1E-05	6.8E-04	1.1E-04
Total	**0.0003**	**0.0003**	**0.0418**	**0.0057**	**0.0003**	**0.0927**	**0.0003**	**0.0192**	**0.0029**
mol/mol		**1.11433**							
g/kg		**0.03356**							
l/l subs		**2.75218**							

Table X: Microbial growth stoichiometry & generated products of aerobic degradation of conventional diesel-type fuel E [S_o=0.3125mg/L, kC=0.015, k_d=0.008, t=1]

E	$S_{tot(0)}g$-$S_{tot(1)}g$	C_xH_y (mol)	O_2 (mol)	C_xH_y (g)	O_2 (g)	CO_2 (g)	H_2O (g)	NH_4 (g)	HCO_3-(g)	$C_5H_7O_2N$ (g)
	1.1E-04	1.1E-04	1.8E-04	2.9E-02	3.3E-03	1.8E-04	5.7E-02	1.8E-04	1.1E-02	1.8E-03
	5.9E-05	5.9E-05	1.1E-04	1.7E-02	2.0E-03	1.1E-04	3.5E-02	1.1E-04	6.9E-03	1.1E-03
	3.4E-04	3.4E-04	6.4E-04	1.0E-01	1.1E-02	6.4E-04	2.0E-01	6.4E-04	3.9E-02	6.3E-03
	2.6E-04	2.6E-04	4.7E-04	7.6E-02	8.5E-03	4.7E-04	1.5E-01	4.7E-04	2.9E-02	4.8E-03
	4.0E-06	4.0E-06	8.7E-06	1.3E-03	1.6E-04	8.7E-06	2.7E-03	8.7E-06	5.3E-04	8.6E-05
Total	**0.0008**	**0.0008**	**0.0014**	**0.2237**	**0.0255**	**0.0014**	**0.4486**	**0.0014**	**0.0863**	**0.0140**
mol/mol			**1.84724**							
g/kg			**0.15087**							
l/l subs			**12.3714**							

APPENDIX III

Table I: Sample input data used for emission modelling

NUMB	X	Y	TINA	PIN	WAIR	FRAIRFF	FRAIRP	FRAIRI	FRAIRD	WF	FACT1	FACT2	FACT3	FACT4	FACT5	TINF	FALT	TAMB	RHAMB
---	---	---	K	atm	kg/s	---	---	---	---	kg/s	---	---	---	---	---	K	m	K	---
////																			
1	17.7	33.1	637.7	12.6	415.0	0.2	0.1	0.2	0.5	10.9	0.2	0.6	0.2	0.2	0.2	420.0	0.0	288.2	0.6
2	17.7	33.1	641.0	12.8	425.3	0.2	0.1	0.2	0.5	10.6	0.2	0.6	0.2	0.2	0.2	420.0	0.0	288.2	0.6
3	17.7	33.1	645.5	12.9	433.3	0.2	0.1	0.2	0.5	10.2	0.2	0.6	0.2	0.2	0.2	420.0	0.0	288.2	0.6
4	17.7	33.1	648.1	12.9	439.1	0.2	0.1	0.2	0.5	9.8	0.2	0.6	0.2	0.2	0.2	420.0	0.0	288.2	0.6
5	17.7	33.1	651.6	13.0	445.5	0.2	0.1	0.2	0.5	9.4	0.2	0.6	0.2	0.2	0.2	420.0	0.0	288.2	0.6
6	17.7	33.1	655.2	13.0	451.2	0.2	0.1	0.2	0.5	9.0	0.2	0.6	0.2	0.2	0.2	420.0	0.0	288.2	0.6
7	17.7	33.1	661.0	13.1	459.1	0.2	0.1	0.2	0.5	8.5	0.2	0.6	0.2	0.2	0.2	420.0	0.0	288.2	0.6
8	17.7	33.1	667.5	13.1	467.7	0.2	0.1	0.2	0.5	8.1	0.2	0.6	0.2	0.2	0.2	420.0	0.0	288.2	0.6
9	17.7	33.1	674.0	13.2	476.6	0.2	0.1	0.2	0.5	7.6	0.2	0.6	0.2	0.2	0.2	420.0	0.0	288.2	0.6

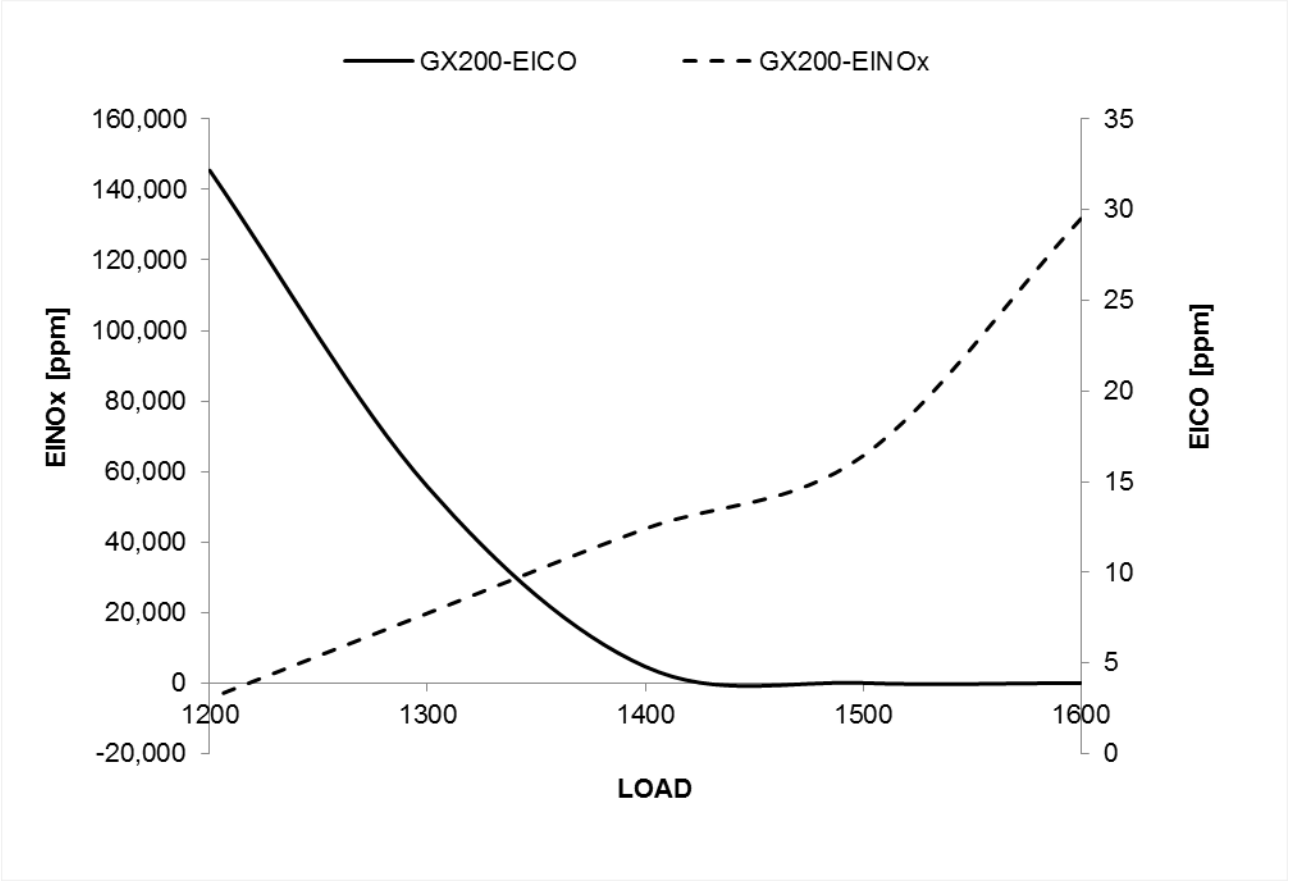

Figure I: NOx and CO emission at vary load conditions for engine GX200.

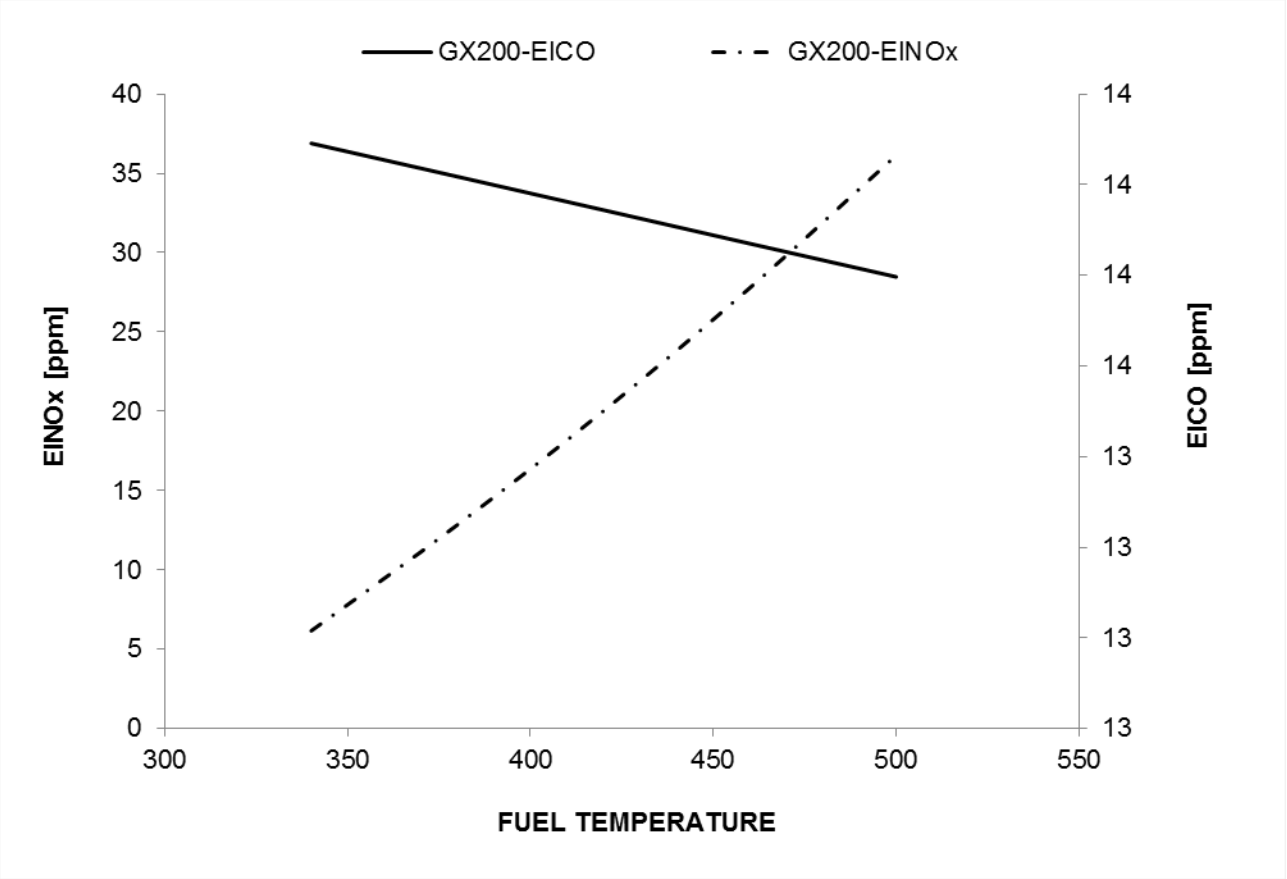

Figure II: Emission analysis at varying fuel temperatures for engine GX200

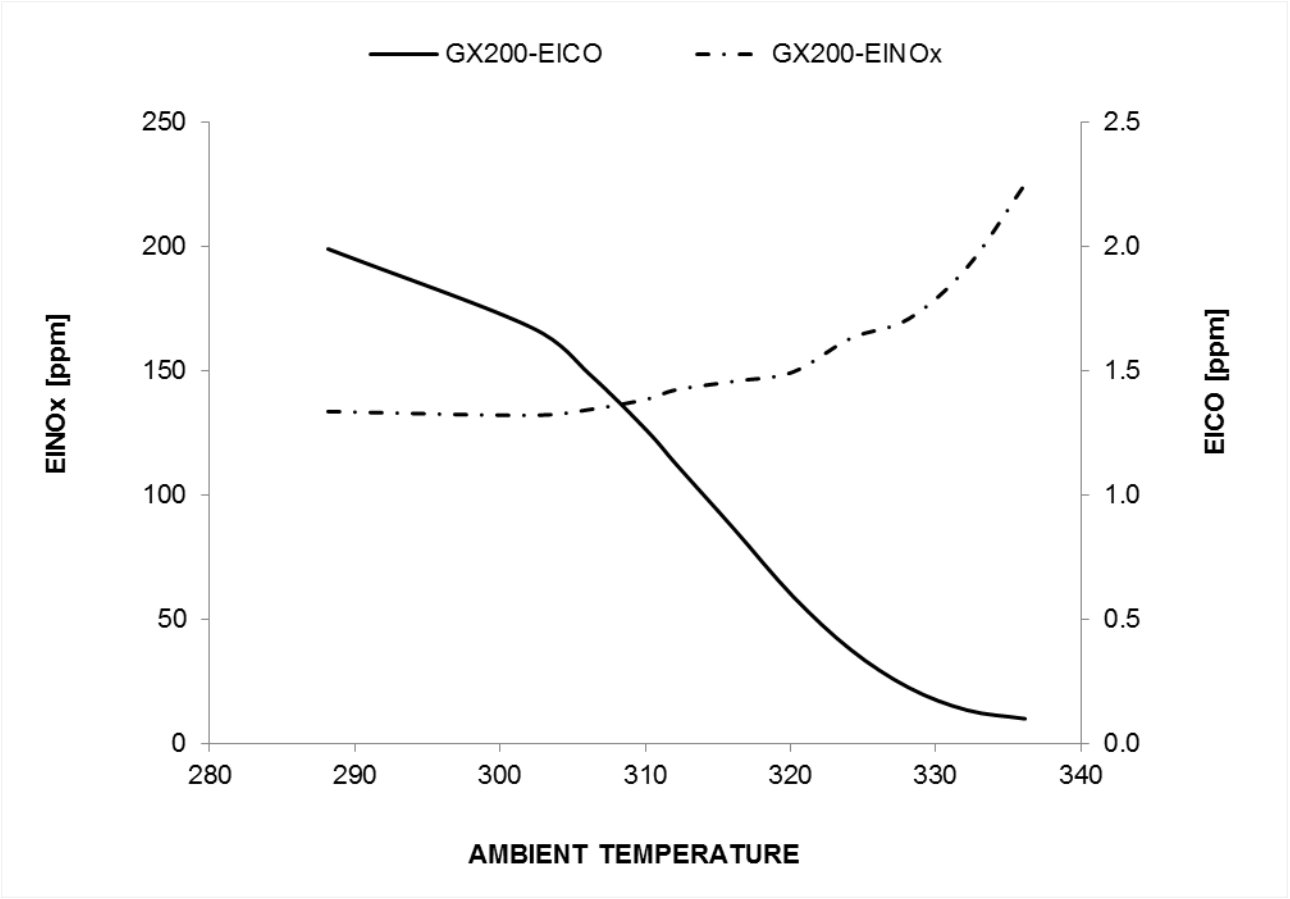

Figure III: Emission analysis at varying ambient temperatures for engine GX200

APPENDIX VI

Table I: Turbine Blade Material Composition

GTD 111	Unit	%
Ni	%	60.39
Cr	%	14.0
Co	%	9.5
Tungsten(W)	%	3.8
Mo	%	1.5
Titanium (Ti)	%	4.9
Al	%	3.0
C	%	0.1
B	%	0.0
Tantalum (Ta)		2.8
Density of Turbine Blade Material	lb/in^3	**0.3077**
-	kg/m^3	**8518**

Table II: Primary data from a Nigerian household and Business Enterprise

Parameters		Business Case	Domestic Case
Engine Rating	kVa	80/100	22
Engine Type	-	Perkins 1100 Series/Duetz	-
Average hours of operation	hrs/day	8-10	6
Energy Cost	$/kWh	0.077	0.077
Total Fuel Cost/Annum	$	40248	13565
Power Factor	%	80%	80%
Engine Power	kW	80	18
Total Operating Hours/Annum	hrs	3650	2190
Total Deficit Hours/Annum	hrs	5658	6570
Fuel Cost	$/kWh	0.1378	0.3519
Capital Cost/Annum	$	1794	776
Total Maintenance Cost/Annum	$	2807	1342
Emission Cost/Annum	$	0	0
Deficit Energy Cost	$	56768	8921